

DISSERTATION

GLOBAL ANALYSIS OF MRNA DECAY RATES AND RNA-BINDING SPECIFICITY  
REVEALS NOVEL ROLES FOR CUGBP1 AND PARN DEADENYLASE IN MUSCLE  
CELLS

Submitted by

Jerome E. Lee

Graduate Degree Program in Cellular and Molecular Biology

In partial fulfillment of the requirements

For the Degree of Doctor of Philosophy

Colorado State University

Fort Collins, Colorado

Summer 2011

Doctoral Committee:

Advisor: Carol J. Wilusz

Co-advisor: Jeffrey Wilusz

Deborah M. Garrity

Norman P. Curthoys

## ABSTRACT

### GLOBAL ANALYSIS OF MRNA DECAY RATES AND RNA-BINDING SPECIFICITY REVEALS NOVEL ROLES FOR CUGBP1 AND PARN DEADENYLASE IN MUSCLE CELLS

Type I Myotonic Dystrophy (DM1) is characterized by myotonia, cardiac conduction defects, muscle wasting, and insulin resistance. In patient muscle cells expression and function of the RNA-binding proteins CUGBP1 and MBNL1 are disrupted, resulting in altered mRNA metabolism at the levels of splicing and translation. Intriguingly, despite strong evidence for CUGBP1 being a regulator of mRNA turnover in humans and other organisms, the possibility that defects in mRNA decay contribute to DM1 pathogenesis has not been investigated to date.

As such, we sought to further characterize the roles of CUGBP1 and its partner, the deadenylase PARN, in mRNA decay in mouse C2C12 muscle cells. The TNF message, which encodes a cytokine known to cause muscle wasting and insulin resistance when over-expressed, was stabilized by depletion of CUGBP1. The normally rapid decay of the TNF mRNA was also disrupted in cells treated with phorbol ester and this coincided with phosphorylation of CUGBP1.

These findings provided impetus to undertake a global analysis of mRNA decay rates in muscle cells. Our investigation revealed that GU- and AU-rich sequence elements are enriched in labile transcripts, which encode cell cycle regulators,

transcription factors, and RNA-processing proteins. Transcripts specifically bound to CUGBP1 in myoblasts are linked with processes such as mRNA metabolism, protein targeting to the endoplasmic reticulum, cytoskeletal organization, and transcriptional regulation, all of which have implications for muscle cell biology. Consistent with this, CUGBP1 depletion profoundly altered the formation of myotubes during differentiation.

Finally we investigated whether PARN, which interacts with CUGBP1 and mediates rapid deadenylation of TNF in HeLa cell extracts, also plays a role in mediating mRNA decay in muscle. We identified 64 mRNA targets whose decay was dependent on PARN. Moreover, deadenylation of the Brf2 mRNA was impaired in PARN knock-down cells supporting that this mRNA is directly and specifically targeted for decay by PARN.

Taken together our findings demonstrate that CUGBP1 and PARN are critical regulators of decay for specific sets of transcripts in muscle cells. It seems likely that some or all of the CUGBP1 targets we have identified may be affected in myotonic dystrophy. Defective mRNA turnover could be linked with defects in myogenesis, TNF over-expression, muscle wasting and/or ER stress, all of which have been documented in DM1.

## Acknowledgements

I would like to begin by thanking my advisors, Drs. Carol and Jeffrey Wilusz. First off, they agreed to take me into their lab with nothing more than a bachelor's degree and a determination to succeed. Throughout this project, they have been outstanding mentors, helping me learn a great deal about molecular biology, experimentation (yes even with hot RNA), and RNA decay. Along the way they have been both encouraging and skeptical of the data and ideas which I possessed. Their advice hasn't always been welcome or easy to hear, but has always kept the "big picture" in mind, and been a very positive influence.

I would also like to thank the American Heart Association for awarding me a pre-doctoral fellowship for three years of this project. I am also grateful for my graduate committee members Dr. Deborah Garrity and Dr. Norm Curthoys. In addition I am thankful to our collaborators, Drs. Ju Youn Lee and Bin Tian who performed nearly all of the bioinformatic analysis of our micro-array data. Without the funding and collaborations this project would have been dramatically reduced.

Finally, I would like to thank my family. Both of my parents and sister have been helpful throughout this project. They have provided a welcome distraction at times, as well as advice on getting through graduate school. Most importantly they have always supported my decision to pursue an advanced degree and encouraged me throughout. Lastly, I would like to thank my future wife Tori. In ways too numerous to describe here, she has helped me get through this period of my life rather smoothly.

## TABLE OF CONTENTS

Abstract .....	ii
Acknowledgements .....	iv
Table of Contents .....	v-xiv
<b>Chapter 1: Introduction</b> .....	<b>1</b>
Gene expression, mRNA decay, and myotonic dystrophy	
1.1 The life cycle of an mRNA .....	1
1.1.1 Transcription .....	2
1.1.2 Capping .....	3
1.1.3 Splicing .....	3
1.1.4 Cleavage and polyadenylation .....	5
1.1.5 The mature mRNA and nuclear surveillance .....	7
1.1.6 mRNA export .....	8
1.1.7 Translation .....	8
1.1.8 Cross-talk in mRNA metabolism .....	9
1.1.9 mRNP remodeling .....	10
1.1.10 mRNA decay .....	11
1.2 Gene expression and the role of mRNA decay .....	11
1.3 Mechanisms of mRNA decay .....	13

1.3.1 Deadenylation-dependent decay .....	13
<b>Figure 1. The primary mRNA decay pathway .....</b>	<b>14</b>
1.3.1.1 Deadenylation .....	15
1.3.1.1.1 PARN .....	15
1.3.1.1.2 The CCR4/NOT complex .....	17
1.3.1.1.3 PAN2/PAN3 .....	18
1.3.2 Deadenylation-independent decay pathways .....	19
1.3.2.1 Decay of aberrant mRNAs .....	19
1.3.2.2 Endoribonucleolytic decay .....	20
1.3.2.3 miRNA-mediated decay .....	20
1.3.3 5'-to-3' Decay .....	21
1.3.4 3'-to-5' Decay .....	22
1.3.5 Sites of mRNA decay .....	23
1.4 <i>Cis</i> -acting determinants of mRNA stability .....	24
1.4.1 The cap and poly(A) tail .....	24
1.4.2 3'UTR regulatory elements .....	25
1.4.2.1 AU-rich elements .....	25
1.4.2.2 GU-rich elements .....	26
1.4.2.3 UGUA elements .....	26
1.4.2.4 miRNA-binding sites .....	27
1.5 <i>Trans</i> -acting factors influence mRNA decay rates .....	27
1.5.1 Destabilizing factors .....	28
1.5.2 Stabilizing factors .....	31
1.6 Modulation of mRNA decay rates .....	32
1.7 Competition between <i>trans</i> -acting factors .....	34
1.8 Muscle biology .....	34

1.9 Muscle differentiation .....	35
<b>Figure 2. Muscle differentiation requires post-transcriptional gene regulation</b> .....	<b>36</b>
1.10 Role of mRNA decay during muscle differentiation.....	36
1.11 Myotonic dystrophy (DM) .....	37
1.11.1 Disease symptoms .....	38
1.11.2 Repeat expansion, anticipation, disease severity, and toxic RNA .....	38
1.11.3 Phosphorylation and over-expression of CUGBP1 in DM1 .....	39
1.11.4 Aberrant splicing regulation by CUGBP1 and MBNL1 .....	40
1.11.5 Aberrant translational regulation by CUGBP1 in DM1 .....	40
1.11.6 Unexplained symptoms of DM1 .....	41
1.11.7 Modifiers of DM phenotype .....	41
<b>Figure 3. Defects in RNA metabolism are hallmarks of DM1</b> .....	<b>42</b>
1.11.8 Therapeutic approaches .....	42
1.12 CUGBP1 .....	43
1.12.1 RNA-binding properties of CUGBP1 .....	44
1.12.2 Nuclear roles of CUGBP1 .....	44
1.12.3 Cytoplasmic roles of CUGBP1 .....	45
1.12.3.1 mRNA Decay .....	45
1.12.3.2 Translational regulator .....	45
1.13 Heritable neuromuscular diseases and CUGBP1 disruption.....	46
1.13.1 OPMD-Oculopharyngeal Muscular Dystrophy .....	46
1.13.2 SBMA-Spinal Bulbar Muscular Atrophy .....	46
1.13.3 FXTAS-Fragile-X Tremor Ataxia Syndrome .....	47
1.14 Rationale and hypothesis .....	47
1.14.1 TNF mRNA decay in muscle cells.....	47

1.14.2 Global rates of mRNA decay in muscle cells .....	48
1.14.3 Identification of CUGBP1 substrate mRNAs .....	49
1.14.4 mRNA decay and deadenylation by PARN in muscle cells .....	49
<b>Chapter 2: Materials and methods .....</b>	<b>51</b>
2.1 Bacterial expression plasmids.....	51
2.1.1 CUGBP1 .....	51
<b>Table 2.1 Primers for generation of GST-tagged CUGBP1 and deletion mutants .....</b>	<b>51</b>
<b>Figure 4. Experimental design for generating GST-tagged CUGBP1 and deletion mutants .....</b>	<b>52</b>
2.1.2 PARN .....	52
<b>Table 2.2 Primers for generation of 6XHis-tagged PARN.....</b>	<b>52</b>
2.1.3 HuR.....	52
2.2 Plasmids for lentivirus expression of shRNAs targeting CUGBP1 and PARN .....	53
2.2.1 CUGBP1 .....	53
2.2.2 PARN .....	53
<b>Table 2.3 Nucleotide sequences for generation of PARN shRNA producing vectors .....</b>	<b>54</b>
2.3 Plasmids for <i>in vitro</i> transcriptions .....	54
2.3.1 pGemT-p21 .....	54
<b>Table 2.4 Primers for amplifying 3'UTRs from mouse cDNA.....</b>	<b>54</b>
2.3.2 pGemT-Zfp36l2 (Brf2), pGemT-Actin.....	55
<b>Table 2.5 Oligonucleotides for generation of 3'UTR probes.....</b>	<b>55</b>
2.4 <i>In vitro</i> transcription reactions .....	55



2.5 Purification of GST-tagged CUGBP1 proteins .....	56
2.6 Purification of 6XHis-tagged PARN protein.....	57
2.7 Purification of 6XHis-tagged HuR protein .....	57
2.8 GST-pulldown assays .....	58
2.9 Cell culture .....	59
2.10 Differentiation of C2C12 cells.....	59
2.11 Phorbol-ester treatment of C2C12 cells.....	59
2.12 Generation of lentivirus particles for shRNA expression.....	59
2.13 Immunofluorescence microscopy.....	60
2.14 Determination of fusion index.....	60
2.15 Generation of PARN and CUGBP1 knock-down cells .....	61
2.15.1 PARN .....	61
2.15.2 CUGBP1 .....	61
2.16 Western blotting .....	62
2.17 Cytoplasmic and nuclear fractionation of C2C12 cells.....	63
2.18 Half-life analysis .....	64
2.19 qRT-PCR.....	65
<b>Table 2.6 List of primers used for (q)RT-PCR experiments .....</b>	<b>66</b>
2.20 RNA immunoprecipitation .....	66
2.21 Preparation of RNA samples and microarray hybridization.....	68
2.22 Half-life analysis by microarray .....	68
2.23 CUGBP1 target identification by RIP-Chip and comparison to other datasets.....	68
2.24 <i>Cis</i> -element analysis .....	69
2.25 Gene ontology analysis.....	70
2.26 Electrophoretic mobility shift assays .....	70

2.27 UV cross-linking assays .....	71
2.28 2D protein gels .....	71
2.29 RNaseH/northern blotting .....	72
<b>Table 2.7 Oligonucleotides used in RNaseH reactions</b> .....	<b>73</b>
<b>Chapter 3: CUGBP1 regulates stability of TNF mRNA in muscle cells</b> .....	<b>74</b>
3.1 CUGBP1 destabilizes TNF mRNA in C2C12 myoblasts .....	75
<b>Figure 5. Knock-down of CUGBP1 by shRNA triggers TNF mRNA abundance and half-life increases</b> .....	<b>76</b>
3.2 PARN deadenylase is dispensable for rapid decay of TNF mRNA in C2C12 cells .....	78
<b>Figure 6. Knock-down of PARN by shRNA does not change TNF mRNA abundance or half-life</b> .....	<b>79</b>
3.3 Protein Kinase C activation increases TNF mRNA abundance and stability	80
<b>Figure 7. CUG-repeat RNA expression and TPA treatment result in CUGBP1 phosphorylation</b> .....	<b>81</b>
3.4 CUGBP1-mediated decay of TNF mRNA is disrupted upon TPA treatment.	81
<b>Figure 8. TNF mRNA abundance and stability are increased upon PKC activation in a CUGBP1-dependent manner</b> .....	<b>82</b>
3.5 Protein kinase C activation disrupts interaction of CUGBP1 with substrate mRNAs .....	84
<b>Figure 9. Myogenin and Jun mRNAs are associated with CUGBP1 and treatment with TPA reduces CUGBP1 association</b> .....	<b>85</b>
<b>Chapter 4: Global analysis of mRNA decay reveals the importance of CUGBP1 in muscle cells</b> .....	<b>88</b>
4.1 Global assessment of mRNA decay in muscle cells .....	89

<b>Figure 10. Experimental design for estimation of mRNA half-lives</b> .....	90
4.2 Global mRNA decay features in myoblasts.....	91
<b>Figure 11. Global decay assay yields 7,398 mRNA half-lives in muscle cells</b> .....	92
4.3 mRNAs involved in cell cycle and ion transport are enriched in short and long-lived mRNAs respectively .....	92
4.4 Identification of <i>cis</i> -acting elements enriched in the 3'UTRs of short and long-lived transcripts .....	93
<b>Table 4.1 GO analysis reveals important processes associated with short and long half-life mRNAs</b> .....	94
<b>Figure 12. Hexamer analysis of stable and unstable mRNAs reveals potential mRNA decay determinants in muscle cells</b> .....	96
4.5 CUGBP1 knock-down impacts mRNA decay rates in muscle cells .....	98
<b>Figure 13. CUGBP1 knock-down stabilizes a subset of mRNAs in muscle cells</b> .....	100
4.6 Identification of direct mRNA targets of CUGBP1 in muscle cells.....	100
<b>Figure 14. Identification of novel mRNA targets of CUGBP1 in muscle cells</b> .....	102
4.7 CUGBP1 binds GU-rich element containing and unstable mRNAs in muscle.....	103
<b>Figure 15. CUGBP1 binds GU-rich element containing mRNAs, correlating with rapid decay in muscle cells</b> .....	104
4.8 CUGBP1 and HuR bind common mRNA targets in muscle cells.....	105
<b>Figure 16. CUGBP1 and HuR bind common mRNA targets</b> .....	106
4.9 CUGBP1 binds transcripts encoding factors involved in cell cycle and mRNA metabolism.....	107
<b>Table 4.2 CUGBP1 binds mRNAs encoding factors involved in the cell cycle and mRNA metabolism</b> .....	108
<b>Table 4.3 CUGBP1 binds mRNAs encoding factors involved in mRNA metabolism, differentiation, and protein secretion</b> .....	109
4.10 CUGBP1 is required for muscle differentiation.....	110

<b>Figure 17. CUGBP1 plays a role in muscle differentiation</b> .....	111
4.11 CUGBP1 plays an important role in muscle differentiation .....	112
<b>Figure 18. CUGBP1 levels are important for appropriate expression of differentiation markers</b> .....	113
4.12 CUGBP1 is phosphorylated upon muscle differentiation .....	114
<b>Figure 19. CUGBP1 is phosphorylated in myotubes</b> .....	115
<b>Chapter 5: Global analysis reveals mRNA substrates for decay by PARN in myoblasts</b> .....	117
5.1 PARN knock-down disrupts decay rates of subset of mRNAs in C2C12 cells .....	117
<b>Table 5.1 Transcripts exhibiting altered decay rates in PARN knock-down myoblasts</b> .....	119
<b>Figure 20. Validation of mRNAs exhibiting PARN-dependent mRNA decay rates</b> .....	121
5.2 PARN knock-down alters poly(A) status of Brf2 mRNA .....	121
<b>Figure 21. PARN knock-down results in altered poly(A) status of the Brf2 mRNA</b> .....	123
<b>Figure 22. PARN knock-down does not alter the poly(A) status of the actin mRNA</b> .....	124
5.3 PARN knock-down disrupts deadenylation of Brf2 .....	124
<b>Figure 23. PARN knock-down inhibits poly(A) tail removal of the Brf2 mRNA</b> .....	126
<b>Chapter 6: Discussion</b> .....	127
6.1 Regulation of TNF mRNA stability by CUGBP1 .....	127
6.1.1 CUGBP1 targets the TNF mRNA for fast decay in muscle cells .....	127

6.1.2 PKC activation disrupts CUGBP1 function.....	128
6.2 mRNA decay and the role of CUGBP1 in muscle cells .....	130
6.2.1 Unique attributes of mRNA decay in muscle cells.....	131
6.2.2 CUGBP1 depletion has wide-ranging effects on mRNA decay in muscle cells .....	131
6.2.3 Direct CUGBP1 targets: substrate competition and differentiation .....	132
6.2.4 Myoblast differentiation is regulated by CUGBP1 .....	134
6.2.5 CUGBP1 is dynamically regulated during muscle differentiation .....	135
6.3 Global approach identifies mRNA substrate for deadenylation by PARN...	135
6.3.1 PARN affects deadenylation in myoblasts .....	136
6.3.2 Brf2 mRNA is subject to deadenylation by PARN .....	137
6.4 Concluding remarks .....	138
Reference List.....	139
Appendices .....	163
Appendix 1. Only full-length CUGBP1 stably interacts with PARN <i>in vitro</i> .....	164
Appendix 2. Knock-down of PARN by shRNA #1520 changes TNF mRNA abundance and half-life .....	165
Appendix 3. Hexamers enriched in the 3'UTRs of the most and least stable mRNAs .....	166
Appendix 4. Transcripts stabilized upon CUGBP1 knock-down.....	168
Appendix 5. Validation of novel mRNA targets of CUGBP1 in muscle cells .....	179
Appendix 6. Transcripts which immunoprecipitate with CUGBP1 .....	181
Appendix 7. Clustering of the top 50 hexamers enriched in CUGBP1 IP dataset reveals binding site .....	191

Appendix 8. Shared transcripts between CUGBP1 knock-down array and top 5% from CUGBP1 RIP-Chip.....	192
Appendix 9. Top 50 hexamers from transcripts stabilized in the CUGBP1 knock-down dataset and in the top 5% of the CUGBP1 IP dataset.....	194
Appendix 10. CUGBP1 knock-down cell line and alternative shRNA (#1320) results in myosac formation and enhanced differentiation .....	195
Appendix 11. A significant number of mRNAs are increased in abundance in both PARN and CUGBP1 knock-down cells. ....	197

## ***Chapter 1: Introduction***

### ***Gene expression, mRNA decay, and myotonic dystrophy***

Gene expression is a multi-step process that must be carefully regulated. A significant proportion of this regulation takes place at the post-transcriptional level at steps such as splicing, polyadenylation, translation, and mRNA decay. Alteration of post transcriptional regulation is observed in the muscle of Myotonic Dystrophy (DM) patients. In this debilitating disease, mRNA metabolism is disrupted by expression of a toxic RNA molecule which results in altered function of two RNA-binding proteins, Muscleblind (MBNL1) and CUG-binding protein (CUGBP1). Herein, with the long term goal of gaining valuable insights into DM pathogenesis, we have examined the regulation of mRNA stability by CUGBP1 and associated factors in muscle cells. Specifically, this study focuses on global control of mRNA decay in muscle cells, the potent mRNA encoding the cytokine Tumor Necrosis Factor (TNF), the RNA-binding protein CUGBP1, and the Poly(A)-specific Ribonuclease PARN.

#### ***1.1 The life cycle of an mRNA***

In eukaryotes formation of a mature messenger RNA (mRNA) requires much more than mere transcription of a DNA template. During and after transcription many tightly regulated events must take place, each of which is associated with a unique array of proteins to form a fully competent mRNP (messenger ribonucleoprotein). Starting from the addition of a cap structure at the 5' end of a nascent mRNA molecule, all the way to

translation and eventual decay of the transcript, proteins carefully chaperone mRNAs through their complex life cycle.

### *1.1.1 Transcription*

Transcription is the first and an absolutely required step in gene expression. Transcription is the copying of a double-stranded DNA molecule into a single stranded RNA molecule by RNA polymerases. Most important here, RNA polymerase II (Pol II) is responsible for transcribing DNA to make mRNAs. This multi-subunit protein complex not only synthesizes RNA from DNA, but also brings many of the mRNA processing enzymes directly to their pre-mRNA substrate. Deposition of the mRNA processing factors is carried out by the carboxy-terminal domain (CTD) of the largest subunit of Pol II. In humans, the CTD is comprised of 52 copies of the hepta-peptide repeat  $Y_1S_2P_3T_4S_5P_6S_7$  (Hirose and Ohkuma, 2007). This domain undergoes a series of phosphorylation and dephosphorylation events as it proceeds from initiation, to elongation, to termination. The phosphorylation state of the CTD correlates with the RNA processing factors which are associated to it and deposited on the forming transcript. At initiation, Ser-5 is phosphorylated to ensure recruitment of the capping machinery (Gu and Lima, 2005). When transcription reaches the elongation phase, phosphorylation of the CTD increases at Ser-2 and decreases at Ser-5 (Bentley, 2005). This causes association of factors of the pre-mRNA splicing machinery. Finally, phosphorylation at Ser-2 further increases near the 3' end of the nascent RNA, resulting in association of factors of the cleavage and polyadenylation machinery with the CTD and its subsequent deposition on the newly made mRNA (Maniatis and Reed, 2002; Ahn et al., 2004).



### 1.1.2 *Capping*

The conventional 7-methylguanosine cap structure found on mammalian mRNAs consists of a non-templated guanosine residue with an unusual 5'-to-5' linkage to the first templated base in the RNA molecule. Capping requires three distinct enzymatic activities, a triphosphatase, a guanylyl-transferase, and a methyltransferase (Wang et al., 1982). Cap addition must be carried out in an efficient manner to protect the mRNA from the cellular 5'→3' exoribonucleases XRN1 and RAT1 (Hsu and Stevens, 1993; Poole and Stevens, 1995), which will readily degrade RNA with a free 5' mono-phosphate. This cap structure is bound by the nuclear Cap-Binding Complex, Cap-Binding Proteins 80/20 (CBP80/20; Izaurralde et al., 1994; Ohno et al., 1990), which protects from decapping, and promotes splicing and export (Lewis and Izaurralde, 1997). In addition, the 5' cap is important for stimulating translation initiation in the cytoplasm (Both et al., 1975). Translation is accomplished by association of the cap with the eukaryotic translation initiation factor 4E (eIF-4E). eIF-4E interacts with eIF-4G which bridges to poly(A) binding protein, resulting in mRNA circularization and translation (Sachs and Varani, 2000).

### 1.1.3 *Splicing*

Splicing is the process responsible for removing intervening portions of mRNA which are not to be translated, termed introns. Like capping, splicing also must be carried out in an efficient manner, and is promoted by associations between the CTD of Pol II and the serine-arginine rich (SR) proteins which interact with the spliceosome (Das et al., 2007). The spliceosome is comprised of well over 100 proteins and RNAs. In higher eukaryotes, CBP80/20, the spliceosome, regulatory RNA-binding proteins,

chromatin structure and transcription rate, all serve to regulate splice site choice (Nilsen and Graveley, 2010).

At its core, splicing is carried out by ubiquitous small nuclear RNAs or U snRNAs complexed with proteins to form small nuclear ribonucleoprotein particles (snRNPs). Through base pairing between the U snRNAs and the unspliced pre-mRNA, the snRNPs are able to guide two nucleophilic attacks. The first attack is by the intron on to the pre-mRNA itself, splitting the molecule in half. The second attack is from the free 3'OH of the mRNA which releases the intron and joins the two exons. Auxiliary factors and RNA-binding proteins, in complex with RNA molecules direct this highly specific process. (McManus and Graveley, 2011).

Completion of splicing is important not only for assembling the proper protein coding sequence, but also for forming a functional mRNP. Successful splicing leaves a specific array of proteins along the mRNA molecule termed exon-junction complexes (EJCs). The position of these EJCs on the mRNA serves as another important quality-control mechanism. EJCs will trigger message decay if improperly positioned relative to the stop codon (Kim et al., 2001). Furthermore, proteins found in the EJC are important for promoting translation (Lee et al., 2009) and nuclear export via interactions with the factors, REF and p15/ALY (Le et al., 2001).

RNA-binding proteins are essential regulators of the splicing process. Nucleotide sequences on the pre-mRNA molecule are specifically recognized by SR proteins, heterogeneous nuclear RNA-binding proteins (hnRNPs), and others (CELF, MBNL, FOX, NOVA, TIA-1, and so on). In general, splicing is enhanced by binding of SR proteins and CELFs (CUGBP and ELAV Like Factors), promoting exon inclusion and repressed by binding of hnRNPs and MBNLs, resulting in exon skipping though there

are many exceptions (McManus and Graveley, 2011). Predicting splicing patterns is very difficult, even with well-characterized binding sites for enhancer and repressor proteins (Barash et al., 2010).

Splicing generates diverse RNA molecules from a limited DNA genome. Alternative splicing contributes to the large phenotypic differences between organisms like humans and mice which exhibit relatively minor differences in gene sequence (only 2% unique at the DNA level; Graveley, 2001). Alternative splicing patterns give distinct tissues many of their unique properties in higher organisms (Graveley, 2001). For example, mis-splicing of the chloride channel-1 (Clcn1) mRNA by loss of MBNL1 function, reverts the Clcn1 mRNA to the embryonic pattern. This results in the inability to quickly relax a muscle once contracted, as the grasp of many newborns exhibit (Mankodi et al., 2002). Shortly after birth the splicing patterns switch to the adult isoform allowing for both contraction and relaxation.

#### *1.1.4 Cleavage and polyadenylation*

The final steps in formation of a mature mRNA are cleavage and polyadenylation. When the last portion (the 3' end) of the message has been transcribed, the 3' end formation machinery, recruited by the CTD of Pol-II assembles and cleaves the newly transcribed RNA. This event is directed by Cleavage/Polyadenylation Specificity Factor (CPSF), which binds the core (AAUAAA) upstream element, in combination with Cleavage Stimulation Factor (CStF) which binds a U-rich downstream element. Cleavage between the upstream and downstream elements is carried out by the 73 kDa subunit of CPSF (Mandel et al., 2006). Following cleavage, around 200 non-templated adenosine residues are added by poly(A) polymerase (Sheets and Wickens, 1989). This poly(A) tail has many important functions

from shielding the mRNA body from 3'→5' exoribonucleases like the exosome to enhancing translation and recruiting mRNA decay factors. In the nucleus the poly(A) tail is complexed with the nuclear Poly(A) Binding Protein (PABPN1) which also influences poly(A) tail length. In the cytoplasm the tail is bound by PABPC1-4, the cytoplasmic poly(A) binding proteins, which promote translation of the message by association with other proteins. The interaction between PABPC1, eIF-4G, and eIF-4E circularizes the mRNP and promotes translation. Following the cleavage event, Pol II continues to transcribe at a slower rate due to CTD phosphorylation. The uncapped nascent RNA is degraded by RAT1, which proceeds rapidly down the RNA triggering termination of transcription upon reaching the polymerase (Buratowski, 2005).

Polyadenylation, like splicing, can be used to produce multiple transcripts from a single gene. Predictive algorithms show nearly all genes possess alternative poly(A) sites, and studies estimate that about 50% of mRNAs exhibit alternative polyadenylation (APA; Tian et al., 2005). Additional downstream poly(A) signals can act as a fail-safe mechanism to ensure 3' end formation and transcription termination. Moreover cells can modulate gene expression by changing the 3' end of a message. Although this can change the coding sequence of a gene, it more often allows for alternative regulatory information to be added or removed from an mRNA. Sequence features in the 3'UTR are bound by proteins and/or miRNAs which dictate how stable the mRNA is, where it localizes to, and how efficiently it is translated. The importance of APA was illustrated nicely by the observation that rapidly dividing cells tend to express short mRNA isoforms (choose the proximal poly(A) site). The reduced regulation of the short 3'UTR containing transcripts was correlated with cancerous cell types (Mayr and Bartel, 2009; Ji et al., 2009; Sandberg et al., 2008).

#### 1.1.4 *The mature mRNA and nuclear surveillance*

A mature messenger RNA should have a 7-methyl guanosine cap, exon-exon junctions marked by EJC, and a 3' poly(A) tail of about 200 nucleotides, though the length of the tail has been shown to vary (Yang et al., 2011). The vast majority of our knowledge regarding mechanisms that monitor these features, termed nuclear surveillance, comes from studies in budding yeast. Relatively little work in this area has been done in mammals. During production of the mature mRNA if any of these processes fail there are a host of nuclear enzymes which will rapidly degrade the aberrant product. Starting at the cap, if addition of the 5' guanosine residue fails or methylation is disrupted, the pyrophosphatase RAI1 will initiate decay of the nascent transcript, and the resulting 5'-monophosphate-containing RNA will be degraded by the RAT1 exoribonuclease (Jiao et al., 2010).

If aberrant products are generated during splicing, specific enzyme complexes exist to destroy the messages. Free 3'-ends which may result from incomplete joining of exons are rapidly degraded by the nuclear exosome (Callahan and Butler, 2010; see below for more discussion). The TRAMP complex enhances the efficiency of nuclear decay by catalyzing the addition of non-templated adenosine residues at the 3' end. In addition to poly(A) polymerase activity, TRAMP also contains an RNA helicase for unwinding structured 3' ends (LaCava et al., 2005). The addition of adenosines to a structured 3' end is thought to create a "toe-hold" for decay to initiate. Thus in this instance, the polyadenylation machinery actually adds adenosines to promote decay as is seen in bacteria (Kushner, 2004).

### 1.1.5 *mRNA export*

Once the mature mRNA has been made, it must be transported to the cytoplasm where it can be translated. This is a process which requires energy in the form of adenosine triphosphate (ATP) and moving the RNA through a 10nm protein tunnel called the nuclear pore complex. The majority of cellular mRNAs leave the nucleus by association of SR proteins and other EJC components, which bind during processing, and interact with adaptor proteins like (REF/p15/ALY) which in turn bind nuclear export factor 1 (NXF1), for a full review see Cook et al., (2007). This mRNP complex associates with the nucleoporin proteins or Nups on the nuclear side of the pore, and is moved into the cytoplasm (Rodriguez et al., 2004b). By linking processing factors deposited during mRNP formation to export, only fully processed mRNAs are efficiently trafficked to the cytoplasm.

### 1.1.6 *Translation*

Translation is the process of converting the open-reading frame of the mRNA into a polypeptide chain. It is carried out by the enormous ribonucleoprotein complex called the ribosome which is composed of a large 60S and small 40S subunit. Translation involves three basic steps, initiation, elongation, and termination.

Initiation is achieved by association of initiation factors with the mRNA and 40S subunit which help to align the 40S subunit with the start codon, and promote large subunit joining for proper initiation, elongation, and eventual termination of the nascent polypeptide (Kapp and Lorsch, 2004). Interestingly, the conformation of the mRNA is important for efficient translation. Message circularization, by eIF-4G bridging the interaction of eIF-4E with PABPC1, synergistically stimulates translation (Gray et al.,

2000; Tarun, Jr. and Sachs, 1996). Initiation is the rate-limiting step in translation, and is extensively regulated, primarily through RNA-binding proteins. For example, the RNA-binding protein ZBP1 binds the *β-actin* mRNA at its 3'UTR blocking translation initiation by inhibiting 60S subunit joining (Dahm and Kiebler, 2005). The ZBP1 protein also associates with myosin motors which travel along the microtubules carrying the *β-actin* mRNA to the edge of the cell, where the SRC kinase phosphorylates ZBP1 reducing its affinity for the mRNA. Release by ZBP1 allows the mRNA to be translated producing actin monomers, which polymerize to elongate the actin filaments (Huttelmaier et al., 2005).

#### *1.1.8 Cross-talk in mRNA metabolism*

Every step along the assembly line of mRNA production seems functionally linked to the processes that precede and follow it. Quality control mechanisms are prevalent along the way. The cell has a multi-layered strategy in place to ensure that the information encoded in DNA is accurately represented in RNA and protein.

Demonstrative of this cross-talk, transcription and decay are linked. In yeast, one of the small subunits of Pol II (Rpb4/7) is an RNA-binding complex that is co-transcriptionally loaded onto some mRNAs. Rpb4/7 promotes mRNA export, enhances translation by recruiting eIF-4G, and targets messages to processing bodies (P-bodies -which are thought to be sites of mRNA storage and decay), during stress (Harel-Sharvit et al., 2010). Splicing and cleavage/polyadenylation are also coupled. Interactions between spliceosomal components (U2AF and U2 snRNP) and cleavage factors (CF1 and the CPSF complex) are necessary to allow for transcript release following the polyadenylation reaction (Rigo and Martinson, 2009). Cleavage and export are linked. Deposition of cleavage factor 1 (CF1<sub>m68</sub>) promotes nuclear export through interactions

with export factor NXF1/TAP (Ruepp et al., 2009). Further cross-talk has been observed between translation and mRNA decay. Decay can be initiated on mRNAs associated with translating ribosomes (polysomes). This decay is carried out in a specific fashion, first deadenylation, then decapping, and finally 5'→3' exoribonucleolytic decay. This ensures that the last ribosome will complete translation of an intact ORF before the coding sequence is destroyed and indicates a link between the two processes (Hu et al., 2009).

### *1.1.9 mRNP remodeling*

mRNPs are incredibly dynamic complexes that change dramatically as they move through their life cycle acquiring and losing proteins at each step. The proteins which bind an RNA molecule determine nearly everything about it, from how much protein is made to how long the message lasts. The sequence, structure, and modification of the RNA molecule determine what those proteins will be. Several examples of remodeling events are described below.

Removal of the 3'-end cleavage and polyadenylation machinery is necessary for export to the cytoplasm and in yeast is promoted by the export factor Mex67p (Qu et al., 2009). Recent studies have shown that the RNA helicase Dbp5p acts at the cytoplasmic surface of the nuclear pore complex where it is activated by Nup159p (a nuclear pore protein) to promote removal of nuclear RNA-binding proteins from the cytoplasmic-bound mRNA (Noble et al., 2011). Furthermore, translation promotes the removal of PABPN1 and replacement by PABPC1 (Sato and Maquat, 2009). The nuclear cap binding protein CBP80 is removed upon arrival to the cytoplasm by importin-β (Sato and Maquat, 2009). The EJCs deposited by splicing are removed during the first round of translation in the cytoplasm (Maquat, 2004). During mRNA decay, there is significant



remodeling to facilitate access of the mRNA decay enzymes. In the nonsense-mediated mRNA decay pathway (see Section 1.3.2.1) the RNA helicase activity of the UPF1 protein is required to remove bound proteins before the transcript can be degraded (Franks et al., 2010). Association of various RNA-binding proteins with the 3'UTR regulates the translation stability, and localization of the mRNA. Protein-mRNA associations are continually modulated based on external cues which can trigger post-translational modifications, relocalization, chaperone interaction, or protein degradation (Parker and Sheth, 2007; Briata et al., 2005; Vlasova et al., 2008).

#### *1.1.10 mRNA decay*

Once a mature mRNA is no longer needed, perhaps due to a change in growth conditions or activation of cell signaling pathways, it is degraded. The process of degradation is carried out by two classes of ribonucleases. Endoribonucleases which can hydrolyze an RNA molecule internally and exoribonucleases which require a free 5' or 3' end for degradation. In addition, enzymes responsible for degrading the cap structure which exhibit special preference for the 5'-to-5' linkage (pyrophosphohydrolases) are also needed. These aspects of mRNA metabolism are covered in detail below (Section 1.2).

### ***1.2 Gene expression and the role of mRNA decay***

Messenger RNA is a requisite intermediate in the production of proteins and its abundance is an important factor in determining levels of gene expression (Schwanhausser et al., 2011). Abundance for a given mRNA in the cytoplasm is dependent on the balance among its rates of synthesis (transcription), processing (capping, splicing, polyadenylation), export to the cytoplasm, and decay. Recently

mRNA decay has received significant attention and has been shown to play an important role in controlling gene expression. Several groups (Cheadle et al., 2005; Dolken et al., 2008; Miller et al., 2011; Sharova et al., 2009; Rabani et al., 2011) have employed various transcriptome-wide technologies to determine the impact of mRNA stability on overall transcript levels in various cell types and conditions. Their findings vary significantly. One study attributed 50% of the changes in overall transcript abundances to alterations in mRNA decay rates (Cheadle et al., 2005). Another estimate predicted that altered decay is the more significant contributor to changes in message abundance for just 17% of mRNAs (Rabani et al., 2011).

In general, these studies conclude that for some messages there is a good correlation between mRNA stability and abundance. For example very stable “housekeeping” messages will be of relatively high abundance and very unstable mRNAs are often low abundance. There are classes of mRNAs where stability is dynamically regulated and does not necessarily correlate with abundance (Rabani et al., 2011). Such regulated mRNAs tend to encode proteins like transcription factors, cytokines, and mRNA-binding proteins (Mukherjee et al., 2009).

The TNF mRNA represents an excellent example of a transcript whose expression is exquisitely dependent on tightly controlled mRNA decay. In unstimulated immune cells, TNF mRNA abundance is low, and the decay rate is high (Carballo et al., 1998). Lipopolysaccharide (LPS) treatment causes TNF mRNA abundance to increase dramatically, through increased transcription and concomitant down-regulation of mRNA decay. Once the biological response has been elicited, transcription rates drop, and decay accelerates, rapidly returning the TNF mRNA to low levels (Hoffmeyer et al., 1999). When appropriate regulation of TNF mRNA half-life is lost, disease ensues in the

form of rheumatoid arthritis, Crohn's disease and other inflammatory conditions (Kontoyiannis et al., 1999). Thus, regulated mRNA decay allows for dramatic, rapid, and transient changes in gene expression necessary for eliciting a cellular response. Failure to appropriately modulate mRNA decay rates can have serious consequences, as mouse models lacking the RNA-binding proteins needed for modulating decay of specific transcripts have demonstrated (Stumpo et al., 2009; Carballo et al., 1998; Ghosh et al., 2009; Kress et al., 2007).

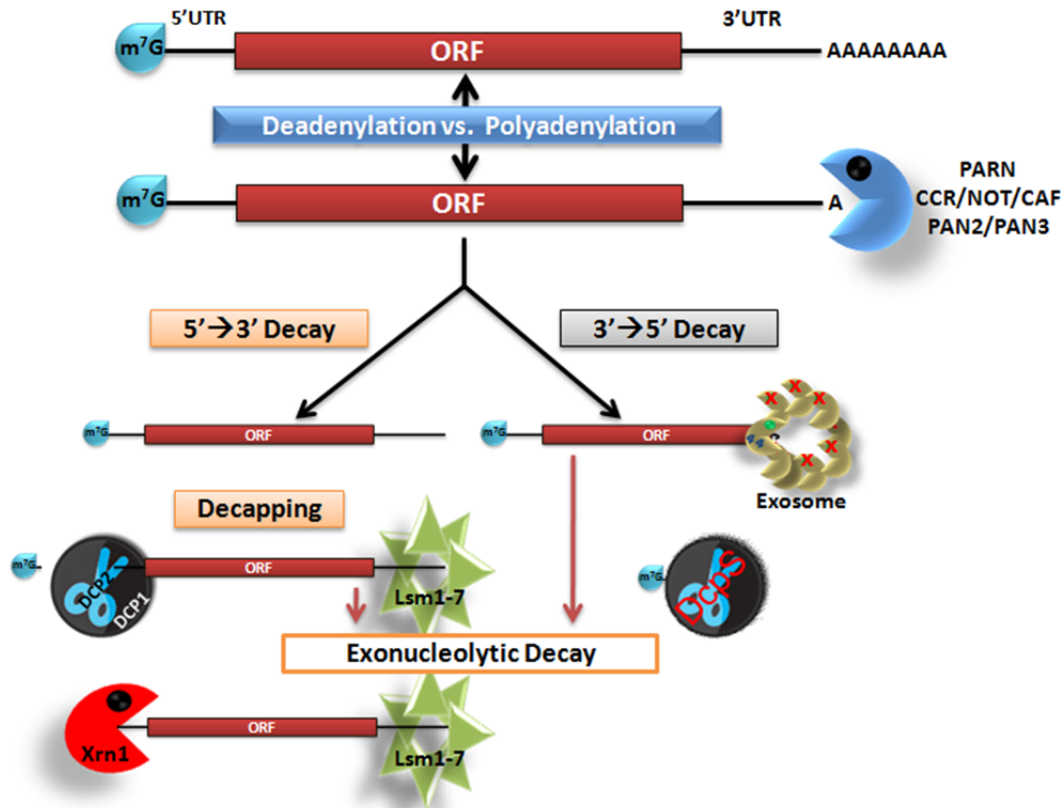
### ***1.3 Mechanisms of mRNA decay***

Decay of mRNAs in the cytoplasm proceeds by two general pathways; the deadenylation-dependent pathway, and the deadenylation-independent (Figure 1). The process of poly(A) tail removal, initiates the deadenylation-dependent decay pathway which is employed for most cellular mRNAs (Garneau et al., 2007). Focus will be given to this primary pathway; however, other pathways will be described briefly to give perspective.

#### ***1.3.1 Deadenylation-dependent decay***

A brief overview of the deadenylation-dependent pathway is given here and followed by detailed information on the specific enzymes and factors required for each step. Deadenylation-dependent decay is unique among decay processes in that the first step is reversible. Poly(A) shortening is generally thought of as a way to destabilize and/or translationally silence a given message. Poly(A) tail lengthening is thought to have the opposite effect, increasing message stability and translatability. CCR4/NOT, PAN2/PAN3, and PARN are the best characterized of the many eukaryotic deadenylases that can shorten the poly(A) tail (Goldstrohm and Wickens, 2008).

Figure 1.



**The primary mRNA decay pathway.** The majority of cellular mRNAs are decayed in a deadenylation-dependent manner. In this pathway, poly(A) tail removal is the first, and rate-limiting step of message decay. This step is uniquely reversible and represents a key regulatory point for control of gene expression. The subsequent decay of the body of the transcript proceeds by 5'→3' and/or 3'→5' decay. 5'→3' decay relies association of the LSM1-7 complex and recruitment of the decapping enzyme DCP1/2 followed by exoribonucleolytic decay by XRN1. 3'→5' decay is carried out by the RRP44 subunit of the exosome, and subsequent cap destruction by the scavenger decapping enzyme DCPS.

Following deadenylation, transcripts can be degraded in both directions, 5'→3' and/or 3'→5'. In 5'→3' decay the LSM1-7 complex associates with the 3' end of the mRNA and facilitates decapping by DCP1/DCP2 (Tharun et al., 2000). Once the cap has been removed, the transcript is susceptible to degradation by XRN1, which recognizes the 5'-monophosphate. The 3'→5' decay pathway is mediated by the exosome, a 10-subunit complex (in mammals) containing one subunit, RRP44, with both 3'→5' exoribonuclease

and endoribonuclease activity (Schaeffer et al., 2009). The remaining cap is recycled by the scavenging enzyme DCPS (Liu et al., 2002).

#### *1.3.1.1 Deadenylation*

Removal of the poly(A) tail is catalyzed by one or more of a family of enzymes termed deadenylases. Eukaryotic cells encode many deadenylases; 10 are predicted for humans. Thus far these enzymes fall into two categories based on the composition of their nuclease domains. The DEDD-type nucleases contain conserved aspartic and glutamic acid residues responsible for coordination of the  $Mg^{2+}$  ion needed for catalysis. CAF1/CNOT7/POP2, PAN2, and PARN deadenylases fall into this group. The second category is the Endonuclease-Exonuclease Phosphatases (EEP) which have conserved aspartic acid and histidine residues in their active site for  $Mg^{2+}$  coordination. CCR4, Nocturnin, Angel, and 2' Phosphodiesterase enzymes are EEPs. The action of these deadenylases can be directly opposed by poly(A) polymerases (Goldstrohm and Wickens, 2008).

##### *1.3.1.1.1 PARN*

PARN is unique in that it is a cap-dependent deadenylase, meaning it deadenylates capped transcripts more efficiently than uncapped (Dehlin et al., 2000; Gao et al., 2000). It is also inhibited by cap-binding proteins (Gao et al., 2001; Balatsos et al., 2006). PARN has a cap-binding pocket and functions as a homodimer (Wu et al., 2009). One monomer binds the cap, while the other degrades the tail. Due to this feature deadenylation by PARN is inhibited by the cap-binding protein CBP80 (Balatsos et al., 2006). It is also inhibited by the Poly(A) Binding Protein PABPC1 (Korner and Wahle, 1997). Furthermore, PARN is the predominant active deadenylase in cytoplasmic extracts derived from tissue culture cells (Gao et al., 2000). Knock-out of the PARN gene

in *Arabidopsis*, an organism with 26 predicted deadenylases, is lethal at the embryo stage (Reverdatto et al., 2004). An additional PARN-related gene, PARN-Like (PNLDC1) is also present in mammals, but has not been characterized.

The best characterized biological role for PARN is in regulating maternal mRNA expression during oocyte maturation. In *Xenopus* oocytes, PARN is required to keep maternally supplied mRNAs such as cyclin B1, Eg-5, and c-mos translationally silent (Kim and Richter, 2006; Paillard et al., 1998). Briefly, Cytoplasmic Polyadenylation Element Binding protein (CPEB) binds to an UUUUAAU motif in the Cyclin B1 3'UTR and forms a complex with GLD2, (a poly(A) polymerase) and PARN. Initially, PARN activity is dominant, the poly(A) tail of cyclin B1 is kept short, and translation is inhibited. Upon maturation of the oocyte, CPEB is phosphorylated, causing PARN to be expelled from the complex, GLD2 then polyadenylates the Cyclin B1 message and translation occurs to allow for cell division (Kim and Richter, 2006).

PARN also plays a role in the nucleus. In response to UV-induced DNA damage, nuclear PARN is activated to prevent the accumulation of aberrant mRNAs. This process is mediated by the 50kDa subunit of Cleavage Stimulation Factor 50 (CSTF50) and the tumor suppressor BARD1. CSTF50 and PARN form a complex which inhibits 3' end formation of erroneous transcripts. Additionally, CSTF50/BARD1 alleviates the inhibition that CBP80 exerts on PARN. This promotes deadenylation and RNA decay (Cevher et al., 2010). Under similar DNA-damaging conditions the MK-2 kinase phosphorylates PARN in the cytoplasm resulting in stabilization of the Gadd45 $\alpha$  mRNA whose gene product is necessary for cell cycle arrest to allow sufficient time for DNA repair to occur (Reinhardt et al., 2010). In addition, PARN is recruited by RNA-binding proteins including

CUGBP1 (Moraes et al., 2006), KSRP (Gherzi et al., 2004), and RHAU (Tran et al., 2004) for poly(A) tail removal.

To summarize, PARN is essential in plants (Reverdatto et al., 2004), and is important for regulation of translation of maternal mRNAs in vertebrates (Copeland and Wormington, 2001). The protein plays a general role in nuclear RNA surveillance following DNA damage (Cevher et al., 2010; Reinhardt et al., 2010). Lastly, PARN also has been shown to impact the stability of at least one mRNA important for cell cycle regulation following genotoxic stress (Reinhardt et al., 2010). Taken together, these findings indicate PARN function is important for control of cell division in higher eukaryotes. Genetic studies are lacking as PARN is absent from yeast and *Drosophila* and there is no knockout mouse thus less is known about PARN function compared with some other deadenylases.

#### 1.3.1.1.2 *The CCR4/NOT complex*

In *S. cerevisiae*, genetic studies have revealed that the CCR4/NOT complex is the primary cytoplasmic deadenylase (Yamashita et al., 2005). In humans, this complex of proteins is very large (0.9-2.0 MDa; Bartlam and Yamamoto, 2010), consisting of the scaffold NOT proteins (CNOT1-5) along with CAF130 and CAF40, as well as the deadenylases (in humans) CNOT6 (CCR4a), CNOT6L (CCR4b), CNOT7 (CAF1) and CNOT8 (CAF2/POP2), which are homologues of the yeast proteins Ccr4p and Caf1p. Current models assert that CCR4/NOT complexes associate with mRNAs by interactions with other proteins. One interacting complex is Tob, which is known to have antiproliferative activities (Bartlam and Yamamoto, 2010). It appears that the association is mediated by mutually hydrophobic regions found on CNOT7 and Tob. In addition, Tob

also associates with PABPC1 and this mutual association with PABPC1 and CCR4/NOT serves to target the deadenylase to its substrate.

Recent reports indicate that the CNOT proteins also promote deadenylation guided by microRNAs (miRNAs). This activity is mediated by direct recruitment of the deadenylase complex to the targeted mRNA by the protein GW182, a subunit of the RNA Induced Silencing Complex (RISC; Chen et al., 2009; Fabian et al., 2009).

Recently, Tristetraprolin (TTP) was shown to recruit the deadenylase CNOT7/CAF1 through mutual associations with the scaffold protein CNOT1. This triggered poly(A) tail removal of an AU-rich element (ARE) containing reporter RNA (Sandler et al., 2011). Work with TTP has also shown that recruitment of cNOT7 is inhibited by TTP phosphorylation upon activation of the p38/MAPK pathway (Marchese et al., 2010). Deadenylation by cNOT7 can be mediated directly through PABPC1 interactions. Eukaryotic Release Factor 3 (eRF3) interacts with both PABPC1 and CNOT7. At translation termination, the mutual associations between eRF3, PABPC1, and CNOT7 facilitate transfer of the message to the deadenylase for poly(A) tail removal (Funakoshi et al., 2007).

#### *1.3.1.1.3 PAN2/PAN3*

Poly(A) Nuclease, PAN2/PAN3, is dependent on PABPC1 being associated with the poly(A) tail. As such, current models have it catalyzing the initial shortening of the poly(A) tail from 200 to ~80 residues (Yamashita et al., 2005). Interestingly, PAN2/PAN3 also deadenylates transcripts following translation termination. In a similar mechanism to that described above for CNOT7/CAF1, mutual associations between PAN2/PAN3, PABPC1, and eRF3 facilitated the hand-off from the translation machinery to the



deadenylation machinery through PABPC1 (Funakoshi et al., 2007). In this way, PABPC1, functions as a destabilizing factor.

### *1.3.2 Deadenylation-independent decay pathways*

Deadenylation-independent decay pathways have two unifying themes. First, by definition they do not rely on poly(A) tail removal. Second, the primary endoribonucleolytic cleavage event permanently inactivates the mRNA. These pathways target both normal and aberrant transcripts and are reviewed in detail elsewhere (Garneau et al., 2007).

#### *1.3.2.1 Decay of aberrant mRNAs*

Decay pathways for mRNAs which contain errors that disrupt appropriate ribosome travel have been classified based on the particular defect found in the transcript; nonsense-mediated, non-stop, and no-go decay. Nonsense-mediated decay (NMD) occurs when the ribosome encounters a premature termination codon (PTC). The PTC is detected due to inappropriate mRNP conformation; either prolonged association of the EJC with the transcript, or excessive distance between the stop codon and poly(A) tail (Isken and Maquat, 2007). NMD can trigger an endoribonucleolytic cleavage, (Huntzinger et al., 2008) or deadenylation-dependent decay (Lejeune et al., 2003). In a complex series of events, the stalled ribosome triggers phosphorylation of the UPF1 helicase which initiates disassembly of the aberrant mRNP. This results in recruitment of deadenylases, the decapping enzyme, and exonucleases to destroy the aberrant message (Franks et al., 2010).

Non-stop decay is initiated when a message lacks a stop codon and the ribosome continues to translate to the 3' terminal of the transcript. Upon reaching the 3'

end of a “broken” mRNA the ribosome stalls, the SKI7 protein which resembles eRF-3, binds to the A-site along with the exosome. The ribosome is released and the message is decayed (Garneau et al., 2007).

No-go decay also results from a stalled ribosome. In this case stalling is caused by strong secondary structure in the mRNA coding sequence. This halted ribosome triggers endoribonucleolytic cleavage by the DOM34 protein in yeast. Cleavage is followed by rapid degradation of the unprotected 5' and 3' fragments (Passos et al., 2009).

#### *1.3.2.2 Endoribonucleolytic decay*

One example of an endoribonucleolytic cleavage occurs during mitosis. Upon completion of cell division many of the cyclin mRNAs must be destroyed. The RNase MRP is a nucleolar localized RNA-protein complex, which initiates decay of the cyclin B2 mRNA by endoribonucleolytic cleavage (Gill et al., 2004). Recent reports indicate that RNase MRP gains access to cytoplasmic mRNAs during nuclear envelope breakdown (Schneider et al., 2010). In another example, the role of the endoribonuclease L (RNase L) in muscle differentiation is quite dramatic. RNase L regulates stability of the MyoD mRNA, and other mRNAs that encode factors which regulate pluripotency. Over-expression of RNase L inhibited muscle differentiation and promoted conversion to adipocytes (Salehzada et al., 2009).

#### *1.3.2.3 miRNA-mediated decay*

miRNAs have garnered an enormous amount of attention in recent years for their ability to post-transcriptionally regulate gene expression (Bartel and Chen, 2004). This is in part due to their ubiquitous nature, and the potential for a single miRNA to

coordinately regulate many mRNA targets. miRNAs are short ~21 base RNA molecules, which are bound by RISC (Shruti et al., 2011). They use the associated RNA molecule (miRNA) as a guide and the Ago2 protein to carry out the endoribonucleolytic cleavage. It appears though that another primary mode of miRNA-initiated decay is through GW182 (a component of RISC) recruiting the deadenylation machinery by interaction with PAN2/PAN3 and CCR4/CAF1 deadenylases (Chen et al., 2009).

### 1.3.3 5'-to-3' Decay

Following poly(A) tail removal, or endoribonucleolytic cleavage, 5'→3' decay proceeds enzymatically by two basic steps. The first step is removal of the 7-methylguanosine cap structure at the 5' end. This is a critical step as it commits the transcript to destruction and is regulated by several enhancer and repressor proteins. The catalysis is carried out by some members of a super-family of proteins called Nudix proteins. They catalyze the hydrolysis of a diphosphate linkage attached to a larger molecule. There are 22 of these Nudix proteins present in mammals. Two have been verified as decapping enzymes: Dcp2 and Nudt16 (Song et al., 2010).

In yeast, enhancers of decapping (Edc1 and Edc2) have been shown to bind RNA, and through interactions with Dcp1, bridge the enzymatic subunit Dcp2 to its substrate. These interactions increase rates of decapping 1000 fold (Borja et al., 2011). Not surprisingly, decapping is linked to other aspects of mRNA regulation. The yeast proteins Pat1p and Dhh1p enhance decapping and repress translation. Interestingly these proteins do this not only by recruiting the decapping enzyme Dcp1p, but also by recruiting the yeast deadenylase Pop2p (CAF1; Collier and Parker, 2005; Collier et al., 2001). This may serve to coordinate the decay of a message with translational arrest.

There are many other proteins whose association has been shown to promote decapping. Following deadenylation, the heptameric Lsm1-7p complex associates with the 3' end of mRNAs, which promotes decapping and subsequent decay (Tharun et al., 2000). In metazoans the protein HEDLS/EDC4 (Human enhancer of decapping large subunit) associates with and stimulates the activity of the decapping complex (DCP1/DCP2; Simon et al., 2006). Furthermore, EDC3 has been shown to mediate interactions between GW182 of the RISC machinery and the decapping factors, providing a link between miRNA-mediated mRNA regulation and decay (Franks and Lykke-Andersen, 2008). Following decapping, the final step is hydrolysis of the remaining RNA body by the 5'→3' exoribonuclease XRN1.

#### 1.3.4 3'-to-5' Decay

Once the poly(A) tail has been removed 3'→5' decay proceeds via the 3'→5' exoribonuclease called the exosome. The exosome is a 10-subunit protein complex that has endo- (Schaeffer et al., 2009) and exoribonucleolytic activities (Gatfield and Izaurralde, 2004). In yeast, the catalytically active subunit is Rrp44 (contains an RNase II domain) in the cytoplasm and Rrp44 and Rrp6 in the nucleus. Studies in yeast have demonstrated that one function of the nuclear exosome is as a quality-control enzyme in conjunction with the nuclear TRAMP complex (LaCava et al., 2005). In mammalian cells the exosome is also important for promoting decay of ARE-containing messages (Chen et al., 2001; Mukherjee et al., 2002), as well as for NMD (van Dijk et al., 2007). Transcriptome-wide studies in *Drosophila* indicate that 25% of exosome substrates contain premature stop codons (Kiss and Andrusis, 2010). Following completion of 3'→5' decay the remaining cap structure is degraded by the scavenger decapping enzyme DCPS.

### 1.3.5 Sites of mRNA decay

Production of high-quality antibodies that recognize proteins which carry out RNA decay along with advances in fluorescence microscopy have allowed scientists to “see” where mRNA decay factors localize. Of the many RNA/protein bodies recorded two have gained significant attention within the mRNA turnover field, namely processing bodies (P-bodies) and stress granules (SGs). P-bodies are cytoplasmic RNA-containing granules which are characterized in mammalian cells by the presence of the AGO1 protein, in addition to the DCP1, XRN1, and LSM proteins (Spector, 2006). P-bodies are hypothesized to be dynamic structures where mRNAs reside when translationally silent, stored, and decayed (Parker and Sheth, 2007). Evidence suggests it's a two-way street and mRNAs also traffic from P-bodies back to polysomes (Brenques et al., 2005). However, P-bodies are yet to be biochemically purified and recent data indicates that mRNA decapping can occur on polysomes (Hu et al., 2009; Hu et al., 2010). As such P-bodies are thought to be sites where mRNAs are stored and sorted during stress conditions requiring bulk movement of RNAs from ribosomes to the decay machinery (Parker and Sheth, 2007). Stress granules (SGs) are also ribonucleoprotein foci which are induced by heat shock and oxidative stressors. They contain mRNAs associated with the small 40S subunit of the ribosome, eIF-3 and other initiation factors. SGs are also thought to result when the macromolecular processing machinery of the cell is overwhelmed, as they are induced by heat-shock and oxidative stress. There is some dynamic exchange of proteins and mRNAs between the P-bodies and SGs indicating a functional relatedness (Balagopal and Parker, 2009).

## **1.4 *Cis-acting determinants of mRNA stability***

Message decay, like transcription, is a highly regulated process. The primary sequence within a given message contains a great deal of information beyond encoding a polypeptide. *Cis-acting* elements are primary sequences which direct interaction of the mRNA with specific proteins and/or miRNAs. These *cis-acting* elements, and the factors they recruit, regulate every step in the life cycle of an mRNA from processing to decay. Sequences that specifically regulate mRNA decay can be found in the 5' and 3' UTRs and the coding sequence (CDS). The majority of these elements described to date are found in the 3'UTR. This is likely for two simple reasons: (1) the 3'UTR has less restriction on length and structure than the 5'UTR, as ribosomes do not have to traverse it, and (2) factors which associate in the CDS or 5'UTR would be displaced with each passing ribosome. Based on the factors they recruit, *cis-acting* elements influence mRNA decay rates (Misquitta et al., 2001).

### **1.4.1 *The cap and poly(A) tail***

The two most ubiquitous determinants of mRNA stability are the 5' cap and the 3' poly(A) tail. All cellular mRNAs have a 5' cap structure. Nearly, all mRNAs have a 3' poly(A) tail, the exception being some histone mRNAs which have a 3' stem-loop structure that fulfills a similar role (Williams and Marzluff, 1995). These features are important as their presence serves as a binding platform for the cytoplasmic cap and poly(A) binding proteins, eIF-4E and PABPC1 respectively. The presence of these proteins is important for promoting translation, and associating with decay enzymes.

### 1.4.2 3'UTR regulatory elements

The 3' UTR is generally the first place one looks for sequence elements which regulate the life span of an mRNA. The best characterized instability elements are AU-rich elements, GU-rich elements, and UGUA motifs, all which recruit RNA-binding proteins. In addition, the presence of miRNA target sites modulates stability. *Cis*-acting elements are context-dependent. The mere presence of a destabilizing element does not mean a message will be unstable. Other factors influence the efficacy of the element such as cellular conditions, RNA secondary structure, mRNP conformation, and the presence of other elements within the transcript.

#### 1.4.2.1 AU-rich elements

One of the best characterized mRNA stability elements in the 3'UTR are the AU-rich elements (AREs) which interact with a plethora of *trans*-acting factors including Tristetraprolin (TTP/ZFP36) and the related BRF1/ZFP36L1 and BRF2/ZFP36L2 (Carballo et al., 1998), AU-rich binding factor (AUF1; Zhang et al., 1993), embryonic lethal abnormal vision like protein, HuR/ELAVL1 (Ma et al., 1996), KH-type splicing regulatory protein (KSRP; Gherzi et al., 2004), and CUGBP1 (CELF1; Moraes et al., 2006). It has been estimated that AREs are present in 5-8% of human transcripts (Bakheet et al., 2006). AREs were subdivided into three classes based on the arrangement of canonical AUUUA pentamers (Wilusz et al., 2001). Class I AREs contain one pentamer flanked by U-rich sequences. Class II contains multiple tandem repeats of the pentamer motif. Class III AREs are generally U-rich and lack AUUUA pentamers (Peng et al., 1996), and in some cases may be GREs (see below). AREs are commonly found in the 3'UTRs of cytokine, growth factor, and transcription factor mRNAs (Caput et al., 1986) where they mediate large changes in expression in response to specific

stimuli. The TNF ARE is an excellent example of the potency of AREs in modulating gene expression. The ARE is absolutely essential for stabilization, decay, and translational de-repression of the TNF mRNA in response to cellular stimuli (Kontoyiannis et al., 1999).

#### *1.4.2.2 GU-rich elements*

In addition to the ARE, *cis*-acting elements called GREs (GU-rich elements) were recently identified (Vlasova et al., 2008). GREs were originally defined as UGUUUGU repeats (Vlasova et al., 2008), but during the course of our study UG-repeats were included in this class (Rattenbacher et al., 2010). GREs are instability elements very similar to AREs. The principle differences are in the proteins which associate with the two types of elements. GREs specifically interact with the RNA-binding protein CUGBP1 (CELF1; Lee et al., 2010; Rattenbacher et al., 2010; Vlasova et al., 2008). HuR has affinity for these types of sequences as well (Lopez et al., 2004). GREs are commonly found in mRNAs encoding transcription factors as well as cytokines (GREs and AREs can often be found on common mRNAs). It is very likely that other uncharacterized proteins also interact with GREs to modulate mRNA metabolism.

#### *1.4.2.3 UGUA elements*

The UGUA element also confers instability to mRNAs through association with RNA-binding proteins in the Pumilio family. Like AREs and GREs, UGUA elements are found on transcription factor, cytokine, and cyclin mRNAs (Morris et al., 2008). These three, AREs, GREs, and UGUA elements, are commonly thought of as instability elements, but this function can be reversed when a stability factor like HuR associates with them (Lopez et al., 2004).



#### 1.4.2.4 miRNA-binding sites

Another class of instability elements commonly found in the 3'UTR are miRNA target sites. These show sequence specificity on a case by case basis for the specific miRNA-mRNA target pair. From the standpoint of the miRNA, the most important region for determining interactions is the 7 base seed sequence at positions 2-8. Efficacy is enhanced by adjacent miRNA target sites, AU-richness near the target, proximity to the stop codon (>15 bases away), and not being in the middle of a long 3'UTR (Grimson et al., 2007). Regulation of gene expression by miRNAs is important in development and in adult tissues (Williams et al., 2009). miRNAs regulate gene expression through translational repression (Wu and Belasco, 2008), endoribonucleolytic cleavage by the AGO2 protein (Yekta et al., 2004), promoting deadenylation (Chen et al., 2009; Fabian et al., 2009), or by translational activation (Vasudevan et al., 2007).

#### 1.5 *Trans-acting factors influence mRNA decay rates*

As mentioned AREs are a regulatory elements that commonly promote instability. Instability is brought about by *trans*-acting factors that recognize primary sequence elements (or secondary structure) within the transcript and promote rapid decay. This is often achieved by recruiting deadenylases followed by rapid poly(A) tail shortening and consequent entry into the mRNA decay pathways (Figure 1). Similarly, RISC-associated miRNAs can bind to mRNAs and either induce endoribonucleolytic cleavage or trigger deadenylation. Tethering experiments have revealed that it is not the *cis*-acting element *per se* that causes stability or instability, but the *trans*-regulatory factors which recognize it (Chou et al., 2006). Thus, the function of the element can be rapidly altered in response to cellular cues that modulate activity of *trans*-acting factors.

### 1.5.1 Destabilizing factors

Destabilizing factors generally exert their effects by directly binding an mRNA substrate, and recruiting (directly or indirectly) components of the decay machinery. They can cause an mRNA to localize to a P-body, sites where decay factors are in close proximity. Finally, destabilizing factors can also displace a stabilizing factor. Each *trans*-acting factor has its own unique mode of action and regulatory mechanisms. Some examples are discussed below.

*AUF1- AU-rich binding factor 1* The AUF1 protein binds to AREs. There are four splice-isoforms of AUF1 (37, 40, 42, and 45kDa) and the best characterized 37kDa isoform mediates instability by binding directly to the exosome (Chen et al., 2001). AUF1 activity can be disrupted by the peptidyl-prolyl isomerase PIN1. PIN1 action inhibits AUF1 binding and stabilizes ARE-containing mRNAs (Esnault et al., 2006). Recent reports have identified heat shock protein 27 (HSP27) as part of the ARE destabilizing AUF1 complex. Interestingly, activation of the mitogen activated protein kinase (p38/MAPK) pathway causes HSP27 phosphorylation, ubiquitination of AUF1 and its destruction by the proteasome, resulting in stabilization of the ARE-containing TNF mRNA (Knapinska et al., 2011). This mechanism is very similar to that described in previous reports linking HSP70 to AUF1, and its destruction following heat-shock (Laroia et al., 1999).

*TTP-Tristetraprolin* is an RNA-binding protein which exhibits strong preference for AREs (Emmons et al., 2008). TTP is the most studied member of the Tis11 family of RNA-binding proteins, which also includes BRF1 and BRF2. BRF1 has been shown to interact with the decay machinery and promote P-body formation (Franks and Lykke-Andersen, 2007). TTP has extensive interactions with the mRNA decay machinery including DCP1 and 2, XRN1, the CCR4/NOT complex of deadenylases, and the exosome (Lykke-

Andersen and Wagner, 2005). One important target of TTP-mediated regulation is the TNF mRNA. TTP restricts TNF production in resting immune cells, but is phosphorylated in response to LPS stimulation. Phospho-TTP associates with a 14-3-3 chaperone leading to stabilization of the TNF mRNA and a large increase in protein production (Sun et al., 2007). Interactions between TTP and cytokine and growth factor messages are very important as a TTP knockout mouse is embryonic lethal due to failed haematopoiesis (Taylor et al., 1996), and derived knockout cell lines exhibit a tumorigenic phenotype (Sanduja et al., 2010). Finally, the TTP homolog ZFP36L1 is increased during muscle differentiation, further underscoring the importance of these RNA-binding proteins (t Hoen et al., 2011).

*KSRP- KH-type splicing regulatory protein* is also an ARE-binding protein. It confers instability to its bound mRNAs by recruiting the decay factors PARN, DCP2, and the exosome (Chou et al., 2006). KSRP plays an important role in muscle differentiation keeping ARE-containing mRNAs unstable in proliferating myocytes. Upon differentiation, p38/MAPK phosphorylates KSRP, disrupting its RNA-binding activity, and resulting in stabilization of transcripts such as myogenin, p21, and MyoD which encode factors essential for myoblast differentiation (Briata et al., 2005).

KSRP also indirectly influences the expression of many genes. In the nucleus KSRP promotes the biogenesis of a subset of microRNAs by binding to AREs in the primary transcript (pri-miRNA) and promoting processing to mature forms through interactions with the pre-miRNA processing factors Drosha and Dicer (Trabucchi et al., 2009). There appears to be an antagonistic relationship between KSRP and hnRNPA1. The two compete for pri-miRNA-binding and the winner appears to be determined by the levels of each protein. In somatic cells KSRP wins out and miRNAs predominate, in

proliferative cells hnRNPA1 wins out and miRNA biogenesis is suppressed (Michlewski and Caceres, 2010).

*Pumilio* or Pum1 is a member of the Puf family of RNA-binding proteins which recognize UGUA motifs. Pufs are the best characterized RNA-binding proteins from the standpoint of RNA-binding as crystal structures in complex with their substrate RNAs have been solved at high resolution (Wang et al., 2009b). The alpha-helical domain of the protein forms a long half-moon shape where individual bases of the RNA intercalate forming base-stacking interactions between amino acid side-chains. With this information researchers are now constructing sequence specific RNA-binding proteins (Lu et al., 2009). Though their biological roles in yeast and some vertebrates have been well characterized, relatively little is known of Pum function in mammalian cells. In *Xenopus*, Pum2 binds the 3'UTR of the RINGO/SPY mRNA. In this context it also binds the cap, thereby repressing translation by inhibiting association of translation initiation factors (Cao et al., 2010). In general, Pumilio proteins confer instability to their mRNA targets, and cause relocalization to P-bodies (Morris et al., 2008).

*CUGBP1/CELF1* CUG-binding protein 1 (CUGBP1) belongs to a family of six RNA-binding proteins called CELF (CUGBP and ELAV like factors). CELF proteins bind GREs, and AREs, and confer instability on mRNAs they target (Paillard et al., 2002; Mukhopadhyay et al., 2003). CUGBP1 is a major focus of this thesis and will be discussed in detail later (Section 1.12).

*miRNAs* microRNAs are a class of small regulatory RNAs whose influence is exerted by canonical Watson-Crick base pairing, and non-canonical G-U base pairing to mRNA targets. miRNAs are expressed as a primary transcript and processed, or result from processing of intronic sequences (Rodriguez et al., 2004a). The pri-miRNA transcript is

processed in the nucleus by Drosha and DGCR8 to form the pre-miRNA, which is a 60-100nt stem-loop. This is exported to the cytoplasm where Dicer processing trims it down to a 22nt. duplex. Loading of the guide strand into RISC forms the mature complex. Target recognition by miRNAs generally results in inhibition of gene expression by translational repression, or in cases of high sequence complementarity between the miRNA and its target, endoribonucleolytic cleavage or deadenylation and mRNA decay (Grimson et al., 2007).

### *1.5.2 Stabilizing factors*

The binding of stabilizing factors with an mRNA generally promotes translation, and disfavors interaction with the RNA decay machinery. Additionally, their association can cause relocalization, out of P-bodies and onto polysomes (Bhattacharyya et al., 2006). Below are two examples of RNA-binding proteins regarded as stability factors.

*HuR* or Embryonic Lethal Abnormal Vision (ELAV) is the most studied mRNA-binding protein. It has been shown to associate with both AREs and GREs (Yoon et al., 2008; Mukherjee et al., 2011). In general *HuR* binding displaces instability factors to promote stabilization and translation (Fan and Steitz, 1998). Competition by *HuR* for target sites is generally accomplished by translocation from the nucleus to the cytoplasm (Atasoy et al., 1998), or by signaling events which disrupt instability factor binding (Kawai et al., 2006). *HuR* is an essential factor but inducible knockout mice show that it is specifically important for regulation of p53-mediated apoptosis (Ghosh et al., 2009). *HuR* function is critical for stabilizing many mRNAs which harbor AREs and GREs when their encoded factors are needed.

*PCBP Poly(C) Binding Proteins* are also well-characterized stability factors. This protein binds poly(C) tracts in the 3'UTR of mRNAs it regulates. This binding is responsible for stabilizing the  $\alpha$ -globin mRNA, which must be translated throughout the life of an erythrocyte (Kiledjian et al., 1995).

### **1.6 Modulation of mRNA decay rates**

Decay of mRNA molecules is a dynamic process mediated by the proteins and/or miRNAs which associate with each transcript. One way responsiveness is achieved in this system is by modulating the function, abundance, and/or access of regulatory RNA-binding proteins as discussed below.

*Regulation of RBP abundance* This is the most basic method employed to modulate function of RNA-binding proteins. Several examples exist, for instance the RNA-binding protein LIN28 is a pluripotency marker expressed in embryonic stem (ES) cells. This protein is responsible for keeping the expression of differentiation promoting miRNAs, including let7a, very low as such it is highly expressed in ES cells, but drops dramatically as distinct cell types arise (Viswanathan et al., 2008). In addition, production of miRNA let7a is inhibited by the RNA-binding protein hnRNPA1, and promoted by KSRP binding. The levels of hnRNPA1 and KSRP correlate with the amount of mature let7a produced in various tissue types (Michlewski and Caceres, 2010). Expression of the ARE-binding protein TTP is induced by growth factors, insulin, and the phorbol-ester TPA. Upon induction TTP can promote the rapid decay of ARE-containing transcripts by association with deadenylases (Sanduja et al., 2010). Finally, AUF1 abundance can be down-regulated by ubiquitination and proteasomal degradation upon activation of the p38/MAPK pathway, stabilizing ARE-containing reporter RNAs (Laroia et al., 1999).

*Localization* This is perhaps the most dramatic from a visual standpoint. Common cellular conditions where RBPs rapidly relocalize include during muscle formation (Lal et al., 2004), viral infection (Sokoloski et al., 2010), and T-cell stimulation (Atasoy et al., 1998). In all of these instances the RNA stability factor HuR can be visualized translocating from the nucleus to the cytoplasm where it stabilizes mRNAs for increased protein production. In addition, activation of the p38/MAPK pathway results in TTP phosphorylation, and association with 14-3-3. This excludes TTP from stress granules, and results in stabilization of ARE containing mRNAs (Stoecklin et al., 2004).

*Phosphorylation/other post-translational modifications* Post-translational modifications are an effective, reversible, and rapid way to modulate activity of RNA-binding proteins. Phosphorylation of TTP reduces both its affinity for RNA substrates and its ability to interact with the decay machinery (Sanduja et al., 2010). Similarly, reduction of eIF-4E phosphorylation triggered by nutrient deprivation reduces its affinity for the cap and consequently promotes deadenylation by PARN (Seal et al., 2005). Activation of the PI<sub>3</sub>-Kinase/AKT pathway triggers KSRP phosphorylation reducing its ability to bind the exosome and stabilizing  $\beta$ -catenin mRNA (Gherzi et al., 2006). Finally, perhaps the most intuitive modification is ubiquitination (which causes proteasomal mediated degradation of the RNA-binding protein itself) as mentioned above for AUF1 promoting cytokine expression (Laroia et al., 1999).

*Chaperone interactions* A final way in which the function of RNA-binding proteins appears to be regulated is through interaction with other proteins. These chaperones can remove an RBP from its substrate or prevent it from recruiting decay factors (as was the case with TTP and 14-3-3). This type of interaction, along with phosphorylation, can also be used to expel a deadenylase from a complex as is the case for PARN in oocytes

(Kim and Richter, 2006). A final example, isomerization by a prolyl-isomerase reduces the affinity of AUF1 for an ARE-containing mRNA promoting HuR association and protein expression (Esnault et al., 2006).

### **1.7 Competition between *trans-acting* factors**

ARE-mediated instability can be dramatically reversed by external cues, like infection or altered growth conditions, which require changes in gene expression. One way this is achieved is through replacement of an instability factor, with a stability factor like HuR. This was observed in stimulated immune cells when HuR moved from the nucleus to the cytoplasm and its movement was closely correlated with increased translation and stability of ARE-containing mRNAs (Atasoy et al., 1998). Another mechanism is by post-translational modification of the instability factor, commonly phosphorylation, resulting in abrogation of its activity. Phosphorylation of *trans-acting* factors has been reported upon activation of the p38/MAPK, and AKT/PI<sub>3</sub> pathways (Lal et al., 2004; Li et al., 2000). Another instance of this comes from differentiating muscle. In this example, nuclear HuR and AUF1 were found on common mRNAs. However, upon reaching the cytoplasm, association of HuR with the cyclin dependent kinase 1A (CDKN1A/p21) mRNA increased as differentiation progressed, and association of AUF1 decreased, promoting translation of the message and cell differentiation (Lal et al., 2004).

### **1.8 Muscle biology**

Muscle is a unique tissue type. By mass, it is the most abundant tissue in the body, and its ability to coordinately contract and relax upon membrane depolarization and polarization allows for movement, breathing, and digestion amongst higher



organisms. Calcium ( $\text{Ca}^{2+}$ ) signaling is central to muscle contraction and stretching, and many of the transcriptional programs in muscle are influenced by  $\text{Ca}^{2+}$  signaling (Berridge et al., 2003).  $\text{Ca}^{2+}$ /Calmodulin Kinase signaling promotes nuclear export of repressive histone deacetylases, allowing for transcription of Myocyte Enhancer Factor-2 (MEF2) regulated genes (McKinsey et al., 2002). MEF2 pairs with the transcription factor MyoD to activate many muscle specific genes (Black and Olson, 1998).

Muscle does more than move. It is sensitive to signaling molecules like insulin and cytokines. Treatment of muscle with insulin causes uptake of glucose for energy metabolism (Kewalramani et al., 2010). Muscle produces low levels of TNF for para/autocrine signaling (Li and Reid, 2001). Exposure of myoblasts to low levels of the cytokine TNF promotes myogenesis by activation of the p38/MAPK pathway, whereas high levels inhibit myogenesis (Chen et al., 2007). Chronic exposure to high TNF levels causes muscle wasting (Flores et al., 1989) and insulin resistance (Li and Reid, 2001).

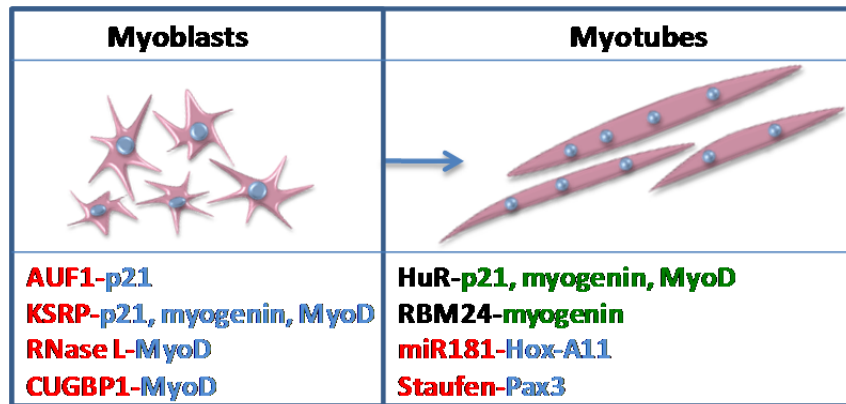
### **1.9 Muscle differentiation**

During development some mesodermal cells will go on to become muscle tissue. This developmental process has been correlated with expression of muscle-specific transcription factors; MyoD, Myf5, and Pax3. Expression of these factors results in conversion of pluripotent cells into myoblasts. Myoblasts can then fuse to become multinucleate myotubes by reduced growth factor stimulation, and/or activation of the p38/MAPK signaling pathway, followed by expression of the transcription factors myogenin and MEF2 (for review see; Molkenin and Olson, 1996). Differentiation is also coupled with the expression of p21 which promotes cell cycle withdrawal (Parker et al., 1995). Early myotubes mature through expression of the transcription factor MRF4 coincident with innervation (Patapoutian et al., 1995). The murine C2C12 myoblast

model has been useful for studying a portion of the differentiation process, as they are proliferative myoblasts that become differentiated myotubes upon serum withdrawal (Blau et al., 1983).

Importantly, muscle has the ability to regenerate. Upon injury, myogenic satellite cells differentiate to myoblasts, and fuse to form myotubes, adjacent myotubes then fuse to form a myofiber. Chronic conditions of muscle injury indicate that depletion of satellite cells has dire consequences (Briata et al., 2005; Wagers and Conboy, 2005).

**Figure 2.**



**Muscle differentiation requires post-transcriptional gene regulation.** Efficient differentiation of myoblasts to myotubes requires dynamic changes in message stability. Shown are destabilizing factors (red), with their corresponding unstable target mRNAs (blue), and stabilizing factors (black) with their stabilized target mRNAs (green).

### **1.10 Role of mRNA decay during muscle differentiation**

The process of muscle differentiation is one that requires dynamic and concerted regulation of gene expression at the post-transcriptional level (Figure 2; Bisbal et al., 2000; Figueroa et al., 2003; Jin et al., 2010; Naguibneva et al., 2007; Briata et al., 2005; Gong et al., 2009). The onset of muscle differentiation is marked by increases in the

abundance of the muscle specific transcription factors MyoD and myogenin mediated in part through post-transcriptional mechanisms (Figuroa et al., 2003). RNase L activity must drop for expression of MyoD (Bisbal et al., 2000). HuR must relocalize transiently from the nucleus to the cytoplasm where it displaces AUF1 (Lal et al., 2004) to stabilize p21, myogenin, and MyoD mRNAs (Figuroa et al., 2003). RBM24 binds to and promotes the stability of the myogenin mRNA (Jin et al., 2010). MiR181 levels increase to down-regulate the proliferation-promoting HoxA11 mRNA (Naguibneva et al., 2007). Phosphorylation of KSRP by p38 disrupts binding to ARE-containing mRNAs promoting the stability of pro-myogenic mRNAs (Briata et al., 2005). Finally, the levels of RNA-binding protein Staufen increase, promoting decay of the Pax3 mRNA and favoring differentiation (Gong et al., 2009). Altered mRNA decay rates and increases in the mRNAs which encode transcription factors result in production of many muscle specific transcripts. Indeed, exogenous expression of MyoD is sufficient to convert fibroblasts into myoblasts (Davis et al., 1987). Additionally, miRNAs have a crucial role to play in the regulation of gene expression in muscle for proper tissue function (Kalsotra et al., 2010; Naguibneva et al., 2007). These findings highlight the importance of modulating mRNA decay in muscle differentiation. mRNA decay is critical for more than just keeping the abundance of certain messages low. Altering the stability of low abundance messages permits a burst of gene expression observed in muscle differentiation.

### **1.11 Myotonic Dystrophy (DM)**

The myotonic dystrophies are dominant heritable neuromuscular diseases, caused by microsatellite repeat expansions in the non-coding region of the affected gene. DM1 is caused by CTG repeat expansion in the 3'UTR of the *dystrophia myotonica* protein kinase (DMPK) mRNA (Buxton et al., 1992), while DM2 results from a

CCTG repeat expansion in intron 1 of the ZNF9 mRNA (Mankodi et al., 2003). DM is the most common form of adult onset muscular dystrophy affecting 1 in 8,000 individuals (Harper et al., 2001). The disease state has been strongly correlated with the production of toxic RNA molecules. As both DM1 and DM2 repeat expansions lie in untranslated regions of mRNAs they affect protein function only minimally (Lee and Cooper, 2009). Here we will focus on DM1, as aberrant CUGBP1 expression is a clear contributor to pathogenesis in DM1 (Kuyumcu-Martinez et al., 2007) whereas it's role, if any, in DM2 is unclear (Margolis et al., 2006).

#### *1.11.1 Disease symptoms*

Symptoms of DM1 include myotonia (the ability to contract but not relax a muscle), insulin resistance (failure of muscle tissue to take up glucose in response to insulin), cardiac conduction defects (failure to coordinate an action potential through the cardiac tissue in an efficient manner), muscle wasting (reduced muscle tissue volume and increased protein catabolism of skeletal muscle), and cataracts (clouding of the lens of the eye; Harper et al., 2001). Congenital DM1 patients exhibit reduced mental capacity and mental retardation in addition to all of the above symptoms, many of which are more severe (Modoni et al., 2004). The congenital form is typically fatal by early adulthood.

#### *1.11.2 Repeat expansion, anticipation, disease severity, and toxic RNA*

DM1, like other repeat expansion diseases, exhibits anticipation, meaning that it tends to get worse with each subsequent generation that harbors the mutation (Harper et al., 2001). This effect is due to repeat expansion in the germline. A grandmother, who experiences mild symptoms such as cataracts late in life, may have few repeats (50-80 CTGs). Her affected child may experience muscle weakness in mid-adulthood and have

100-500 repeats. A grandchild born with congenital DM1 will likely have over 1000 CUG repeats.

Expansion of the CUG repeat in the DMPK 3'UTR beyond 50-100 repeats results in formation of toxic RNA (Musova et al., 2009). Many primary symptoms of the disease result from the presence of the repeat RNA. Analysis by fluorescence microscopy has indicated that the repeat accumulation in nuclear foci containing mRNAs, and that the RNA-binding protein and splicing factor MBNL1 is bound to them (Jiang et al., 2004). This sequesters MBNL1 from its natural mRNA targets, perturbing the antagonistic relationship between CUGBP1 and MBNL1 resulting in many mis-splicing events (Ladd et al., 2001; Philips et al., 1998; Du et al., 2010). The length and context of the CUG repeats, and the abundance of the toxic RNA species are important determinants of disease severity (Logigian et al., 2004).

#### *1.11.3 Phosphorylation and over-expression of CUGBP1 in DM1*

Increased abundance of CUGBP1 in DM1 patient muscle was noted quite soon after identification of the DMPK gene (Philips et al., 1998). However the mechanisms behind over-expression are only now coming to light. Expression of repeat RNA results in elevated Protein Kinase C (PKC) activity through an uncharacterized pathway (Kuyumcu-Martinez et al., 2007). PKC activation leads to hyperphosphorylation of CUGBP1. One effect of hyperphosphorylation is increased stability of the CUGBP1 protein, leading to its over-expression in the nucleus (Kuyumcu-Martinez et al., 2007). It is of note that to date CUGBP1 over-expression has been observed only in mouse models of DM1 that exhibit the muscle wasting phenotype (Kuyumcu-Martinez et al., 2007; Mahadevan et al., 2006). In one such mouse model, elevated CUGBP1 levels are observed in as little as 6 hours after tamoxifen induction of CUG repeat expression

indicating that in this case CUGBP1 over-expression is a primary effect and not due to long term damage of the muscle (Wang et al., 2007). Moreover, over-expression of CUGBP1 in the absence of repeat-containing toxic RNAs is sufficient on its own to induce many symptoms of DM1 (Ward et al., 2010; Timchenko et al., 2004).

#### *1.11.4 Aberrant splicing regulation by CUGBP1 and MBNL1*

Much effort has been invested in characterizing the nuclear roles of MBNL1 and CUGBP1 with respect to splice site selection in muscle-specific transcripts (Kalsotra et al., 2008; Ladd et al., 2001). Indeed, many observed symptoms of DM1 are likely due to mis-splicing. Documented mis-splicing events include: myotonia (chloride channel 1, intron 2 retention,  $\beta$ -tropomyosin exon 6B inclusion), insulin resistance (insulin receptor exon 11 skipping), and cardiac conduction defects (cardiac troponin T exon 5 inclusion). (Ladd et al., 2001; Charlet et al., 2002; Philips et al., 1998; Kalsotra et al., 2008; Philips et al., 1998; Savkur et al., 2001). In DM1, MBNL1 loss of function and CUGBP1 gain of function are both thought to contribute to splicing changes. Comparisons between CUG-repeat expressing mice and MBNL1 knock-out mice indicate that loss of MBNL1 function is responsible for 80% of the splicing changes in DM1. However, the authors noted that 50% of the mRNA abundance changes are currently inexplicable (Du et al., 2010).

#### *1.11.5 Aberrant translational regulation by CUGBP1 in DM1*

There have been few studies conducted to address the possible roles of altered activity of CUGBP1 from the standpoint of mRNA translation. Studies looking at stress granules found CUGBP1 was a component of them (Fujimura et al., 2008). Further work with purified components of SGs from DM1 patient cells, found evidence for activation of protein kinase R (PKR) and reduction in protein synthesis by phosphorylation of eIF-2

(Huichalaf et al., 2010). These studies indicate that translation may be impacted in by aberrant CUGBP1 function DM1.

#### *1.11.6 Unexplained symptoms of DM1*

Muscle wasting is a common symptom in severe cases of DM1. However, no molecular defect, splicing or otherwise, has been identified to explain the muscle wasting symptom. One study found elevated serum TNF levels in DM1 patients (Mammarella et al., 2002). TNF is known to cause muscle wasting (Flores et al., 1989), is expressed by muscle and its expression is extensively regulated at the level of mRNA stability (Carballo et al., 1998; Garnon et al., 2005; Lai et al., 1999).

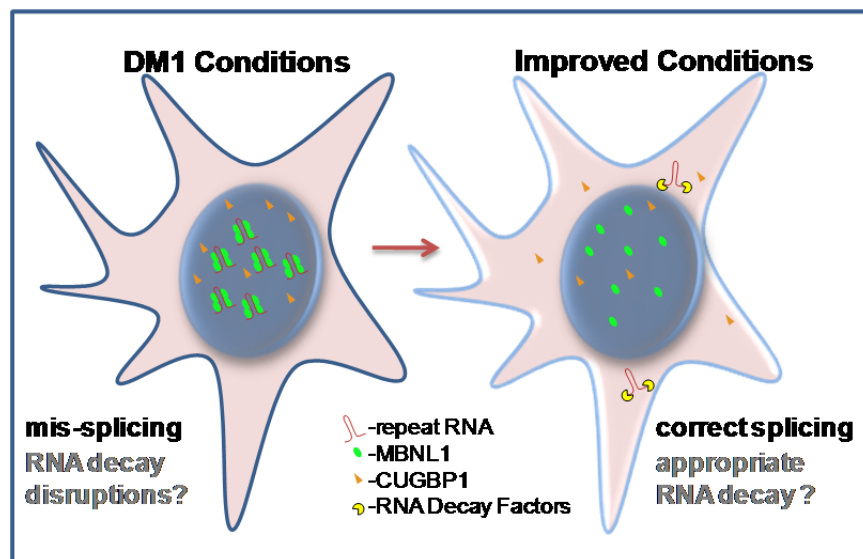
The insulin resistance observed in DM1 patients is often attributed to mis-splicing of the insulin receptor (Savkur et al., 2001). However, this study merely identified a correlation between the mis-splicing event and insulin resistance. Exposure of muscle cells to elevated levels of TNF also causes insulin resistance (Li and Schwartz, 2001). Currently it is unclear which molecular changes are responsible for insulin resistance in DM1 patients.

#### *1.11.7 Modifiers of DM phenotype*

Several DM1 models have been generated in both mice and *Drosophila* and have greatly aided in characterizing the disorder. Interestingly, over-expression of the MBNL1 protein in CUG-repeat expressing mice alleviates the phenotype (Kanadia et al., 2006). These findings have been corroborated in *Drosophila* models of the disease. The muscle wasting phenotype in DM1 flies (express 480 CUG repeats introduced by targeted mutagenesis) worsened in MBNL1-depleted lines, and improved in MBNL1 over-expressing lines (De Haro et al., 2006). Additionally, over-expression of CUGBP1

in DM1 flies further worsened the phenotype (De Haro et al., 2006). DM1 flies also showed improvement in phenotype in conjunction with over-expression of the RNA export factor ALY, consistent with the finding that the repeat-containing mRNAs are less toxic when located in the cytoplasm (Garcia-Lopez et al., 2008). All told, these findings indicate that RNA metabolism and the levels of CUGBP1/MBNL1 are important determinants of disease severity in DM1.

**Figure 3.**



**Defects in RNA metabolism are hallmarks of DM1.** CUG-repeat containing RNA is primarily confined to the nucleus of DM1 cells. MBNL1 is strongly associated with repeats and unable to carry out normal functions including splicing regulation, while nuclear CUGBP1 levels are increased. Disruption of repeat RNA/MBNL1 complexes improves conditions, through correcting splicing, perhaps enhancing decay of repeat containing mRNAs, and returning CUGBP1 to normal function.

### 1.11.8 Therapeutic approaches

Currently there is no therapy or cure for DM1, but mouse models have demonstrated that the effects of toxic CUG RNA are reversible (Mahadevan et al., 2006). Development of therapies is focused on destruction or inactivation of the toxic RNA. One idea is to introduce a morpholino that binds to the CUG-repeat RNA and



releases MBNL1 (and any other sequestered factors ) to carry out its normal function (Figure 3). Attempts at this have been successful at improving phenotype in mouse models, showing a reduction in RNA-foci and corrected splicing defects (Mulders et al., 2009). The biggest challenge with this approach is getting the morpholino into the tissue, and bringing the cost down. As direct targeting of nucleic acids is challenging, one alternative might be treating with PKC inhibitors. These inhibitors correct the CUGBP1-mediated defects, but not the MBNL1-mediated defects (Wang et al., 2009a). A drawback of this approach in humans may be off-target effects. This would likely not correct all the splicing defects, but may alleviate the muscle wasting phenotype. As such, approaches to degrade the toxic RNA are most promising.

### **1.12 CUGBP1**

The *trans*-acting factor of primary interest in this study is the CELF-family protein CUGBP1. CELF proteins are well-characterized regulators of mRNA metabolism (Ladd et al., 2005; Timchenko et al., 2005; Vlasova et al., 2008; Zhang et al., 2008; Goracznik and Gunderson, 2008). The protein has three tandem RNA recognition motifs (RRMs) with RRM2 and RRM3 separated by a linker region (Figure 4). This layout is common for all six proteins of the human CELF family, and is also found in ELAV family members including HuR/ELAVL1. The human CUGBP1 protein was originally identified *in vitro* (HeLa cell lysates) based on its ability to cause a shift in the migration pattern of (CUG)<sub>8</sub> RNA during gel electrophoresis (Timchenko et al., 1996). While the affinity of CUGBP1 for CUG repeats has since been refuted (Marquis et al., 2006; Vlasova et al., 2008), the protein has remained associated with the human disease DM1, as its function is dramatically altered in the presence of CUG repeat containing mRNAs (Kuyumcu-Martinez et al., 2007).

### *1.12.1 RNA-binding properties of CUGBP1*

Based on early studies implicating CUGBP1 in DM1, many have sought to further define the role of CUGBP1 in cells. Firstly, multiple studies have examined the binding preferences of CUGBP1 (Marquis et al., 2006; Vlasova et al., 2008; Graindorge et al., 2008; Mori et al., 2008; Takahashi et al., 2000; Graindorge et al., 2008; Tsuda et al., 2009). Most have found a strong preference for U-rich regions interspersed with G residues. CUGBP1 protein also exhibits strong affinity for UG repeats, primarily by RRM3 association with RNA (Graindorge et al., 2008; Tsuda et al., 2009). Quantitative experiments looking at binding to CUG repeats revealed that the protein has 100-fold lower affinity for them than UG repeats (Mori et al., 2008).

### *1.12.2 Nuclear roles of CUGBP1*

From a molecular standpoint, CUGBP1 has been most thoroughly characterized as a splicing enhancer. CUGBP1 association with pre-mRNAs promotes exon inclusion for a subset of muscle transcripts (Kalsotra et al., 2008). CUGBP1 expression is decreased during muscle development by miRNA targeting the CUGBP1 message (Kalsotra et al., 2010) Reduction in CUGBP1 protein levels in muscle correlated with observed splicing changes in target transcripts that favor expression of adult splice isoforms over embryonic ones. As muscle develops, reduction of CUGBP1 levels favors MBNL1 activity and promotes exon-skipping (Ladd et al., 2001). In addition to modulating alternative splicing events, binding of CUGBP1 to GREs near a viral poly(A) site inhibits cleavage and polyadenylation (Goracznik and Gunderson, 2008).

### 1.12.3 Cytoplasmic roles of CUGBP1

In addition to roles in the nucleus mediating alternative splicing, CUGBP1 has important cytoplasmic functions as detailed below.

#### 1.12.3.1 mRNA Decay

Work with the *Xenopus* homolog of CUGBP1, EDEN-BP, demonstrated that binding of this factor triggered deadenylation of the *c-mos* transcript (Paillard et al., 1998). Similar findings have been made in mammalian systems as well (Graindorge et al., 2008; Moraes et al., 2006; Mori et al., 2008; Rattenbacher et al., 2010; Vlasova et al., 2008). Previous work in the Wilusz lab has demonstrated that CUGBP1 binds to the 3'UTR of the TNF mRNA, where it recruits PARN to initiate poly(A) shortening (Moraes et al., 2006). In support of these findings, array studies conducted in T-cells demonstrated that a significant proportion of regulated mRNAs contained GREs. These GREs bind CUGBP1 and thereby destabilize reporter transcripts in transfected HeLa cells (Vlasova et al., 2008).

#### 1.12.3.2 Translational regulator

Additional reports imply that CUGBP1 associates with the 5'UTR of the C/EBP- $\beta$  mRNA and enhances translation initiation by recruiting initiation factors (Timchenko et al., 2005), as well as modulating translational start site selection (Timchenko et al., 1999). Under certain conditions CUGBP1 is associated with translationally repressive stress granules (Fujimura et al., 2008). In support of a repressive role in translational control, the *Drosophila* CUGBP1 homologue, Bruno inhibits translation of the *oskar* mRNA in oocytes through association with the 3'UTR. Repression was achieved by two mechanisms, first by binding Cup, an eIF-4E binding protein that represses 40S subunit

joining. Secondly, in the absence of Cup, Bruno was capable of mediating mRNA oligomerization of large translationally repressed complexes (Chekulaeva et al., 2006).

### ***1.13 Heritable neuromuscular diseases and CUGBP1 disruption***

Several heritable neuromuscular diseases show disruption of CUGBP1 expression: Oculopharyngeal Muscular Dystrophy (OPMD), Spinal Bulbar Muscular Atrophy (SBMA), Fragile-X Tremor Ataxia Syndrome (FXTAS), and DM1. In DM1 CUGBP1 disruption is a direct effect of the disorder (Wang et al., 2007). For the others, that remains an open question. Nevertheless, the link remains that a common feature of these diseases is misregulation of CUGBP1. Future studies must address if this is a primary symptom of each disease, or due to the continual regenerative process of the affected muscle (Orengo et al., 2011).

#### ***1.13.1 OPMD-Oculopharyngeal Muscular Dystrophy***

OPMD is an adult-onset muscular dystrophy caused by a (GCN)<sub>12-17</sub> expansion in the open-reading frame of the nuclear poly(A) binding protein (PABPN1). This results in a polyalanine expansion in the N-terminus of the protein. Expression of this mutant PABNP1 causes formation of intranuclear inclusions, which contain many other RNA-binding proteins, one of which is CUGBP1 (Corbeil-Girard et al., 2005).

#### ***1.13.2 SBMA-Spinal Bulbar Muscular Atrophy***

Like DM1, SBMA is caused by a trinucleotide repeat expansion, this time CAG repeats in the androgen receptor mRNA resulting in a receptor containing a polyglutamine tract (La Spada et al., 1991). Interestingly, mouse models of SBMA exhibit over-expression of CUGBP1, but not muscle wasting. These mice also exhibit mis-splicing events consistent with CUGBP1 overexpression. In this case, CUGBP1

overexpression likely results from muscle denervation rather than being a direct consequence of repeat expression (Yu et al., 2009).

### **1.13.3 FXTAS-Fragile-X Tremor Ataxia Syndrome**

FXTAS is found in older individuals who carry a premutation allele (CGG)<sub>60-200</sub> in the 5'UTR of the fragile-X mental retardation gene (FMRP)(Jacquemont et al., 2003). This disease is thought to be caused in part by toxic CGG RNA sequestering RNA-binding proteins (Iwahashi et al., 2006). A *Drosophila* model of FXTAS which expresses the CGG repeat RNA (in the context of the 5'UTR of the FMRP mRNA) found the RNA was associated with hnRNP A1/B2 (Sofola et al., 2007). CUGBP1 was also found in this complex through interactions with hnRNP A1/B2. Over-expression of CUGBP1 alleviated the neural degeneration phenotype in the transgenic fly model of FXTAS (Sofola et al., 2007).

In summary, defects in RNA metabolism are common in expanded repeat neuromuscular disorders. Furthermore, there is a significant body of evidence implicating CUGBP1 in these muscle diseases. The predominantly muscular symptoms of these RNA-mediated defects are demonstrative of the importance of proper control of mRNP dynamics in muscle cells. When those dynamics are disrupted, the results are severe.

## **1.14 Rationale and hypotheses**

### **1.14.1 TNF mRNA decay in muscle cells**

A previous report identified CUGBP1 and PARN as direct mediators of rapid deadenylation of a TNF reporter RNA in HeLa cytoplasmic extracts (Moraes et al., 2006). TNF is a significant modulator of muscle differentiation (Li and Schwartz, 2001),

and over-expression triggers muscle wasting (Taylor et al., 1996). Aberrant myogenesis and muscle wasting are hallmarks of myotonic dystrophy (Lee and Cooper, 2009). Moreover, although TNF is primarily produced by immune cells it is also secreted at low levels by muscle and other cell types (Hotamisligil et al., 1995; Li and Reid, 2001). However, no prior studies have examined the post-transcriptional regulation of TNF in muscle. **We hypothesized that in muscle cells, where CUGBP1 appears to have a unique influence on mRNA metabolism, CUGBP1 and PARN collaborate to promote rapid decay of the TNF message.**

#### *1.14.2 Global rates of mRNA decay of in muscle cells*

By mass, skeletal muscle is the most abundant tissue type in the body, and it exhibits its own distinct pattern of gene expression that can change dramatically during development and in response to extracellular cues (Molkentin and Olson, 1996). Several transcription factors which control myogenesis (MyoD, myogenin, and PAX3) are encoded by short-lived mRNAs (Figuroa et al., 2003; Gong et al., 2009). For these mRNAs, and likely for numerous other transcripts, post-transcriptional control is essential for robust and transient response to differentiation cues (Wagers and Conboy, 2005).

Establishment of basal rates of mRNA decay on a global scale is a necessary step to permit the discovery and characterization of novel post-transcriptional regulatory pathways in muscle cells. **We hypothesized that global mRNA decay profiling would identify characteristic features of mRNAs that influence decay in muscle, reveal cellular processes impacted by regulated mRNA decay, and identify those transcripts which are degraded through CUGBP1-dependent mechanisms.**

### 1.14.3 Identification of CUGBP1 substrate mRNAs

CUGBP1 influences many aspects of mRNA metabolism including splicing, translation and mRNA decay. CUGBP1 function is disrupted in DM1 and other neuromuscular diseases and over-expression of CUGBP1 is sufficient to induce many aspects of DM1 pathogenesis in mice (Timchenko et al., 2004). The contribution of altered splicing to DM1 pathogenesis has been studied extensively (Du et al., 2010; Jiang et al., 2004; Mankodi et al., 2002), but nothing is known about the impact of aberrant CUGBP1 expression on mRNA decay in this debilitating muscle disease. **We reasoned that identification of direct targets of CUGBP1 in muscle would uncover novel mechanisms that may be disrupted in DM1 and contribute to pathogenesis.**

### 1.14.4 mRNA decay and deadenylation by PARN in muscle cells

Many sequence-specific RNA-binding proteins specifically recruit components of the decay machinery to accelerate mRNA turnover. CUGBP1 (Moraes et al., 2006), KSRP (Gherzi et al., 2004), RHAU (Tran et al., 2004), and TTP (Sandler and Stoecklin, 2008) all interact directly with the deadenylase PARN. Some of these RNA-binding proteins also interact with other deadenylases; for example, TTP binds the CAF1 deadenylase (Lykke-Andersen and Wagner, 2005). However, it is not known whether the many eukaryotic deadenylases each show preference for different mRNA substrates or are redundant in function and can each be recruited to any transcript destined for decay. Given that CUGBP1 and PARN directly collaborate for TNF message destruction *in vitro*, we predicted that they would also extensively collaborate to initiate decay of other transcripts *in vivo*. **We hypothesized that assessment of the rates of mRNA decay in the absence of PARN would reveal the full extent to which PARN influences this process in muscle cells.**

The overarching goal of this study was to fully characterize the targets of post-transcriptional control mediated by CUGBP1 and PARN in muscle cells. We anticipated that the results would also provide essential insights into transcripts and processes that may be affected by aberrant CUGBP1 function in DM1 patients.



## Chapter 2: Materials & methods

### 2.1 Bacterial expression plasmids

#### 2.1.1 CUGBP1

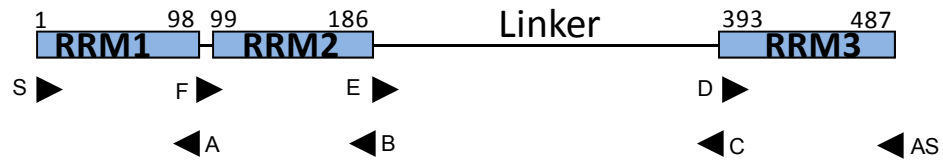
A bacterial expression vector to produce recombinant N-terminal GST-tagged *H. sapiens* CUGBP1 protein was generated by PCR amplification using primers CUGBP **S** and CUGBP **AS** (see Table 2.1) from the pcDNA3.1CUG-BP (transcript variant 3 accession # NM\_001025596.2) which was a gift from Dr. T.A. Cooper (Baylor College of Medicine). PCR amplicons were digested with *BamH1* and *EcoR1* and ligated into pGex2TZQ vector (Qian and Wilusz, 1994) which had been digested with the same enzymes. Locations of primers for generation of mutant vectors are indicated with arrow heads (Figure 4).

**Table 2.1**

Primers for generation of GST tagged CUGBP1 and deletion mutants		
Name	Primer Name (restriction site)	Nucleotide Sequence (5' to 3')
CUGBP-S	CUGBP <b>S</b> (BamH1)	GCTGGATCCATGAACGGCACCCTGGACC
CUGBP-AS	CUGBP <b>AS</b> (EcoR1)	GCTGAATTCTCAGTAGGGCTTGCTGTCA
CUGBP-A	CUGBP <b>A</b> (EcoR1)	ACAGAATTCTAAGCAGGTTTTCATCTGT
CUGBP-B	CUGBP <b>B</b> (EcoR1)	ACAGAATTCTAAGCAAATTTTACCACC
CUGBP-C	CUGBP <b>C</b> (EcoR1)	ACAGAATTCTATCCAGCAGCACCAATA
CUGBP-D	CUGBP <b>D</b> (BamH1)	ACAGGATCCAGCCAGAAGGAAGGTCCAG
CUGBP-E	CUGBP <b>E</b> (BamH1)	ACAGGATCCGCTGATACACAGAAGGACA
CUGBP-F	CUGBP <b>F</b> (BamH1)	ACAGGATCCAGTGAGAAGAACAATGCAG

**Note:** Underlined sequence corresponds to the CUGBP1 cDNA sequence, bold indicates translation stop codon.

**Figure 4.**



**Experimental design for generating GST-tagged CUGBP1 and deletion mutants.** PCR primers are represented as arrow heads, RNA recognition motifs (RRM) as boxes and the linker region as a line. Numbers listed above represent amino acid positions.

### 2.1.2 PARN

A bacterial expression vector to produce recombinant N-Terminal 6 histidine (6XHis) tagged *H. sapiens* PARN protein was generated as follows. The PARN cDNA was PCR amplified using pcDNA3.1+hPARN as template (a kind gift from J. Anderson) and the primers listed below in Table 2.2. Amplified product was digested and cloned into the bacterial expression vector pTrcHis A between the *Kpn1* and *Xho1* sites to produce pTrcHis-A-hPARN.

**Table 2.2**

Primers for generation of 6XHis tagged PARN		
Primer Name	Primer Name (restriction site)	Nucleotide Sequence (5' to 3')
PARN-S	PARN <b>S</b> (Xho1)	GT <u>CGAGAACCTCGAGATGGAGATAATCAGGA</u>
PARN-AS	PARN <b>AS</b> (Kpn1)	GGT <u>ACCCAAGGTACCTTACCATGTGTCAGGAA</u>

**Note:** Underlined sequence corresponds to the PARN cDNA sequence, non-underlined is the restriction site.

### 2.1.3 HuR

A bacterial expression vector to produce recombinant 6XHis tagged mouse HuR protein pET21aHuR (Ma et al., 1996) was kindly provided by Dr. N. Curthoys.

## **2.2 Plasmids for lentivirus expression of shRNAs targeting CUGBP1 and PARN**

### **2.2.1 CUGBP1**

CUGBP1 targeting lentivirus vectors were obtained from the Broad Institute Mission collection and were purchased as bacterial stocks from Sigma Aldrich (NM\_198683.1-**868**s1c1, NM\_198683.1-**869**s1c1, NM\_198683.1-**1279**s1c1, NM\_198683.1-**1320**s1c1, and NM\_198683.1-**1739**s1c1). The numbers in bold indicate the first nucleotide of the region targeted within the CUGBP1 transcript (accession# NM\_198683.1).

### **2.2.2 PARN**

PARN targeting shRNA vectors were generated by subcloning oligos (see Table 2.3 below) into the empty pLKO.1puro plasmid (a gift from R. Schneider; Stewart et al., 2003). Oligonucleotide sequences were chosen by selecting the 6 highest scoring hits from the Broad Institute's RNAi Consortium database. Briefly, the plasmid was digested with *Age1* and *EcoR1* and phosphatased. Annealed oligonucleotide pairs bearing compatible cohesive ends were kinased and ligated into the vector using T4 DNA ligase. pCMVR $\Delta$ 8.2 and pCMV-VSVG plasmids for packaging and pseudotyping lentiviruses were described previously (Stewart et al., 2003) and were obtained from R. Schneider of New York University Langone Medical Center.

**Table 2.3**

Nucleotide sequences for generation of PARN shRNA producing vectors		
Name	mRNA Position(region)	Oligonucleotide Sequence (5' to 3')
PARN1	384 (ORF)	CCGGCCAAGCATGTAACGAAGTCATCTCGAGATGACTTCGTTACATGCTTGGTTTTTG
		AATTCAAAAACCAAGCATGTAACGAAGTCATCTCGAGATGACTTCGTTACATGCTTGG
PARN2	1349 (ORF)	CCGGGCCAGATCAAAGCTCATTGAACTCGAGTTCAATGAGCTTTGATCTGGCTTTTTG
		AATTCAAAAAGCCAGATCAAAGCTCATTGAACTCGAGTTCAATGAGCTTTGATCTGGC
PARN3	1520 (ORF)	CCGGGCCTTCGGTAACATTAGATTCTCGAGAATCTGAATGTTACCGAAGGCTTTTTG
		AATTCAAAAAGCCTTCGGTAACATTAGATTCTCGAGAATCTGAATGTTACCGAAGGC
PARN4	1866 (ORF)	CCGGCGGAGCTTGAACAGACAGATTCTCGAGAATCTGTCTGTTCAAGCTCCGTTTTTG
		AATTCAAAAACGGAGCTTGAACAGACAGATTCTCGAGAATCTGTCTGTTCAAGCTCCG
PARN5	2211 (3'UTR)	CCGGGCGTGTGTATTATTAATACTCGAGATTAGTTAATAACACACACGCTTTTTG
		AATTCAAAAAGCGTGTGTATTATTAATACTCGAGATTAGTTAATAACACACACGC
PARN6	2475 (3'UTR)	CCGGCCAGGCTTTGAGAGCTTGTACTCGAGTAACAAGCTCTCAAAGCCTGGTTTTTG
		AATTCAAAAACCAAGCCTTTGAGAGCTTGTACTCGAGTAACAAGCTCTCAAAGCCTGG

### 2.3 Plasmids for *in vitro* transcriptions

#### 2.3.1 pGemT-p21

Total RNA from C2C12 myoblasts was isolated and subjected to RT-PCR (using p21 3'UTR F and p21 3'UTR R in Table 2.4). The 1290bp PCR product represents the majority of the p21 3'UTR (20nt. at the 5'end and 18nt. at the 3' end were omitted). This amplicon was ligated into the pGemT-Easy vector (Promega). The clone was sequenced and found to match the Genbank sequence. This plasmid pGemTp21 was used as a template (linearized with *EcoRV*) for transcriptions to generate RNA for use in ultra-violet (UV) crosslinking assays (Section 2.26). Additionally, this plasmid served as a template for generating short 120bp PCR amplicons which were then used as a template for preparing p21 RNA for electrophoretic mobility shift assays (Section 2.25)

**Table 2.4**

Primers for amplifying 3'UTRs from mouse cDNA		
Name	Gene Name (accession #)	Oligonucleotide Sequence (5' to 3')
p21 3'UTR F	Cdkn1a/p21 (NM_007669.4)	CCTCTTCTGCTGTGGGTCAG
p21 3'UTR R		ATTGAGCACCAGCTTTGGG
p21 T7 F	p21 120nt. Fragment	TAATACGACTCACTATAGAGGCCTCTTCCCCATCTTC
p21 T7 R		GACTGGGAGAGGGCAGGCAG

### 2.3.2 pGemT-Zfp36l2 (Brf2), pGemT-Actin

Plasmids used as transcription templates to generate probes for RNase H northern blots were generated as follows. Total RNA was isolated from proliferating C2C12 cells, and the poly(A) tails were removed by RNase H and oligo dT<sub>18</sub> treatment (Section 2.29). An RNA linker (Integrated DNA Technologies Linker 3) was ligated to the 3' ends of the RNAs using T4 RNA ligase treatment as described previously (Garneau et al., 2008). Ligated RNAs were subjected to reverse transcription using a specific primer complementary to the RNA linker (Table 2.5). The resulting cDNA, which corresponded to the 3' ends of the actin or Brf2 mRNAs, were then PCR amplified using the linker complement and the DNA oligo originally designed for the Poly(A) Tail (PAT) assay and ligated into the pGemT Easy vector as described above. This process generated the pGemT-Brf2 and pGemT-Actin plasmids which encode the 3'-most 300nt of the Actin mRNA and the 3'-most 183nt of the Brf2 message.

**Table 2.5**

Oligonucleotides for generation of 3'UTR probes				
Primer Name	Gene ID	Gene name	Nucleic Acid (5' to 3')	Type
Linker	-	RNA Linker	ApppTTTAACCGCGAATTCCAGddC	RNA
RT-Linker	-	Linker complement	CTGGAATTTCGCGGTTAAA	DNA
Actin-PAT	109711	Actin	CACTCCTAAGAGGAGGATGGTCGCGTC	DNA
Zfp-PAT	12193	Zfp36l2 (Brf2)	CAGTTGGAGCACCGCGTGTG	DNA

### 2.4 *In vitro* transcription reactions

Internally radio-labeled RNAs were generated by *in vitro* transcription (20U T7 or SP6 RNA polymerase, 10U RNase inhibitor, 40mM Tris pH7.9, 6mM MgCl<sub>2</sub>, 10mM DTT, 10mM NaCl, 2mM spermidine, 500µM ATP, GTP, CTP, 50µM UTP and 4.0µl/10µl reaction [ $\alpha$ -<sup>32</sup>P]UTP(4.5µCi/µl), 716Ci/mmol). Reactions were carried out for 3 hours at

37°C, using 100ng of PCR template or 1µg of plasmid template. For the RNaseH/northern blot probes, the pGemT-Brf2 construct was linearized with *SpeI* and transcribed with T7 RNA polymerase. The pGemT-Actin construct was linearized with *SacII* and transcribed with SP6 RNA polymerase. Restriction enzymes were purchased from New England Biolabs, and plasmids digested according to the manufacturer's instructions. The p21 RNA was transcribed with T7 RNA polymerase, run at ~10V/cm on a 5% polyacrylamide gel containing 7M urea, excised and eluted overnight in 400mM NaCl, 50mM Tris-Cl pH7.5, and 0.1% SDS (w/v) at 22°C. RNA was precipitated and resuspended in H<sub>2</sub>O. Typical reactions yielded 3-5million counts per minute.

### **2.5 Purification of GST-tagged CUGBP1 proteins**

500ml of log phase culture of *E.coli* BL21 (DE3) cells containing the pGex2TZQ-CUGBP1 plasmid (Section 2.1.1) was grown at 30°C in Luria Broth (LB) containing 100µg/ml ampicillin. The bacteria were induced to express N-terminal tagged human CUGBP1 protein by addition of isopropyl β-D-1-thiogalactopyranoside (IPTG) to 1mM for 3 hours. Cells were harvested by centrifugation at 2,500xg for 10 minutes at 4°C, resuspended in 10ml lysis buffer (50mM HEPES pH 7.9, 150mM KCl, 1mM MgCl<sub>2</sub>, 0.1% triton-X 100, 0.1mM phenylmethylsulfonylfluoride (PMSF), and Complete Protease Inhibitor Cocktail (Roche)) and lysed via sonication on ice (Fisher Scientific Sonic Dismembrator Model 100; three 10 second pulses at level 7). Debris was pelleted via centrifugation at 11,000xg for 20 minutes at 4°C, and supernatants were then added to 2mls of 50% slurry of glutathione-agarose in lysis buffer. Beads were rocked with lysates for 1 hour at 4°C, then washed 5 times with 10ml of lysis buffer. GST-CUGBP1 protein was eluted by adding 1ml of lysis buffer containing 50mM reduced glutathione and

rocking on ice for 10 minutes. Elution was repeated two more times and the eluates were pooled, dialyzed into lysis buffer containing 20% glycerol and stored at -80°C. Deletion mutants were prepared in a similar manner.

### **2.6 Purification of 6XHis-tagged PARN protein**

500ml of log phase *E.coli* BL21 (DE3) culture containing the pTrcHisA hPARN plasmid was grown in LB with 100µg/ml ampicillin at 30°C. Cells were induced to express 6XHis tagged human PARN protein for 4 hours by addition of IPTG to 1mM. Cells were harvested by centrifugation at 2,500xg for 10 minutes at 4°C, resuspended in lysis buffer and lysed by sonication on ice (three 10 second pulses at level 7). Debris was pelleted via centrifugation at 25,000xg for 10 minutes at 4°C. Supernatant was incubated with pre-charged Ni-NTA resin (Invitrogen R901-01) which had been pre-equilibrated in lysis buffer for 1 hour at 4°C. Resin was washed three times in 10mls of lysis buffer containing 20mM imidazole, then three times with 60mM imidazole, and finally three times with 80mM imidazole also in lysis buffer. 6XHis-hPARN was eluted by rocking for 10 minutes at 4°C with 1ml of 250mM imidazole. Purified protein was dialyzed in lysis buffer with 20% glycerol and stored at -80°C.

### **2.7 Purification of 6XHis-tagged HuR protein**

500ml of log phase *E.coli* BL21 (DE3) culture containing the pET21aHuR plasmid was grown in LB with 100µg/ml ampicillin at 30°C. Cells were induced to express 6XHis N-terminal tagged mouse HuR protein for 4 hours by addition of IPTG to 1mM. Cells were harvested by centrifugation at 2,500xg for 10 minutes at 4°C, resuspended in 10ml

lysis buffer and lysed via sonication on ice (three 10 second pulses at level 7). Debris was pelleted via centrifugation at 50,000xg for 20 minutes at 4°C. Supernatant was loaded onto a column containing 1ml Ni-NTA resin (Invitrogen R901-01) which had been pre-equilibrated in lysis buffer containing 10mM imidazole for 1 hour at 4°C. Unbound material was allowed to flow through the resin, and the column was then washed 3 times with 4mls of lysis buffer containing 50mM imidazole. HuR protein was eluted by the addition of 1ml of lysis buffer containing 250mM imidazole, and then with 1M imidazole in lysis buffer. The eluates were collected separately, dialyzed into lysis buffer with 20% glycerol (without imidazole), aliquoted, and stored at -80°C.

## **2.8 GST-pulldown assays**

20µl of 50% slurry of glutathione-agarose pre-equilibrated in 1X phosphate buffered saline (PBS) was incubated with 5µg of rGST-CUGBP1 or deletion variant for 2 hours at 4°C. Beads were washed three times in 1.1X PBS (10% more salt than conventional 1XPBS), and then incubated with 1µg of r6XhisPARN in 1.1X PBS containing 0.3% triton-X 100 (1.1XPBS-T) for 1 hour at 4°C. Beads were washed 4 times with 1.1X PBS-T, then resuspended in 6X protein loading dye (600mM Tris-Cl pH 6.8, 10% sodium dodecyl sulfate (SDS), 30% glycerol, 0.6M dithiothreitol (DTT) and 0.001% w/v bromophenol blue), boiled, and resolved on 10% Tris-Glycine SDS-polyacrylamide gels. Proteins were detected by western blotting (Section 2.14). Blots were probed for the presence of rPARN using rabbit anti-PARN serum (generated in-house; Moraes et al., 2006) at 1:20,000 dilution and goat anti-rabbit horseradish peroxidase conjugated secondary (BioRad #170-6515) at 1:20,000 dilution.



## **2.9 Cell culture**

Murine C2C12 myoblasts (ATCC# CRL1772) cultures were maintained at or below 60% confluency in Dulbecco's Modified Eagle's Medium (DMEM) containing 10% fetal bovine serum (FBS), penicillin (10 units/ml) and streptomycin (10 $\mu$ g/ml) in 5% CO<sub>2</sub> at 37°C. Cells were detached from culture flasks by rinsing two times with sterile PBS, and adding 0.25% trypsin. Cells were diluted in complete culture medium and split at a ratio no greater than 1:20.

## **2.10 Differentiation of C2C12 cells**

3.0x10<sup>5</sup> C2C12 myoblasts were seeded on 60mm dishes in DMEM growth media (described above). Once cells had reached a density of ~90% confluency (typically 12-16 hours later) the media was replaced with differentiation media (DMEM, 2% donor equine serum, penicillin 10 units/ml, and streptomycin 10 $\mu$ g/ml). Differentiating cells were cultured for 0 to 7 days in 5% CO<sub>2</sub> at 37°C, with fresh media each day.

## **2.11 Phorbol-ester treatment of C2C12 cells**

For experiments involving phorbol-ester treatment, 100 ng/ml of 12-O-tetradecanoyl-phorbol-13-acetate (TPA Sigma Aldrich) or an equivalent volume of DMSO was added, to cells. Cells were incubated for 3 h prior to either lysis for immunoprecipitation or Trizol collection for RNA analyses.

## **2.12 Generation of lentivirus particles for shRNA expression**

Infectious lentivirus was generated by cotransfection of 10 $\mu$ g each of packaging (pCMVR $\Delta$ 8.2), pseudotyping (pCMV-VSVG), and targeting plasmids (pLKO.1puro+shRNA) into 293T cells by the calcium phosphate method (Jordan et al.,

1996). Twelve hours post-transfection 6mls (for 75cm<sup>2</sup> dishes) of fresh culture media (DMEM, 10% FBS, penicillin (10 units/ml), and streptomycin (10µg/ml)) was added containing 60µl of a 5% butyric acid solution in PBS. Virus-containing supernatants were collected every day for three days following syncytia formation (Stewart et al., 2003), and stored in 1.5ml aliquots at -80°C.

### **2.13 Immunofluorescence Microscopy**

Cells were grown on glass coverslips for the indicated period of time, fixed and permeabilized in PBS containing 0.05% triton-X 100 and 1% paraformaldehyde for 15 minutes at room temperature. Fixed cells were washed 3 times in PBS with 0.05% triton-X 100 (wash buffer) and blocked in wash buffer containing 3% bovine serum albumin (BSA). Primary antibodies were added to block solution at the following dilutions: myosin heavy chain 1:20 (MF20), myogenin 1:20 (F5D), CUGBP1 1:1000 (3B1), and HuR 1:1000 (3A2) for 1 hour at room temperature. Following incubation coverslips were washed 3 times, probed with fluorophore conjugated donkey anti-mouse Cy-2 (Jackson Labs Cat # 715226020), goat anti-mouse Texas Red (Santa Cruz Cat.# sc-3797), or donkey anti-mouse Dylight-488™ (Cat.# 715486150). They were then washed 3 times and mounted on a glass slide in DAPI containing ProLong-Gold (Invitrogen). Actin was visualized using Texas-Red conjugated phalloidin (Invitrogen Cat.# T7471; 1:1000).

### **2.14 Determination of fusion index**

Nuclei residing within myosin heavy chain positive cells were counted and represented as a ratio of total number of nuclei per field of view. Random fields of view were selected and scored in triplicate for three independent experiments.

## **2.15 Generation of PARN and CUGBP1 knock-down cells**

### **2.15.1 PARN**

Wild type C2C12 myoblasts were transfected as described in Mercer et al., (2005) using Lipofectamine 2000 (Invitrogen) with the six PARN targeting vectors from Table 2.3. Two days post-transfection cells were switched to media containing 4.0µg/ml puromycin. Once puromycin resistance had been established, PARN expression was evaluated by qRT-PCR using primers listed in Table 2.6, and by western blot using rabbit anti-PARN antibodies. Constructs #1520 and #2211 gave the best knock-down (consistently around 90%). These vectors were therefore chosen for generation of infectious lentivirus particles. Wild type C2C12 cells were transduced with PARN-targeting or LKO-1 control lentivirus and puromycin resistant cell pools were selected. From these pools single clones were isolated by seeding ~10 cells per 100mm dish. Five to ten clonal cell lines were isolated using glass cloning rings, grown up and re-screened for gene knock-down by western and/or qRT-PCR. All experiments involving PARN Knock Down (KD) cells, were conducted with a clonal cell line stably expressing #2211, as those expressing #1520 failed to differentiate.

### **2.15.2 CUGBP1**

Glycerol stocks of lentivirus vectors bearing shRNAs targeting CUGBP1 were purchased from Sigma Aldrich (SHCLNG-NM 198683). Plasmids were transfected into C2C12 cells and selected with 4.0µg/ml puromycin. CUGBP1 expression was evaluated by qRT-PCR using CUGBP1-specific primers listed below (Table 2.6) and by western blotting. Of the five constructs supplied, #1320 and #1739 gave the best knock-down and #1739 was used for the majority of experiments. These constructs were used to

generate knock-down cell lines by transfection and subsequent selection of stable clones with puromycin. For later experiments involving differentiation, pools of CUGBP1 knock-down cells were generated by infecting with lentivirus and selecting stable pools of CUGBP1-depleted cells. Stable pools were generated with both construct #1739 and #1320.

Control cells were generated in a similar fashion as described for PARN (Section 2.15.1). For experiments involving clonal cell lines, controls were generated by transfection of empty pLKO.1puro vector, selection of puromycin resistant pools, and selection of clonal cell lines. Clones were tested for the ability to differentiate and line 6-3 was utilized for all experiments involving clonal CUGBP1 and PARN KD cells (including the global half life analysis). For experiments involving CUGBP1 knock-down pools, cells were infected with virus containing empty pLKO.1puro. Puromycin-resistant pools were then selected in an identical fashion.

### **2.16 Western blotting**

For CUGBP1 western blots, 40 µg of whole cell lysate was prepared by lysis of cells in RIPA buffer (50 mM Tris-HCl (pH 7.4), 150 mM NaCl, 1.0% deoxycholate, 1% triton-X 100, 1mM EDTA, and 0.1% SDS). The lysates were boiled in 6X protein loading buffer, and resolved on a 10% SDS-polyacrylamide gel. Gels were blotted to Polyvinylidene Fluoride (PVDF) membrane, using Bio-Rad Semi-Dry transfer apparatus at 18V for 25 minutes in Transfer Buffer (25mM Tris-HCl, 190mM Glycine, and 15% methanol). Membranes were blocked for one hour in PBS-T (PBS containing 0.05% Tween-20) and 5% (w/v) non-fat dry milk. Primary antibodies were added directly to blocking solution. Following one hour incubation with primary antibody, membranes were washed three times with PBS-T, 5 minutes per wash, fresh blocking solution was added,

secondary antibody added for one hour at room temperature, membranes again washed three times for five minutes each in PBS-T, and signal detected using Pierce Pico Chemiluminescent detection kit. CUGBP1 was detected using monoclonal antibody 3B1 (1:20,000 dilution; Santa Cruz Biotechnology), HuR was detected using monoclonal antibody 3A2 (1:10,000 dilution; Santa Cruz Biotechnology), phospho-PKC was detected with rabbit polyclonal antibody SC-12356-R (1:2000 dilution; Santa Cruz Biotechnology) PARN was detected using rabbit anti-sera (1:20,000; Moraes et al., 2006). GAPDH was used as a loading control (1:20,000 dilution; Chemicon mAB374). Differentiation markers, namely myogenin and myosin heavy chain were detected using hybridoma supernatants F5D and MF20 respectively at 1:20 dilution (Developmental Studies Hybridoma Bank, University of Iowa). Quantification was performed using QuantityOne software (BioRad). Reported values are a measure of the pixel intensity of the band of interest relative to the pixel intensity of the loading control (GAPDH in most cases). These ratios were then normalized relative to control samples.

### ***2.17 Cytoplasmic and nuclear fractionation of C2C12 cells***

Cells were collected by trypsinization and washed three times in ice-cold PBS. Cells were pelleted by centrifugation at 500xg for 5 minutes at 4°C. Cell pellets were resuspended in an equal volume of Buffer A (10mM HEPES pH 7.5, 10mM NaCl, 1.5mM MgCl<sub>2</sub>, 0.5mM DTT, and Complete Protease Inhibitor Cocktail (Roche)) and swollen on ice for 10 minutes with intermittent mixing. Cells were pelleted by spinning at 500xg for 5 minutes at 4°C. Supernatant was removed and the cell pellet was resuspended in an equal volume of Buffer A containing 0.5% (v/v) Nonidet-P40 (NP-40). Cells were lysed by vigorously passage through a 25-gauge needle about 20 times. Cytoplasmic lysis was confirmed by microscopy. Nuclei were pelleted by centrifugation at 4,000xg in a 4°C

bench top microcentrifuge. Cytosolic supernatant was collected and stored at  $-80^{\circ}\text{C}$ . Pellets containing nuclei were subjected to 4 washes in Buffer A containing 0.5% NP-40, each of which was approximately 4 packed nuclei volumes. Nuclear pellets were resuspended in an equal volume Buffer C (20mM HEPES pH7.9, 420mM NaCl, 0.2mM EDTA, 1.5mM  $\text{MgCl}_2$ , 0.5mM DTT, 25% glycerol, and Complete Protease Inhibitor Cocktail (Roche)) and incubated on ice for 30 minutes with intermittent vortexing. The mixture was then centrifuged at 16,000xg at  $4^{\circ}\text{C}$  in a bench top microcentrifuge for 10 minutes. Supernatant containing nucleoplasm was stored at  $-80^{\circ}\text{C}$  for future use.

### **2.18 Half-life analysis**

C2C12 cells were grown in 100mm dishes to 60-70% confluency. Transcription was shut off by treating cells with Actinomycin-D ( $8\mu\text{g/ml}$  Sigma-Aldrich) for 20 minutes. Cells were collected in Trizol™ (Invitrogen) at the indicated time points post transcription shutoff. Total RNA was isolated according to the manufacturer's instructions. Equivalent amounts (1-2 $\mu\text{g}$ ) were reverse transcribed, and analyzed by real-time PCR (BioRad MyIQ or, BioRad CFX96) using the  $\Delta\Delta\text{C}_t$  method (Vandesompele et al., 2002). Primer sets were designed using qPrimer Depot (Cui et al., 2007) or Primer3 plus (Untergasser et al., 2007) and are shown in Table 2.6 below. Except where otherwise noted, graphed data represents the mean values from at least three independent experiments; error bars represent the pooled standard deviations.

For microarray experiments RNA concentration, purity, and quality were assessed via Bioanalyzer (Agilent). Transcription shut-off was confirmed using 1 $\mu\text{g}$  of total RNA from each time point in qRT-PCR assays (described previously Section 2.16) for either MyoD or myogenin, using GAPDH as a reference mRNA. Samples displaying adequate transcriptional shut off were then used for microarray hybridization.

### **2.19 qRT-PCR**

For reverse transcriptase reaction (RT) 1-4µg of total RNA was annealed to 500ng of random hexamers (for TNF, 1µl of 10µM gene-specific primer was used) in 5µl total volume by heating to 70°C for five minutes then cooling on ice. Reverse transcriptions were done in the following reaction mixture (35mM Tris-Cl pH8.3, 50mM NaCl, 5mM MgCl<sub>2</sub>, 5mM DTT, 500ng random hexamers, 10U RNase Inhibitor, 1µl Improm II Reverse Transcriptase (Promega)). Following the RT step, 2.5µl of cDNA template was used for qPCR with BioRad Supermix (170-8860) according to manufacturer's instructions. A two-step amplification protocol was used with an annealing temperature of 60°C for 30 seconds and a melting temperature of 95°C for 30 seconds for 40 cycles. A melt curve was generated by starting at 65°C and heating 0.5°C every 30 seconds until a temperature of 95°C was reached. Primer pairs were standardized by amplifying six 5-fold serial dilutions (each done in triplicate) of cDNA reactions and fitting the data to a line. Primer pairs which generated a PCR efficiency between 80 and 120% and an R<sup>2</sup> value (correlation coefficient) of >0.98 were deemed acceptable.

**Table 2.6**

List of primers used for (q)RT-PCR experiments					
Name	Gene ID	Gene name	Left Primer (5' to 3')	Right Primer (5' to 3')	Efficiency
Actin	109711	Actin	AGAGGGAAATCGTGCGTGAC	CAATAGTGATGACCTGGCCGT	108.8%
Adora2b	11541	Adora2b	TGCTCACACAGAGCTCCATC	TGTCCCAGTGACCAAACCTT	108.2%
Ankrd54	223690	Ankrd54	CAATGCCAACGACGTAGAAA	ATTGCAGGAAGCAAAATGGA	105.3%
Arl8a	68724	Arl8a	CAGTACTCGGGCAAGACCAC	CCTTTGGTGATTTTTTCGCAT	N/D
Bcl6	12053	Bcl6	AGTTTCTAGGAAAGGCCGGA	GATACAGCTGTCAGCCGGG	103.5%
p21	12575	Cdkn1a	CTCAGGTAGACCTTGGGCAG	GTGTGCCGTTGTCTCTTCGG	89.2%
cJun	11767	cJun	AAAACCTTGAAAGCGCAAAA	GTTTGCAACTGCTGCGTTAG	99.8%
Myc	17869	cMyc	CTGTCCATTCAAGCAGACGA	TCCAGCTCCTCCTCGAGTTA	N/D
Cox-2	19225	Ptgs2	CAAGACAGATCATAAGCGAGGA	GGCGCAGTTTATGTTGTCTGT	116.0%
CUGBP	13046	Cugbp1	GATCAGTGCAGCGTCTGTGT	GTGTTGAGGTTCCCAGAGGA	107.1%
GAPDH	14433	GAPDH	TCACCACCATGGAGAAGGC	GCTAAGCAGTTGGTGGTGCA	98.8%
Gata4	14463	Gata4	CTGGAAGACACCCCAATCTC	CAGGCATTGCACAGGTAGTG	107.2%
Gnb1l	54584	Gnb1l	AGCGGAGCCTCTGATCCT	GACAAATCTGGGACCAGGC	112.6%
GPSM	67839	Gpsm1	CTGACTAGCCCAGCAGCAG	TCTCGGCACTCAGCCTCT	98.4%
Gemin4	276919	Gemin4	GAAGTGCAGGACATGCTCAA	AGCTCCAAGTTTTGGCTGAA	106.3%
Id2	15902	Id2	GTCCTTGCAGGCATCTGAAT	AGAAAAGAAAAGTCCCAATG	99.5%
Il-6	16193	Il6	GAGGATACCACTCCCAACAGACC	AAGTGCATCATCGTTGTTTCATACA	99.9%
Infy	16173	Il18	ACGGCACAGCTATTGAAAGCCTA	CTCACCATCCTTTTGGCAGTCC	97.9%
JunD	16478	JunD	GACCCTCAAAGCCAGAACA	GTTGACGTGGCTGAGGACTT	N/D
Lsm7	66094	Lsm7	CATCGATAAGACCATTCCGGG	AGCACCAGGTTGAGCAGTG	N/D
MyoD	17927	Myod	TGGGATATGGAGCTTCTATCGC	GGTGAGTCGAAACACGGATCAT	107.1%
Myogenin	17928	Myog	ACTCCCTTACGTCCATCGTG	CAGGGCTGTTTTCTGGACAT	110.4%
Ncoa5	228869	Ncoa5	GGCAGCGGAAAGAAGAAATA	TCTCCTTGGACTTCCCTCGAA	112.5%
Net1	56349	Net1	TGTTCCCATTTCTAGACCAAG	CAGCTCTGCGTCGAGTTTTT	N/D
PARN	74108	PARN	CTCAGCCAGCCAGAACAAGT	TGCTGCCTTCTGCTTCTT	98.3%
Plk2	20620	Plk2	GGCAAGAAGGACAAAGCAAG	TTGCTAGGCTGCTGGGTTAT	N/D
Ppp1r15b	108954	Ppp1r15b	GTGAGGCTCTTGCTGGAGAA	TCCTTTGCGATCCTCATCAC	110.1%
Rnd3	74194	Rnd3	CACTGCCAGTTTTGAAATCG	GGTAAGAGAGTGGACGGACG	114.5%
Smad7	17131	Smad7	GAACGAATTATCTGGCCCCT	GACACAGTAGAGCCTCCCA	113.2%
Sox9	20682	Sox9	AGGAAGCTGGCAGACCAGTA	TCCACGAAGGCTCTCTTCTC	118.1%
TNF	21926	TNF	CATCTTCTCAAATTCGAGTGACAA	TGGGAGTAGACAAGGTACAACCC	94.9%
Xist	213742	Xist	CCAGGAACCATTTCTTGCCCTA	GGAAAGCCCCAAGTAAAAGG	N/D
Zfp36l2	12193	Zfp36l2 (Bfr2)	CCTCCTTTGTGGTGGTTGTT	ACACTACGTGGTGGCAATGA	109.1%

**Note:** N/D indicates that the PCR efficiency was not measured as these primer pairs were used in traditional end-point RT-PCR assays.

## 2.20 RNA immunoprecipitation

Cell lysates were collected from proliferating C2C12 cells (~70% confluency) as previously described (Tenenbaum et al., 2002). This involved rinsing the cells three times in ice cold PBS, and collecting the cells by trypsinizing. Cells were then pelleted by



centrifuging at 500xg for 5 minutes at 4°C, and washing thrice in PBS. Cells were lysed by resuspension of the pellet in an equal volume of Polysome Lysis Buffer (100mM KCl, 5 mM MgCl<sub>2</sub>, 10 mM HEPES, pH 7.0, 0.5% Nonidet P-40, 1 mM DTT, 100 units/ml RiboLock RNase Inhibitor (Fermentas), 0.2% vanadyl ribonucleoside complexes (New England Biolabs), 0.2mM PMSF, and 1X Complete Protease Inhibitor Cocktail (Roche)) and snap freezing to -80°C. Immunoprecipitates were isolated by incubating 100µl of cleared lysate with 7µl mouse control IgG (Santa Cruz sc-3877) or αCUGBP1 antibody (Santa Cruz sc-3B1) for 1 hour on ice. Following centrifugation at 16,000x g for 3 minutes at 4°C, the reaction was transferred to a tube containing 100µl of a 10% slurry of Protein-G sepharose beads (Sigma) in NT-2 buffer (50 mM Tris-Cl, pH 7.4, 150 mM NaCl, 1 mM MgCl<sub>2</sub>, and 0.05% Nonidet P-40) and rocked for 1 hour at 4°C. Beads were washed two times with 250µl of NT-2 buffer, transferred to a micro-spin column (Pierce Cat.# 89879) and washed four more times with 200µL of NT-2 buffer. Beads were collected, divided in half, and analyzed for associated RNAs or proteins, by qRT-PCR or western blot respectively. For array validations, RNA was eluted by vortexing beads in 60µl of Trizol (Invitrogen). RNA was purified according to manufacturer's recommendations and resuspended in 5µl of water. 1 µl of RNA was reverse-transcribed with random hexamers, subjected to 30-40 cycles of PCR and run on a 2% agarose gel. Proteins were collected by elution with 10µl 6X protein loading buffer, boiled for 5 minutes, resolved by SDS-PAGE (10% gels) and analyzed by western blot. For co-immunoprecipitation, lysates were prepared as described above except cells were sonicated on ice (3 times 5 second pulses at level 7) prior to snap freezing.

### **2.21 Preparation of RNA samples and microarray hybridization**

RNA samples were isolated from Trizol™ (Invitrogen). 300ng of total RNA for half-life, and 100ng of immunoprecipitated RNA were used to generate labeled cDNA fragments for hybridization to Affymetrix Gene 1.0 ST Arrays (Cat.# 901168) following the manufacturer's protocols for the Sense Target Labeling Kit (cat.# 900652). Half life experiments were conducted in triplicate, using a total of 45 arrays. For immunoprecipitation the experiment was conducted in duplicate and input RNA, control IgG precipitated RNA, and  $\alpha$ -CUGBP1 precipitated RNA samples were assayed.

### **2.22 Half-life analysis by microarray**

Relative fluorescence unit (RFU) values for each probe were normalized to the 5<sup>th</sup> percentile value of the range of RFUs on each array. Array probes exhibiting signal that was above background in the 0 time point (P-value <0.05) were considered present. Half-lives were calculated in R (Dessau and Pipper, 2008) using a non-linear model fit to the normalized RFU values and time points. The calculated value for the mRNA half-life was considered reliable if it met the following two criteria in at least two of the three experimental replicates. First, the data points had to fit the decay curve within the acceptable error range (P-value <0.05). Second, the range of the 95% confidence intervals must be less than twice the calculated half-life. For comparisons between control and CUGBP1 KD and control and PARN KD cells only mRNAs which yielded reliable half-lives in both sets were used.

### **2.23 CUGBP1 target identification by RIP-Chip and comparison to other datasets**

Probe intensities and expressed genes were normalized and determined as described in the preceding section. The data from the Input RNA arrays was not used for

the final analysis. The ratio of the  $\log_2$  values of the CUGBP1 IP sample over the  $\log_2$  values of the normal mouse IgG sample were calculated for each gene and the genes were ranked by this value. Genes in the top 95<sup>th</sup> percentile were considered significantly associated with CUGBP1. The significantly associated genes were compared to other datasets for Pum1 (Morris et al., 2008) and HuR (Mukherjee et al., 2009) using Ingenuity Pathway Analysis (Ingenuity® Systems, [www.ingenuity.com](http://www.ingenuity.com)).

### **2.24 Cis-element analysis**

In order to identify sequence elements significantly enriched in unstable and stable transcripts the following approach was taken. mRNAs with reliable half-lives in C2C12 LKO-1 cells were ranked from shortest to longest. The transcripts with the shortest (10<sup>th</sup> percentile and below) and longest (90<sup>th</sup> percentile and above) half-lives were selected for comparison. Each set contained 739 mRNAs. The 3'UTR of each mRNA from both sets was examined for the occurrence of each of 4096 possible hexamers. Hexamer occurrence for the unstable and stable sets were compared by Fisher's exact test to identify those that were significantly over-represented in one set as compared to the other (P-values <0.05 were considered significant). Related hexamers were clustered, and used to generate sequence logos via a Position Specific Scoring Matrix using Perl. In the sequence logo the probability for a particular nucleotide to be found in that position is represented by character height, where full height equals >99%. Sequence logos were generated by Web Logo Tool (Crooks et al., 2004). This process was repeated for the CUGBP1 RIP-Chip data using a method similar to that described previously.

### **2.25 Gene ontology analysis**

Gene Ontology (GO) analyses were performed on various sets of mRNAs (e.g. unstable transcripts, transcripts bound by CUGBP1, transcripts affected by PARN knock-down) in order to identify functional relationships within each set. Significantly over-represented GO terms were identified using R script and Perl script by Dr. Ju Youn Lee, University of Medicine & Dentistry of New Jersey Medical School.

### **2.26 Electrophoretic mobility shift assays**

The 120nt p21 RNA (Section 2.3.1) was *in vitro* transcribed from 100ng of PCR-generated template in the presence of ( $\alpha$ -<sup>32</sup>P) UTP (4.0 $\mu$ l in 10 $\mu$ l total) using 10U T7 RNA polymerase in 1X transcription buffer (40mM Tris-HCl (pH 7.9), 6mM MgCl<sub>2</sub>, 10mM DTT, 10mM NaCl, and 2mM spermidine) containing 0.5mM NTPs. Precipitated RNA was gel purified on a 5% denaturing polyacrylamide gel (see section 2.3 for electrophoresis conditions). Increasing amounts of recombinant human GST-CUGBP1, mouse 6XHis HuR, or both were incubated with 3 fmol of RNA in the presence of 20 units of RNase inhibitor, 0.15mM spermidine, 20 mM HEPES (pH 7.9), 8% glycerol, 100 mM KCl, 1mM DTT and 2 mM MgCl<sub>2</sub> for 5 min at 30 °C in a total volume of 10  $\mu$ l. Low molecular weight heparin (Sigma Cat.# H2149) was added to a final concentration of 4mg/ml. Samples were chilled on ice for an additional 5 min, and 2  $\mu$ l of loading buffer (0.5% bromophenol blue, 0.5% xylene cyanol, 30% glycerol) was added, followed by electrophoresis at room temperature on 5% native polyacrylamide gels in 1X TBE buffer (89mM Tris-Cl, 89mM boric acid, and 1mM EDTA) at 10 V/cm for 90 minutes. Dried gels were exposed to storage phosphor screens and visualized by Phosphor-Imaging using a Typhoon Trio Imager (GE Healthcare) and Image Quant software. The fraction of RNA bound was calculated by quantifying the amount of RNA associated with protein and dividing it by

the total amount of RNA in each lane. Excel (Microsoft) was used to plot the graphs shown, and dissociation constants ( $K_D$ ) were defined as the protein concentration required to achieve half-maximal binding at equilibrium. Reported  $K_D$ s are the average of at least three experiments  $\pm$  the standard deviation.

### **2.27 UV cross-linking assays**

The p21 3'UTR RNA substrate was generated using *EcoRV* digested pGemTp21 as a template for transcription (Section 2.4). The RNA contains the first 395nt of the murine p21 3'UTR. 0.3 fmols of RNA were incubated for 20 minutes at 22°C with the indicated concentration of recombinant proteins in binding buffer (20mM HEPES pH 7.9, 100mM KCl, and 1mM DTT) as described previously (Sureban et al., 2007). Heparin was then added to a final concentration of 5mg/ml. After 5 minutes reactions were crosslinked at 250mJ/cm<sup>2</sup> at a wavelength of 254nm, and were subsequently treated with 5 units of RNase One (Promega) for 10 minutes at 37°C, mixed with 6X protein loading dye and resolved by SDS-PAGE (10% gels). Dried gels were exposed to storage phosphor screens and imaged on the Typhoon Trio Imager (GE Healthcare).

### **2.28 2D protein gels**

Total protein from RIPA lysed C2C12 cells (0.2mg) was precipitated in 4 volumes acetone at -20°C for 20 minutes followed by centrifugation for 20 minutes at 5,000 x g at 4°C. Pellets were wash four times in 80% acetone, air dried, and resuspended in IEF sample buffer (8M urea, 2M thiourea, 2% w/v CHAPS, 0.3% DTT, 0.2% triton-X 100, 1% bromophenol blue, and 2.5% carrier ampholytes). For calf-intestinal phosphatase (CIP) treated samples 0.2mg of protein was resuspended in 1X CIP buffer containing: 50 mM Tris-HCl pH7.9, 100 mM NaCl, 10 mM MgCl<sub>2</sub>, 1 mM Dithiothreitol, and 100 units CIP

(New England BioLabs) and incubated at 37°C for two hours. Mock samples were incubated in identical conditions lacking enzyme. First dimension focusing was done on Bio-Rad Ready Strips pH 3-10 following 12 hours of active rehydration (in IEF sample buffer) at 50V, focusing was done initially at 250V for 15 minutes, then for a total of 30kV-hours using the BioRad Protean IEF Cell. Strips were equilibrated for 15 minutes in equilibration buffer (6M urea, 30% glycerol, 2% SDS, and 25mM Tris pH 6.8) first containing 2% DTT, then containing 2.5% iodoacetamide. Second dimensions were resolved on 10% SDS-PAGE, and blotted to PVDF membrane at 18V for 40 minutes, which were probed and visualized as described Section 2.16.

### **2.29 RNaseH/northern blotting**

In order to shorten mRNAs to facilitate analysis of mRNA poly(A) tail lengths 10µg of total RNA was incubated with 2µM DNA oligos (sequence listed in Table 2.7), heated to 95°C for 3 minutes and slow cooled (drop of 1.5°C/minute) to 4°C. RNaseH (7 units) and RNase Inhibitor (20 units) were added in the supplied reaction buffer (Fermentas Cat.# EN0201). For generating poly(A) tail minus (A<sub>0</sub>) controls 100ng/µl of oligo dT<sub>18</sub> was included. Reactions were incubated at 37°C for 30 minutes. RNAs were then resolved on a 5% denaturing polyacrylamide gel (7M urea, 1X TBE), electroblotted to nylon membrane (Hybond-XL GE Healthcare) at 700mA for 30 minutes in 1X TBE. Nucleic acids were immobilized by UV-crosslinking (Stratalinker, Auto-Crosslink Feature). Membranes were pre-hybridized for 1 hour at 60°C in 25ml hybridization buffer (50% formamide, 750mM NaCl, 75mM sodium citrate, 1% SDS, 0.1mg/ml salmon sperm DNA, 1mg/ml polyvinylpyrrolidone, 1mg/ml ficoll, 1mg/ml bovine serum albumin (BSA)). Membranes were then hybridized to radio-labeled probe over night at 60°C, also in hybridization buffer. Blots were washed two times in 25ml non-stringent wash buffer

(0.1% SDS, 300mM NaCl, 30mM sodium citrate) and two times in 25ml stringent wash buffer (0.1% SDS, 30mM NaCl, 3mM sodium citrate) for 20 minutes each time at 60°C. Membranes were exposed to storage phosphor screens and imaged on the Typhoon Trio Imager (GE Healthcare). Results were analyzed using Image Quant software (GE Healthcare).  $\alpha^{32}\text{P}$ -labeled RNA probes were generated by *in vitro* transcription reactions as described (Section 2.4). Briefly pGemTZfp36l2 (Brf2) was linearized with *Spe1* and transcribed with T7 RNA polymerase to generate RNA complementary to the Zfp36l2 message. The pGemTActin plasmid, was linearized with *SacII* and transcribed with SP6 RNA polymerase. In some experiments, cells were treated with Actinomycin-D (8 $\mu\text{g}/\text{ml}$  Sigma-Aldrich) in growth media (Section 2.9) for the indicated length of time prior to harvesting.

**Table 2.7**

Oligonucleotides used in RNaseH reactions		
Gene ID	Gene name	DNA oligo (5' to 3')
109711	Actin	AAGCAATGCTGTCACCTTCC
12193	Zfp36l2 (Brf2)	CGCGGTGCTCCAACCTGTACCTA

## **Chapter 3: CUGBP1 regulates stability of TNF mRNA in muscle cells**

Many of the results presented in Chapter 3 appeared in: The RNA-binding Protein CUGBP1 Regulates Stability of Tumor Necrosis Factor mRNA in Muscle Cells: *Implications for Myotonic Dystrophy* Journal of Biological Chemistry Vol. 283, No. 33, pg. 22457–22463, August 15, 2008.

A previous study in the Wilusz lab sought to address the mechanism by which ARE-mediated decay of TNF mRNA is achieved (Moraes et al., 2006). A cell-free RNA decay system which can be used to accurately assess rates of deadenylation was employed (Ford and Wilusz, 1999). Through UV-crosslinking and competition assays, it was demonstrated that CUGBP1 specifically binds to a fragment of the 3'UTR of TNF mRNA in cytoplasmic extracts. Later experiments showed CUGBP1 was not associated exclusively with the ARE, but also recognized a UGUU element adjacent to the ARE. Additional experiments demonstrated that the TNF 3'UTR RNA was rapidly deadenylated in cytoplasmic extracts. This activity was dependent on CUGBP1 binding and PARN was the enzyme responsible. Finally, evidence was presented that PARN and CUGBP1 could directly interact, and that this interaction was RNA-independent. Unfortunately, attempts to further characterize the interaction between PARN and CUGBP1 have been unsuccessful to date (Appendix 1). Overall, these *in vitro* results demonstrate that direct recruitment of a deadenylase to an RNA substrate by CUGBP1 enhances mRNA decay.

TNF is a potent cytokine produced primarily in immune cells (Tracey and Cerami, 1994), but also in other cell types, including adipocytes (Prins et al., 1997) and myocytes (Li and Schwartz, 2001). Importantly, TNF over-expression has many



pathogenic effects; it has been directly linked with muscle wasting (Reid and Li, 2001), rheumatoid arthritis (Kontoyiannis et al., 1999), and Crohn's disease (Kontoyiannis et al., 2002). Moreover, TNF is commonly over-expressed in skeletal muscle diseases like Duchenne Muscular Dystrophy, DM1, and polymyositis (Mammarella et al., 2002; Saito et al., 2000; Shimizu et al., 2000).

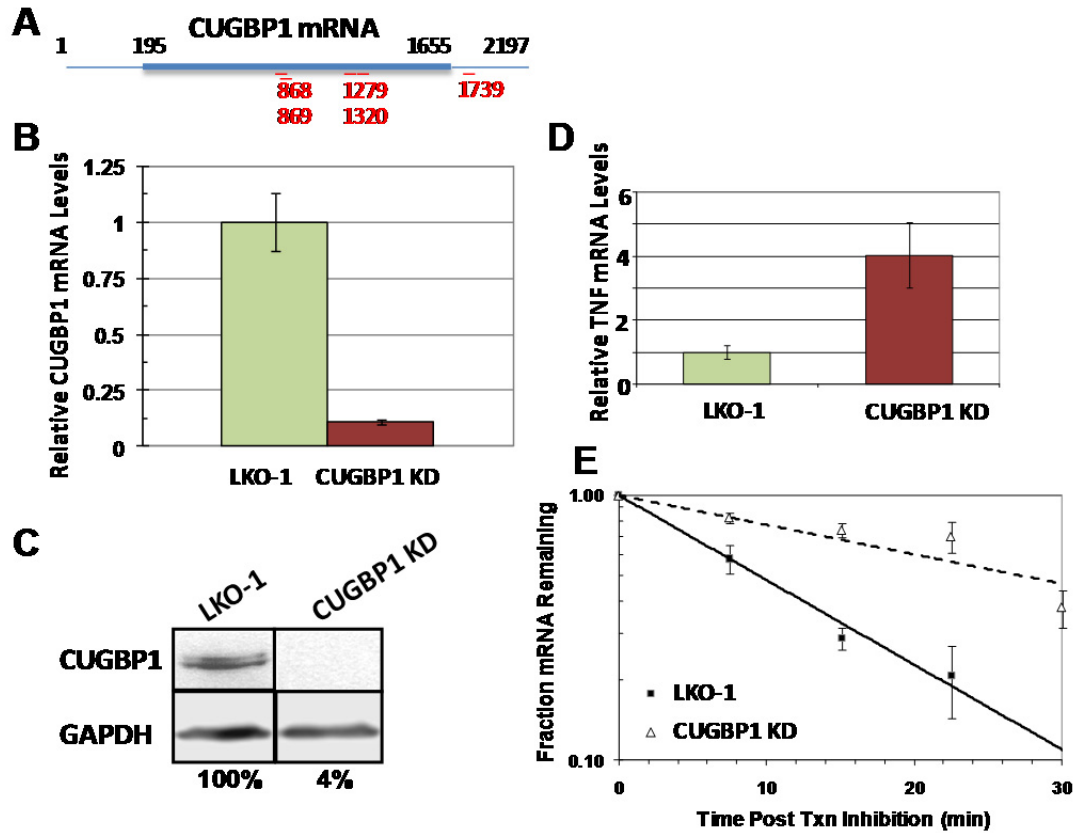
As stated above, the TNF mRNA is a probable target of CUGBP1, which likely regulates decay of several mRNAs in immune cells (Vlasova et al., 2008). However, CUGBP1 appears to play a more significant role in muscle than in immune and other cell types as its function is disrupted in the neuromuscular disorders including DM1, OPMD, FXTAS, and SBMA (Corbeil-Girard et al., 2005; Sofola et al., 2007; Yu et al., 2009; Mammarella et al., 2002). Based on these observations we hypothesized that disruption of CUGBP1 function in DM1 leads to stabilization of TNF mRNA and TNF over-expression, which might promote muscle wasting. We therefore examined whether the CUGBP1-mediated regulation of TNF mRNA decay observed in HeLa extracts (Moraes et al 2006) could be recapitulated in proliferating muscle cells.

### **3.1 CUGBP1 destabilizes TNF mRNA in C2C12 myoblasts**

We chose to use C2C12 muscle cells for this study because they are a well-characterized and easily cultured model that can be induced to differentiate *in vitro* (Blau et al., 1983). In order to examine the role of CUGBP1 in regulating TNF expression in C2C12 cells we first generated a knock-down cell line. Five commercially available lentivirus vectors containing shRNAs predicted to target CUGBP1 were tested for efficacy by transient transfection into C2C12 cells (Figure 5A). Cell pools which exhibited the best knock-down when compared to empty vector (LKO-1), as assessed by qRT-PCR and western blot, were used for selection of clonal lines. Two cell lines were

selected for further experiments – LKO-1 (bearing empty vector) and CUGBP1 knock-down (KD; bearing construct #1739, which targets all splice isoforms of CUGBP1) (Figure 5A). As shown in Figures 5B and C, CUGBP1 expression was reduced approximately 90% at the mRNA and protein levels in the CUGBP1 KD cell line.

Figure 5.



**Knock-down of CUGBP1 by shRNA triggers TNF mRNA abundance and half-life increases.**

(A) Schematic of CUGBP1 mRNA, ORF as box, lines as UTRs, red line indicates approximate position of targeting shRNA, numbers indicate nucleotide boundaries of described features. (B) Abundance of CUGBP1 mRNA in CUGBP1 KD and control (LKO-1) cells determined by qRT-PCR, normalized to GAPDH mRNA. (C) Western blot for CUGBP1 and GAPDH (loading control) of extracts from LKO-1 and CUGBP1 KD cell lines. (D) TNF mRNA levels in LKO-1 and CUGBP1 KD cell lines assessed by qRT-PCR normalized to GAPDH. (E) Rate of decay for TNF mRNA in the LKO-1 (solid line) and CUGBP1 KD cell lines (dashed line) was assessed following actinomycin-D treatment. mRNA levels were measured at each time point and normalized to GAPDH (the average of 3 separate experiments is shown).

As an initial experiment, the levels of TNF mRNA were measured by qRT-PCR in both LKO-1 and CUGBP1 KD cell lines (Figure 5D). In CUGBP1 KD cells the relative abundance of the TNF transcript was, on average, increased 4-fold over the levels in the control cells, consistent with an increase in mRNA stability. Next, TNF mRNA stability was assessed in control and CUGBP1 knock-down cell lines (Figure 5E) by treating cells with the transcription inhibitor actinomycin-D, isolating total RNA at each time point, and measuring the abundance of both a stable reference mRNA (GAPDH) and TNF mRNA for each sample. The measured half life for TNF mRNA in control cells was  $10.0 \pm 1.0$  min. This is slightly less stable than previously reported in lymphocytes and macrophages where the message had a half-life of 15-20 minutes for lymphocytes and 30-40 minutes for macrophages (Garnon et al., 2005; Wang et al., 2006). This may be due to muscle not being a primary TNF producer, or be indicative of the sensitive nature of muscle to TNF levels.

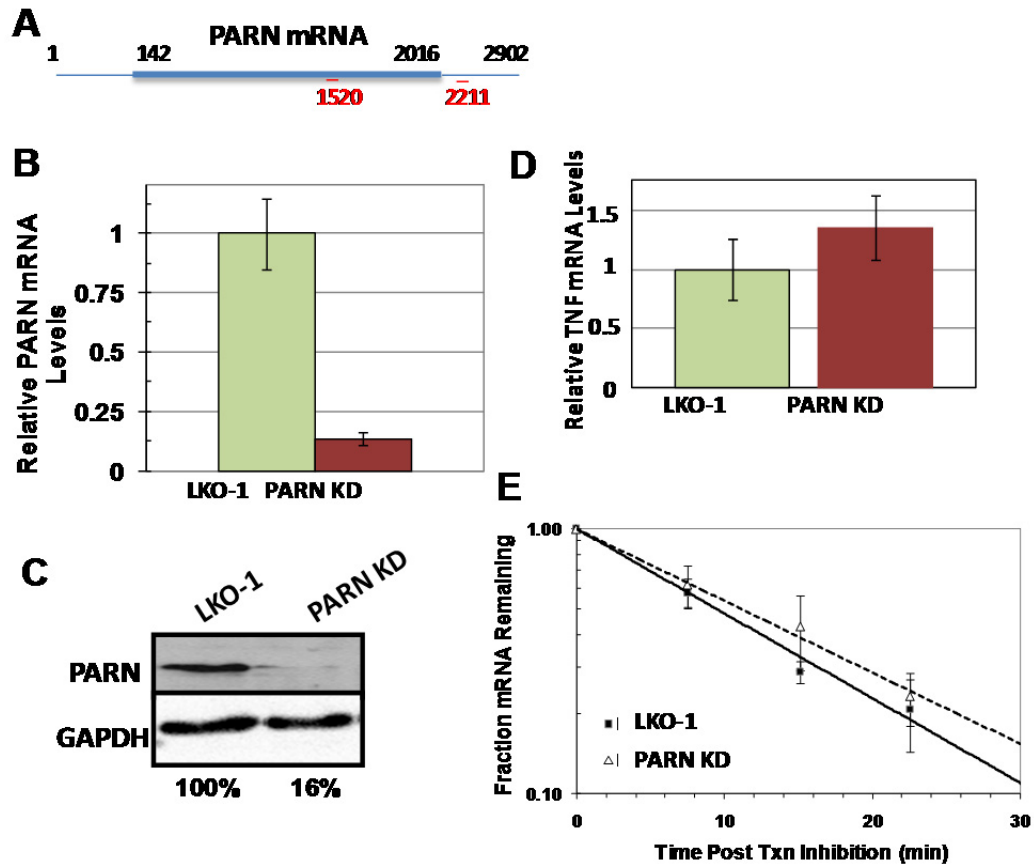
In the CUGBP1 KD cells the half-life of the TNF mRNA was markedly increased ( $27.0 \pm 3.5$  min). This result conforms nicely with the *in vitro* data generated in the previous study (Moraes et al., 2006) which first suggested that decay of TNF was regulated by CUGBP1. This finding adds CUGBP1 to the growing list of RNA-binding proteins which post-transcriptionally regulates TNF mRNA, which currently includes: TIA-1 (Piecyk et al., 2000), FXR1 (Garnon et al., 2005), TTP (Carballo et al., 1998), and HuR (Rajasingh et al., 2006). This is the first study to identify an RNA-binding protein that regulates TNF mRNA decay in muscle. Previous studies focused on the TNF expression in immune responses of haematopoietic cells (Garnon et al., 2005; Wang et al., 2006).

### **3.2 PARN deadenylase is dispensable for rapid decay of TNF mRNA in C2C12 cells**

*In vitro*, CUGBP1 initiated rapid poly(A) tail removal by directly interacting with PARN (Moraes et al., 2006). We were therefore interested to learn whether PARN influences TNF mRNA decay in proliferating myoblasts. To test this, six oligo pairs encoding sequences predicted by The Broad Institute's RNAi Consortium to specifically target the PARN mRNA were subcloned into the pLKO.1puro vector. Again, these were transfected into C2C12 cells, and cells were screened by qRT-PCR and western blot for those exhibiting the best knock-down. The two most effective vectors (#1520 and #2211) from Table 2.3 were chosen for production of infectious lentiviral particles. C2C12 cells were then transduced with PARN-targeting lentivirus, and clonal cell lines were selected. As shown in Figure 6B and C for construct #2211, PARN mRNA and protein levels were both reduced about 85%. We focused our efforts on construct #2211, because cells generated by #1520 failed to differentiate upon serum withdrawal (data not shown).

In the PARN KD cells, there was no detectable difference in TNF mRNA abundance (Figure 6D). As mRNA half-life and abundance do not necessarily correlate (Dolken et al., 2008; Rabani et al., 2011), the rate of TNF mRNA decay was measured in LKO-1 and PARN KD cells. TNF mRNA consistently decayed at the same rate in both cell types (Figure 6E; half-life around 11 minutes in both cases). The fact that PARN knock-down does not affect TNF mRNA half life could be for several reasons. First, it is possible that another deadenylase is acting in its place. As mentioned earlier, there are multiple deadenylases (10 encoded in humans; Garneau et al., 2007). Secondly, PARN was chosen for study based on observations from HeLa cytoplasmic extracts where it is the major active deadenylase, but this may not be the case for C2C12 muscle cells. Alternatively, TNF mRNA may be decayed by a deadenylation-independent route in

Figure 6.



**Knock-down of PARN by shRNA does not change TNF mRNA abundance or half-life.** (A) Schematic of PARN mRNA, ORF as box, lines as UTRs, red line indicates position of targeting shRNA. (B) Abundance of PARN mRNA in (PARN KD) and empty vector (LKO-1) expressing cells determined by qRT-PCR and normalized to GAPDH. (C) Western blot for PARN and GAPDH (loading control) of extracts from LKO-1 and PARN knock-down cell lines. (D) TNF mRNA levels assessed by qRT-PCR from LKO-1 and PARN KD cell lines normalized to GAPDH. (E) Rate of decay for TNF mRNA in the LKO-1 (solid line) and PARN KD cell line (dashed line) was assessed following actinomycin-D treatment. mRNA levels were measured at each time point and normalized to GAPDH.

myoblasts. Finally, the level of PARN knock-down may simply be insufficient to elicit an effect on the half life of the TNF mRNA. On a related note the PARN KD cells generated using shRNA construct #1520 (which showed similar levels of knock down) did exhibit significant stabilization of the TNF mRNA, by about 2-fold (Appendix 2). However, the

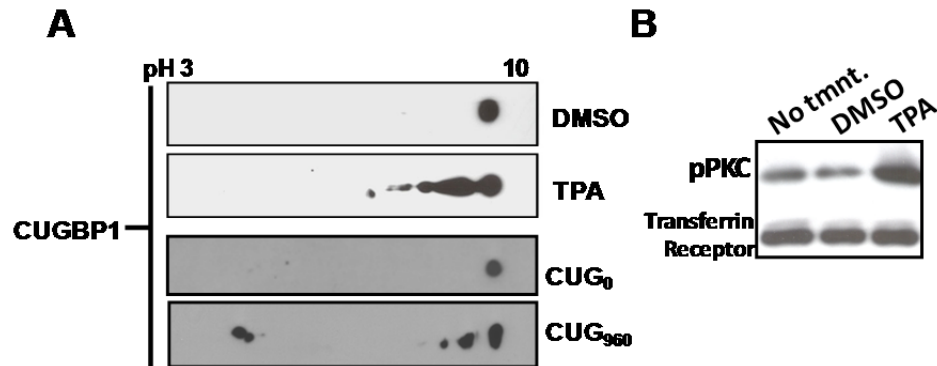
validity of these results is questionable as the finding (1) was not corroborated by an add-back experiment showing a return to normal decay rates and (2) could be the result of an off-target effect as the cells generated using shRNA #1520 failed to differentiate (data not shown).

### **3.3 Protein Kinase C activation increases TNF mRNA abundance and stability**

The experiments described above indicated that PARN is dispensable for rapid TNF mRNA decay. As CUGBP1 was found necessary for rapid decay of the TNF mRNA additional experiments were focused there. We were drawn to a report by the Cooper lab which indicated that CUGBP1 function is altered in DM1 by phosphorylation via activation of the Protein Kinase C (PKC) pathway (Kuyumcu-Martinez et al., 2007). We therefore hypothesized that either expression of CUG-repeat containing mRNAs or PKC activation by treatment with the phorbol ester 12-O-tetradecanoyl-phorbol-13-acetate (TPA) would impact TNF mRNA stability by inducing phosphorylation of CUGBP1. Experiments conducted in our lab by Dr. Libin Zhang showed that transfection of C2C12 cells with an expression plasmid bearing 960 CUG repeats (CUG<sub>960</sub>) within the DMPK 3'UTR (Philips et al., 1998) triggers CUGBP1 phosphorylation, whereas an otherwise identical control plasmid bearing zero CUG repeats (CUG<sub>0</sub>) does not (Figure 7A). Additionally treatment of C2C12 myoblasts with TPA triggers PKC activation (Figure 7B) and a reduction in isoelectric point (pI) of CUGBP1. Interestingly, both repeat RNA and TPA treatment apparently result in multiple phosphorylation events, however the exact number could not be precisely determined as no isoelectric focusing standard was included with the samples. These data are consistent with a phosphorylation event (Dr. Libin Zhang Figure 7A). In DM1 patient cells CUGBP1 is increased in abundance in the nucleus (Kuyumcu-Martinez et al., 2007) but we saw no effect on abundance or

localization of CUGBP1 in C2C12 cells expressing CUG repeat RNA (Dr. Libin Zhang, data not shown).

**Figure 7.**



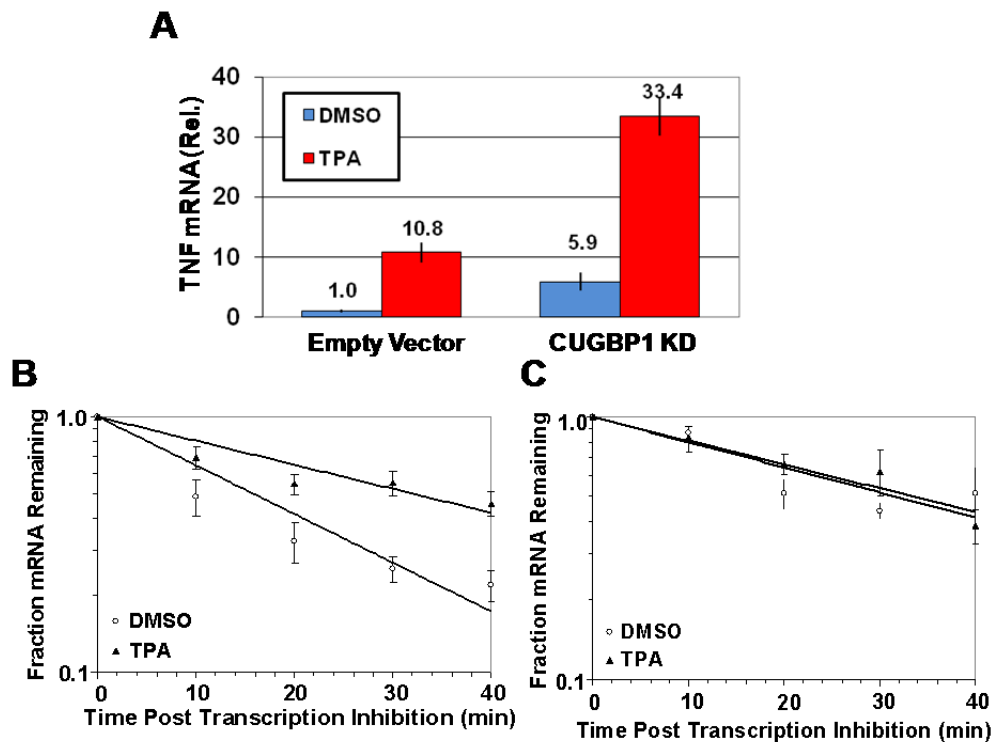
**CUG-repeat RNA expression and TPA treatment result in CUGBP1 phosphorylation.** (A) Extracts from C2C12 cells treated with DMSO or TPA or transfected with 0 or 960 CUG repeat expressing plasmids were subjected to 2D-PAGE followed by western blot for CUGBP1. (B) Western blot of extracts from untreated, DMSO, and TPA treated C2C12 myoblasts probed for active (pPKC) and transferrin receptor as loading control.

### ***3.4 CUGBP1-mediated decay of TNF mRNA is disrupted upon TPA treatment***

To address the effect of PKC activation on TNF mRNA levels and stability we first treated the control LKO-1 myoblasts with TPA or DMSO (solvent only control). TPA treatment resulted in TNF mRNA abundance being increased 10-fold over the levels in DMSO treated myoblasts (Figure 8A). This large increase in mRNA levels indicated that TPA induces TNF expression in C2C12 cells as was reported previously for monocytes (Kelker et al., 1985) but does not distinguish between regulation at transcriptional and post-transcriptional levels. To determine the contribution of changes in mRNA decay to this large increase in steady-state TNF mRNA levels, we assessed TNF mRNA half-life in myoblasts which had been pre-treated for 3 hours with TPA or DMSO. In myoblasts treated with DMSO, the TNF mRNA half-life was  $14.9 \pm 1.2$  minutes, which was slightly longer than in the untreated control myoblasts (Figure 5E). For the TPA treated control cells the TNF mRNA half-life was  $32.7 \pm 2.8$  minutes (Figure 8B).

The two-fold change in stability of the TNF message indicated that upon TPA treatment, at least some of the ten-fold increase in mRNA abundance was due to an increase in mRNA stability. The remainder of the increase in abundance can be attributed to increased rates of transcription. Indeed, TPA treatment has been shown to increase TNF transcription rates in T-lymphocytes (Hoffmeyer et al., 1999) by activating the transcription factor, Activator Protein-1 (AP-1 or Jun; Lee et al., 1987).

**Figure 8.**



**TNF mRNA abundance and stability are increased upon PKC activation in a CUGBP1-dependent manner.** (A) TNF mRNA levels were assessed following TPA or DMSO (carrier) treatment in control, and CUGBP1 knock-down myoblasts by qRT-PCR. (B) TNF mRNA half life following treatment of control cells with TPA or DMSO, and (C) TNF mRNA half life in CUGBP1 KD cells following treatment with DMSO or TPA. In all cases GAPDH was used as the reference mRNA.



To test whether CUGBP1 phosphorylation plays a role in stabilizing TNF mRNA upon TPA treatment we repeated these experiments in our CUGBP1 KD myoblasts. When TPA was added to CUGBP1 KD cells, there was a large increase in TNF mRNA levels (Figure 8A) much as was seen in the LKO1 controls. However, the TNF mRNA half-life was identical in both DMSO and TPA treated CUGBP1 KD cells ( $31.4 \pm 4.1$  minutes for DMSO and  $33.3 \pm 3.0$  minutes for TPA treated cells, Figure 8C).

This result indicates that the TNF transcript was fully stabilized by CUGBP1 depletion, and could not be further stabilized by TPA treatment. Thus phosphorylation or depletion of CUGBP1 have similar effects on TNF mRNA stability. These observations strongly support the idea that phosphorylation of CUGBP1 abrogates its destabilizing activity. Furthermore, it indicates that the ten-fold increase in TNF mRNA abundance observed in TPA treated control cells (Figure 8A) was due to both a transcriptional increase, and disruption of CUGBP1-mediated mRNA decay. The idea that the ten-fold increase is caused by changes in transcription and stabilization, is supported by similar experiments in the CUGBP1 knock-down cells. In the KD cells the TNF mRNA is already stabilized, so the five-fold abundance increase would represent just the transcriptional induction. The effect of TPA treatment on TNF mRNA could be mediated through loss of CUGBP1 binding, or could require recruitment of a stability factor like HuR. This is plausible as HuR has been shown to bind the TNF 3'UTR and regulate mRNA stability in NIH 3T3 fibroblasts (Stoecklin et al., 2003).

Exhaustive attempts were made to measure TNF protein levels in control and CUGBP1 KD myoblasts, DMSO and TPA treated myoblasts, differentiated myotubes, and in media supernatants both by western blot and enzyme-linked immunosorbent assay (ELISA). The levels of TNF protein expressed in C2C12 cells were too low to

permit detection of TNF in these cells. In the future, it would be interesting to determine whether the changes we observed at the mRNA level are reflected in increased TNF protein levels.

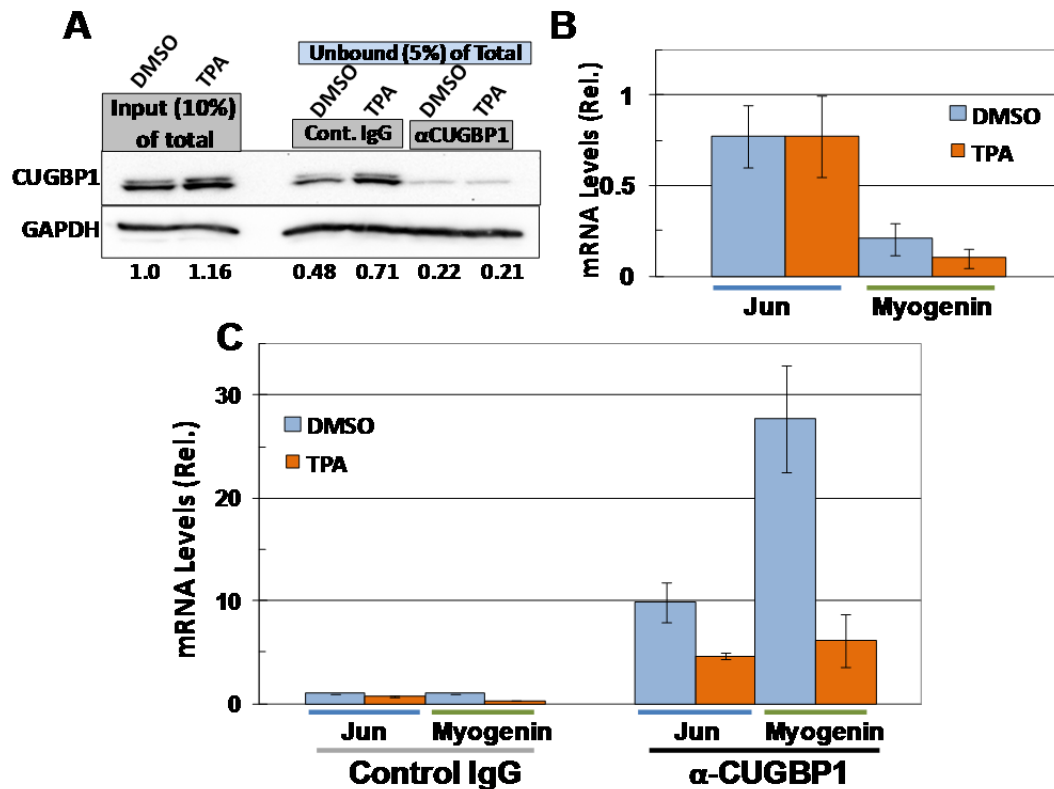
### **3.5 Protein kinase C activation disrupts interaction of CUGBP1 with substrate mRNAs**

As we had demonstrated that TPA treatment of cells results in stabilization of an mRNA target of CUGBP1, and that this event is correlated with CUGBP1 phosphorylation, we next sought to address the possible mechanism by which CUGBP1 loses its ability to destabilize TNF mRNA. One hypothesis was that phosphorylation of CUGBP1 resulted in loss of RNA-binding ability and consequently decreased association with mRNA targets. Alternatively, it could be that phospho-CUGBP1 no longer efficiently recruits PARN and/or other mRNA decay factors. We focused on testing the first hypothesis –that CUGBP1 association with its RNA targets is decreased upon phosphorylation.

We chose an RNA immunoprecipitation (RIP) approach that has been successful for others (Schmidt et al., 2011; Galban et al., 2008; Kawai et al., 2006; Jin et al., 2010). For these experiments we were forced to examine mRNA targets other than TNF, as it was expressed at too low a level for reliable detection in this assay (data not shown). The Jun mRNA was selected because it is bound avidly by the *Xenopus* homolog of CUGBP1, and by human CUGBP1 (Paillard et al., 2002). Myogenin was selected as a muscle-specific and post-transcriptionally regulated mRNA which has extensive UG-rich elements in its 3'UTR (Figuroa et al., 2003; Jin et al., 2010). These elements strongly resemble those previously identified as CUGBP1 binding sites (Vlasova et al., 2008; Rattenbacher et al., 2010).

C2C12 myoblasts were pre-treated for 3 hours with TPA or DMSO, lysed, and the extracts subjected to immunoprecipitation with  $\alpha$ CUGBP1 antibody (3B1) or an equivalent volume of control IgG. Efficient isolation of CUGBP1 from both DMSO and TPA treated cells was confirmed by western blot, (Figure 9A). Associated mRNAs were detected by qRT-PCR.

**Figure 9.**



**Myogenin and Jun mRNAs are associated with CUGBP1 and treatment with TPA reduces CUGBP1 association.** (A) Western blot of lysates from DMSO and TPA treated cells probed for CUGBP1 and GAPDH (loading control). Shown is the relative quantitation of CUGBP1 in each fraction following immunoprecipitation. (B) Levels of Jun and myogenin mRNAs were assessed by qRT-PCR from total RNA samples isolated from DMSO and TPA treated myoblasts. (C) qRT-PCR of bound fractions from negative control IgG and  $\alpha$ -CUGBP1 immunoprecipitation reactions show abundance of each mRNA associated with CUGBP1 normalized to GAPDH mRNA. These experiments were repeated in triplicate and the average of the three independent trials is shown, where error bars represent the pooled standard deviations.

For Jun mRNA the results in cells treated with DMSO were promising in that the transcript was enriched in the CUGBP1 immunoprecipitate, as expected, based on published results from another lab (Paillard et al., 2002). In fact, Jun mRNA shows on

average a ten-fold enrichment in the CUGBP1 immunoprecipitate over the control IgG precipitated samples. There is a marked reduction in the amount of Jun mRNA associated with CUGBP1 in TPA treated extracts (Figure 9C) despite that the overall abundance of Jun mRNA is not affected by TPA treatment (Figure 9A).

Myogenin mRNA also associated with CUGBP1 (Figure 9C). In DMSO treated C2C12 cells, myogenin mRNA was enriched on average 30-fold in the CUGBP1 immunoprecipitate over control IgG. This is exciting as myogenin is a potent transcription factor necessary for muscle differentiation (Parker et al., 1995), which has been shown to be regulated at the post-transcriptional level by the RNA-binding proteins HuR (Figuroa et al., 2003) and RBM24 (Jin et al., 2010). Our result indicates that CUGBP1 may also regulate expression of myogenin and thus impact muscle differentiation. Interestingly, the pretreatment of myoblasts with TPA dramatically reduced the amount of myogenin mRNA associated with CUGBP1 (Figure 9C) even though TPA treatment had a negligible effect on myogenin mRNA abundance (Figure 9B). This indicates that PKC activation may disrupt muscle differentiation through CUGBP1.

As CUGBP1 bound specifically to Jun and myogenin mRNAs, we measured the half-life of these transcripts in our control and CUGBP1 KD myoblasts, but found no significant differences. Jun had a half life of ~12 minutes in both KD and control cell types, and myogenin had a half life of ~1.3 hours in both. CUGBP1 may impact other aspects of mRNA metabolism for these two messages, such as translational efficiency. Alternatively, instability of these critical transcripts may be maintained through multiple redundant pathways such that CUGBP1 knock-down is not sufficient on its own to disrupt their degradation. The fact that multiple RBPs are known to associate with both of these transcripts to regulate their decay is consistent with this possibility (Figuroa et al., 2003; Jin et al., 2010; Paillard et al., 2002).

In summary, we have demonstrated that TNF mRNA has a very short half-life (~10 minutes) in C2C12 cells. This rapid decay requires CUGBP1 activity, as knock-down experiments showed marked stabilization of the TNF transcript. However, PARN depletion had no significant impact on the TNF mRNA. Following activation of PKC, which results in CUGBP1 phosphorylation, TNF mRNA is induced and stabilized in a CUGBP1-dependent fashion. Activation of PKC, a condition observed in DM1 (Kuyumcu-Martinez et al., 2007), disrupts CUGBP1 association with Jun and myogenin mRNAs. Taken together this work underscores a critical gap in the understanding of DM1 and other diseases of muscle. Inappropriate expression of CUGBP1 is strongly correlated with muscle disease, yet the cytoplasmic mRNA targets for which CUGBP1 targets for decay are wholly uncharacterized in muscle.

## ***Chapter 4: Global analysis of mRNA decay reveals the importance of CUGBP1 in muscle cells***

Many of the results presented in Chapter 4 appeared in: Systematic Analysis of Cis-Elements in Unstable mRNAs Demonstrates that CUGBP1 Is a Key Regulator of mRNA Decay in Muscle Cells. PLoS ONE 5(6): e11201.

As we had now demonstrated that CUGBP1 regulated TNF mRNA stability in muscle cells, we sought to identify additional mRNA targets of CUGBP1 in these cells. Our focus was on the role of CUGBP1 in muscle, primarily because it is misregulated in several muscle disorders (FXTAS (Sofola et al., 2007), SBMA (Yu et al., 2009), OPMD (Corbeil-Girard et al., 2005), and DM1 (Philips et al., 1998)). In one mouse model of DM1, a global approach revealed that approximately half of the changes in mRNA abundance were due to sequestration of MBNL1 by CUG-repeat RNA (Du et al., 2010). We hypothesized that some of the remaining changes could be due to aberrant CUGBP1 function. Thus identifying the mRNA targets of CUGBP1 in muscle was a primary goal.

The methods we chose to identify additional mRNA targets of CUGBP1 utilized whole genome microarrays. The approach is two-pronged, employing microarrays to measure mRNA decay rates on a global scale in both control and CUGBP1 KD cells. Comparison of half-life datasets revealed mRNAs exhibiting CUGBP1-dependent decay kinetics. The second approach involves an RNA ImmunoPrecipitation followed by microarray (RIP-Chip) to identify mRNA targets bound by CUGBP1.

Microarray-based strategies have been successful for measuring mRNA decay rates on a global scale in bacteria (Bernstein et al., 2002), yeast (Wang et al., 2002), and mammalian cells (Raghavan et al., 2002; Sharova et al., 2009). These studies have found that abundance and mRNA half-life do not necessarily correlate (Bernstein et al., 2002), that functionally related mRNAs decay with similar kinetics (Wang et al., 2002), and that functionally related messages are co-regulated in response to external cues (Raghavan et al., 2002; Sharova et al., 2009).

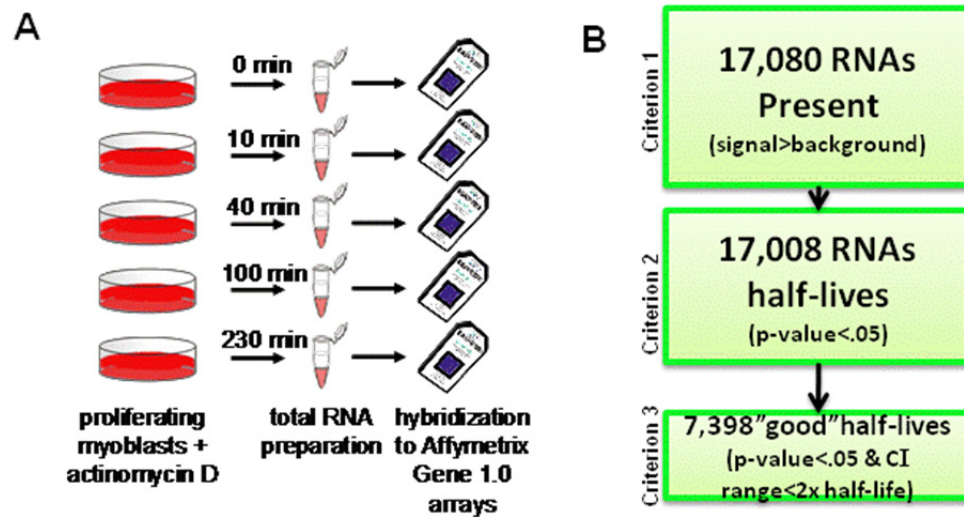
The RIP-Chip approach has identified mRNA targets for regulation by HuR (Mazan-Mamczarz et al., 2008), Pum1 (Morris et al., 2008), TTP (Emmons et al., 2008), and Ago2 (miRNAs; Wang et al., 2010). These studies have yielded significant insight to the cellular roles of mRNA-binding proteins. HuR was implicated in transformation of cells to a tumorigenic phenotype (Mazan-Mamczarz et al., 2008). Pum1 was found to be important for cell cycle regulation (Morris et al., 2008). TTP was associated with many mRNAs encoding factors important for regulating protein synthesis (Emmons et al., 2008). By applying these global approaches to study CUGBP1, significant progress should be made towards understanding mRNA decay in muscle cells in general as well as better characterizing the role of CUGBP1 as a regulator of mRNA decay in this tissue.

#### ***4.1 Global assessment of mRNA decay in muscle cells***

A microarray-based approach (Wang et al., 2002) was used to measure mRNA decay rates in C2C12 LKO-1 muscle cells in triplicate. Similar to the TNF mRNA half-life experiments described in Chapter 3, we utilized actinomycin-D for transcriptional arrest, collected cell samples at 0, 10, 40, 100, and 230 minutes post drug treatment, and isolated RNA (Figure 10A). Total RNA samples were used to generate probes for hybridization to the arrays. This time course was chosen for two reasons: First,

prolonged transcriptional inhibition is toxic to cells (Reich et al., 1961), and second, other studies indicated many post-transcriptionally regulated genes have shorter half-lives (Vlasova et al., 2008; Dolken et al., 2008; Rabani et al., 2011).

**Figure 10.**



**Experimental design for estimation of mRNA half-lives.** (A) Proliferating myoblasts were treated with transcription inhibitor and collected in Trizol at the indicated time points. Total RNA was isolated and used to prepared cDNA probes which were hybridized to Affymetrix Gene 1.0 ST Arrays. (B) Criteria applied to probe intensities for determining reliable half-lives.

For all of the arrays, generation of biotinylated cDNA probes, hybridization, and detection were performed by Erin Petrilli of the Colorado State University Genomics and Proteomics Core. Drs. Bin Tian and Ju Youn Lee at the University of Medicine and Dentistry of New Jersey (UMDNJ)-New Jersey Medical School performed the majority of the bioinformatic analyses described below. Drs. Tian and Lee calculated mRNA half-lives by monitoring diminished fluorescence on each spot on the arrays over the experimental time course, and fitting to a non-linear model as described previously (Wang et al., 2002).

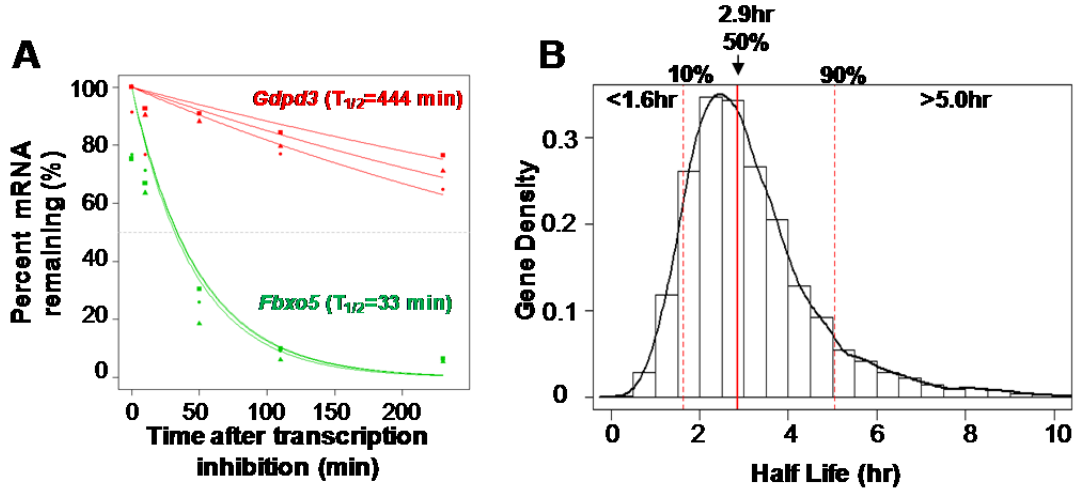


## **4.2 Global mRNA decay features in myoblasts**

In total, 17,080 transcripts were expressed in the C2C12 myoblasts (signal significantly above background in the 0 time point for all three replicates). Half-lives were determined by fitting the data to a first order exponential curve. Highly selective criteria (Fig 10B) were applied to each gene to ascertain that only reliable half lives were reported. First, the decay curve had to be a good fit to the exponential ( $p < 0.05$ ). Second, the range of the 95% confidence interval had to be less than twice the calculated half life. These two criteria had to apply for at least two of the three replicates. 17,008 transcripts met the first criterion (fit well to the exponential curve) and 7,398 of these also met the second criteria (acceptable confidence interval). This represents 41% of the detected mRNAs.

Examples of calculated mRNA decay curves for an unstable (Fbxo5) and stable message (Gdpd3) are shown in Figure 11A. The median half-life of all 7,398 mRNAs was 2.9 hours (Figure 11B) which is somewhat shorter than expected, as other global mRNA decay studies reported medians of ~10 hours for fibroblasts and hepatocytes (Yang et al., 2003), and 7.1 hours for embryonic stem cells (Sharova et al., 2009). We attribute these differences to the stringent criteria that we have used (many genes we have excluded had long half-lives), differences in cell types, and our shorter experimental time course. The lower and upper 10<sup>th</sup> percentiles, at 0-1.6 hours and greater than 5.0 hours, were chosen for in-depth analysis (dashed lines in Figure 11B).

Figure 11.



**Global decay assay yields 7,398 mRNA half-lives in muscle cells.** (A) Change in abundance of representative mRNAs over time as determined by microarray for an unstable (Fbxo5) and stable (Gdpd3) transcript. (B) Distribution plot of the 7,398 reliable half lives from C2C12 cells, red dashed lines indicate the upper and lower 10<sup>th</sup> percentiles and solid line indicates the median.

#### ***4.3 mRNAs involved in cell cycle and ion transport are enriched in short and long-lived mRNAs respectively***

To identify functional relationships between transcripts with similar half-lives Gene Ontology (GO) analyses were performed. For this we focused on the least and most stable transcripts (lower and upper 10<sup>th</sup> percentiles Figure 11B). GO analysis was performed by retrieving assigned GO terms from the NCBI database and comparing the normalized frequency of occurrence for each term in the lowest 10<sup>th</sup> percentile with its normalized frequency in the entire dataset. P-values for GO terms were calculated by Fisher's exact test. Terms with a p-value of <0.05 were considered significantly enriched.

The top 20 GO terms (by significance) for the least and most stable transcripts are listed in Table 4.1. Short half-life messages were enriched for factors involved in cell cycle, transcriptional regulation, and mRNA metabolism. The longest-lived transcripts

were enriched for factors involved in ion transport. These results are similar to those reported in other global mRNA decay experiments which concluded that short half-life mRNAs frequently encode factors which mediate rapid responses to external cues (Miller et al., 2011; Mukherjee et al., 2009; Vlasova et al., 2008). Conversely, long half-life mRNAs encode factors that are typically involved in “house-keeping” functions (Miller et al., 2011).

We were most interested in the unstable messages as they were likely to be dynamically regulated at the level of mRNA stability. For muscle short-lived mRNAs are involved in cell cycle, transcriptional regulation, and mRNA metabolism. As other studies have shown, it is common for mRNAs whose gene products need to be regulated dynamically to have a short half-life (Miller et al., 2011; Vlasova et al., 2008). Global half-life experiments conducted in embryonic stem (ES) cells found that short half-life mRNAs encode factors involved in conversion of stem cells into differentiated cell types (Sharova et al., 2009). For T-cells, short half-life mRNAs encode factors involved in eliciting an immune response (Mukherjee et al., 2009; Vlasova et al., 2008). In yeast, short half-life mRNAs encode factors critical for response to heat-shock or osmotic stress (Miller et al., 2011).

#### ***4.4 Identification of cis-acting elements enriched in the 3'UTRs of short and long-lived transcripts***

To identify sequence elements within the short and long lived transcripts which could be responsible for their decay rate, hexamer analysis of 3'UTRs was performed.

**Table 4.1**

P-value	GO ID, GO Term
<b>Short half life mRNAs</b>	
6.30E-07 (56,14)	GO:0007049,cell cycle
6.07E-06 (31,4)	GO:0006325,establishment or maintenance of chromatin architecture
1.19E-05 (55,17)	GO:0006366,transcription from RNA polymerase II promoter
3.49E-05 (51,16)	GO:0006357,regulation of transcription from RNA polymerase II promoter
6.51E-05 (31,6)	GO:0051276,chromosome organization
1.64E-04 (40,12)	GO:0009892,negative regulation of metabolic process
1.64E-04 (40,12)	GO:0031324,negative regulation of cellular metabolic process
2.78E-04 (16,1)	GO:0016071,mRNA metabolic process
3.39E-04 (35,10)	GO:0010629,negative regulation of gene expression
3.39E-04 (35,10)	GO:0045934,negative regulation of nucleobase, nucleoside, nucleotide and nucleic acid metabolic process
4.00E-04 (38,12)	GO:0010605,negative regulation of macromolecule metabolic process
4.08E-04 (18,2)	GO:0048534,hemopoietic or lymphoid organ development
4.83E-04 (29,7)	GO:0045892,negative regulation of transcription, DNA-dependent
4.83E-04 (29,7)	GO:0051253,negative regulation of RNA metabolic process
4.96E-04 (20,3)	GO:0006396,RNA processing
5.56E-04 (24,5)	GO:0000122,negative regulation of transcription from RNA polymerase II promoter
5.56E-04 (24,5)	GO:0000278,mitotic cell cycle
7.39E-04 (17,2)	GO:0006333,chromatin assembly or disassembly
8.45E-04 (33,10)	GO:0016481,negative regulation of transcription
9.87E-04 (14,1)	GO:0006397,mRNA processing
<b>Long half life mRNAs</b>	
1.63E-08 (36,4)	GO:0006811,ion transport
1.45E-04 (12,0)	GO:0006820,anion transport
1.63E-04 (20,3)	GO:0006812,cation transport
3.06E-04 (11,0)	GO:0015698,inorganic anion transport
1.35E-03 (9,0)	GO:0015674,di-, tri-valent inorganic cation transport
2.82E-03 (8,0)	GO:0006816,calcium ion transport
2.82E-03 (8,0)	GO:0006817,phosphate transport
2.82E-03 (8,0)	GO:0006887,exocytosis
3.11E-03 (17,4)	GO:0007610,behavior
3.11E-03 (17,4)	GO:0044255,cellular lipid metabolic process
3.17E-03 (15,3)	GO:0030001,metal ion transport
4.68E-03 (10,1)	GO:0006836,neurotransmitter transport
4.68E-03 (10,1)	GO:0007268,synaptic transmission
4.68E-03 (10,1)	GO:0008610,lipid biosynthetic process
5.49E-03 (12,2)	GO:0007626,locomotory behavior
5.90E-03 (7,0)	GO:0006631,fatty acid metabolic process
9.08E-03 (15,4)	GO:0046903,secretion
9.82E-03 (13,3)	GO:0019226,transmission of nerve impulse
9.82E-03 (13,3)	GO:0032940,secretion by cell
1.23E-02 (6,0)	GO:0007601,visual perception

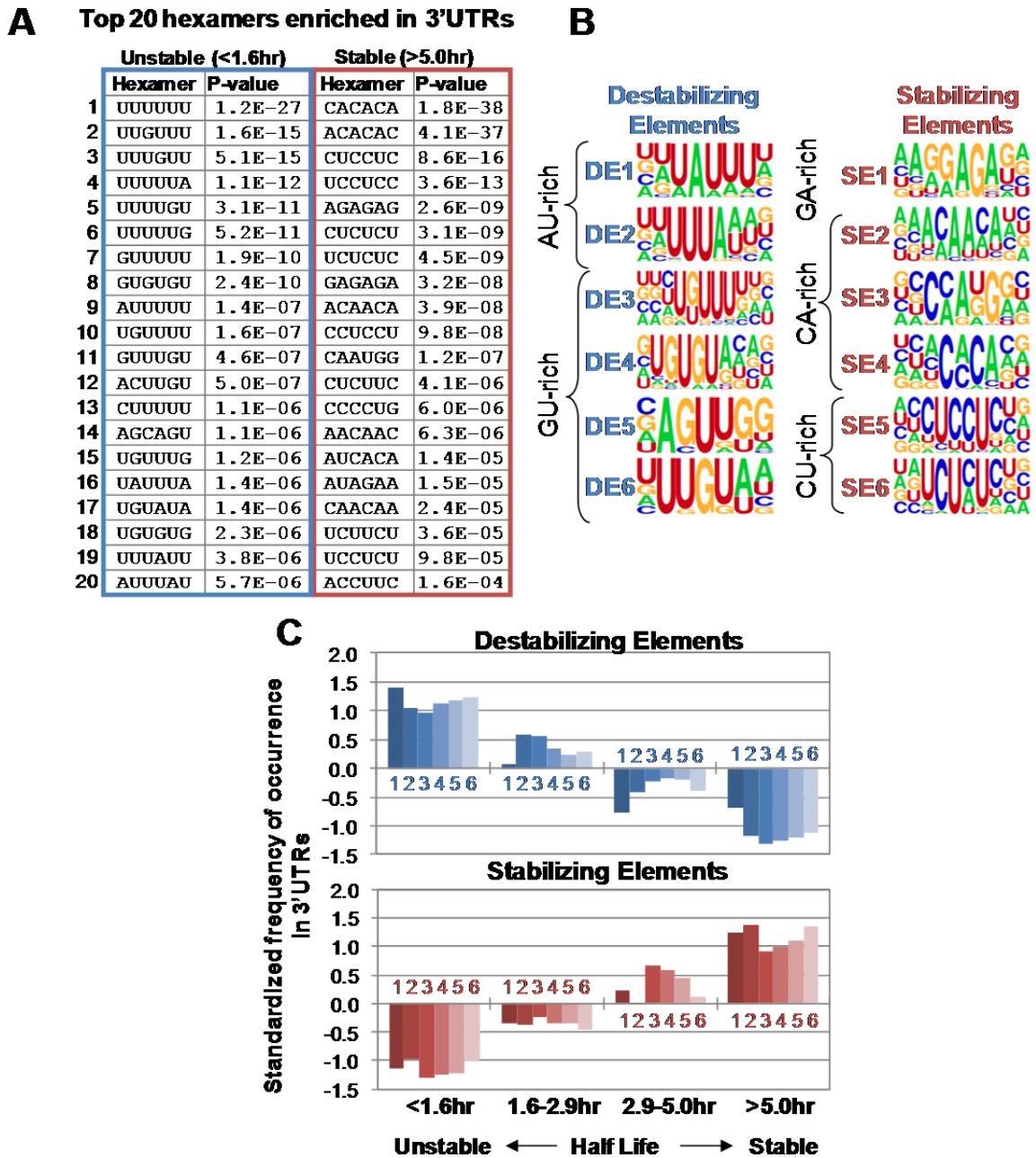
**GO analysis reveals important processes associated with short and long half-life mRNAs.** The top 20 GO terms are shown for the short and long half-life mRNAs. Calculation of p-values was done by Fisher's exact test. The first number in parentheses corresponds to the number of mRNAs for the indicated half-life category, and the second number corresponds to the number of mRNAs for the category of the opposite half-life group.

Briefly, this involved scanning the 3'UTR with a 6 nucleotide window and counting each occurrence of the 4,096 possible hexamers. From there, frequencies of occurrence were compared between the least and most stable mRNAs (bottom 10<sup>th</sup> percentile and the most stable 90-100<sup>th</sup> percentile). P-values were calculated from these observed frequencies using Fisher's exact test (Figure 12A). Significant hexamers were clustered by relatedness of sequence (Appendix 3). Sequence logos were generated (Figure 12B) for clustered hexamers using WebLOGO, as described previously (Hu et al., 2005). These logos are hereafter referred to as Destabilizing or Stabilizing Elements based on the transcripts they were identified from.

Encouragingly, we found that the transcripts with the shortest half-lives (0-10<sup>th</sup> percentile or a half-life of less than 1.6 hours) contained a high frequency of AU and GU-rich sequences within their 3'UTRs (Figure 12A and B). This was promising for several reasons. Firstly, AU-rich elements (AREs) were one of the first mRNA *cis*-elements to be discovered (Shaw and Kamen, 1986) and are often found within notoriously unstable cytokine mRNAs, among others (Emmons et al., 2008; Caput et al., 1986; Miller et al., 2011). Identifying ARE-like sequences (Figure 12, Destabilizing Element (DE)1 and 2) via our hexamer analysis indicated the method was both specific and sensitive.

Identifying GU-rich sequences (DE3-DE6) was even more encouraging. GREs, though more recently discovered than AREs, appear to have an analogous function as regulators of mRNA stability. In addition, GREs are bound by CUGBP1 (Paillard et al., 1998; Vlasova et al., 2008; Goraczniak and Gunderson, 2008). Identification of GREs correlating significantly with mRNA instability in muscle cells potentially links muscle function and post-transcriptional control of mRNAs to CUGBP1, and provides strong

Figure 12.



**Hexamer analysis of unstable and stable mRNAs reveals potential mRNA decay determinants in muscle cells.** (A) The top 20 hexamers (ranked by P-value) enriched in the least and most stable mRNA 3'UTRs. (B) Sequence logos of significantly enriched cis-elements in the least stable transcripts (half life ranking in the bottom 10<sup>th</sup> percentile) and sequence elements associated with the most stable transcripts (top 10<sup>th</sup> percentile). (C) Standardized frequency of occurrence of identified *cis*-elements in mRNA 3'UTRs plotted as a function of half-life category.

support for the idea that post-transcriptional control may be disrupted in DM1 and other neuromuscular diseases.

In contrast to the short-lived mRNAs, the longest lived transcripts (90 -100<sup>th</sup> percentile, or a half life greater than 5.0 hours) harbored GA (Stabilizing Element (SE)1), CA (SE2 and 4), and CU (SE5 and 6) containing elements. These results were exciting as there was literary precedent for each element promoting stabilization of mRNAs. CA elements have been shown to bind the stability factor hnRNP L (Hui et al., 2003), CU repeat-containing mRNAs are stabilized by PCBP1/PCBP2 and the stability factor HuR (Kong et al., 2006; Wein et al., 2003), and GA-containing elements have been shown to stabilize the elastin mRNA (Hew et al., 2000). Overall, the hexamer approach was a specific and sensitive systematic approach to identify putative 3'UTR stability elements in muscle cells.

Next we investigated whether the occurrence of putative stabilizing and destabilizing elements correlated with mRNA half-life (Figure 12C). The occurrences of all significant hexamers (Figure 12A and Appendix 3) were normalized for 3'UTR length and grouped based on what *cis*-element they mapped to in Figure 12B. The resulting normalized frequency of occurrence was plotted as a function of mRNA half-life. Half-lives were grouped as indicated in Figure 12C. This analysis showed that Destabilizing elements are enriched in the 3'UTRs of the shortest lived mRNAs, and occur at a much decreased frequency in very stable mRNAs. Stabilizing elements show the opposite trend. Interestingly, the intermediated half-life mRNAs (1.6-5.0 hours) show some enrichment of both destabilizing and stabilizing elements, indicating that the elements may act combinatorially. This finding is supported by the observation that in some very unstable mRNAs, destabilizing elements are generally repeated multiple times. For

instance the TNF 3'UTR has a Class II ARE consisting of 4 overlapping repeats of AUUUA (Caput et al., 1986).

The process of scanning for enriched hexamers was repeated in the 5'UTR and the coding-sequence. However, no significant enrichment was observed between the identified elements and their frequencies in other regions of the mRNAs. This observation strongly supports the accepted idea that elements which regulate transcript stability are most prevalent in the 3'UTR.

#### ***4.5 CUGBP1 knock-down impacts mRNA decay rates in muscle cells***

At the same time as we conducted the half-life analysis with the control myoblasts, we also performed a parallel analysis with CUGBP1 KD myoblasts. Our goal in doing this was to compare half-lives between the two cell lines to reveal novel mRNAs whose stability was regulated by CUGBP1. Identification of these targets would aid in understanding the CUGBP1-related pathology of DM1. A similar array-based approach revealed CUGBP1 may be important in modulating mRNA stability in stimulated immune cells (Vlasova et al., 2008).

The CUGBP1 KD dataset was generated and analyzed in an identical fashion to the control myoblast dataset described previously. There were 14,619 transcripts present; half-lives were calculated for 14,505 mRNAs (good match to the exponential curve  $p < 0.05$  for two out of the three replicates). Transcripts were omitted, where the range of the 95% confidence intervals was greater than twice the half-life (Criterion 3 Figure 10B) leaving just 959 mRNAs half-lives. This was just 6.5% of the mRNAs present and far fewer than the 7,398 half-lives obtained for the control. Finally, only 924 genes had reliable half-lives in both the control and CUGBP1 KD dataset. Reasons for

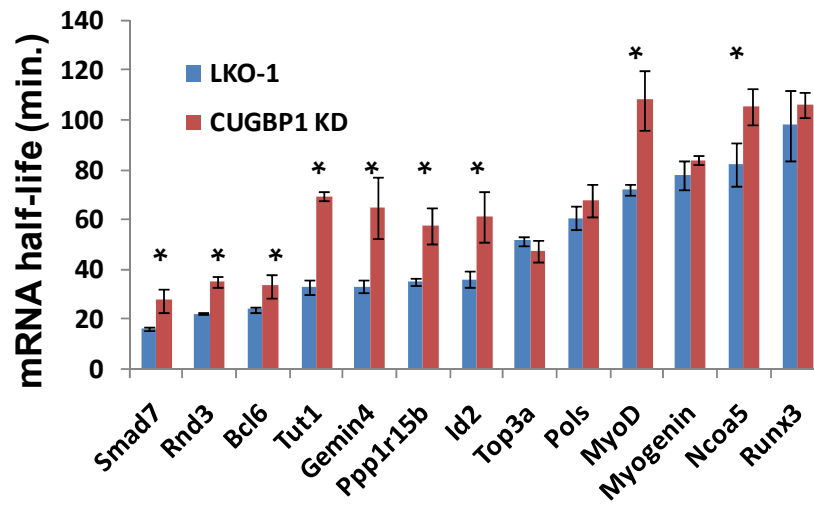


the increased variability in the CUGBP1 KD dataset are not clear, as the experiment was done in parallel with the control set. One possibility is that the knock-down cells were differentiating precociously leading to unwanted variations in gene expression between the replicates. This idea is based on the fact that we later found dramatic differences in differentiation of the knock-down cells (see below).

Differentially stabilized genes were identified by comparing the average calculated half-lives from the three CUGBP1 KD replicates to the average obtained from the three control cell replicates. Student's T-test was used to calculate p-values within similar sets and significant differences in half-life were noted when the p-value was less than 0.05. In total, we identified 480 transcripts whose half-lives had increased significantly in the CUGBP1 KD cell line compared to the control (Appendix 4) These half-life increases ranged from 5.3-fold stabilized to 1.2-fold stabilized. Surprisingly, no mRNAs showed a significant decrease in half-life in the CUGBP1 KD cells.

From the analysis of our control data, we had identified a set of short lived transcripts bearing GREs. We hypothesized that these GREs could be functioning as CUGBP1 binding sites. As such, these GRE-containing transcripts were likely to be stabilized by CUGBP1 KD. To test this hypothesis and to validate the microarray data, stabilities of 13 transcripts were examined by qRT-PCR. In total, 9 out of 12 mRNAs stabilized in the CUGBP1 KD cells by microarray analysis were also stabilized by qRT-PCR (Figure 13 and Appendix 5). Of the 9 stabilized genes, 5 of them (MyoD, Rnd3, Smad7, Ppp1r15b, and Id2) bear hexamer sequences that match to the GU-rich DEs from Figure 12.

Figure 13.



**CUGBP1 knock-down stabilizes a subset of mRNAs in muscle cells.** Half-lives of indicated mRNAs were determined in LKO-1 and CUGBP1 KD cell lines by linear regression of qRT-PCR data from half-life experiments. Error bars represent the standard deviation. Myogenin was chosen as a negative control as it showed no change in stability by array, and here, by qRT-PCR. Decay curves for each mRNA can be found in Appendix 5.

These results demonstrate that CUGBP1 impacts the decay of mRNA targets other than TNF in muscle. MYOD, ID2, RND3, and SMAD7 all are factors important for myogenesis (Fortier et al., 2008; Melnikova et al., 1999; Miyake et al., 2010; Rudnicki et al., 1993), and our results show that decay of the mRNAs encoding them is dependent on CUGBP1. We conclude that CUGBP1 has a significant role in regulating gene expression in muscle. However, since only five of the nine stabilized mRNAs we examined had GU-rich elements in their 3'UTRs, CUGBP1 KD may also have indirect effects on mRNA decay or be recruited to other sequence elements.

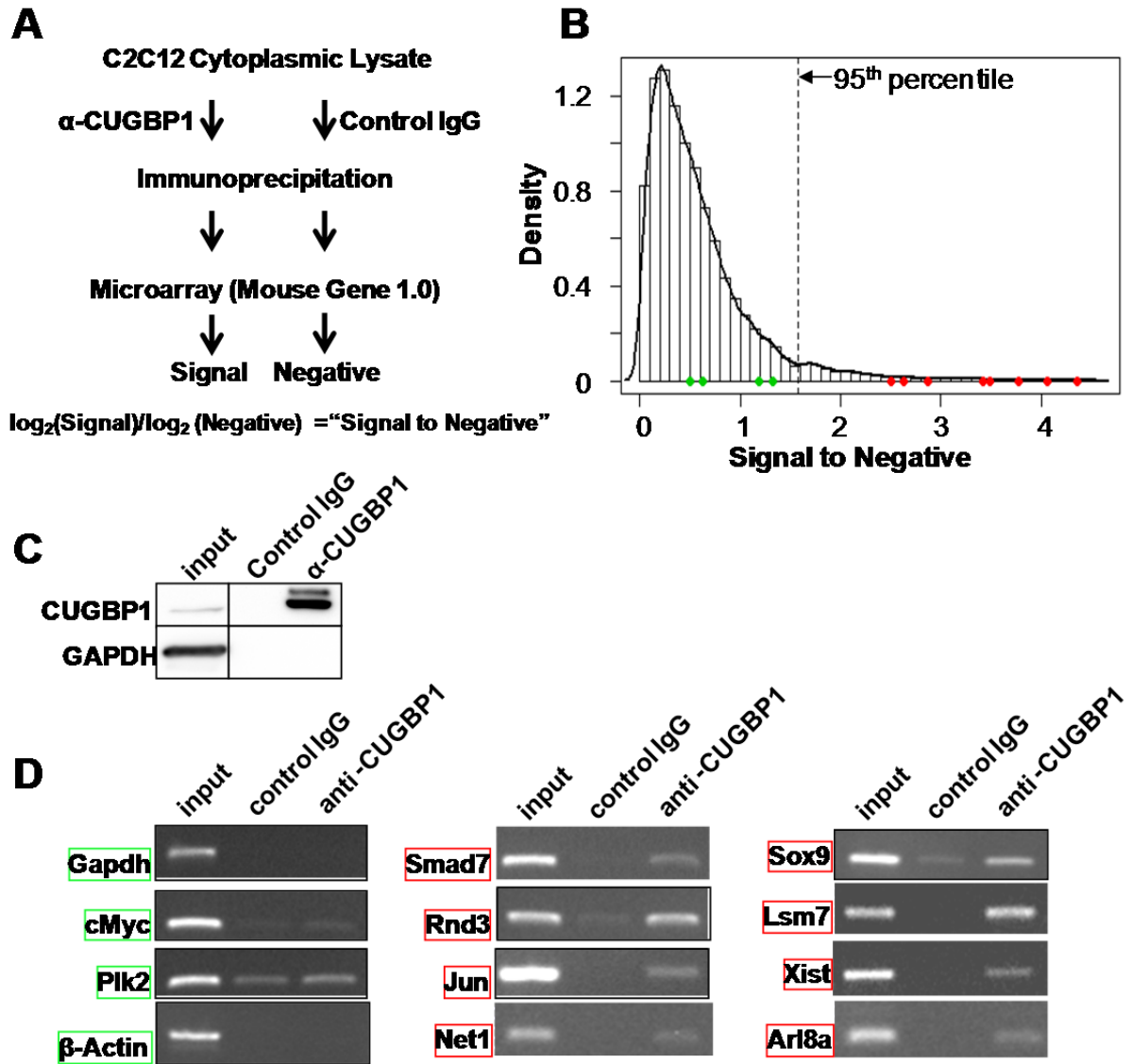
#### **4.6 Identification of direct mRNA targets of CUGBP1 in muscle cells**

In the preceding section, comparisons between half-life data sets from CUGBP1 KD and control cells identified 480 transcripts stabilized in the CUGBP1 KD cells. The methods used to identify these 480 transcripts made no distinction between direct and

indirect mRNA targets of CUGBP1. We therefore sought to identify direct mRNA targets of CUGBP1 in muscle cells. To do this on a global scale we performed a well characterized RIP-Chip protocol (Tenenbaum et al., 2002).

RNAs bound by CUGBP1 were immuno-purified from C2C12 cytoplasmic lysates using anti-CUGBP1 monoclonal antibody 3B1 (Santa Cruz Biotechnology). As a negative control an equal volume of non-specific mouse IgG antibody was used. Column resins were washed extensively in ice cold NT-2 buffer (Chapter 2) and RNAs were eluted by addition of Trizol. Following confirmation of specific and efficient pull-down (by western blot and qRT-PCR for Jun and myogenin mRNAs), total RNA was prepared from input, CUGBP1 bound, and control IgG bound samples. RNA (100ng each) from two independent experiments was used to generate probes for hybridization to microarrays (Affymetrix Gene 1.0 ST). RNAs that were bound in the  $\alpha$ -CUGBP1 immunoprecipitate were compared to those in control mouse IgG immunoprecipitate. Transcripts were ranked by ratio of the  $\alpha$ -CUGBP1 signal to control mouse IgG signal (Signal to Negative, Figure 14A). The top 5% of these (881 transcripts see Appendix 6) were defined as being bound specifically by CUGBP1 (Figure 14B). Several of these targets have been validated by RT-PCR (Figure 14C).

Figure 14.



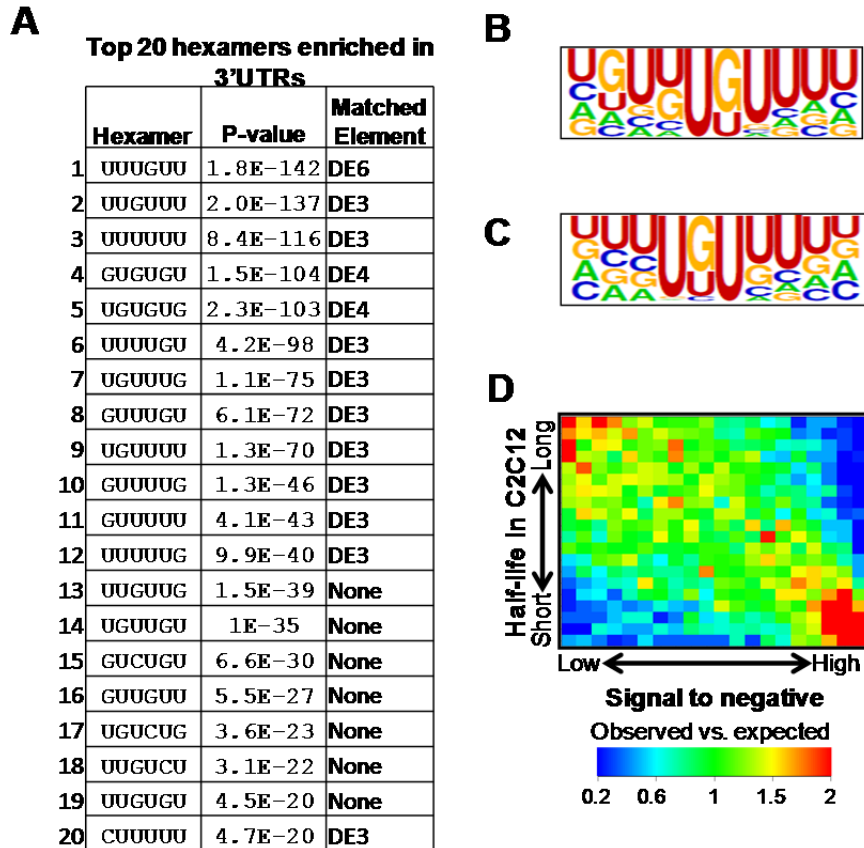
**Identification of novel mRNA targets of CUGBP1 in muscle cells.** (A) Experimental approach to identify direct mRNA targets of CUGBP1 from myoblast lysates. (B) Gene densities were plotted as a function of the mean ratio of the CUGBP1 immunoprecipitate signal to control IgG immunoprecipitate signal (Signal to Negative). 95<sup>th</sup> percentile is indicated by a dashed line, corresponding colored dots indicate where RT-PCR samples from D lie in the analysis. (C) Western blot probed for CUGBP1 and GAPDH (loading control) indicates specificity and efficiency of protein pull-down. (D) Ethidium bromide stained 2% agarose gels of RT-PCR from CUGBP1 and control mouse IgG immunoprecipitation (remaining panels). Colored boxes correspond to position of dots on chart in panel B.

#### ***4.7 CUGBP1 binds GU-rich element containing and unstable mRNAs in muscle cells***

We used a hexamer analysis similar to that described above to identify enriched sequences in the CUGBP1 associated transcripts. The 3'UTRs of the transcripts associated with CUGBP1 (upper 95<sup>th</sup> percentile of the Signal to Negative ratio) were scanned using a 6-base window. The number of occurrences of each hexamer was counted. Fisher's exact test was used to identify hexamers significantly enriched in the "bound" set as compared to the unbound set of transcripts. This approach identified enriched hexamers which are generally U-rich within the CUGBP1 associated 3'UTRs (Figure 15A). The top 50 significant hexamers were clustered and the highest ranking group (by mean of p-values) was used to generate a sequence logo using WebLOGO (Figure 15B and Appendix 7). The hexamers and the sequence logo shown in Figure 15B very closely match with CUGBP1 binding sites identified in other cell types (Marquis et al., 2006; Rattenbacher et al., 2010; Vlasova et al., 2008). We hypothesized that a significant fraction of the 480 transcripts stabilized in the CUGBP1 KD half-life arrays were stabilized due to loss of CUGBP1 binding. Shared transcripts between the significantly stabilized group from the CUGBP1 KD dataset, and the top 5% of the signal to negative ratio of the CUGBP1 RIP-Chip dataset were identified. In total 88 transcripts were common between the two groups (Appendix 8). Hexamer analysis, clustering, and a sequence logo were generated from this set of transcripts as well (Appendix 9). The resulting sequence logo (Figure 15C) is nearly identical to those generated from the CUGBP1 IP dataset. We conclude that this represents the canonical CUGBP1 binding site in muscle. The 88 transcripts common between datasets are mRNAs that are both bound by CUGBP1 and regulated at the level of mRNA stability. These are likely only a

subset of the CUGBP1 targets given the small size of the CUGBP1 KD half-life dataset, but nevertheless are highly likely to be regulated by CUGBP1 in muscle cells.

Figure 15.



**CUGBP1 binds GU-rich element containing mRNAs, correlating with rapid decay in muscle cells.** (A) Top 20 hexamer sequences (ranked by p-value) enriched in the 3'UTR of genes found in 95<sup>th</sup> percentile and higher (bound) from the CUGBP1 RIP-Chip (signal-to-negative ratio). Matching sequence element from Figure 12, is given. (B) Corresponding sequence logo generated from the most-significant group of RIP-Chip hexamers after clustering. (C) Sequence logo from the hexamer analysis of the 88 immunoprecipitated and stabilized transcripts. (D) Heat map comparing the half-life data from control myoblasts (y-axis) to the CUGBP1 RIP-Chip data (x-axis) where enrichment is shown in red and depletion in blue.

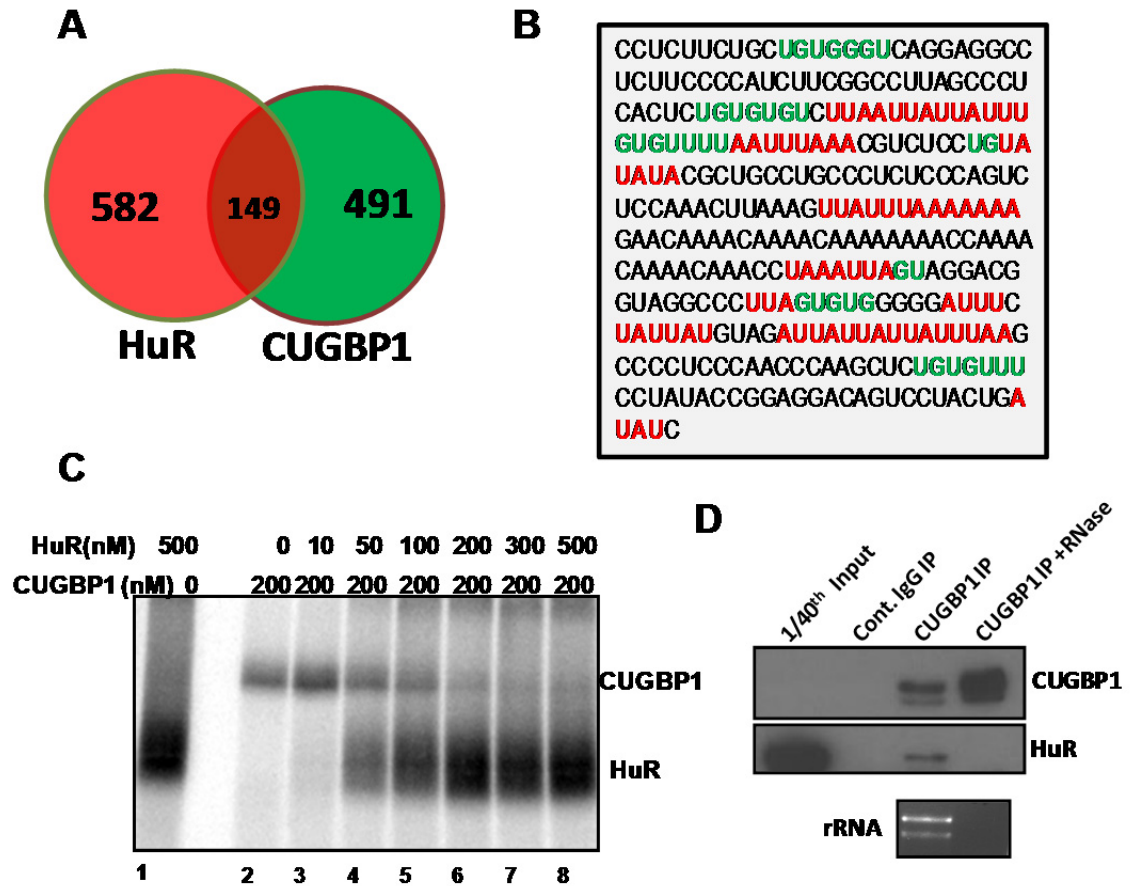
CUGBP1 has been reported by us (Moraes et al., 2006; Zhang et al., 2008) and others (Paillard et al., 1998; Rattenbacher et al., 2010; Vlasova et al., 2008) to destabilize the mRNAs it binds. To address whether this is a general phenomenon in muscle cells, we compared our global half-life data from the control myoblasts to our

RIP-Chip data of “bound” mRNAs (Figure 15C). The half-life and RIP-Chip datasets were each divided at every 5<sup>th</sup> percentile, based on rank. Half-lives were assigned to the y-axis and Signal to negatives from the RIP-Chip were assigned to the x-axis. Each box of the resulting 20x20 matrix was assigned a color (red for enrichment, blue for depletion) based on the observed number of genes which fell in that box, versus number expected if the partitioning were random (Figure 15D). This reveals that short-lived transcripts in muscle (low on the y-axis) tend to be bound by CUGBP1 (far right on the x-axis). The opposite is also true; long-lived transcripts (high on y-axis) are less likely to be bound by CUGBP1 (far left on x-axis). Overall, this shows that CUGBP1 binding correlates with instability in muscle cells.

#### ***4.8 CUGBP1 and HuR bind common mRNA targets in muscle cells***

With a set of CUGBP1 target transcripts in hand we had achieved one of our primary goals. Upon examining the hexamers and sequence logos over-represented in CUGBP1 bound mRNAs, we noticed that they closely resembled those recognized by the stabilizing factor HuR (Dormoy-Raclet et al., 2007; Mukherjee et al., 2009; Ray et al., 2009; Vlasova et al., 2008). To test whether the two proteins might bind common mRNA targets, a recently published HuR RIP-Chip dataset from human T-lymphocytes (Mukherjee et al., 2009) was compared to our list of CUGBP1-bound mRNAs using Ingenuity Pathway Analysis (Figure 16A). Of our 881 identified targets, 640 could easily be compared to the HuR dataset as they had common gene identifiers in humans. Comparison of the 640 CUGBP1 targets with the 731 HuR targets revealed that 23% of mRNAs bound by CUGBP1 in C2C12 cells were bound by HuR in lymphocytes (Mukherjee et al., 2009). This result was perhaps not surprising, given the related nature of the sequences the two proteins recognize.

Figure 16.



**CUGBP1 and HuR bind common RNA targets.** (A) Venn diagram showing the overlap of mRNAs bound by both CUGBP1 and HuR as determined by RIP-Chip experiments (Lee et al., 2010; Mukherjee et al., 2009). (B) Sequence of the first 336nt of the p21 3'UTR, GU-rich sequences in green, and AU-rich sequences in red. (C) UV-crosslinking of radiolabeled p21 3'UTR with recombinant HuR alone and with CUGBP1 protein. (D) Western blot of CUGBP1 immunoprecipitates probed for CUGBP1 and HuR (top panels), and ethidium bromide stained formaldehyde agarose gel of RNA isolated from immunoprecipitated reaction supernatants (bottom panel).

To follow up on this *in silico* result we utilized an *in vitro* approach to examine binding of HuR and CUGBP1 to one putative shared substrate mRNA –p21/Cdkn1a. Similar experiments were used to characterize the interactions of HuR and CUGBP2 with the Cox2 ARE (Sureban et al., 2007). p21 is an important factor in muscle whose expression peaks early in the differentiation process and promotes cell cycle withdrawal (Parker et al., 1995). Moreover, the first 336nt of the p21 3'UTR harbors extensive AU



and GU-rich elements (Figure 16B). Radiolabeled p21 3'UTR RNA was incubated with 200nM GST-CUGBP1 and increasing amounts of 6XHis-HuR, heparin was added, and stable complexes were cross-linked with 254nm light. This mixture was RNase treated and resolved by 10% SDS-PAGE. Both HuR and CUGBP1 could be cross-linked to the RNA efficiently (Figure 16C). However based on the loss of CUGBP1 cross-linking as the concentration of HuR is increased, the two proteins appear to compete for RNA-binding *in vitro* (Figure 16B lanes 3 and 4). This is consistent with these two factors sharing a binding site(s) within the p21 3'UTR. These results indicate that CUGBP1 may also compete with HuR for mRNA substrates during differentiation much like AUF1 does to regulate muscle differentiation (Lal et al., 2004).

We next examined whether HuR and CUGBP1 also share substrate mRNAs in myoblasts. C2C12 lysates were immunoprecipitated with anti-CUGBP1 antibodies, and the immunoprecipitates were probed for CUGBP1 and HuR by western blotting (Figure 16D). HuR was clearly detected in the CUGBP1 immunoprecipitates, but RNase treatment of the lysates prior to immunoprecipitation disrupted the interaction. The effectiveness of RNase treatment was confirmed by visualization of rRNA (lower panel Figure 16D). Therefore, although HuR and CUGBP1 probably do not interact directly, they are able to bind the same RNA simultaneously.

#### ***4.9 CUGBP1 binds transcripts encoding factors involved in cell cycle and mRNA metabolism***

Given the target overlap between CUGBP1 and HuR (Figure 16), the well-documented role for HuR in muscle differentiation (Figuroa et al., 2003; Lal et al., 2004), and the involvement of CUGBP1 in muscle diseases, we speculated that CUGBP1 function was also critical in muscle specific processes. As with the global half-

life experiments, GO analysis of the RIP-Chip dataset yielded insights into CUGBP1 regulated processes. GO terms enriched in CUGBP1-associated transcripts were compiled. At first glance, the enriched GO terms that were most interesting were cell cycle and RNA processing (Table 4.2).

**Table 4.2**

<b>P-value</b>	<b>GO ID, GO Term</b>
5.60E-15	GO:0007049, cell cycle
5.07E-13	GO:0046907, intracellular transport
6.51E-13	GO:0008104, protein localization
1.11E-12	GO:0051641, cellular localization
7.98E-11	GO:0048522, positive regulation of cellular process
1.01E-10	GO:0048523, negative regulation of cellular process
1.46E-10	GO:0050793, regulation of developmental process
1.02E-09	GO:0006996, organelle organization
3.66E-09	GO:0009887, organ morphogenesis
7.94E-09	GO:0007242, intracellular signaling cascade
1.72E-08	GO:0006915, apoptosis
1.05E-07	GO:0000278, mitotic cell cycle
1.31E-07	GO:0009790, embryonic development
2.20E-07	GO:0006396, RNA processing
2.22E-07	GO:0016192, vesicle-mediated transport
4.20E-07	GO:0040007, growth
6.54E-07	GO:0065008, regulation of biological quality
1.64E-06	GO:0008283, cell proliferation
3.66E-06	GO:0000087, M phase of mitotic cell cycle
1.73E-05	GO:0000279, M phase

**CUGBP1 binds mRNAs encoding factors involved in the cell cycle and mRNA metabolism.** Top 20 GO terms associated with CUGBP1 bound mRNAs (by P-value ranking).

As the terms used in the NCBI GO database are vague and somewhat arbitrary, they were manually broken down into more descriptive terms (Table 4.3). For example, “RNA processing” from Table 4.2 was sub-divided into RNA Binding, RNA Splicing, and RNA Decay. The CUGBP1-bound transcripts that fell into these categories are listed. This table (Table 4.3) reveals that CUGBP1 binds to transcripts involved in muscle homeostasis, which is of great interest considering its role in DM1. Additionally, many of the RNAs bound by CUGBP1 encode other RNA-binding proteins. This cross-regulation amongst RNA-binding proteins has been documented previously and is likely a common

occurrence (Pullmann, Jr. et al., 2007). As we were interested in muscle differentiation we also focused on CUGBP1-associated mRNAs which encode factors involved in that process.

**Table 4.3**

<b>Gene Ontology of mRNAs that directly associate with CUGBP1</b>	
<b>Gene Ontology</b>	<b>mRNAs that immunoprecipitate with CUGBP1</b>
<b>RNA-Binding</b>	ELAVL1 (HuR), Pum1 (Pumilio), hnRNP A3, hnRNP K, hnRNP A1, PABPN1, PABPC4, RBM5, RBM9, RBMS1, CUGBP1, CUGBP2, LARP1, RBM3, ROD1
<b>mRNA Splicing</b>	ASF/SF2 (SFS1), SRp20 (SFRS3), SRp40 (SFRS5), SF1, RNPS1, UAP56 (BAT1A), CUGBP1, CUGBP2
<b>mRNA Decay</b>	Lsm6, Lsm7, Lsm8, Lsm12, Lsm14a, Cnot6 (Ccr4), CUGBP1, CUGBP2
<b>Protein targeting to ER and protein processing in the ER</b>	<i>SRP components: Srp54b, Srp68, Srp72</i> <i>Translocon Components: Tram1</i>
	<i>Translocon Associated Protein Complex: Ssr1,</i> <i>Signal Peptidases: Spcs2</i>
	<i>Signal Peptide Peptidase: Sppl3</i> <i>Oligosaccharyltransferase: Stt3a, Dad1,</i> <i>Krtcap2</i>
	<i>ER Glycoprotein Chaperones: Calr</i> <i>(Calreticulin), Canx (Calnexin)</i>
<b>Muscle development and function</b>	<i>Transcription Regulators: MyoD1, Myog, Sox9,</i> <i>Mef2D, Six4, Epc1</i>
	<i>Others: Cdon, Kras, p38MAPK<math>\alpha</math> (Mapk14),</i> <i>Chrna1, Mylip, Cdkn1a (p21<sub>Waf1</sub>), Rnd3, Smad7</i>
<b>Non-coding RNAs</b>	Xist, H19, Rny1, SnorD22
<b>Tubulins</b>	Tuba1c, Tubb2a, Tubb3, Tubb5

**CUGBP1 binds mRNAs encoding factors involved in mRNA metabolism, differentiation, and protein secretion.** GO terms of interest from the standpoint of post-transcriptional control and muscle homeostasis found to be enriched in mRNAs that interact with CUGBP1 by RIP-Chip.

One of the novel CUGBP1 regulated processes identified by this GO analysis is protein targeting to the ER (Srp components). Furthermore, cellular structure (tubulins)

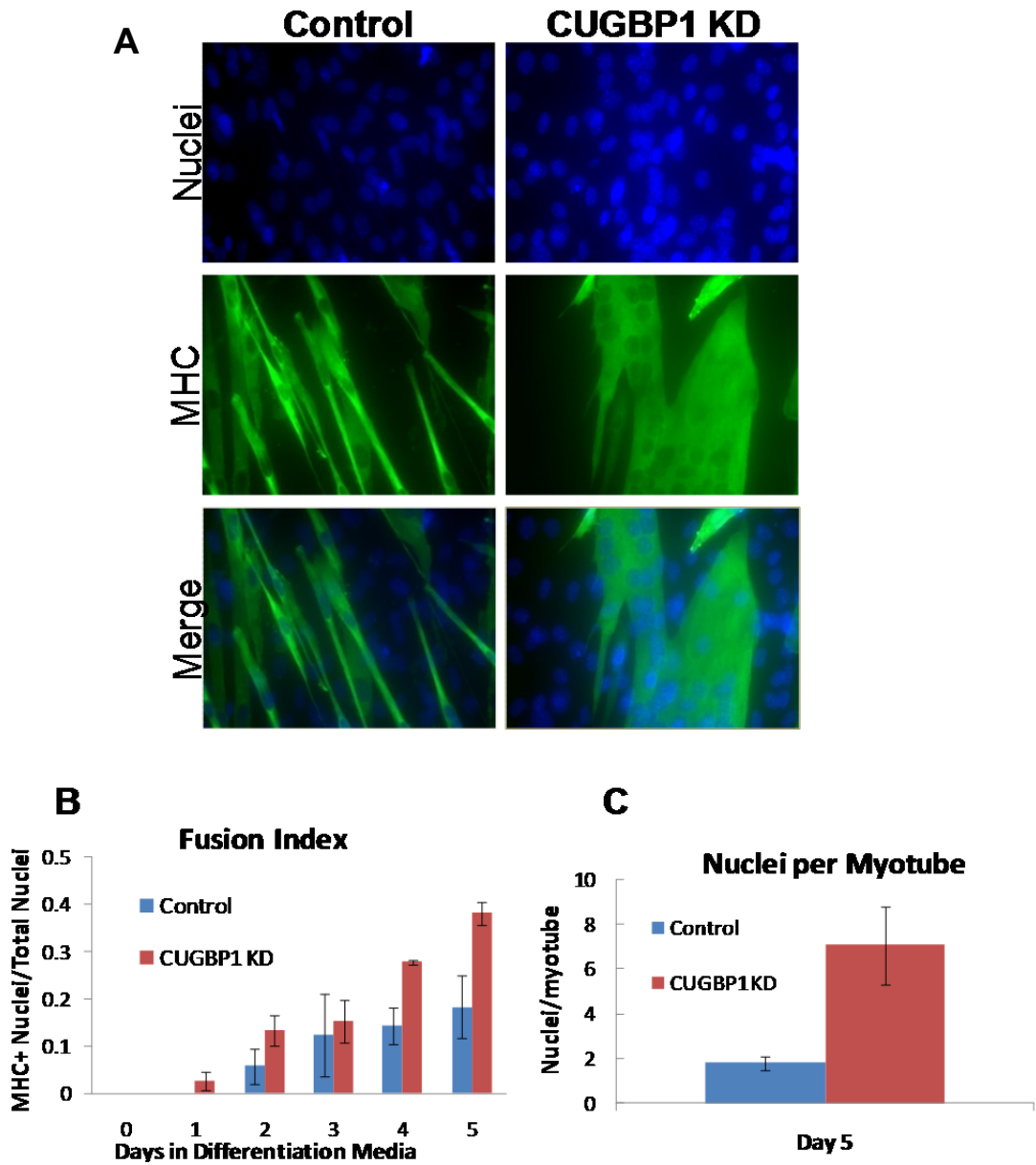
and non-coding RNAs are also apparently regulated by CUGBP1. It will be interesting to learn how CUGBP1 is involved in all of these processes.

#### ***4.10 CUGBP1 is required for muscle differentiation***

A primary goal at the start of this project was to further characterize mRNA decay in muscle and determine the involvement of CUGBP1. The RIP-Chip experiment identified many CUGBP1-bound mRNAs encoding factors important for muscle differentiation (Table 4.3). We therefore sought to address the impact of CUGBP1 on myoblast differentiation. The process of muscle differentiation can be observed quite simply in C2C12 cultures by growing to near confluence and switching to a low-serum media (2% horse serum) triggering spontaneous differentiation to myotubes (Andres and Walsh, 1996).

Control and CUGBP1 KD myoblast cell pools were generated by lentiviral transduction and puromycin selection with empty vector and CUGBP1 targeting vector (see Materials and Methods 2.11). Knock-down was as effective as in the clonal cell line established previously (data not shown). Cells were induced to differentiate, and samples collected daily throughout the differentiation process. Immunofluorescence against the differentiation marker myosin heavy chain (MHC shown in green in Figure 17A) was used to track differentiation (Andres and Walsh, 1996). Differentiation was quantified by calculating a fusion index. This involved counting MHC positive nuclei and dividing by total nuclei per field of view. As seen in Figure 17B, the CUGBP1 KD myoblasts showed MHC positive nuclei earlier, indicating that they initiated differentiation more rapidly (Days 1 and 2). Additionally, they displayed a disorganized differentiation phenotype. Instead of forming long thin myotubes with aligned nuclei (as is common and the controls show) the CUGBP1 KD myoblasts form broad poorly-

Figure 17.



**CUGBP1 plays a role in muscle differentiation.** (A) Immunofluorescence microscopy of day 5 myotubes from control and CUGBP1 KD cell pools (nuclei were stained with DAPI and are colored blue, MHC was detected with monoclonal antibody MF20, and Cy-2 goat anti-mouse conjugated secondary antibody (colored green). (B) Fusion index in control and CUGBP1 KD cells (average of 3 independent experiments where error bars represent the standard error). (C) Average number of nuclei per MHC positive myotube compared between day 5 CUGBP1 KD and control cells (average of 3 random fields of view from 3 independent experiments, where error bars represent the standard error from the mean).

organized syncytia or myosacs (Figure 17A). This is clearly quantified in Figure 17C, where the numbers of nuclei per myotube are compared. There is a large increase in

nuclei per myotube in the CUGBP1 KD compared to empty vector controls. As this phenotype occasionally arises spontaneously these results were confirmed by repeating these differentiation experiments in a different clonal cell line that utilized the same 1739 shRNA, and in an alternatively transduced pool of cells made using the #1320 shRNA that targets a different region of the CUGBP1 mRNA (Appendix 10). Both of these cell lines gave a similar phenotype.

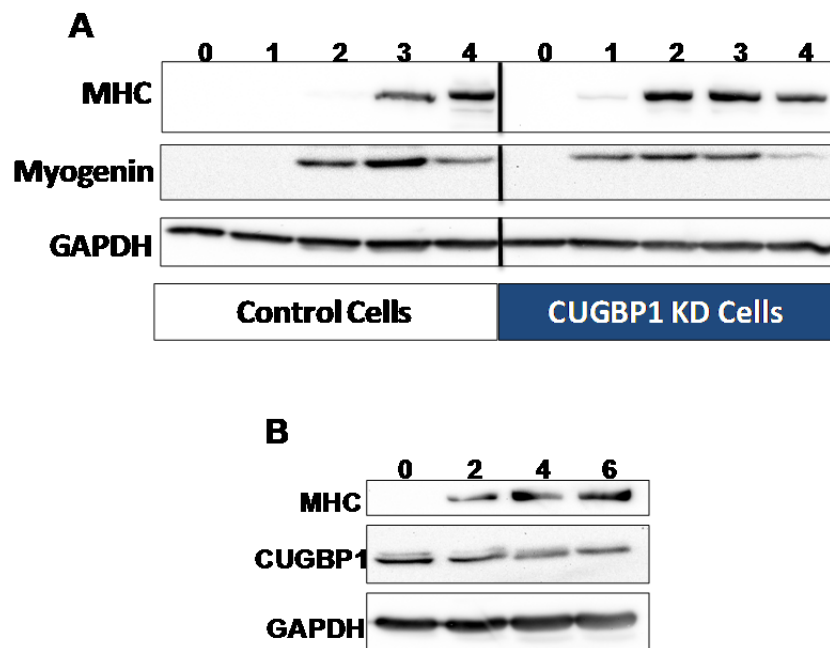
There are many possible explanations for the myosac phenotype which likely reflects cytoskeletal disorganization. One CUGBP1 target mRNA Rnd3 (RhoE) encodes a small GTPase required for differentiation (Fortier et al., 2008). RhoE regulates RhoA which is responsible for organization of actin filaments during differentiation of C2C12 myoblasts (Castellani et al., 2006). Thus one could imagine that aberrant expression of RhoE in CUGBP1 KD cells might lead to defects in the cytoskeleton. In addition, TPA treatment of C2C12 cells, which we have shown induces CUGBP1 phosphorylation, also induces myosac formation (Mermelstein et al., 1996). Finally, disruption of microtubules with nocodazole results in formation of myosacs, thus it may be relevant that CUGBP1 is associated with several tubulin mRNAs (Table 4.3).

#### ***4.11 CUGBP1 plays an important role in muscle differentiation***

As the previous experiment indicated, the CUGBP1 KD cells appeared to be initiating differentiation more rapidly than the control myoblasts (see Figure 17B days 1 and 2). To address this possibility differentiation was monitored by western blot to examine expression of myogenin, a marker of muscle differentiation. Whole cell lysates were collected from control and CUGBP1 KD myoblasts and probed for the differentiation markers MHC and myogenin. In good agreement with our microscopy data we observed that CUGBP1 KD cells expressed MHC at an earlier time during

differentiation (Figure 18). In addition, the transcription factor myogenin was also expressed at an earlier time. This result is significant, because expression of myogenin signals the end of myoblast proliferation (Katagiri et al., 1997). Premature expression of myogenic factors like myogenin results in depletion of progenitor cells necessary for maintenance of muscle in adult tissue, as well as muscle hypotrophy (Schuster-Gossler et al., 2007).

**Figure 18.**



**CUGBP1 levels are important for appropriate expression of differentiation factors.**  
 (A) Western blot of whole cell lysates collected from myoblasts induced to differentiate in low-serum media for the indicated number of days (number above lane). Samples were probed for the presence of the differentiation markers MHC and myogenin, as well as a GAPDH as loading control. (B) 35µg of whole cell lysate was resolved on 10% SDS-PAGE, blotted and probed for MHC and CUGBP1 during differentiation (day indicated at top of lane), GAPDH is a loading control.

The relationship between onset of differentiation, and absence of CUGBP1 led us to wonder how CUGBP1 expression changed during the process of normal myoblast differentiation. To address this question, western blots of whole cell lysates from normal

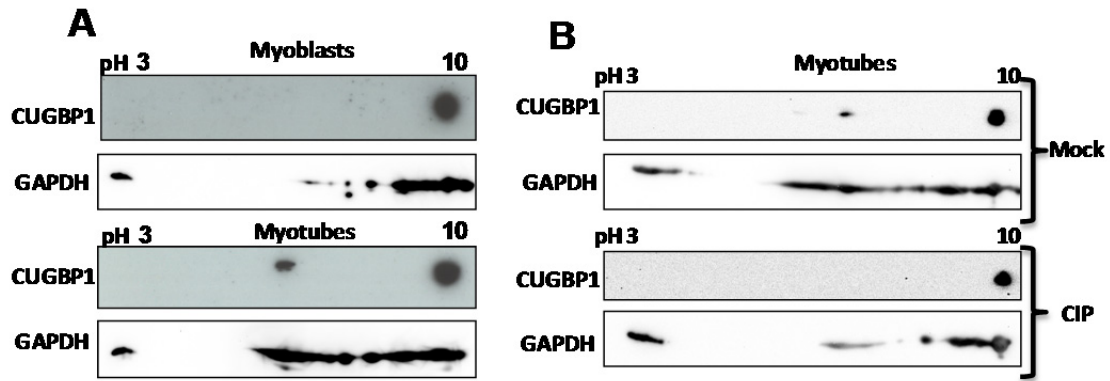
myoblasts induced to differentiate were probed for CUGBP1 levels (Figure 18B). These showed that CUGBP1 protein levels decrease as the cells are differentiating, similar to a finding in a report published during the course of this study (Bland et al., 2010). qRT-PCR analysis of CUGBP1 mRNA indicated that levels dropped ~80% between proliferating and 6-day differentiated cultures (*J. Allredge* personal communication). A previous report indicated that murine CUGBP1 is down-regulated by the miRNAs miR23a and miR23b in developing cardiac tissue (Kalsotra et al., 2008). This data provides a strong correlation between reduction in CUGBP1 protein levels, and increased expression of the differentiation markers MHC and myogenin.

#### ***4.12 CUGBP1 is phosphorylated upon myotube formation***

Finally, as the phosphorylation status of CUGBP1 is modulated upon expression of CUG repeat RNA or PKC activation (Figure 7) and in DM1 patients (Kuyumcu-Martinez et al., 2007) we wondered if this were the case in differentiating muscle. To address this possibility C2C12 myoblast cultures were again induce to differentiate. Cells were collected and lysates prepared for isoelectric focusing, and 2<sup>nd</sup> dimension PAGE. Samples were blotted and probed for CUGBP1 and GAPDH as a loading control. Interestingly, CUGBP1 exhibits a shift in isoelectric point (pI) in the 5 day differentiated myotubes (Figure 19A lower panel). This phosphorylated species was not present in the proliferating cultures. GAPDH was multiply phosphorylated as was also shown in another study (Choudhary et al., 2000). To confirm that what we observed was indeed a phospho-state of CUGBP1, these same extracts were treated with phosphatase (CIP) and CUGBP1 then migrated at a single pI similar to that predicted for unmodified protein (Figure 19B).



Figure 19.



**CUGBP1 is phosphorylated in myotubes.** (A) Western blot for CUGBP1 and GAPDH loading control from 2D-PAGE on whole cell lysates of proliferating myoblast cultures (top) and 5 day differentiated myotube cultures (bottom). (B) Western blot for CUGBP1 and GAPDH of 2D-PAGE on whole cell lysates from differentiated myotube cultures mock treated (top) or calf intestinal phosphatase treated (bottom).

In addition, samples isolated at different times during differentiation were also subject to 2D-PAGE, revealing that the phosphorylated species appeared as myotubes formed (data not shown). These results indicate that phosphorylation of CUGBP1 occurs during the process of muscle differentiation. Interestingly, the relative amounts of phosphorylation observed here (Figure 19) and in response to TPA treatment or CUG repeat RNA expression seem to be rather distinct. During differentiation, only a small fraction of CUGBP1 is phosphorylated, whereas the other conditions appear to elicit phosphorylation of a much larger proportion of the protein. These results indicate that phosphorylation of CUGBP1 in DM1 is likely distinct from CUGBP1 phosphorylation during myotube formation. This is perhaps expected as DM1 conditions result in PKC activation and CUGBP1 phosphorylation (Kuyumcu-Martinez et al., 2007) while differentiation involves different kinase pathways from PKC (Akt/PI<sub>3</sub>, p38 MAPK, and Erk6; Lechner et al., 1996; Li et al., 2000; Xu and Wu, 2000)

To summarize, a great deal has been learned about mRNA decay and CUGBP1. In these studies we have identified important elements for decay, and what RNA sequences CUGBP1 recognizes. Targets for CUGBP1 regulation have been identified in muscle, and CUGBP1 differentiation defects have been observed. Finally, we have documented the expression characteristics of CUGBP1 in normal myoblasts induced to differentiate. These studies will serve as a solid foundation for future endeavors looking at post-transcriptional control of mRNAs in muscle.

## ***Chapter 5: Global analysis reveals mRNA substrates for decay by PARN in myoblasts***

There is strong evidence that PARN is critical for survival in plants (Reverdatto et al., 2004), for oocyte maturation in *Xenopus*, (Kim and Richter, 2006) and in the response to DNA damage in mammalian cells (Cevher et al., 2010). Nevertheless, very few specific targets of this, or any other deadenylase have been identified. We hypothesized that PARN is recruited to a specific subset of mRNAs by RNA-binding proteins such as CUGBP1 (Moraes et al., 2006) and KSRP (Gherzi et al., 2004). A global approach to identify mRNAs that are dependent on PARN for their catabolism was undertaken. We chose to use C2C12 cells in order to allow comparison with the control and CUGBP1 KD datasets described in the previous sections.

### ***5.1 PARN knock-down disrupts decay rates for a subset of mRNAs in C2C12 cells***

Given that PARN had been implicated in the regulation of mRNA decay both on its own (Reverdatto et al., 2004) and in conjunction with CUGBP1 (Moraes et al., 2006), we carried out global half-life array experiments with our PARN KD cell line (Figure 6). These experiments were carried out in an identical manner to those described previously for the control and CUGBP1 KD cells. Briefly, transcription was inhibited by actinomycin-D treatment and total RNA was collected at 0,10,40,100, and 230 minutes after transcriptional arrest. Lastly probes for array hybridization were generated from 300ng of total RNA. The results were analyzed by Drs. Bin Tian and Ju Youn Lee at UMDNJ-New Jersey Medical School. There were 19,385 transcripts detected in the PARN KD cells,

which is slightly more than the control (17,080) and CUGBP1 KD (14,619) datasets (13% and 32% more respectively). Half-lives were calculated for the 19,385 transcripts, those with a p-value greater than 0.05 were omitted, leaving 19,162 mRNAs. Ninety-five percent confidence intervals were calculated for these 19,162 half lives. Transcripts where the range of the confidence intervals was over 2 times the calculated half-life for two of the three replicates were omitted. This left 1,581 mRNAs with a “reliable” half-life. These transcripts were compared to the control dataset, leaving 1,389 genes with “reliable” half lives in both sets.

Next we sought to identify mRNAs whose stability had changed significantly in the PARN KD cells. Half-lives were compared between the control and PARN KD myoblasts. As with the previous datasets, Student’s t-test was used to determine significant differences in decay rates between the control and PARN KD cells. Surprisingly, this yielded a mere 64 mRNAs whose half-lives had changed significantly (Table 5.1). Forty of these mRNAs showed an increase in stability ranging from 2.4-fold to 1.2-fold stabilized. Many of the stabilized transcripts encode RNA-binding proteins (LIN37, ZFP36L2 (BRF2), TOE1 (CAF1Z) and EDC3) and transcription factors (GATA4, ZFP219, KLF14, and NUFIP1). This relatively small number of stabilized mRNAs is perhaps unsurprising when the number of cellular deadenylases is kept in mind (10 are predicted for humans). In the absence of PARN it is likely that other deadenylases substitute for its function to some degree, or that more transcripts undergo deadenylation-independent decay. This idea is supported by the fact that the greatest increase in stability was 2.4-fold (ADORA2B).

**Table 5.1**

Significantly stabilized mRNAs in PARN KD cells				
Gene Name	Control HL (min)	PARN KD HL (min)	Fold Change	p-value
<b>Adora2b</b>	80	189	2.4	2.70E-02
Lin37	107	240	2.2	4.32E-02
Mrgprf	125	279	2.2	4.21E-02
Mat2a	52	111	2.1	3.73E-03
Gnb1l	73	145	2.0	1.94E-02
<b>Ptpn3</b>	145	262	1.8	2.07E-02
Ankrd54	112	201	1.8	7.00E-03
Gpsm1	149	265	1.8	3.87E-03
Klf16	102	176	1.7	3.24E-02
1300010M03Rik	88	151	1.7	2.66E-02
Caly	246	421	1.7	4.11E-02
Nsun5	160	270	1.7	4.41E-02
<b>Zfp36l2</b>	58	97	1.7	2.75E-02
Xkr8	117	194	1.7	1.92E-02
Kcnk5	89	146	1.6	3.88E-02
Anapc7	129	208	1.6	1.84E-02
Polm	220	340	1.5	4.56E-02
Kcnn4	103	158	1.5	2.19E-02
Rnf122	96	144	1.5	1.98E-02
<b>Jtv1</b>	156	233	1.5	4.29E-02
Tacc2	109	159	1.5	4.62E-02
<b>Rfxap</b>	109	159	1.5	4.91E-02
Toe1	71	102	1.4	6.02E-03
Trip10	110	159	1.4	3.12E-02
Nufip1	68	99	1.4	3.25E-02
Sipa1l2	134	193	1.4	4.82E-02
Zfp219	134	193	1.4	1.37E-02
Cdk5r1	88	125	1.4	4.24E-02
<b>Itpr1l1</b>	179	251	1.4	4.57E-02
Akirin2	75	106	1.4	2.05E-02
Gata2	114	159	1.4	4.63E-02
<b>Traf2</b>	71	98	1.4	3.60E-02
<b>Tbc1d10a</b>	134	184	1.4	3.34E-02
Dgcr14	97	133	1.4	2.88E-02
Psrc1	115	158	1.4	3.50E-02
<b>Zbtb45</b>	96	129	1.3	1.41E-02
<b>Edc3</b>	76	100	1.3	9.91E-03
Gfer	119	151	1.3	4.30E-02
Fadd	128	153	1.2	9.53E-03
Stx5a	104	124	1.2	2.67E-02

Significantly destabilized mRNAs in PARN KD cells				
Gene Name	Control HL (min)	PARN KD HL (min)	Fold Change	p-value
Sema4f	410	153	-2.7	4.72E-02
<b>Tnfaip3</b>	73	32	-2.3	2.04E-02
<b>Rnf144b</b>	285	127	-2.3	1.94E-02
Clk1	49	22	-2.2	2.83E-02
Psg29	536	263	-2.0	1.52E-02
<b>Ccdc99</b>	136	83	-1.6	2.20E-02
<b>Phlda1</b>	52	32	-1.6	1.84E-03
Ngf	83	52	-1.6	3.58E-02
3010003L21Rik	214	138	-1.6	2.02E-03
<b>Gdf15</b>	163	107	-1.5	3.95E-03
Snapc1	150	101	-1.5	7.73E-03
<b>Foxc2</b>	50	35	-1.4	1.22E-03
<b>Zcchc7</b>	110	77	-1.4	2.75E-02
<b>Dusp16</b>	92	66	-1.4	4.97E-02
Chchd4	97	70	-1.4	6.61E-03
<b>Nanp</b>	91	66	-1.4	1.22E-02
<b>Hist3h2a</b>	55	40	-1.4	3.42E-02
<b>4732471D19Rik</b>	80	60	-1.3	4.49E-02
Eif1b	134	101	-1.3	1.41E-02
<b>2310057M21Rik</b>	87	66	-1.3	3.94E-02
Prmt6	125	98	-1.3	4.02E-02
Thra	63	52	-1.2	3.94E-02
<b>Tmem171</b>	132	115	-1.2	2.42E-02
<b>Rabif</b>	84	74	-1.1	3.16E-02

**Transcripts exhibiting altered decay rates in PARN knock-down myoblasts.** Global half-life approach reveals 64 mRNAs exhibiting altered stability upon PARN KD. Impacted transcripts are listed with their corresponding half-lives. Transcripts shown in red were stabilized in the CUGBP1 KD dataset. Destabilized mRNAs bearing an ARE are shown in bold and underlined.

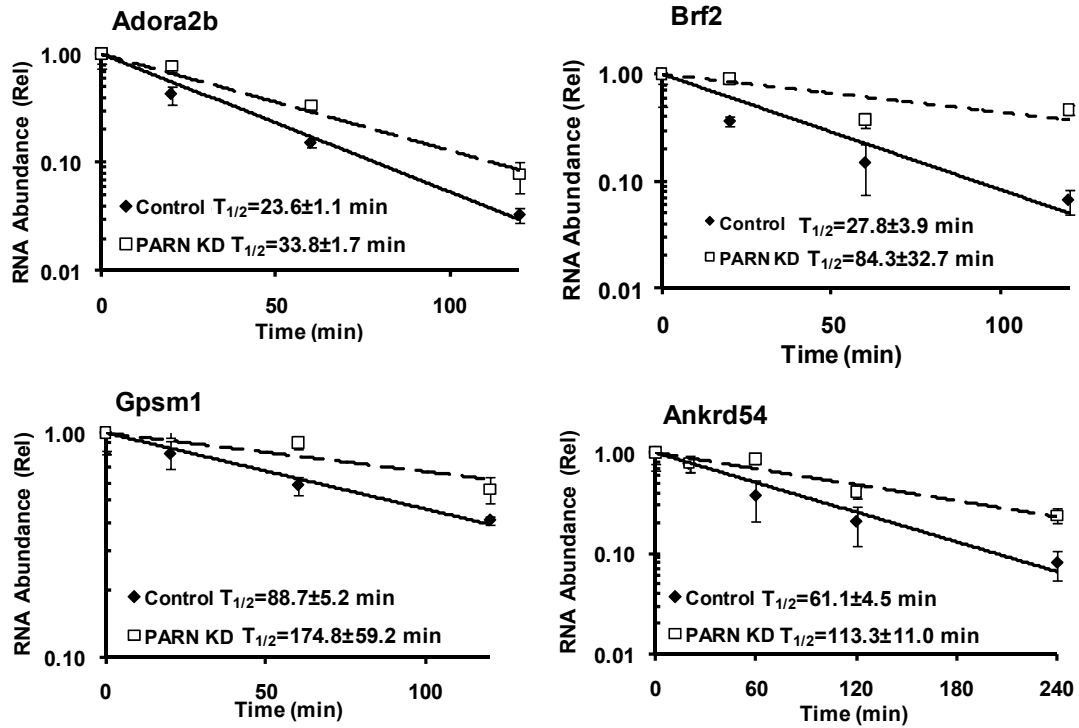
Unexpectedly, 24 mRNAs showed a significant *decrease* in stability ranging from 1.1-fold to 2.5-fold destabilized in the PARN KD dataset. We speculate that this is due to indirect effects of PARN KD. For example PARN KD could result in stabilization of an mRNA encoding a destabilizing factor. In fact, this is observed for the Edc3 mRNA, which is stabilized 1.3-fold, and encodes a factor which recruits the decapping enzyme DCP1/2 to mRNA substrates (Badis et al., 2004; Fenger-Gron et al., 2005). Zfp3612 (Brf2) mRNA, is also stabilized (1.7-fold) in PARN KD cells (Table 5.1). Closely related homologues of BRF2 (TTP and BRF1) have been shown to mediate decay of ARE-containing transcripts by recruiting CNOT6 and DCP2 (Lykke-Andersen and Wagner, 2005). If this factor is limiting in normal myoblasts, but is increased in PARN KD cells, it might acquire additional targets, or act more effectively on its normal targets. In support of this idea, 11/24 destabilized transcripts harbor an ARE (Table 5.1 bold and underlined; Bakheet et al., 2006).

Comparisons between the 40 genes exhibiting increased stability in the PARN KD and the 480 stabilized transcripts in the CUGBP1 KD cell line, showed little overlap (10 transcripts in total shown in red Table 5.1). This indicates that CUGBP1 and PARN are not exclusive partners in triggering deadenylation of CUGBP1-substrate RNAs in muscle. However, given the relatively small datasets for the two factors, the possibility of them co-regulating decay of a significant number of substrates has certainly not been ruled out.

As before, we validated the findings from the microarrays. Transcription was shut off by actinomycin-D treatment and qRT-PCR was performed to monitor mRNA decay rates in control and PARN KD cells (Figure 20). Encouragingly, all four of the mRNAs tested upheld the trend predicted by the microarray results, and were stabilized in the

PCR-based assay. These stabilized mRNAs therefore represent the first reported endogenous targets for regulation by PARN in mammalian cells.

**Figure 20.**



**Validation of mRNAs exhibiting PARN-dependent mRNA decay rates.** Decay rates in control and PARN KD myoblasts of mRNAs identified by global half-life approach measured by qRT-PCR. Representative experiments are shown. Half-lives ( $T_{1/2}$ ) are reported with corresponding standard deviations.

## 5.2 PARN knock-down alters poly(A) status of Brf2 mRNA

As demonstrated by the microarray experiments, and in Figure 20, PARN is necessary for normal decay rates of a subset of mRNAs. We next sought to address the mechanism for this regulation. As PARN has deadenylase activity, we chose to start with the simplest hypothesis: that PARN levels impact the poly(A) status of the Brf2 mRNA. Brf2 mRNA was chosen as it was over three-fold stabilized by qRT-PCR. In addition, as mentioned BRF1 is important for ARE-mediated decay, and the Tis11/TTP family

members, BRF1 and BRF2 share homology at their N-termini, where the interactions with decay machinery (DCP1, DCP2, CNOT6) likely occur (Lykke-Andersen and Wagner, 2005). BRF2 knockout mice die within two weeks of birth due to failed haematopoiesis (Stumpo et al., 2009) and cells lacking both BRF1 and BRF2 resemble T-lymphoblast leukemic cells (Hodson et al., 2010). For these reasons we concluded that BRF2 is an important mediator of mRNA decay, and that disruption of PARN function may impact the expression of BRF2 and thereby affect expression of other genes.

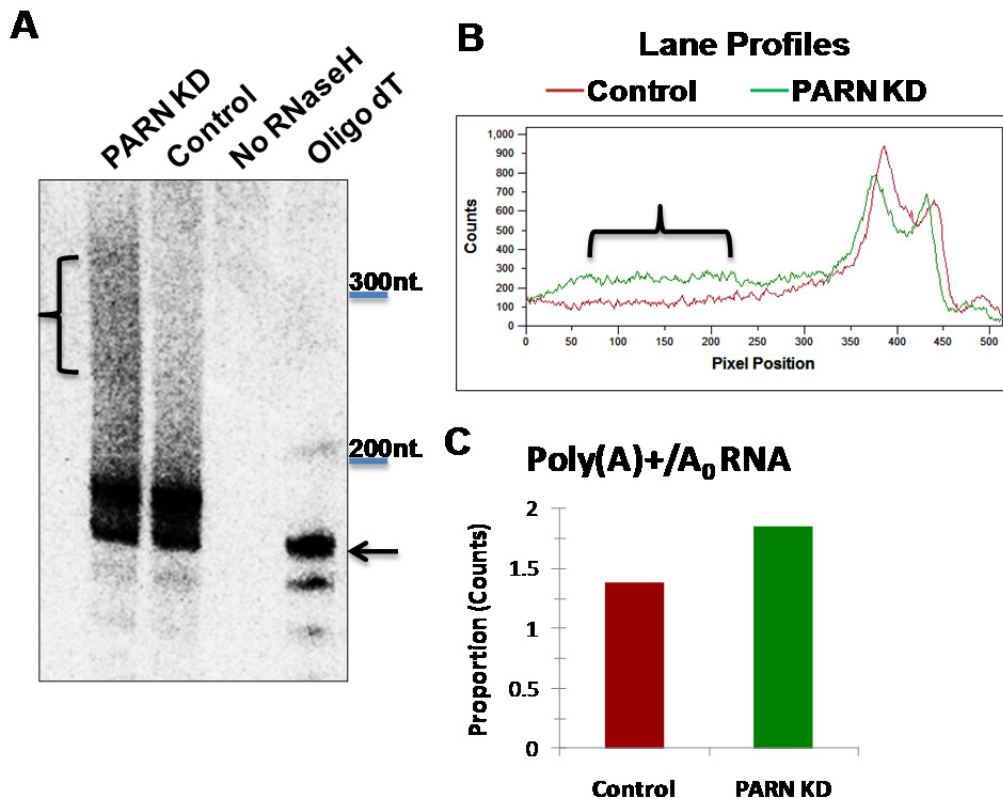
To test the poly(A) tail length of Brf2 mRNAs, an RNase H/northern blot was employed. Briefly, 10µg of total cellular RNA was annealed with a DNA oligonucleotide complementary to the 3'UTR of Brf2 and treated with RNaseH. Brf2 mRNA was detected by northern blotting using a probe specific for the 3' UTR. As shown in Figure 21A, treatment with the Brf2-specific DNA oligo and oligo-dT<sub>18</sub> generates a poly(A) minus band (A<sub>0</sub>) at ~170nt (see arrow). The expected length from the RefSeq database is 168nt. The control lane (treated only with Brf2 specific oligo) shows a higher molecular weight smear corresponding to the last 168nt of the Brf2 message plus the poly(A) tail. When control and PARN KD samples are compared there is a greater proportion of poly(A)<sup>+</sup> species with a long poly(A) tail in the PARN KD (see brackets in Figure 21A). This observation is further supported by profiles of the pixel density in each lane (Figure 21B) and by quantitation of the proportion of poly(A)<sup>+</sup> RNA to deadenylated RNA (Figure 21C). Thus we conclude that the Brf2 poly(A)-status is dependent on levels of PARN.

To confirm that the altered poly(A) status of the Brf2 mRNA observed in PARN knock-down myoblasts was specific to the Brf2 transcript, RNaseH/northern blots were repeated for the β-actin mRNA. As before, 10µg of total cellular RNA was annealed with a DNA oligonucleotide complementary to the 3'UTR of actin and treated with RNaseH.



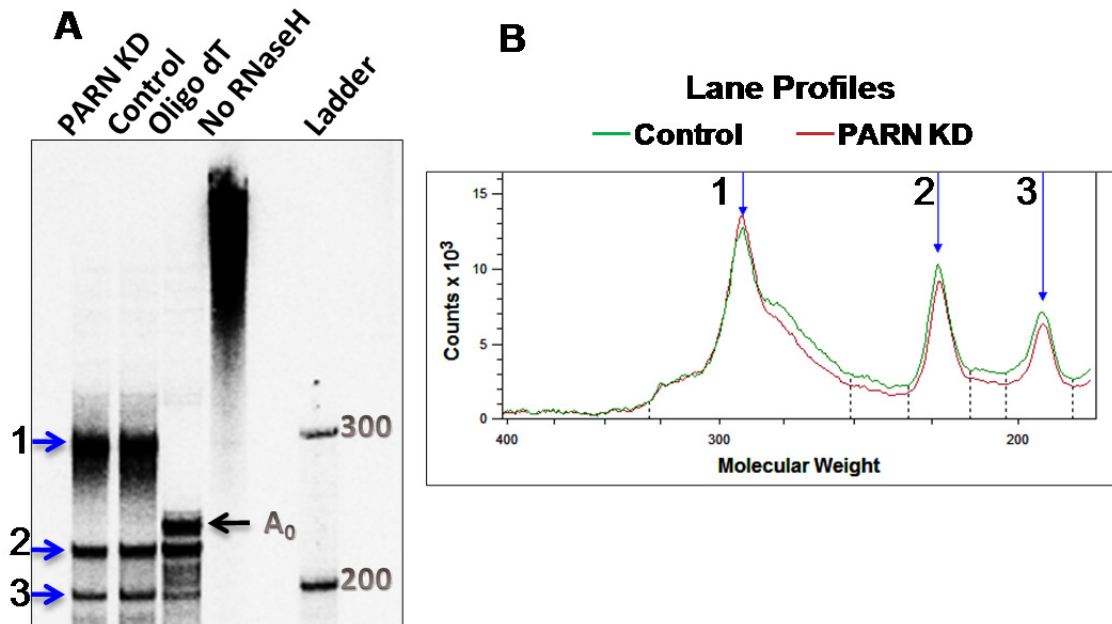
The actin mRNA was detected by northern blotting using a probe specific for the 3' UTR. The expected size for the  $A_0$  species was 232nt, which is consistent with what is shown in Figure 22A. The results from Figure 22A indicate that PARN KD has no effect on the overall poly(A) status of the actin mRNA, comparing the control and PARN KD lanes. This finding is confirmed by the lane profile counts in panel B, which also show no difference between control and PARN KD samples. The difference observed for the Brf2 mRNA poly(A) status is likely specific to that mRNA, and not the result of a general disruption of poly(A) states in the PARN KD cells.

**Figure 21.**



**PARN knock-down results in altered poly(A) status of the Brf2 mRNA.** (A) Oligo annealing/RNaseH treatment followed by northern blot of the Brf2 mRNA in control and PARN KD myoblasts. Position of arrow indicates the  $A_0$  species, blue lines correspond with migration of molecular weight markers. (B) Profile of pixel density in control (red) and PARN KD (green) lanes indicate an increase proportion of poly(A)<sup>+</sup> mRNA in PARN KD samples. (C) Quantitation of the proportion of poly(A)<sup>+</sup> to  $A_0$  Brf2 mRNA.

Figure 22.



**PARN knock-down does not alter the poly(A) status of the actin mRNA.** (A) Oligo annealing/RNaseH treatment followed by northern blot of the  $\beta$ -actin mRNA in control and PARN KD myoblasts. Position of black arrow indicates the  $A_0$  species, blue arrows and numbers correspond to the profile counts shown in B. (B) Profile of pixel density in control (green) and PARN KD (red) lanes indicate no change in the proportion of poly(A)<sup>+</sup> mRNA in PARN KD samples compared with control samples.

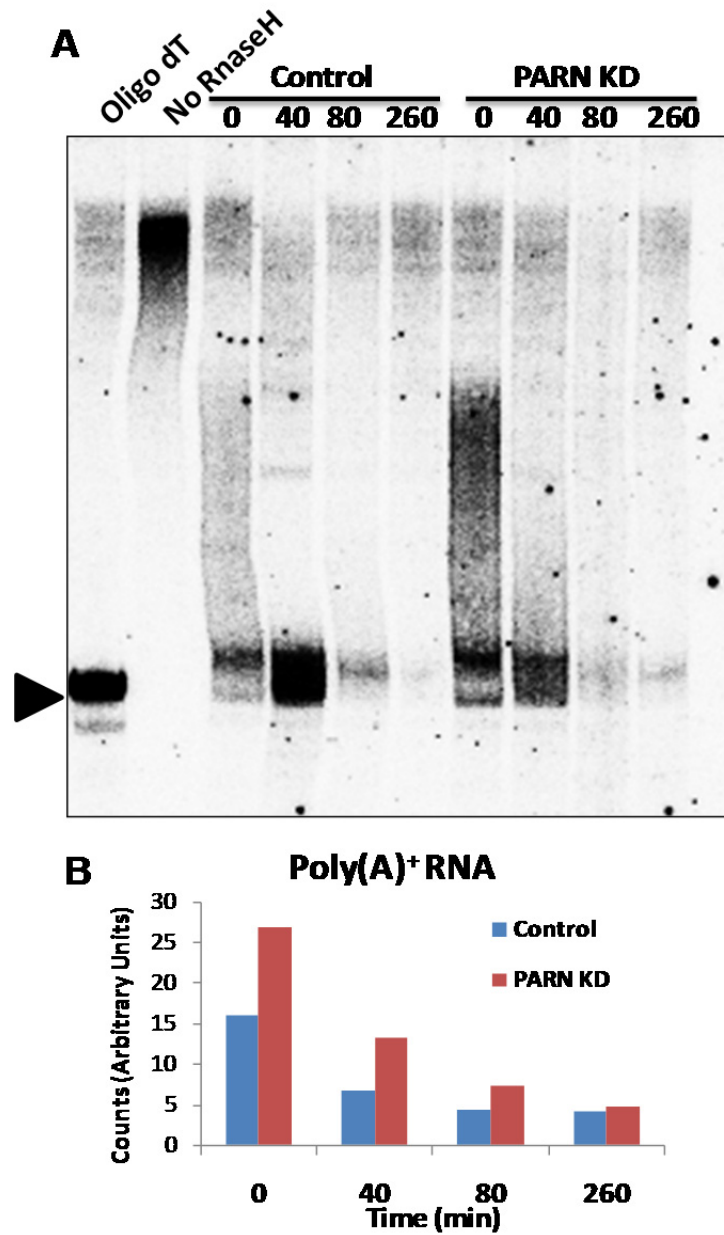
### 5.3 PARN knock-down disrupts deadenylation of Brf2 mRNA

Encouraged by the finding that PARN levels impacted the poly(A) status of the Brf2 mRNA, we next investigated the impact on deadenylation rates. Rates of deadenylation for the Brf2 mRNA were examined by transcriptional arrest using actinomycin-D in control and PARN KD myoblasts. Total RNA samples were collected from the actinomycin-D treated time course. 10 $\mu$ g of total RNA from each sample was again treated with RNase H and the Brf2-specific oligo. As before there is a striking difference in poly(A) status of the mRNA between the control and PARN KD samples at

the 0 time point (Figure 23A and B). In the control, a large reduction in the levels of poly(A)<sup>+</sup> Brf2 mRNA was evident by 40 minutes, with nearly all of the Brf2 mRNA migrating at a molecular weight consistent with a very short poly(A) tail species at that time (Figure 23A). This is in contrast to the PARN KD cells where the poly(A) tail is not completely shortened until the 80 minute time point (Figure 23A and B). Taken together these results support and extend those shown in Figure 21. We conclude that PARN impacts Brf2 mRNA decay by mediating poly(A) shortening. Interestingly, as the Brf2 message is still deadenylated in the PARN KD cells there may be sufficient PARN remaining in this cell line to carry out some decay. Alternatively, a different deadenylase may be acting in its place (CCR4/NOT, or PARN-L). The fact that deadenylase enzymes may substitute for one another to some degree is indicative of the importance of mRNA decay. Post-transcriptional control of mRNA levels must be efficient for survival. (Stumpo et al., 2009; Williams et al., 2009).

This is the first time PARN has been shown to impact the poly(A) status of an endogenous transcript in muscle cells and establishes PARN as significant initiator of mRNA decay in mammalian cells. Furthermore, as Brf2 is an ARE-binding protein that confers instability to bound transcripts, aberrant expression of Brf2 may in part explain why we had a subset of mRNAs that were destabilized in the PARN KD dataset. Therefore PARN deadenylase needs to be considered as an active contributor to deadenylation-dependent decay in mammalian cells.

Figure 23.



**PARN knock-down inhibits poly(A) tail removal of the Brf2 mRNA.** (A) Oligo/RNaseH treatment of RNA isolated from control and PARN KD cells following actinomycin D addition was followed by northern blot for the Brf2 mRNA. Migration of  $A_0$  is marked with an arrowhead. Samples labeled 0 were not exposed to actinomycin-D. (B) Quantitation of poly(A)<sup>+</sup> Brf2 mRNA as a function of time treated with Actinomycin-D.

## **Chapter 6: Discussion**

### **6.1 Regulation of TNF mRNA stability by CUGBP1**

Prior to this study, CUGBP1 and PARN had been demonstrated to be necessary for rapid deadenylation of TNF reporter RNA *in vitro* (Moraes et al., 2006). We hypothesized that this regulation might have biological impact in myoblasts, given the muscle-specific effects of CUGBP1 over-expression (Timchenko et al., 2004). Our experiments showed that CUGBP1 indeed regulates TNF mRNA decay in muscle cells (Figure 5; Zhang et al., 2008). However, PARN knock-down did not alter TNF mRNA stability (Figure 6). Interestingly, CUGBP1-mediated instability of TNF mRNA was disrupted by PKC activation (Figures 7 and 8). Lastly, interactions between CUGBP1 and the Jun and Myogenin mRNAs were reduced by TPA treatment (Figure 9).

#### **6.1.1 CUGBP1 targets the TNF mRNA for fast decay in muscle cells**

TNF mRNA exhibits rapid decay in myoblasts in a CUGBP1-dependent manner. This is perhaps surprising as TNF mRNA decay was shown previously to be promoted by four other ARE-binding factors: AUF1 (Lu et al., 2006), TIA1 (Piecyk et al., 2000), TIAR (Gueydan et al., 1999), and TTP (Sun et al., 2007). The half-life reported here (~10 minutes) is even shorter than reported in immune cells (20-40 minutes), which are primary TNF producers (Garnon et al., 2005; Wang et al., 2006). In muscle cells, this very high decay rate may ensure that TNF production is tightly controlled. Such control is necessary as TNF can both induce and inhibit terminal differentiation of muscle dependent on its concentration (Chen et al., 2007). Chronic exposure of muscle to high

TNF levels causes muscle wasting and insulin resistance (Flores et al., 1989; Kewalramani et al., 2010). The relatively high rate of decay for TNF mRNA (~30 minutes) even in the CUGBP1 KD cells is likely due to ARE recognition by one of the aforementioned factors. Such extensive regulation of TNF mRNA is required because of the potency of the TNF cytokine (Kontoyiannis et al., 1999).

The mechanism by which CUGBP1 induces TNF mRNA levels remains an open question, as PARN knock-down did not alter the rate of TNF mRNA decay (Figure 6). Although it is possible that PARN was not knocked down sufficiently, CUGBP1 could well recruit an alternate deadenylase in PARN KD myoblasts, or may act through a deadenylation-independent pathway. Although PARN is the only decay enzyme known to interact with CUGBP1, other RNA-binding proteins have been shown to interact with a multitude of cellular decay factors: TTP recruits the decapping machinery, the exosome, and CNOT6 (Lykke-Andersen and Wagner, 2005) to promote decay. The possibility of CUGBP1 interacting with other decay factors could be tested by co-immunoprecipitation assays.

#### *6.1.2 PKC activation disrupts CUGBP1 function*

Phorbol ester treatment causes PKC activation, which resulted in stabilization of the TNF mRNA (Figure 8), phosphorylation of CUGBP1 and a reduction in CUGBP1/mRNA association (Figure 9). Hyperphosphorylation of CUGBP1 is observed in DM1, and in a mouse model expressing CUG-repeat transcripts (Kuyumcu-Martinez et al., 2007). Moreover, treatment of this DM1 mouse with PKC inhibitors reduces CUGBP1 phosphorylation and abundance, corrects CUGBP1-mediated mis-splicing, and improves muscle function (Wang et al., 2009a). This could indicate that the phosphorylation changes observed for CUGBP1 in TPA-treated myoblasts mirror those

observed in DM1 patients (Kuyumcu-Martinez et al., 2007). One question remains, do CUGBP1-dependent changes in TNF mRNA stability occur in DM1 patients and if so, are they sufficient to cause TNF over-expression? There is one published report of TNF over-expression in DM1 patients (Mammarella et al., 2002), but the mechanism is not known. Our results are encouraging and should be followed up by investigating TNF mRNA abundance in DM1 patient muscle cells and in mouse models of the disease.

The immunoprecipitation experiments from cytoplasmic lysates demonstrated that mRNA associations with CUGBP1 were reduced upon TPA activation, which was correlated with CUGBP1 phosphorylation. Changes in the phospho-state of CUGBP1 are also evident during differentiation. It is currently not clear how phosphorylation results in reduced affinity of CUGBP1 for RNA. It could result in CUGBP1 sequestration in the nucleus. However this appears not to be the case in TPA treated cells (*Dr. L. Zhang unpublished observation*). DM1 models seemingly indicate that phospho-CUGBP1 retains affinity for RNA. In the DM1 mouse model (Kuyumcu-Martinez et al., 2007), CUGBP1 is phosphorylated, and rates of exon inclusion in CUGBP1 targets are increased. This would seem to indicate that phospho-CUGBP1 retains affinity for RNA. However, in this mouse model nuclear levels of CUGBP1 are increased. Therefore, comparing rates of exon inclusion is not likely a reliable indicator of binding affinity. Phospho-CUGBP1 may have reduced affinity for RNA, but the increased concentration may offset that in the nucleus. In the cytoplasm, reduced affinity has a significant impact as less CUGBP1 is available. Phosphorylation could alter the binding preference of CUGBP1 for other proteins, like splicing factors, similar to TTP showing increased affinity for the 14-3-3 chaperone upon phosphorylation (Sun et al., 2007). In this instance the RNA-binding function of the complex would likely be influenced by other proteins in addition to CUGBP1.

To summarize findings from Chapter 3, we have determined that CUGBP1 regulates the stability of TNF mRNA in muscle. Upon PKC activation, conditions similar to DM1, the destabilization is disrupted, and mRNA substrate association is reduced allowing TNF levels and half-life to increase. These findings establish a common link between disrupted CUGBP1 function and increased levels and stability of the TNF mRNA. Increased TNF levels have been shown to disrupt insulin signaling and promote muscle wasting (Li and Reid, 2001). Elevation of potent cytokine TNF, by disruption of CUGBP1 function in muscle cells, may be responsible for some unexplained symptoms of DM1 -muscle wasting and insulin resistance.

## ***6.2 mRNA decay and the role of CUGBP1 in muscle cells***

As CUGBP1 likely targets many mRNAs in addition to TNF, we sought to characterize mRNA decay in muscle, and identify CUGBP1 targets on a global scale. We reported half-lives for 7,398 mRNAs in C2C12 cells. Cell cycle and transcriptional regulation were identified as processes likely to be post-transcriptionally regulated in muscle, and AU-rich and GU-rich sequence elements were considered likely to mediate this regulation as they were over-represented in unstable mRNAs. We went on to identify over 800 CUGBP1-associated transcripts, and distinguish CUGBP1 binding motifs. RNA metabolism, protein targeting to the ER, and muscle differentiation were all identified as processes likely to be impacted by CUGBP1. CUGBP1 and HuR were found to share common mRNA targets. Finally CUGBP1 protein expression was essential for normal myogenesis and was down-regulated as cells completed the transition to myotubes.



### *6.2.1 Unique attributes of mRNA decay in muscle cells*

The global half-life experiments revealed muscle-specific features of mRNA decay. GU-rich sequences were found to be more significant than AU-rich ones (Figure 12A). Muscle cells were unique in this regard, as comparison of GU and AU-rich sequences with proliferative ES cells, neuronal-like ES cells, and immune-like ES cells identified AU-rich sequences as most significant in those three (Lee et al., 2010). This finding indicates that in muscle cells GREs are a more important regulatory element than AREs. This may in part explain why over-expression of CUGBP1 primarily causes symptoms in muscle (Kuyumcu-Martinez et al., 2007).

For muscle cells, transcription factors and cell cycle regulators tend to be encoded by unstable mRNAs; as was noted by previous studies in other cell types (Miller et al., 2011; Raghavan et al., 2002; Sharova et al., 2009). In these studies it was hypothesized that mRNAs with short half-lives can most readily be induced in response to external cues. Stabilization in conjunction with transcriptional induction allows for synergistic effects on mRNA levels and corresponding increase in protein levels. In addition, keeping the mRNA half-life short for groups of transcripts, allows for a rapid induction of mRNA levels.

### *6.2.2 CUGBP1 depletion has wide ranging effects on mRNA decay in muscle cells*

CUGBP1 knock-down significantly stabilized 480 mRNAs in myoblasts which represents more than half of the transcripts for which half-lives were obtained. Confirmation of these observations was obtained for 9/13 transcripts examined by qRT-PCR. Hexamer analyses were not useful for identifying over-represented elements in CUGBP1-regulated mRNAs. This is partly due to the much smaller size of the dataset (924 mRNAs in total vs. 7,398 mRNAs in controls). In retrospect, the indirect effects of CUGBP1 on mRNA decay may be wide-ranging given that the protein binds to a large

number of mRNAs encoding proteins required for mRNA metabolism including 26 RNA-binding proteins, 11 splicing factors, and 10 decay factors (Table 4.3). All told, finding 480 putative CUGBP1 targets represents a marked advance in characterizing the cytoplasmic roles of the protein.

### *6.2.3 Direct CUGBP1 targets: substrate competition and differentiation*

As our initial attempts to identify CUGBP1 targets by half-life analysis did not give a clear result, direct CUGBP1 targets were identified by RIP-Chip. Stringent analysis of RIP-Chip data conservatively identified 881 targets for regulation by CUGBP1. GO analysis of this dataset indicated that regulation of transcription, muscle differentiation, protein secretion, and cytoskeletal genes are all likely to be post-transcriptionally regulated by CUGBP1 in muscle. Two CUGBP1 binding motifs were predicted from the hexamer analyses. Comparison of our CUGBP1 RIP-Chip dataset with a similar dataset of mRNAs associated with the human HuR protein in T-cells indicated a significant degree of overlap in the transcripts recognized by these two opposing mRNA stability factors. CUGBP1 and HuR were found to compete for RNA-binding *in vitro*, similar to the competition between CUGBP2 and HuR that was previously reported (Sureban et al., 2007). During myoblast differentiation, HuR stabilizes the Myogenin, MyoD, and p21 mRNAs (Lal et al., 2004; Figueroa et al., 2003). We found CUGBP1 bound to Myogenin, MyoD, and p21 mRNAs, and showed that CUGBP1 destabilizes the MyoD transcript (Figure 13). It now seems likely that CUGBP1 may be repressing the expression of these three factors in proliferative myoblasts.

GO analysis of the CUGBP1 RIP-Chip dataset linked CUGBP1 with expression patterns of functionally related mRNAs in muscle. CUGBP1-bound mRNAs encode factors involved in cell cycle, transcription, and RNA metabolism, these findings were in agreement with previous reports where global approaches were applied to TTP targets,

PUM1 targets, HuR targets, and T-cell responses (Emmons et al., 2008; Morris et al., 2008; Mukherjee et al., 2009; Vlasova et al., 2008). Our analysis has identified processes which are likely to be mis-regulated upon disruption of CUGBP1 function. Many of the short half-life mRNAs identified have an important role in muscle differentiation including: (1) CEBP/β a transcription factor that can repress myocyte growth (Bostrom et al., 2010), (2) Rnd3 (RhoE) constitutively active G-protein which when ablated in mice causes delayed neuromuscular maturation and very early mortality (Mocholi et al., 2011), (3) Jun, a transcription factor whose activity levels can promote myogenic differentiation of ES cells (Wu et al., 2010), and (4) MyoD a transcription factor that increases during muscle differentiation for transcription of muscle-specific genes (Rudnicki et al., 1993). The complete list of mRNAs now provides a large dataset for studies looking at mRNA regulation in muscle cells.

It has been proposed that a single RNA-binding protein can regulate gene expression for hundreds of mRNA targets (Keene, 2007). This model is similar to transcriptional efficiency of related bacterial polycistronic genes being regulated by a common factor, in an operon. Extending this model to mRNA decay in eukaryotes, it is thought that functionally-related classes of messages are controlled by a common RNA-binding protein, thus eliciting a concerted response. Our data strongly supports this model. We found CUGBP1 associated with mRNAs encoding factors involved in mRNA metabolism (including its own mRNA), muscle differentiation, cytoskeleton, and protein targeting to the ER. Finding an RNA-binding protein associated with many other mRNAs encoding other RNA-binding proteins supports the “regulator of regulators” idea. This is a concept that has emerged from several RIP-Chip studies which have found the RNA-binding protein of interest associated with mRNAs which encode for RNA-binding proteins. This phenomenon likely represents a method of feedback by which mRNA-

binding proteins exert far-reaching effects post-transcriptionally (Pullmann, Jr. et al., 2007).

#### 6.2.4 Myoblast differentiation is regulated by CUGBP1

As shown in Chapter 4, knock-down of CUGBP1 significantly alters myotube formation. We hypothesize this may be due to aberrant stabilization of one or more CUGBP1-regulated mRNAs. Our work here demonstrated that TNF mRNA abundance and stability are elevated in CUGBP1 KD myoblasts. If we extend this finding to the protein level, then elevated TNF functioning in an autocrine fashion may be partly to blame for the precocious differentiation. A previous report demonstrated that: (1) TNF mRNA levels increase 3-fold upon initiation of differentiation, (2) depletion of TNF from culture media inhibits myotube formation, and (3) slightly elevated TNF levels promote differentiation of C2C12 cells (Li and Schwartz, 2001).

The finding that CUGBP1 depletion causes myosac formation upon differentiation is particularly interesting and could be linked with aberrant expression of any one of several mRNAs associated with CUGBP1. The RhoE mRNA encodes a factor important for cytoskeletal organization (Fortier et al., 2008; Mocholi et al., 2011). CUGBP1 also binds to four mRNAs that encode tubulins, and curiously, disruption of microtubules with drugs also causes a myosac phenotype (Saitoh et al., 1988). Finally, it is noteworthy that TPA treatment of differentiating C2C12 cells also induces formation of myosacs (Mermelstein et al., 1996). CUGBP1 binds to (Table 4.3) and regulates the mRNA stability of factors critical for protein targeting to the ER, and secretion (*C. Lopez personal communication*). Disruption of these processes in CUGBP1 knock-down cells may hamper the movement of proteins to the extracellular space. This is of note because mutations in extra cellular matrix (ECM) components cause Duchenne and other muscular dystrophies (Kanagawa and Toda, 2006) and effects on ECM were

recently documented in DM1 mouse models (Du et al., 2010). In addition, DM1 patient cells exhibit hallmarks of ER stress that could also be linked with defective CUGBP1 function (Ikezoe et al., 2007).

#### ***6.2.5 CUGBP1 is dynamically regulated during muscle differentiation***

Differentiation of C2C12 cells from myoblast to myotubes required CUGBP1 for normal kinetics. We sought to characterize the expression profile of CUGBP1 in the differentiation process. CUGBP1 levels drop in C2C12 cultures (Figure 18) and murine cardiac tissues as differentiation proceeds (Kalsotra et al., 2010). Interestingly, phosphorylation of CUGBP1 also changes during differentiation, however the relative pattern may be distinct from that observed in TPA treatment or repeat RNA expression. As several pathways involving kinase signaling are activated upon muscle differentiation including PI<sub>3</sub>K/Akt (Xu and Wu, 2000) and p38/MAPK (Briata et al., 2005) it would be interesting to test which, if any, of these are responsible for CUGBP1 phosphorylation under normal differentiation conditions compared with the DM1/PKC activated conditions.

#### ***6.3 Global approach identifies mRNA substrate for deadenylation by PARN***

Prior to this work no direct substrates of PARN had been characterized in mammalian cells. While this work was in progress, Gadd45 $\alpha$  was found to be regulated by PARN at the level of stability in response to DNA damage (Reinhardt et al., 2010). PARN had been shown to interact with RNA-binding proteins including CUGBP1, TTP, KSRP, RHAU (Gherzi et al., 2004; Sandler and Stoecklin, 2008; Tran et al., 2004), and promote deadenylation *in vitro* (Moraes et al., 2006) but little evidence for a cytoplasmic role in living cells was available. Here we detected 64 mRNAs with significantly different

half-lives in PARN knock-down cells. One of these transcripts, Brf2, is directly affected at the level of deadenylation. This transcript, Brf2, encodes an RNA-binding protein which likely confers instability onto mRNA targets of its own (Lykke-Andersen and Wagner, 2005). From the 40 mRNAs stabilized in the PARN knock-down cells, many may represent direct substrates for deadenylation by PARN. In addition, 24 of the mRNAs expressed in the PARN KD cells were destabilized. As mentioned, this could be due to increased amounts of BRF2, an ARE-binding protein, as 11/24 destabilized transcripts were found to contain AREs (Bakheet et al., 2006). In addition, increases in the levels of the deadenylase TOE1 (CAF1Z) and/or the enhancer of decapping EDC3 could also promote mRNA decay of some of the 24 identified destabilized transcripts.

#### *6.3.1 PARN affects deadenylation in myoblasts*

Efforts here to implicate PARN deadenylase in the regulation of TNF mRNA stability were inconclusive. Interestingly, the PARN KD array data yields a plausible explanation. Upon PARN KD it was discovered that the Brf2 mRNA was stabilized. The closely related ARE-binding protein TTP has been shown previously to enhance decay of the TNF mRNA (Carballo et al., 1998). In addition TTP and BRF1 were both found to recruit DCP2 and CNOT6, but not PARN. No detectable changes in the overall abundance of the mRNA of Brf2 were detected in the PARN KD relative to controls, this is expected as BRF2 protein auto-regulates its own mRNA (Rabani et al., 2011). Nevertheless, Brf2 mRNA exhibits an increase in average poly(A) tail length in PARN KD cells, which might enhance translation. If excess BRF2 protein bound the ARE in the TNF mRNA, it might recruit DCP2 and/or CNOT6 thereby compensating for lack of PARN and keeping the TNF mRNA unstable.

### 6.3.2 *Brf2* mRNA is subject to deadenylation by PARN

The relatively small number of mRNAs impacted by PARN knock-down is consistent with redundancy of targets between different deadenylases. Knock-down of the deadenylase CNOT6 in human breast adenocarcinoma cells (MCF7) resulted in no significant mRNA abundance changes. Double knock down of CNOT6/CNOT6L resulted in 79 mRNA abundance changes of 1.5-fold or greater (up and down), and CNOT7/CNOT8 double knock down resulted in 229 abundance changes (up and down; Mittal et al., 2011). Analysis of the zero time point data from our PARN KD cells reveals 263 abundance changes (68 increased, and 195 decreased 2-fold or greater). Intriguingly, the Mittal study indicates that different deadenylases examined regulate distinct classes of messages. This is somewhat surprising considering the deadenylases compared can all associate with the NOT scaffolding proteins. Further bioinformatic comparisons with the PARN KD abundance data may reveal whether distinct classes of mRNAs are targets for regulation by PARN. In addition, comparison of abundances from our global studies between PARN and CUGBP1 KD cells has revealed that the two proteins may cooperatively regulate a small subset (20 mRNAs) of transcripts which are involved in neuronal function (Appendix 11).

Finally, to our knowledge this is the first data demonstrating that PARN modulates poly(A) tail status of an endogenous mRNA in the cytoplasm of mammalian cells. At this point it is unclear what features make *Brf2* mRNA a PARN substrate in muscle, the 3'UTR has both AU- and GU-rich sequences. Future experiments will be directed towards looking at protein levels and translation rates of a *Brf2* reporter RNA in control and PARN KD myoblasts. Future studies could be directed at elucidating what features the 40 transcripts stabilized in the PARN KD cells make them PARN substrates.

#### **6.4 Concluding remarks**

At the inception of this study, the regulation of TNF mRNA decay in muscle was uncharacterized. The processes of mRNA decay and CUGBP1-mediated decay were uncharacterized in muscle. Finally, the role, if any, of PARN in mRNA decay in mammalian cells was unclear. TNF mRNA decay was characterized for the first time in muscle cells. CUGBP1 was demonstrated necessary for rapid decay of the TNF message (Zhang et al., 2008). This study provided a potential link between unexplained symptoms of DM1 and CUGBP1 overexpression.

For the first time we have measured mRNA decay rates on a global scale in muscle cells, revealing important concepts about mRNA decay dynamics in muscle. We have identified a set of RNAs whose half-life is dependent of the presence of CUGBP1 protein in muscle, identified direct mRNA targets of CUGBP1 (Lee et al., 2010), and differentiation defects dependent on CUGBP1 were characterized. Prior to these findings CUGBP1 was primarily characterized as a splicing factor in mammalian cells, and a mediator of translational activation/repression in transcriptionally silent oocytes (Kalsotra et al., 2008; Paillard et al., 1998). Our results have now firmly established CUGBP1 as an important post-transcriptional regulator in mammalian cells beyond splicing.

Lastly we identified a subset of mRNAs whose decay rates are dependent on PARN levels, and have implicated PARN as an important deadenylase from the standpoint of transcript regulation in muscle cells. To conclude, these findings have significantly advanced the understanding mRNA decay in muscle cells, the role of CUGBP1 in muscle, and identified an endogenous mRNA substrate for deadenylation by PARN, establishing them as potent factors in the post-transcriptional control of gene expression.



## Reference List

- Ahn,S.H., Kim,M., and Buratowski,S. (2004). Phosphorylation of serine 2 within the RNA polymerase II C-terminal domain couples transcription and 3' end processing. *Mol. Cell* **13**, 67-76.
- Andres,V. and Walsh,K. (1996). Myogenin expression, cell cycle withdrawal, and phenotypic differentiation are temporally separable events that precede cell fusion upon myogenesis. *J. Cell Biol.* **132**, 657-666.
- Atasoy,U., Watson,J., Patel,D., and Keene,J.D. (1998). ELAV protein HuA (HuR) can redistribute between nucleus and cytoplasm and is upregulated during serum stimulation and T cell activation. *J. Cell Sci.* **111** ( Pt 21), 3145-3156.
- Badis,G., Saveanu,C., Fromont-Racine,M., and Jacquier,A. (2004). Targeted mRNA degradation by deadenylation-independent decapping. *Mol. Cell* **15**, 5-15.
- Bakheet,T., Williams,B.R., and Khabar,K.S. (2006). ARED 3.0: the large and diverse AU-rich transcriptome. *Nucleic Acids Res.* **34**, D111-D114.
- Balagopal,V. and Parker,R. (2009). Polysomes, P bodies and stress granules: states and fates of eukaryotic mRNAs. *Curr. Opin. Cell Biol.* **21**, 403-408.
- Balatsos,N.A., Nilsson,P., Mazza,C., Cusack,S., and Virtanen,A. (2006). Inhibition of mRNA deadenylation by the nuclear cap binding complex (CBC). *J. Biol. Chem.* **281**, 4517-4522.
- Barash,Y., Calarco,J.A., Gao,W., Pan,Q., Wang,X., Shai,O., Blencowe,B.J., and Frey,B.J. (2010). Deciphering the splicing code. *Nature* **465**, 53-59.
- Bartel,D.P. and Chen,C.Z. (2004). Micromanagers of gene expression: the potentially widespread influence of metazoan microRNAs. *Nat. Rev. Genet.* **5**, 396-400.
- Bartlam,M. and Yamamoto,T. (2010). The structural basis for deadenylation by the CCR4-NOT complex. *Protein Cell* **1**, 443-452.
- Bentley,D.L. (2005). Rules of engagement: co-transcriptional recruitment of pre-mRNA processing factors. *Curr. Opin. Cell Biol.* **17**, 251-256.
- Bernstein,J.A., Khodursky,A.B., Lin,P.H., Lin-Chao,S., and Cohen,S.N. (2002). Global analysis of mRNA decay and abundance in *Escherichia coli* at single-gene resolution using two-color fluorescent DNA microarrays. *Proc. Natl. Acad. Sci. U. S. A* **99**, 9697-9702.
- Berridge,M.J., Bootman,M.D., and Roderick,H.L. (2003). Calcium signalling: dynamics, homeostasis and remodelling. *Nat. Rev. Mol. Cell Biol.* **4**, 517-529.

- Bhattacharyya, S.N., Habermacher, R., Martiny-Bar, U., Closs, E.I., and Filipowicz, W. (2006). Stress-induced reversal of microRNA repression and mRNA P-body localization in human cells. *Cold Spring Harb. Symp. Quant. Biol.* **71**, 513-521.
- Bisbal, C., Silhol, M., Laubenthal, H., Kaluza, T., Carnac, G., Milligan, L., Le, R.F., and Salehzada, T. (2000). The 2'-5' oligoadenylate/RNase L/RNase L inhibitor pathway regulates both MyoD mRNA stability and muscle cell differentiation. *Mol. Cell Biol.* **20**, 4959-4969.
- Black, B.L. and Olson, E.N. (1998). Transcriptional control of muscle development by myocyte enhancer factor-2 (MEF2) proteins. *Annu. Rev. Cell Dev. Biol.* **14**, 167-196.
- Blau, H.M., Chiu, C.P., and Webster, C. (1983). Cytoplasmic activation of human nuclear genes in stable heterocaryons. *Cell* **32**, 1171-1180.
- Borja, M.S., Piotukh, K., Freund, C., and Gross, J.D. (2011). Dcp1 links coactivators of mRNA decapping to Dcp2 by proline recognition. *RNA*. **17**, 278-290.
- Bostrom, P., Mann, N., Wu, J., Quintero, P.A., Plovie, E.R., Panakova, D., Gupta, R.K., Xiao, C., MacRae, C.A., Rosenzweig, A., and Spiegelman, B.M. (2010). C/EBPbeta controls exercise-induced cardiac growth and protects against pathological cardiac remodeling. *Cell* **143**, 1072-1083.
- Both, G.W., Furuichi, Y., Muthukrishnan, S., and Shatkin, A.J. (1975). Ribosome binding to reovirus mRNA in protein synthesis requires 5' terminal 7-methylguanosine. *Cell* **6**, 185-195.
- Bregues, M., Teixeira, D., and Parker, R. (2005). Movement of eukaryotic mRNAs between polysomes and cytoplasmic processing bodies. *Science* **310**, 486-489.
- Briata, P., Forcales, S.V., Ponassi, M., Corte, G., Chen, C.Y., Karin, M., Puri, P.L., and Gherzi, R. (2005). p38-dependent phosphorylation of the mRNA decay-promoting factor KSRP controls the stability of select myogenic transcripts. *Mol. Cell* **20**, 891-903.
- Buratowski, S. (2005). Connections between mRNA 3' end processing and transcription termination. *Curr. Opin. Cell Biol.* **17**, 257-261.
- Buxton, J., Shelbourne, P., Davies, J., Jones, C., Van, T.T., Aslanidis, C., de, J.P., Jansen, G., Anvret, M., Riley, B., and . (1992). Detection of an unstable fragment of DNA specific to individuals with myotonic dystrophy. *Nature* **355**, 547-548.
- Callahan, K.P. and Butler, J.S. (2010). TRAMP complex enhances RNA degradation by the nuclear exosome component Rps6. *J. Biol. Chem.* **285**, 3540-3547.
- Cao, Q., Padmanabhan, K., and Richter, J.D. (2010). Pumilio 2 controls translation by competing with eIF4E for 7-methyl guanosine cap recognition. *RNA*. **16**, 221-227.
- Caput, D., Beutler, B., Hartog, K., Thayer, R., Brown-Shimer, S., and Cerami, A. (1986). Identification of a common nucleotide sequence in the 3'-untranslated region of mRNA

- molecules specifying inflammatory mediators. *Proc. Natl. Acad. Sci. U. S. A.* **83**, 1670-1674.
- Carballo,E., Lai,W.S., and Blakeshear,P.J. (1998). Feedback inhibition of macrophage tumor necrosis factor- $\alpha$  production by tristetraprolin. *Science* **281**, 1001-1005.
- Castellani,L., Salvati,E., Alema,S., and Falcone,G. (2006). Fine regulation of RhoA and Rock is required for skeletal muscle differentiation. *J. Biol. Chem.* **281**, 15249-15257.
- Cevher,M.A., Zhang,X., Fernandez,S., Kim,S., Baquero,J., Nilsson,P., Lee,S., Virtanen,A., and Kleiman,F.E. (2010). Nuclear deadenylation/polyadenylation factors regulate 3' processing in response to DNA damage. *EMBO J.* **29**, 1674-1687.
- Charlet,B., Logan,P., Singh,G., and Cooper,T.A. (2002). Dynamic antagonism between ETR-3 and PTB regulates cell type-specific alternative splicing. *Mol. Cell* **9**, 649-658.
- Cheadle,C., Fan,J., Cho-Chung,Y.S., Werner,T., Ray,J., Do,L., Gorospe,M., and Becker,K.G. (2005). Control of gene expression during T cell activation: alternate regulation of mRNA transcription and mRNA stability. *BMC Genomics* **6**, 75.
- Chekulaeva,M., Hentze,M.W., and Ephrussi,A. (2006). Bruno acts as a dual repressor of oskar translation, promoting mRNA oligomerization and formation of silencing particles. *Cell* **124**, 521-533.
- Chen,C.Y., Gherzi,R., Ong,S.E., Chan,E.L., Raijmakers,R., Pruijn,G.J., Stoecklin,G., Moroni,C., Mann,M., and Karin,M. (2001). AU binding proteins recruit the exosome to degrade ARE-containing mRNAs. *Cell* **107**, 451-464.
- Chen,C.Y., Zheng,D., Xia,Z., and Shyu,A.B. (2009). Ago-TNRC6 triggers microRNA-mediated decay by promoting two deadenylation steps. *Nat. Struct. Mol. Biol.* **16**, 1160-1166.
- Chen,S.E., Jin,B., and Li,Y.P. (2007). TNF- $\alpha$  regulates myogenesis and muscle regeneration by activating p38 MAPK. *Am. J. Physiol Cell Physiol* **292**, C1660-C1671.
- Chou,C.F., Mulky,A., Maitra,S., Lin,W.J., Gherzi,R., Kappes,J., and Chen,C.Y. (2006). Tethering KSRP, a decay-promoting AU-rich element-binding protein, to mRNAs elicits mRNA decay. *Mol. Cell Biol.* **26**, 3695-3706.
- Choudhary,S., De,B.P., and Banerjee,A.K. (2000). Specific phosphorylated forms of glyceraldehyde 3-phosphate dehydrogenase associate with human parainfluenza virus type 3 and inhibit viral transcription in vitro. *J. Virol.* **74**, 3634-3641.
- Coller,J. and Parker,R. (2005). General translational repression by activators of mRNA decapping. *Cell* **122**, 875-886.
- Coller,J.M., Tucker,M., Sheth,U., Valencia-Sanchez,M.A., and Parker,R. (2001). The DEAD box helicase, Dhh1p, functions in mRNA decapping and interacts with both the decapping and deadenylase complexes. *RNA.* **7**, 1717-1727.

- Cook,A., Bono,F., Jinek,M., and Conti,E. (2007). Structural biology of nucleocytoplasmic transport. *Annu. Rev. Biochem.* 76, 647-671.
- Copeland,P.R. and Wormington,M. (2001). The mechanism and regulation of deadenylation: identification and characterization of *Xenopus* PARN. *RNA.* 7, 875-886.
- Corbeil-Girard,L.P., Klein,A.F., Sasseville,A.M., Lavoie,H., Dicaire,M.J., Saint-Denis,A., Page,M., Duranceau,A., Codere,F., Bouchard,J.P., Karpati,G., Rouleau,G.A., Massie,B., Langelier,Y., and Brais,B. (2005). PABPN1 overexpression leads to upregulation of genes encoding nuclear proteins that are sequestered in oculopharyngeal muscular dystrophy nuclear inclusions. *Neurobiol. Dis.* 18, 551-567.
- Crooks,G.E., Hon,G., Chandonia,J.M., and Brenner,S.E. (2004). WebLogo: a sequence logo generator. *Genome Res.* 14, 1188-1190.
- Cui,W., Taub,D.D., and Gardner,K. (2007). qPrimerDepot: a primer database for quantitative real time PCR. *Nucleic Acids Res.* 35, D805-D809.
- Dahm,R. and Kiebler,M. (2005). Cell biology: silenced RNA on the move. *Nature* 438, 432-435.
- Das,R., Yu,J., Zhang,Z., Gygi,M.P., Krainer,A.R., Gygi,S.P., and Reed,R. (2007). SR proteins function in coupling RNAP II transcription to pre-mRNA splicing. *Mol. Cell* 26, 867-881.
- Davis,R.L., Weintraub,H., and Lassar,A.B. (1987). Expression of a single transfected cDNA converts fibroblasts to myoblasts. *Cell* 51, 987-1000.
- De Haro.M., Al-Ramahi,I., De,G.B., Ukani,L., Rosa,A., Faustino,N.A., Ashizawa,T., Cooper,T.A., and Botas,J. (2006). MBNL1 and CUGBP1 modify expanded CUG-induced toxicity in a *Drosophila* model of myotonic dystrophy type 1. *Hum. Mol. Genet.* 15, 2138-2145.
- Dehlin,E., Wormington,M., Korner,C.G., and Wahle,E. (2000). Cap-dependent deadenylation of mRNA. *EMBO J.* 19, 1079-1086.
- Dessau,R.B. and Pipper,C.B. (2008). "R"--project for statistical computing. *Ugeskr. Laeger* 170, 328-330.
- Dolken,L., Ruzsics,Z., Radle,B., Friedel,C.C., Zimmer,R., Mages,J., Hoffmann,R., Dickinson,P., Forster,T., Ghazal,P., and Koszinowski,U.H. (2008). High-resolution gene expression profiling for simultaneous kinetic parameter analysis of RNA synthesis and decay. *RNA.* 14, 1959-1972.
- Dormoy-Raclet,V., Menard,I., Clair,E., Kurban,G., Mazroui,R., Di,M.S., von,R.C., Pause,A., and Gallouzi,I.E. (2007). The RNA-binding protein HuR promotes cell migration and cell invasion by stabilizing the beta-actin mRNA in a U-rich-element-dependent manner. *Mol. Cell Biol.* 27, 5365-5380.

- Du,H., Cline,M.S., Osborne,R.J., Tuttle,D.L., Clark,T.A., Donohue,J.P., Hall,M.P., Shiue,L., Swanson,M.S., Thornton,C.A., and Ares,M., Jr. (2010). Aberrant alternative splicing and extracellular matrix gene expression in mouse models of myotonic dystrophy. *Nat. Struct. Mol. Biol.* *17*, 187-193.
- Emmons,J., Townley-Tilson,W.H., Deleault,K.M., Skinner,S.J., Gross,R.H., Whitfield,M.L., and Brooks,S.A. (2008). Identification of TTP mRNA targets in human dendritic cells reveals TTP as a critical regulator of dendritic cell maturation. *RNA.* *14*, 888-902.
- Esnault,S., Shen,Z.J., Whitesel,E., and Malter,J.S. (2006). The peptidyl-prolyl isomerase Pin1 regulates granulocyte-macrophage colony-stimulating factor mRNA stability in T lymphocytes. *J. Immunol.* *177*, 6999-7006.
- Fabian,M.R., Mathonnet,G., Sundermeier,T., Mathys,H., Zipprich,J.T., Svitkin,Y.V., Rivas,F., Jinek,M., Wohlschlegel,J., Doudna,J.A., Chen,C.Y., Shyu,A.B., Yates,J.R., III, Hannon,G.J., Filipowicz,W., Duchaine,T.F., and Sonenberg,N. (2009). Mammalian miRNA RISC recruits CAF1 and PABP to affect PABP-dependent deadenylation. *Mol. Cell* *35*, 868-880.
- Fan,X.C. and Steitz,J.A. (1998). Overexpression of HuR, a nuclear-cytoplasmic shuttling protein, increases the *in vivo* stability of ARE-containing mRNAs. *EMBO J.* *17*, 3448-3460.
- Fenger-Gron,M., Fillman,C., Norrild,B., and Lykke-Andersen,J. (2005). Multiple processing body factors and the ARE binding protein TTP activate mRNA decapping. *Mol. Cell* *20*, 905-915.
- Figuerola,A., Cuadrado,A., Fan,J., Atasoy,U., Muscat,G.E., Munoz-Canoves,P., Gorospe,M., and Munoz,A. (2003). Role of HuR in skeletal myogenesis through coordinate regulation of muscle differentiation genes. *Mol. Cell Biol.* *23*, 4991-5004.
- Flores,E.A., Bistran,B.R., Pomposelli,J.J., Dinarello,C.A., Blackburn,G.L., and Iltfan,N.W. (1989). Infusion of tumor necrosis factor/cachectin promotes muscle catabolism in the rat. A synergistic effect with interleukin 1. *J. Clin. Invest* *83*, 1614-1622.
- Ford,L.P. and Wilusz,J. (1999). An *in vitro* system using HeLa cytoplasmic extracts that reproduces regulated mRNA stability. *Methods* *17*, 21-27.
- Fortier,M., Comunale,F., Kucharczak,J., Blangy,A., Charrasse,S., and Gauthier-Rouviere,C. (2008). RhoE controls myoblast alignment prior fusion through RhoA and ROCK. *Cell Death. Differ.* *15*, 1221-1231.
- Franks,T.M. and Lykke-Andersen,J. (2007). TTP and BRF proteins nucleate processing body formation to silence mRNAs with AU-rich elements. *Genes Dev.* *21*, 719-735.
- Franks,T.M. and Lykke-Andersen,J. (2008). The control of mRNA decapping and P-body formation. *Mol. Cell* *32*, 605-615.

- Franks,T.M., Singh,G., and Lykke-Andersen,J. (2010). Upf1 ATPase-dependent mRNP disassembly is required for completion of nonsense- mediated mRNA decay. *Cell* 143, 938-950.
- Fujimura,K., Kano,F., and Murata,M. (2008). Dual localization of the RNA binding protein CUGBP-1 to stress granule and perinucleolar compartment. *Exp. Cell Res.* 314, 543-553.
- Funakoshi,Y., Doi,Y., Hosoda,N., Uchida,N., Osawa,M., Shimada,I., Tsujimoto,M., Suzuki,T., Katada,T., and Hoshino,S. (2007). Mechanism of mRNA deadenylation: evidence for a molecular interplay between translation termination factor eRF3 and mRNA deadenylases. *Genes Dev.* 21, 3135-3148.
- Galban,S., Kuwano,Y., Pullmann,R., Jr., Martindale,J.L., Kim,H.H., Lal,A., Abdelmohsen,K., Yang,X., Dang,Y., Liu,J.O., Lewis,S.M., Holcik,M., and Gorospe,M. (2008). RNA-binding proteins HuR and PTB promote the translation of hypoxia-inducible factor 1alpha. *Mol. Cell Biol.* 28, 93-107.
- Gao,M., Fritz,D.T., Ford,L.P., and Wilusz,J. (2000). Interaction between a poly(A)-specific ribonuclease and the 5' cap influences mRNA deadenylation rates *in vitro*. *Mol. Cell* 5, 479-488.
- Gao,M., Wilusz,C.J., Peltz,S.W., and Wilusz,J. (2001). A novel mRNA-decapping activity in HeLa cytoplasmic extracts is regulated by AU-rich elements. *EMBO J.* 20, 1134-1143.
- Garcia-Lopez,A., Monferrer,L., Garcia-Alcover,I., Vicente-Crespo,M., varez-Abril,M.C., and Artero,R.D. (2008). Genetic and chemical modifiers of a CUG toxicity model in *Drosophila*. *PLoS. One.* 3, e1595.
- Garneau,N.L., Wilusz,C.J., and Wilusz,J. (2008). Chapter 5. In vivo analysis of the decay of transcripts generated by cytoplasmic RNA viruses. *Methods Enzymol.* 449, 97-123.
- Garneau,N.L., Wilusz,J., and Wilusz,C.J. (2007). The highways and byways of mRNA decay. *Nat. Rev. Mol. Cell Biol.* 8, 113-126.
- Garnon,J., Lachance,C., Di,M.S., Hel,Z., Marion,D., Ruiz,M.C., Newkirk,M.M., Khandjian,E.W., and Radzioch,D. (2005). Fragile X-related protein FXR1P regulates proinflammatory cytokine tumor necrosis factor expression at the post-transcriptional level. *J. Biol. Chem.* 280, 5750-5763.
- Gatfield,D. and Izaurralde,E. (2004). Nonsense-mediated messenger RNA decay is initiated by endonucleolytic cleavage in *Drosophila*. *Nature* 429, 575-578.
- Gherzi,R., Lee,K.Y., Briata,P., Wegmuller,D., Moroni,C., Karin,M., and Chen,C.Y. (2004). A KH domain RNA binding protein, KSRP, promotes ARE-directed mRNA turnover by recruiting the degradation machinery. *Mol. Cell* 14, 571-583.
- Gherzi,R., Trabucchi,M., Ponassi,M., Ruggiero,T., Corte,G., Moroni,C., Chen,C.Y., Khabar,K.S., Andersen,J.S., and Briata,P. (2006). The RNA-binding protein KSRP

promotes decay of beta-catenin mRNA and is inactivated by PI3K-AKT signaling. *PLoS Biol.* 5, e5.

Ghosh,M., Aguila,H.L., Michaud,J., Ai,Y., Wu,M.T., Hemmes,A., Ristimaki,A., Guo,C., Furneaux,H., and Hla,T. (2009). Essential role of the RNA-binding protein HuR in progenitor cell survival in mice. *J. Clin. Invest* 119, 3530-3543.

Gill,T., Cai,T., Aulds,J., Wierzbicki,S., and Schmitt,M.E. (2004). RNase MRP cleaves the CLB2 mRNA to promote cell cycle progression: novel method of mRNA degradation. *Mol. Cell Biol.* 24, 945-953.

Goldstrohm,A.C. and Wickens,M. (2008). Multifunctional deadenylase complexes diversify mRNA control. *Nat. Rev. Mol. Cell Biol.* 9, 337-344.

Gong,C., Kim,Y.K., Woeller,C.F., Tang,Y., and Maquat,L.E. (2009). SMD and NMD are competitive pathways that contribute to myogenesis: effects on PAX3 and myogenin mRNAs. *Genes Dev.* 23, 54-66.

Goracznik,R. and Gunderson,S.I. (2008). The regulatory element in the 3'-untranslated region of human papillomavirus 16 inhibits expression by binding CUG-binding protein 1. *J. Biol. Chem.* 283, 2286-2296.

Graindorge,A., Le,T.O., Thuret,R., Pollet,N., Osborne,H.B., and Audic,Y. (2008). Identification of CUG-BP1/EDEN-BP target mRNAs in *Xenopus tropicalis*. *Nucleic Acids Res.* 36, 1861-1870.

Graveley,B.R. (2001). Alternative splicing: increasing diversity in the proteomic world. *Trends Genet.* 17, 100-107.

Gray,N.K., Collier,J.M., Dickson,K.S., and Wickens,M. (2000). Multiple portions of poly(A)-binding protein stimulate translation *in vivo*. *EMBO J.* 19, 4723-4733.

Grimson,A., Farh,K.K., Johnston,W.K., Garrett-Engele,P., Lim,L.P., and Bartel,D.P. (2007). MicroRNA targeting specificity in mammals: determinants beyond seed pairing. *Mol. Cell* 27, 91-105.

Gu,M. and Lima,C.D. (2005). Processing the message: structural insights into capping and decapping mRNA. *Curr. Opin. Struct. Biol.* 15, 99-106.

Gueydan,C., Droogmans,L., Chalon,P., Huez,G., Caput,D., and Kruijs,V. (1999). Identification of TIAR as a protein binding to the translational regulatory AU-rich element of tumor necrosis factor alpha mRNA. *J. Biol. Chem.* 274, 2322-2326.

Harel-Sharvit,L., Eldad,N., Haimovich,G., Barkai,O., Duek,L., and Choder,M. (2010). RNA polymerase II subunits link transcription and mRNA decay to translation. *Cell* 143, 552-563.

Harper,P.S., Brook,J.D., and Newman,E. (2001). *Myotonic dystrophy*. (London: W.B. Saunders).

- Hew, Y., Lau, C., Grzelczak, Z., and Keeley, F.W. (2000). Identification of a GA-rich sequence as a protein-binding site in the 3'-untranslated region of chicken elastin mRNA with a potential role in the developmental regulation of elastin mRNA stability. *J. Biol. Chem.* *275*, 24857-24864.
- Hirose, Y. and Ohkuma, Y. (2007). Phosphorylation of the C-terminal domain of RNA polymerase II plays central roles in the integrated events of eucaryotic gene expression. *J. Biochem.* *141*, 601-608.
- Hodson, D.J., Janas, M.L., Galloway, A., Bell, S.E., Andrews, S., Li, C.M., Pannell, R., Siebel, C.W., MacDonald, H.R., De, K.K., Ferrando, A.A., Grutz, G., and Turner, M. (2010). Deletion of the RNA-binding proteins ZFP36L1 and ZFP36L2 leads to perturbed thymic development and T lymphoblastic leukemia. *Nat. Immunol.* *11*, 717-724.
- Hoffmeyer, A., Grosse-Wilde, A., Flory, E., Neufeld, B., Kunz, M., Rapp, U.R., and Ludwig, S. (1999). Different mitogen-activated protein kinase signaling pathways cooperate to regulate tumor necrosis factor alpha gene expression in T lymphocytes. *J. Biol. Chem.* *274*, 4319-4327.
- Hotamisligil, G.S., Arner, P., Caro, J.F., Atkinson, R.L., and Spiegelman, B.M. (1995). Increased adipose tissue expression of tumor necrosis factor-alpha in human obesity and insulin resistance. *J. Clin. Invest* *95*, 2409-2415.
- Hsu, C.L. and Stevens, A. (1993). Yeast cells lacking 5'-->3' exoribonuclease 1 contain mRNA species that are poly(A) deficient and partially lack the 5' cap structure. *Mol. Cell Biol.* *13*, 4826-4835.
- Hu, J., Lutz, C.S., Wilusz, J., and Tian, B. (2005). Bioinformatic identification of candidate cis-regulatory elements involved in human mRNA polyadenylation. *RNA.* *11*, 1485-1493.
- Hu, W., Petzold, C., Collier, J., and Baker, K.E. (2010). Nonsense-mediated mRNA decapping occurs on polyribosomes in *Saccharomyces cerevisiae*. *Nat. Struct. Mol. Biol.* *17*, 244-247.
- Hu, W., Sweet, T.J., Chamnongpol, S., Baker, K.E., and Collier, J. (2009). Co-translational mRNA decay in *Saccharomyces cerevisiae*. *Nature* *461*, 225-229.
- Hui, J., Reither, G., and Bindereif, A. (2003). Novel functional role of CA repeats and hnRNP L in RNA stability. *RNA.* *9*, 931-936.
- Huichalaf, C., Sakai, K., Jin, B., Jones, K., Wang, G.L., Schoser, B., Schneider-Gold, C., Sarkar, P., Pereira-Smith, O.M., Timchenko, N., and Timchenko, L. (2010). Expansion of CUG RNA repeats causes stress and inhibition of translation in myotonic dystrophy 1 (DM1) cells. *FASEB J.* *24*, 3706-3719.
- Huntzinger, E., Kashima, I., Fauser, M., Sauliere, J., and Izaurralde, E. (2008). SMG6 is the catalytic endonuclease that cleaves mRNAs containing nonsense codons in metazoan. *RNA.* *14*, 2609-2617.



- Huttelmaier,S., Zenklusen,D., Lederer,M., Dichtenberg,J., Lorenz,M., Meng,X., Bassell,G.J., Condeelis,J., and Singer,R.H. (2005). Spatial regulation of beta-actin translation by Src-dependent phosphorylation of ZBP1. *Nature* 438, 512-515.
- Ikezoe,K., Nakamori,M., Furuya,H., Arahata,H., Kanemoto,S., Kimura,T., Imaizumi,K., Takahashi,M.P., Sakoda,S., Fujii,N., and Kira,J. (2007). Endoplasmic reticulum stress in myotonic dystrophy type 1 muscle. *Acta Neuropathol.* 114, 527-535.
- Isken,O. and Maquat,L.E. (2007). Quality control of eukaryotic mRNA: safeguarding cells from abnormal mRNA function. *Genes Dev.* 21, 1833-1856.
- Iwahashi,C.K., Yasui,D.H., An,H.J., Greco,C.M., Tassone,F., Nannen,K., Babineau,B., Lebrilla,C.B., Hagerman,R.J., and Hagerman,P.J. (2006). Protein composition of the intranuclear inclusions of FXTAS. *Brain* 129, 256-271.
- Izaurralde,E., Lewis,J., McGuigan,C., Jankowska,M., Darzynkiewicz,E., and Mattaj,I.W. (1994). A nuclear cap binding protein complex involved in pre-mRNA splicing. *Cell* 78, 657-668.
- Jacquemont,S., Hagerman,R.J., Leehey,M., Grigsby,J., Zhang,L., Brunberg,J.A., Greco,C., Des,P., V, Jardini,T., Levine,R., Berry-Kravis,E., Brown,W.T., Schaeffer,S., Kissel,J., Tassone,F., and Hagerman,P.J. (2003). Fragile X premutation tremor/ataxia syndrome: molecular, clinical, and neuroimaging correlates. *Am. J. Hum. Genet.* 72, 869-878.
- Ji,Z., Lee,J.Y., Pan,Z., Jiang,B., and Tian,B. (2009). Progressive lengthening of 3' untranslated regions of mRNAs by alternative polyadenylation during mouse embryonic development. *Proc. Natl. Acad. Sci. U. S. A* 106, 7028-7033.
- Jiang,H., Mankodi,A., Swanson,M.S., Moxley,R.T., and Thornton,C.A. (2004). Myotonic dystrophy type 1 is associated with nuclear foci of mutant RNA, sequestration of muscleblind proteins and deregulated alternative splicing in neurons. *Hum. Mol. Genet.* 13, 3079-3088.
- Jiao,X., Xiang,S., Oh,C., Martin,C.E., Tong,L., and Kiledjian,M. (2010). Identification of a quality-control mechanism for mRNA 5'-end capping. *Nature* 467, 608-611.
- Jin,D., Hidaka,K., Shirai,M., and Morisaki,T. (2010). RNA-binding motif protein 24 regulates myogenin expression and promotes myogenic differentiation. *Genes Cells* 15, 1158-1167.
- Jordan,M., Schallhorn,A., and Wurm,F.M. (1996). Transfecting mammalian cells: optimization of critical parameters affecting calcium-phosphate precipitate formation. *Nucleic Acids Res.* 24, 596-601.
- Kalsotra,A., Wang,K., Li,P.F., and Cooper,T.A. (2010). MicroRNAs coordinate an alternative splicing network during mouse postnatal heart development. *Genes Dev.* 24, 653-658.

- Kalsotra,A., Xiao,X., Ward,A.J., Castle,J.C., Johnson,J.M., Burge,C.B., and Cooper,T.A. (2008). A postnatal switch of CELF and MBNL proteins reprograms alternative splicing in the developing heart. *Proc. Natl. Acad. Sci. U. S A* *105*, 20333-20338.
- Kanadia,R.N., Shin,J., Yuan,Y., Beattie,S.G., Wheeler,T.M., Thornton,C.A., and Swanson,M.S. (2006). Reversal of RNA missplicing and myotonia after muscleblind overexpression in a mouse poly(CUG) model for myotonic dystrophy. *Proc. Natl. Acad. Sci. U. S. A* *103*, 11748-11753.
- Kanagawa,M. and Toda,T. (2006). The genetic and molecular basis of muscular dystrophy: roles of cell-matrix linkage in the pathogenesis. *J. Hum. Genet.* *51*, 915-926.
- Kapp,L.D. and Lorsch,J.R. (2004). The molecular mechanics of eukaryotic translation. *Annu. Rev. Biochem.* *73*, 657-704.
- Katagiri,T., Akiyama,S., Namiki,M., Komaki,M., Yamaguchi,A., Rosen,V., Wozney,J.M., Fujisawa-Sehara,A., and Suda,T. (1997). Bone morphogenetic protein-2 inhibits terminal differentiation of myogenic cells by suppressing the transcriptional activity of MyoD and myogenin. *Exp. Cell Res.* *230*, 342-351.
- Kawai,T., Lal,A., Yang,X., Galban,S., Mazan-Mamczarz,K., and Gorospe,M. (2006). Translational control of cytochrome c by RNA-binding proteins TIA-1 and HuR. *Mol. Cell Biol.* *26*, 3295-3307.
- Keene,J.D. (2007). RNA regulons: coordination of post-transcriptional events. *Nat. Rev. Genet.* *8*, 533-543.
- Kelker,H.C., Oppenheim,J.D., Stone-Wolff,D., Henriksen-DeStefano,D., Aggarwal,B.B., Stevenson,H.C., and Vilcek,J. (1985). Characterization of human tumor necrosis factor produced by peripheral blood monocytes and its separation from lymphotoxin. *Int. J. Cancer* *36*, 69-73.
- Kewalramani,G., Bilan,P.J., and Klip,A. (2010). Muscle insulin resistance: assault by lipids, cytokines and local macrophages. *Curr. Opin. Clin. Nutr. Metab Care* *13*, 382-390.
- Kiledjian,M., Wang,X., and Liebhaber,S.A. (1995). Identification of two KH domain proteins in the alpha-globin mRNP stability complex. *EMBO J.* *14*, 4357-4364.
- Kim,J.H. and Richter,J.D. (2006). Opposing polymerase-deadenylase activities regulate cytoplasmic polyadenylation. *Mol. Cell* *24*, 173-183.
- Kim,V.N., Kataoka,N., and Dreyfuss,G. (2001). Role of the nonsense-mediated decay factor hUpf3 in the splicing-dependent exon-exon junction complex. *Science* *293*, 1832-1836.
- Kiss,D.L. and Andrulis,E.D. (2010). Genome-wide analysis reveals distinct substrate specificities of Rrp6, Dis3, and core exosome subunits. *RNA.* *16*, 781-791.

- Knapinska,A.M., Gratacos,F.M., Krause,C.D., Hernandez,K., Jensen,A.G., Bradley,J.J., Wu,X., Pestka,S., and Brewer,G. (2011). Chaperone Hsp27 modulates AUF1 proteolysis and AU-rich element-mediated mRNA degradation. *Mol. Cell Biol.* 31, 1419-1431.
- Kong,J., Sumaroka,M., Eastmond,D.L., and Liebhaber,S.A. (2006). Shared stabilization functions of pyrimidine-rich determinants in the erythroid 15-lipoxygenase and alpha-globin mRNAs. *Mol. Cell Biol.* 26, 5603-5614.
- Kontoyiannis,D., Boulougouris,G., Manoloukos,M., Armaka,M., Apostolaki,M., Pizarro,T., Kotlyarov,A., Forster,I., Flavell,R., Gaestel,M., Tschlis,P., Cominelli,F., and Kollias,G. (2002). Genetic dissection of the cellular pathways and signaling mechanisms in modeled tumor necrosis factor-induced Crohn's-like inflammatory bowel disease. *J. Exp. Med.* 196, 1563-1574.
- Kontoyiannis,D., Pasparakis,M., Pizarro,T.T., Cominelli,F., and Kollias,G. (1999). Impaired on/off regulation of TNF biosynthesis in mice lacking TNF AU-rich elements: implications for joint and gut-associated immunopathologies. *Immunity.* 10, 387-398.
- Korner,C.G. and Wahle,E. (1997). Poly(A) tail shortening by a mammalian poly(A)-specific 3'-exoribonuclease. *J. Biol. Chem.* 272, 10448-10456.
- Kress,C., Gautier-Court, Osborne,H.B., Babinet,C., and Paillard,L. (2007). Inactivation of CUG-BP1/CELF1 causes growth, viability, and spermatogenesis defects in mice. *Mol. Cell Biol.* 27, 1146-1157.
- Kushner,S.R. (2004). mRNA decay in prokaryotes and eukaryotes: different approaches to a similar problem. *IUBMB. Life* 56, 585-594.
- Kuyumcu-Martinez,N.M., Wang,G.S., and Cooper,T.A. (2007). Increased steady-state levels of CUGBP1 in myotonic dystrophy 1 are due to PKC-mediated hyperphosphorylation. *Mol. Cell* 28, 68-78.
- La Spada,A.R., Wilson,E.M., Lubahn,D.B., Harding,A.E., and Fischbeck,K.H. (1991). Androgen receptor gene mutations in X-linked spinal and bulbar muscular atrophy. *Nature* 352, 77-79.
- LaCava,J., Houseley,J., Saveanu,C., Petfalski,E., Thompson,E., Jacquier,A., and Tollervey,D. (2005). RNA degradation by the exosome is promoted by a nuclear polyadenylation complex. *Cell* 121, 713-724.
- Ladd,A.N., Charlet,N., and Cooper,T.A. (2001). The CELF family of RNA binding proteins is implicated in cell-specific and developmentally regulated alternative splicing. *Mol. Cell Biol.* 21, 1285-1296.
- Ladd,A.N., Stenberg,M.G., Swanson,M.S., and Cooper,T.A. (2005). Dynamic balance between activation and repression regulates pre-mRNA alternative splicing during heart development. *Dev. Dyn.* 233, 783-793.
- Lai,W.S., Carballo,E., Strum,J.R., Kennington,E.A., Phillips,R.S., and Blackshear,P.J. (1999). Evidence that tristetraprolin binds to AU-rich elements and promotes the

deadenylation and destabilization of tumor necrosis factor alpha mRNA. *Mol. Cell Biol.* **19**, 4311-4323.

Lal,A., Mazan-Mamczarz,K., Kawai,T., Yang,X., Martindale,J.L., and Gorospe,M. (2004). Concurrent versus individual binding of HuR and AUF1 to common labile target mRNAs. *EMBO J.* **23**, 3092-3102.

Laroia,G., Cuesta,R., Brewer,G., and Schneider,R.J. (1999). Control of mRNA decay by heat shock-ubiquitin-proteasome pathway. *Science* **284**, 499-502.

Le,H.H., Gatfield,D., Izaurrealde,E., and Moore,M.J. (2001). The exon-exon junction complex provides a binding platform for factors involved in mRNA export and nonsense-mediated mRNA decay. *EMBO J.* **20**, 4987-4997.

Lechner,C., Zahalka,M.A., Giot,J.F., Moller,N.P., and Ullrich,A. (1996). ERK6, a mitogen-activated protein kinase involved in C2C12 myoblast differentiation. *Proc. Natl. Acad. Sci. U. S. A* **93**, 4355-4359.

Lee,H.C., Choe,J., Chi,S.G., and Kim,Y.K. (2009). Exon junction complex enhances translation of spliced mRNAs at multiple steps. *Biochem. Biophys. Res. Commun.* **384**, 334-340.

Lee,J.E. and Cooper,T.A. (2009). Pathogenic mechanisms of myotonic dystrophy. *Biochem. Soc. Trans.* **37**, 1281-1286.

Lee,J.E., Lee,J.Y., Wilusz,J., Tian,B., and Wilusz,C.J. (2010). Systematic analysis of cis-elements in unstable mRNAs demonstrates that CUGBP1 is a key regulator of mRNA decay in muscle cells. *PLoS. One.* **5**, e11201.

Lee,W., Mitchell,P., and Tjian,R. (1987). Purified transcription factor AP-1 interacts with TPA-inducible enhancer elements. *Cell* **49**, 741-752.

Lejeune,F., Li,X., and Maquat,L.E. (2003). Nonsense-mediated mRNA decay in mammalian cells involves decapping, deadenylating, and exonucleolytic activities. *Mol. Cell* **12**, 675-687.

Lewis,J.D. and Izaurrealde,E. (1997). The role of the cap structure in RNA processing and nuclear export. *Eur. J. Biochem.* **247**, 461-469.

Li,Y., Jiang,B., Ensign,W.Y., Vogt,P.K., and Han,J. (2000). Myogenic differentiation requires signalling through both phosphatidylinositol 3-kinase and p38 MAP kinase. *Cell Signal.* **12**, 751-757.

Li,Y.P. and Reid,M.B. (2001). Effect of tumor necrosis factor-alpha on skeletal muscle metabolism. *Curr. Opin. Rheumatol.* **13**, 483-487.

Li,Y.P. and Schwartz,R.J. (2001). TNF-alpha regulates early differentiation of C2C12 myoblasts in an autocrine fashion. *FASEB J.* **15**, 1413-1415.

- Liu,H., Rodgers,N.D., Jiao,X., and Kiledjian,M. (2002). The scavenger mRNA decapping enzyme DcpS is a member of the HIT family of pyrophosphatases. *EMBO J.* *21*, 4699-4708.
- Logigian,E.L., Moxley,R.T., Blood,C.L., Barbieri,C.A., Martens,W.B., Wiegner,A.W., Thornton,C.A., and Moxley,R.T., III (2004). Leukocyte CTG repeat length correlates with severity of myotonia in myotonic dystrophy type 1. *Neurology* *62*, 1081-1089.
- Lopez,d.S., I, Zhan,M., Lal,A., Yang,X., and Gorospe,M. (2004). Identification of a target RNA motif for RNA-binding protein HuR. *Proc. Natl. Acad. Sci. U. S. A* *101*, 2987-2992.
- Lu,G., Dolgner,S.J., and Hall,T.M. (2009). Understanding and engineering RNA sequence specificity of PUF proteins. *Curr. Opin. Struct. Biol.* *19*, 110-115.
- Lu,J.Y., Sadri,N., and Schneider,R.J. (2006). Endotoxic shock in AUF1 knockout mice mediated by failure to degrade proinflammatory cytokine mRNAs. *Genes Dev.* *20*, 3174-3184.
- Lykke-Andersen,J. and Wagner,E. (2005). Recruitment and activation of mRNA decay enzymes by two ARE-mediated decay activation domains in the proteins TTP and BRF-1. *Genes Dev.* *19*, 351-361.
- Ma,W.J., Cheng,S., Campbell,C., Wright,A., and Furneaux,H. (1996). Cloning and characterization of HuR, a ubiquitously expressed Elav-like protein. *J. Biol. Chem.* *271*, 8144-8151.
- Mahadevan,M.S., Yadava,R.S., Yu,Q., Balijepalli,S., Frenzel-McCardell,C.D., Bourne,T.D., and Phillips,L.H. (2006). Reversible model of RNA toxicity and cardiac conduction defects in myotonic dystrophy. *Nat. Genet.* *38*, 1066-1070.
- Mammarella,A., Ferroni,P., Paradiso,M., Martini,F., Paoletti,V., Morino,S., Antonini,G., Gazzaniga,P.P., Musca,A., and Basili,S. (2002). Tumor necrosis factor-alpha and myocardial function in patients with myotonic dystrophy type 1. *J. Neurol. Sci.* *201*, 59-64.
- Mandel,C.R., Kaneko,S., Zhang,H., Gebauer,D., Vethantham,V., Manley,J.L., and Tong,L. (2006). Polyadenylation factor CPSF-73 is the pre-mRNA 3'-end-processing endonuclease. *Nature* *444*, 953-956.
- Maniatis,T. and Reed,R. (2002). An extensive network of coupling among gene expression machines. *Nature* *416*, 499-506.
- Mankodi,A., Takahashi,M.P., Jiang,H., Beck,C.L., Bowers,W.J., Moxley,R.T., Cannon,S.C., and Thornton,C.A. (2002). Expanded CUG repeats trigger aberrant splicing of CIC-1 chloride channel pre-mRNA and hyperexcitability of skeletal muscle in myotonic dystrophy. *Mol. Cell* *10*, 35-44.
- Mankodi,A., Teng-Umnuay,P., Krym,M., Henderson,D., Swanson,M., and Thornton,C.A. (2003). Ribonuclear inclusions in skeletal muscle in myotonic dystrophy types 1 and 2. *Ann. Neurol.* *54*, 760-768.

- Maquat,L.E. (2004). Nonsense-mediated mRNA decay: splicing, translation and mRNP dynamics. *Nat. Rev. Mol. Cell Biol.* 5, 89-99.
- Marchese,F.P., Aubareda,A., Tudor,C., Saklatvala,J., Clark,A.R., and Dean,J.L. (2010). MAPKAP kinase 2 blocks tristetraprolin-directed mRNA decay by inhibiting CAF1 deadenylase recruitment. *J. Biol. Chem.* 285, 27590-27600.
- Margolis,J.M., Schoser,B.G., Moseley,M.L., Day,J.W., and Ranum,L.P. (2006). DM2 intronic expansions: evidence for CCUG accumulation without flanking sequence or effects on ZNF9 mRNA processing or protein expression. *Hum. Mol. Genet.* 15, 1808-1815.
- Marquis,J., Paillard,L., Audic,Y., Cosson,B., Danos,O., Le,B.C., and Osborne,H.B. (2006). CUG-BP1/CELF1 requires UGU-rich sequences for high-affinity binding. *Biochem. J.* 400, 291-301.
- Mayr,C. and Bartel,D.P. (2009). Widespread shortening of 3'UTRs by alternative cleavage and polyadenylation activates oncogenes in cancer cells. *Cell* 138, 673-684.
- Mazan-Mamczarz,K., Hagner,P.R., Corl,S., Srikantan,S., Wood,W.H., Becker,K.G., Gorospe,M., Keene,J.D., Levenson,A.S., and Gartenhaus,R.B. (2008). Post-transcriptional gene regulation by HuR promotes a more tumorigenic phenotype. *Oncogene* 27, 6151-6163.
- McKinsey,T.A., Zhang,C.L., and Olson,E.N. (2002). MEF2: a calcium-dependent regulator of cell division, differentiation and death. *Trends Biochem. Sci.* 27, 40-47.
- McManus,C.J. and Graveley,B.R. (2011). RNA structure and the mechanisms of alternative splicing. *Curr. Opin. Genet. Dev.*
- Melnikova,I.N., Bounpheng,M., Schatteman,G.C., Gilliam,D., and Christy,B.A. (1999). Differential biological activities of mammalian Id proteins in muscle cells. *Exp. Cell Res.* 247, 94-104.
- Mercer,S.E., Ewton,D.Z., Deng,X., Lim,S., Mazur,T.R., and Friedman,E. (2005). Mirk/Dyrk1B mediates survival during the differentiation of C2C12 myoblasts. *J. Biol. Chem.* 280, 25788-25801.
- Mermelstein,C.S., Costa,M.L., Chagas,F.C., and Moura,N., V (1996). Intermediate filament proteins in TPA-treated skeletal muscle cells in culture. *J. Muscle Res. Cell Motil.* 17, 199-206.
- Michlewski,G. and Caceres,J.F. (2010). Antagonistic role of hnRNP A1 and KSRP in the regulation of let-7a biogenesis. *Nat. Struct. Mol. Biol.* 17, 1011-1018.
- Miller,C., Schwalb,B., Maier,K., Schulz,D., Dumcke,S., Zacher,B., Mayer,A., Sydow,J., Marcinowski,L., Dolken,L., Martin,D.E., Tresch,A., and Cramer,P. (2011). Dynamic transcriptome analysis measures rates of mRNA synthesis and decay in yeast. *Mol. Syst. Biol.* 7, 458.

- Misquitta,C.M., Iyer,V.R., Werstiuk,E.S., and Grover,A.K. (2001). The role of 3'-untranslated region (3'-UTR) mediated mRNA stability in cardiovascular pathophysiology. *Mol. Cell Biochem.* 224, 53-67.
- Mittal,S., Aslam,A., Doidge,R., Medica,R., and Winkler,G.S. (2011). The Ccr4a (CNOT6) and Ccr4b (CNOT6L) deadenylase subunits of the human Ccr4-Not complex contribute to the prevention of cell death and senescence. *Mol. Biol. Cell* 22, 748-758.
- Miyake,T., Alli,N.S., and McDermott,J.C. (2010). Nuclear function of Smad7 promotes myogenesis. *Mol. Cell Biol.* 30, 722-735.
- Mocholi,E., Ballester-Lurbe,B., Arque,G., Poch,E., Peris,B., Guerri,C., Dierssen,M., Guasch,R.M., Terrado,J., and Perez-Roger,I. (2011). RhoE deficiency produces postnatal lethality, profound motor deficits and neurodevelopmental delay in mice. *PLoS One.* 6, e19236.
- Modoni,A., Silvestri,G., Pomponi,M.G., Mangiola,F., Tonali,P.A., and Marra,C. (2004). Characterization of the pattern of cognitive impairment in myotonic dystrophy type 1. *Arch. Neurol.* 61, 1943-1947.
- Molkentin,J.D. and Olson,E.N. (1996). Defining the regulatory networks for muscle development. *Curr. Opin. Genet. Dev.* 6, 445-453.
- Moraes,K.C., Wilusz,C.J., and Wilusz,J. (2006). CUG-BP binds to RNA substrates and recruits PARN deadenylase. *RNA.* 12, 1084-1091.
- Mori,D., Sasagawa,N., Kino,Y., and Ishiura,S. (2008). Quantitative analysis of CUG-BP1 binding to RNA repeats. *J. Biochem.* 143, 377-383.
- Morris,A.R., Mukherjee,N., and Keene,J.D. (2008). Ribonomic analysis of human Pum1 reveals cis-trans conservation across species despite evolution of diverse mRNA target sets. *Mol. Cell Biol.* 28, 4093-4103.
- Mukherjee,D., Gao,M., O'Connor,J.P., Raijmakers,R., Pruijn,G., Lutz,C.S., and Wilusz,J. (2002). The mammalian exosome mediates the efficient degradation of mRNAs that contain AU-rich elements. *EMBO J.* 21, 165-174.
- Mukherjee,N., Corcoran,D.L., Nusbaum,J.D., Reid,D.W., Georgiev,S., Hafne, M., Ascano,M. Jr, Tuschl,T., Ohle, U., Keene,J.D. (2011) Integrative Regulatory Mapping Indicates that the RNA-Binding Protein HuR Couples Pre-mRNA Processing and mRNA Stability. *Mol. Cell Epub In Press.*
- Mukherjee,N., Lager,P.J., Friedersdorf,M.B., Thompson,M.A., and Keene,J.D. (2009). Coordinated posttranscriptional mRNA population dynamics during T-cell activation. *Mol. Syst. Biol.* 5, 288.
- Mukhopadhyay,D., Houchen,C.W., Kennedy,S., Dieckgraefe,B.K., and Anant,S. (2003). Coupled mRNA stabilization and translational silencing of cyclooxygenase-2 by a novel RNA binding protein, CUGBP2. *Mol. Cell* 11, 113-126.

Mulders, S.A., van den Broek, W.J., Wheeler, T.M., Croes, H.J., van Kuik-Romeijn, P., de Kimpe, S.J., Furling, D., Platenburg, G.J., Gourdon, G., Thornton, C.A., Wieringa, B., and Wansink, D.G. (2009). Triplet-repeat oligonucleotide-mediated reversal of RNA toxicity in myotonic dystrophy. *Proc. Natl. Acad. Sci. U. S. A* *106*, 13915-13920.

Musova, Z., Mazanec, R., Krepelova, A., Ehler, E., Vales, J., Jaklova, R., Prochazka, T., Koukal, P., Marikova, T., Kraus, J., Havlovicova, M., and Sedlacek, Z. (2009). Highly unstable sequence interruptions of the CTG repeat in the myotonic dystrophy gene. *Am. J. Med. Genet. A* *149A*, 1365-1374.

Naguibneva, I., Poleskaya, A., meyar-Zazoua, M., Souidi, M., Groisman, R., Cuvellier, S., Ait-Si-Ali, S., Pritchard, L.L., and Harel-Bellan, A. (2007). Micro-RNAs and muscle differentiation. *J. Soc. Biol.* *201*, 367-376.

Nilsen, T.W. and Graveley, B.R. (2010). Expansion of the eukaryotic proteome by alternative splicing. *Nature* *463*, 457-463.

Noble, K.N., Tran, E.J., cazar-Roman, A.R., Hodge, C.A., Cole, C.N., and Wentz, S.R. (2011). The Dbp5 cycle at the nuclear pore complex during mRNA export II: nucleotide cycling and mRNP remodeling by Dbp5 are controlled by Nup159 and Gle1. *Genes Dev.* *25*, 1065-1077.

Ohno, M., Kataoka, N., and Shimura, Y. (1990). A nuclear cap binding protein from HeLa cells. *Nucleic Acids Res.* *18*, 6989-6995.

Orengo, J.P., Ward, A.J., and Cooper, T.A. (2011). Alternative splicing dysregulation secondary to skeletal muscle regeneration. *Ann. Neurol.* *69*, 681-690.

Paillard, L., Legagneux, V., Maniey, D., and Osborne, H.B. (2002). c-Jun ARE targets mRNA deadenylation by an EDEN-BP (embryo deadenylation element-binding protein)-dependent pathway. *J. Biol. Chem.* *277*, 3232-3235.

Paillard, L., Omilli, F., Legagneux, V., Bassez, T., Maniey, D., and Osborne, H.B. (1998). EDEN and EDEN-BP, a cis element and an associated factor that mediate sequence-specific mRNA deadenylation in *Xenopus* embryos. *EMBO J.* *17*, 278-287.

Parker, R. and Sheth, U. (2007). P bodies and the control of mRNA translation and degradation. *Mol. Cell* *25*, 635-646.

Parker, S.B., Eichele, G., Zhang, P., Rawls, A., Sands, A.T., Bradley, A., Olson, E.N., Harper, J.W., and Elledge, S.J. (1995). p53-independent expression of p21Cip1 in muscle and other terminally differentiating cells. *Science* *267*, 1024-1027.

Passos, D.O., Doma, M.K., Shoemaker, C.J., Muhlrads, D., Green, R., Weissman, J., Hollien, J., and Parker, R. (2009). Analysis of Dom34 and its function in no-go decay. *Mol. Biol. Cell* *20*, 3025-3032.

Patapoutian, A., Yoon, J.K., Miner, J.H., Wang, S., Stark, K., and Wold, B. (1995). Disruption of the mouse MRF4 gene identifies multiple waves of myogenesis in the myotome. *Development* *121*, 3347-3358.



- Peng,S.S., Chen,C.Y., and Shyu,A.B. (1996). Functional characterization of a non-AUUUA AU-rich element from the c-jun proto-oncogene mRNA: evidence for a novel class of AU-rich elements. *Mol. Cell Biol.* 16, 1490-1499.
- Philips,A.V., Timchenko,L.T., and Cooper,T.A. (1998). Disruption of splicing regulated by a CUG-binding protein in myotonic dystrophy. *Science* 280, 737-741.
- Pieczyk,M., Wax,S., Beck,A.R., Kedersha,N., Gupta,M., Maritim,B., Chen,S., Gueydan,C., Kruys,V., Streuli,M., and Anderson,P. (2000). TIA-1 is a translational silencer that selectively regulates the expression of TNF-alpha. *EMBO J.* 19, 4154-4163.
- Poole,T.L. and Stevens,A. (1995). Comparison of features of the RNase activity of 5'-exonuclease-1 and 5'-exonuclease-2 of *Saccharomyces cerevisiae*. *Nucleic Acids Symp. Ser.* 79-81.
- Prins,J.B., Niesler,C.U., Winterford,C.M., Bright,N.A., Siddle,K., O'Rahilly,S., Walker,N.I., and Cameron,D.P. (1997). Tumor necrosis factor-alpha induces apoptosis of human adipose cells. *Diabetes* 46, 1939-1944.
- Pullmann,R., Jr., Kim,H.H., Abdelmohsen,K., Lal,A., Martindale,J.L., Yang,X., and Gorospe,M. (2007). Analysis of turnover and translation regulatory RNA-binding protein expression through binding to cognate mRNAs. *Mol. Cell Biol.* 27, 6265-6278.
- Qian,Z. and Wilusz,J. (1994). GRSF-1: a poly(A)+ mRNA binding protein which interacts with a conserved G-rich element. *Nucleic Acids Res.* 22, 2334-2343.
- Qu,X., Lykke-Andersen,S., Nasser,T., Saguez,C., Bertrand,E., Jensen,T.H., and Moore,C. (2009). Assembly of an export-competent mRNP is needed for efficient release of the 3'-end processing complex after polyadenylation. *Mol. Cell Biol.* 29, 5327-5338.
- Rabani,M., Levin,J.Z., Fan,L., Adiconis,X., Raychowdhury,R., Garber,M., Gnirke,A., Nusbaum,C., Hacohen,N., Friedman,N., Amit,I., and Regev,A. (2011). Metabolic labeling of RNA uncovers principles of RNA production and degradation dynamics in mammalian cells. *Nat. Biotechnol.* 29, 436-442.
- Raghavan,A., Ogilvie,R.L., Reilly,C., Abelson,M.L., Raghavan,S., Vasdevani,J., Krathwohl,M., and Bohjanen,P.R. (2002). Genome-wide analysis of mRNA decay in resting and activated primary human T lymphocytes. *Nucleic Acids Res.* 30, 5529-5538.
- Rajasingh,J., Bord,E., Luedemann,C., Asai,J., Hamada,H., Thorne,T., Qin,G., Goukassian,D., Zhu,Y., Losordo,D.W., and Kishore,R. (2006). IL-10-induced TNF-alpha mRNA destabilization is mediated via IL-10 suppression of p38 MAP kinase activation and inhibition of HuR expression. *FASEB J.* 20, 2112-2114.
- Rattenbacher,B., Beisang,D., Wiesner,D.L., Jeschke,J.C., von,H.M., St Louis-Vlasova,I.A., and Bohjanen,P.R. (2010). Analysis of CUGBP1 targets identifies GU-repeat sequences that mediate rapid mRNA decay. *Mol. Cell Biol.* 30, 3970-3980.

- Ray,D., Kazan,H., Chan,E.T., Pena,C.L., Chaudhry,S., Talukder,S., Blencowe,B.J., Morris,Q., and Hughes,T.R. (2009). Rapid and systematic analysis of the RNA recognition specificities of RNA-binding proteins. *Nat. Biotechnol.* 27, 667-670.
- Reich,E., Franklin,R.M., Shatkin,A.J., and Tatum,E.L. (1961). Effect of actinomycin D on cellular nucleic acid synthesis and virus production. *Science* 134, 556-557.
- Reid,M.B. and Li,Y.P. (2001). Tumor necrosis factor-alpha and muscle wasting: a cellular perspective. *Respir. Res.* 2, 269-272.
- Reinhardt,H.C., Hasskamp,P., Schmedding,I., Morandell,S., van Vugt,M.A., Wang,X., Linding,R., Ong,S.E., Weaver,D., Carr,S.A., and Yaffe,M.B. (2010). DNA damage activates a spatially distinct late cytoplasmic cell-cycle checkpoint network controlled by MK2-mediated RNA stabilization. *Mol. Cell* 40, 34-49.
- Reverdatto,S.V., Dutko,J.A., Chekanova,J.A., Hamilton,D.A., and Belostotsky,D.A. (2004). mRNA deadenylation by PARN is essential for embryogenesis in higher plants. *RNA* 10, 1200-1214.
- Rigo,F. and Martinson,H.G. (2009). Polyadenylation releases mRNA from RNA polymerase II in a process that is licensed by splicing. *RNA*. 15, 823-836.
- Rodriguez,A., Griffiths-Jones,S., Ashurst,J.L., and Bradley,A. (2004a). Identification of mammalian microRNA host genes and transcription units. *Genome Res.* 14, 1902-1910.
- Rodriguez,M.S., Dargemont,C., and Stutz,F. (2004b). Nuclear export of RNA. *Biol. Cell* 96, 639-655.
- Rudnicki,M.A., Schnegelsberg,P.N., Stead,R.H., Braun,T., Arnold,H.H., and Jaenisch,R. (1993). MyoD or Myf-5 is required for the formation of skeletal muscle. *Cell* 75, 1351-1359.
- Ruepp,M.D., Aringhieri,C., Vivarelli,S., Cardinale,S., Paro,S., Schumperli,D., and Barabino,S.M. (2009). Mammalian pre-mRNA 3' end processing factor CF-68 functions in mRNA export. *Mol. Biol. Cell* 20, 5211-5223.
- Sachs,A.B. and Varani,G. (2000). Eukaryotic translation initiation: there are (at least) two sides to every story. *Nat. Struct. Biol.* 7, 356-361.
- Saito,K., Kobayashi,D., Komatsu,M., Yajima,T., Yagihashi,A., Ishikawa,Y., Minami,R., and Watanabe,N. (2000). A sensitive assay of tumor necrosis factor alpha in sera from Duchenne muscular dystrophy patients. *Clin. Chem.* 46, 1703-1704.
- Saitoh,O., Arai,T., and Obinata,T. (1988). Distribution of microtubules and other cytoskeletal filaments during myotube elongation as revealed by fluorescence microscopy. *Cell Tissue Res.* 252, 263-273.
- Salehzada,T., Cambier,L., Vu,T.N., Manchon,L., Regnier,L., and Bisbal,C. (2009). Endoribonuclease L (RNase L) regulates the myogenic and adipogenic potential of myogenic cells. *PLoS. One.* 4, e7563.

- Sandberg,R., Neilson,J.R., Sarma,A., Sharp,P.A., and Burge,C.B. (2008). Proliferating cells express mRNAs with shortened 3' untranslated regions and fewer microRNA target sites. *Science* 320, 1643-1647.
- Sandler,H., Kreth,J., Timmers,H.T., and Stoecklin,G. (2011). Not1 mediates recruitment of the deadenylase Caf1 to mRNAs targeted for degradation by tristetraprolin. *Nucleic Acids Res.* 39, 4373-4386.
- Sandler,H. and Stoecklin,G. (2008). Control of mRNA decay by phosphorylation of tristetraprolin. *Biochem. Soc. Trans.* 36, 491-496.
- Sanduja,S., Blanco,F.F., and Dixon,D.A. (2010). The roles of TTP and BRF proteins in regulated mRNA decay. *Wiley. Interdiscip. Rev. RNA.* 2, 42-57.
- Sato,H. and Maquat,L.E. (2009). Remodeling of the pioneer translation initiation complex involves translation and the karyopherin importin beta. *Genes Dev.* 23, 2537-2550.
- Savkur,R.S., Philips,A.V., and Cooper,T.A. (2001). Aberrant regulation of insulin receptor alternative splicing is associated with insulin resistance in myotonic dystrophy. *Nat. Genet.* 29, 40-47.
- Schaeffer,D., Tsanova,B., Barbas,A., Reis,F.P., Dastidar,E.G., Sanchez-Rotunno,M., Arraiano,C.M., and Van Hoof, A. (2009). The exosome contains domains with specific endoribonuclease, exoribonuclease and cytoplasmic mRNA decay activities. *Nat. Struct. Mol. Biol.* 16, 56-62.
- Schmidt,M.J., West,S., and Norbury,C.J. (2011). The human cytoplasmic RNA terminal U-transferase ZCCHC11 targets histone mRNAs for degradation. *RNA.* 17, 39-44.
- Schneider,M.D., Bains,A.K., Rajendra,T.K., Dominski,Z., Matera,A.G., and Simmonds,A.J. (2010). Functional characterization of the *Drosophila* MRP (mitochondrial RNA processing) RNA gene. *RNA.* 16, 2120-2130.
- Schuster-Gossler,K., Cordes,R., and Gossler,A. (2007). Premature myogenic differentiation and depletion of progenitor cells cause severe muscle hypotrophy in Delta1 mutants. *Proc. Natl. Acad. Sci. U. S. A* 104, 537-542.
- Schwanhausser,B., Busse,D., Li,N., Dittmar,G., Schuchhardt,J., Wolf,J., Chen,W., and Selbach,M. (2011). Global quantification of mammalian gene expression control. *Nature* 473, 337-342.
- Seal,R., Temperley,R., Wilusz,J., Lightowers,R.N., and Chrzanowska-Lightowers,Z.M. (2005). Serum-deprivation stimulates cap-binding by PARN at the expense of eIF4E, consistent with the observed decrease in mRNA stability. *Nucleic Acids Res.* 33, 376-387.
- Sharova,L.V., Sharov,A.A., Nedorezov,T., Piao,Y., Shaik,N., and Ko,M.S. (2009). Database for mRNA half-life of 19 977 genes obtained by DNA microarray analysis of pluripotent and differentiating mouse embryonic stem cells. *DNA Res.* 16, 45-58.

- Shaw,G. and Kamen,R. (1986). A conserved AU sequence from the 3' untranslated region of GM-CSF mRNA mediates selective mRNA degradation. *Cell* 46, 659-667.
- Sheets,M.D. and Wickens,M. (1989). Two phases in the addition of a poly(A) tail. *Genes Dev.* 3, 1401-1412.
- Shimizu,T., Tomita,Y., Son,K., Nishinarita,S., Sawada,S., and Horie,T. (2000). Elevation of serum soluble tumour necrosis factor receptors in patients with polymyositis and dermatomyositis. *Clin. Rheumatol.* 19, 352-359.
- Shruti,K., Shrey,K., and Vibha,R. (2011). Micro RNAs: tiny sequences with enormous potential. *Biochem. Biophys. Res. Commun.* 407, 445-449.
- Simon,E., Camier,S., and Seraphin,B. (2006). New insights into the control of mRNA decapping. *Trends Biochem. Sci.* 31, 241-243.
- Sofola,O.A., Jin,P., Qin,Y., Duan,R., Liu,H., de,H.M., Nelson,D.L., and Botas,J. (2007). RNA-binding proteins hnRNP A2/B1 and CUGBP1 suppress fragile X CGG premutation repeat-induced neurodegeneration in a *Drosophila* model of FXTAS. *Neuron* 55, 565-571.
- Sokoloski,K.J., Dickson,A.M., Chaskey,E.L., Garneau,N.L., Wilusz,C.J., and Wilusz,J. (2010). Sindbis virus usurps the cellular HuR protein to stabilize its transcripts and promote productive infections in mammalian and mosquito cells. *Cell Host. Microbe* 8, 196-207.
- Song,M.G., Li,Y., and Kiledjian,M. (2010). Multiple mRNA decapping enzymes in mammalian cells. *Mol. Cell* 40, 423-432.
- Spector,D.L. (2006). SnapShot: Cellular bodies. *Cell* 127, 1071.
- Stewart,S.A., Dykxhoorn,D.M., Palliser,D., Mizuno,H., Yu,E.Y., An,D.S., Sabatini,D.M., Chen,I.S., Hahn,W.C., Sharp,P.A., Weinberg,R.A., and Novina,C.D. (2003). Lentivirus-delivered stable gene silencing by RNAi in primary cells. *RNA*. 9, 493-501.
- Stoecklin,G., Lu,M., Rattenbacher,B., and Moroni,C. (2003). A constitutive decay element promotes tumor necrosis factor alpha mRNA degradation via an AU-rich element-independent pathway. *Mol. Cell Biol.* 23, 3506-3515.
- Stoecklin,G., Stubbs,T., Kedersha,N., Wax,S., Rigby,W.F., Blackwell,T.K., and Anderson,P. (2004). MK2-induced tristetraprolin:14-3-3 complexes prevent stress granule association and ARE-mRNA decay. *EMBO J.* 23, 1313-1324.
- Stumpo,D.J., Broxmeyer,H.E., Ward,T., Cooper,S., Hangoc,G., Chung,Y.J., Shelley,W.C., Richfield,E.K., Ray,M.K., Yoder,M.C., Aplan,P.D., and Blackshear,P.J. (2009). Targeted disruption of Zfp36l2, encoding a CCCH tandem zinc finger RNA-binding protein, results in defective hematopoiesis. *Blood* 114, 2401-2410.
- Sun,L., Stoecklin,G., Van,W.S., Hinkovska-Galcheva,V., Guo,R.F., Anderson,P., and Shanley,T.P. (2007). Tristetraprolin (TTP)-14-3-3 complex formation protects TTP from

dephosphorylation by protein phosphatase 2a and stabilizes tumor necrosis factor- $\alpha$  mRNA. *J. Biol. Chem.* 282, 3766-3777.

Sureban,S.M., Murmu,N., Rodriguez,P., May,R., Maheshwari,R., Dieckgraefe,B.K., Houchen,C.W., and Anant,S. (2007). Functional antagonism between RNA binding proteins HuR and CUGBP2 determines the fate of COX-2 mRNA translation. *Gastroenterology* 132, 1055-1065.

't Hoen,P.A., Hirsch,M., de Meijer,E.J., de Menezes,R.X., van Ommen,G.J., and den Dunnen,J.T. (2011). mRNA degradation controls differentiation state-dependent differences in transcript and splice variant abundance. *Nucleic Acids Res.* 39, 556-566.

Takahashi,N., Sasagawa,N., Suzuki,K., and Ishiura,S. (2000). The CUG-binding protein binds specifically to UG dinucleotide repeats in a yeast three-hybrid system. *Biochem. Biophys. Res. Commun.* 277, 518-523.

Tarun,S.Z., Jr. and Sachs,A.B. (1996). Association of the yeast poly(A) tail binding protein with translation initiation factor eIF-4G. *EMBO J.* 15, 7168-7177.

Taylor,G.A., Carballo,E., Lee,D.M., Lai,W.S., Thompson,M.J., Patel,D.D., Schenkman,D.I., Gilkeson,G.S., Broxmeyer,H.E., Haynes,B.F., and Blackshear,P.J. (1996). A pathogenetic role for TNF  $\alpha$  in the syndrome of cachexia, arthritis, and autoimmunity resulting from tristetraprolin (TTP) deficiency. *Immunity.* 4, 445-454.

Tenenbaum,S.A., Lager,P.J., Carson,C.C., and Keene,J.D. (2002). Ribonomics: identifying mRNA subsets in mRNP complexes using antibodies to RNA-binding proteins and genomic arrays. *Methods* 26, 191-198.

Tharun,S., He,W., Mayes,A.E., Lennertz,P., Beggs,J.D., and Parker,R. (2000). Yeast Sm-like proteins function in mRNA decapping and decay. *Nature* 404, 515-518.

Tian,B., Hu,J., Zhang,H., and Lutz,C.S. (2005). A large-scale analysis of mRNA polyadenylation of human and mouse genes. *Nucleic Acids Res.* 33, 201-212.

Timchenko,L.T., Miller,J.W., Timchenko,N.A., DeVore,D.R., Datar,K.V., Lin,L., Roberts,R., Caskey,C.T., and Swanson,M.S. (1996). Identification of a (CUG) $_n$  triplet repeat RNA-binding protein and its expression in myotonic dystrophy. *Nucleic Acids Res.* 24, 4407-4414.

Timchenko,N.A., Patel,R., Iakova,P., Cai,Z.J., Quan,L., and Timchenko,L.T. (2004). Overexpression of CUG triplet repeat-binding protein, CUGBP1, in mice inhibits myogenesis. *J. Biol. Chem.* 279, 13129-13139.

Timchenko,N.A., Wang,G.L., and Timchenko,L.T. (2005). RNA CUG-binding protein 1 increases translation of 20-kDa isoform of CCAAT/enhancer-binding protein beta by interacting with the alpha and beta subunits of eukaryotic initiation translation factor 2. *J. Biol. Chem.* 280, 20549-20557.

- Timchenko,N.A., Welm,A.L., Lu,X., and Timchenko,L.T. (1999). CUG repeat binding protein (CUGBP1) interacts with the 5' region of C/EBPbeta mRNA and regulates translation of C/EBPbeta isoforms. *Nucleic Acids Res.* 27, 4517-4525.
- Trabucchi,M., Briata,P., Garcia-Mayoral,M., Haase,A.D., Filipowicz,W., Ramos,A., Gherzi,R., and Rosenfeld,M.G. (2009). The RNA-binding protein KSRP promotes the biogenesis of a subset of microRNAs. *Nature* 459, 1010-1014.
- Tracey,K.J. and Cerami,A. (1994). Tumor necrosis factor: a pleiotropic cytokine and therapeutic target. *Annu. Rev. Med.* 45, 491-503.
- Tran,H., Schilling,M., Wirbelauer,C., Hess,D., and Nagamine,Y. (2004). Facilitation of mRNA deadenylation and decay by the exosome-bound, DExH protein RHAU. *Mol. Cell* 13, 101-111.
- Tsuda,K., Kuwasako,K., Takahashi,M., Someya,T., Inoue,M., Terada,T., Kobayashi,N., Shirouzu,M., Kigawa,T., Tanaka,A., Sugano,S., Guntert,P., Muto,Y., and Yokoyama,S. (2009). Structural basis for the sequence-specific RNA-recognition mechanism of human CUG-BP1 RRM3. *Nucleic Acids Res.*
- Untergasser,A., Nijveen,H., Rao,X., Bisseling,T., Geurts,R., and Leunissen,J.A. (2007). Primer3Plus, an enhanced web interface to Primer3. *Nucleic Acids Res.* 35, W71-W74.
- van Dijk,E.L., Schilders,G., and Pruijn,G.J. (2007). Human cell growth requires a functional cytoplasmic exosome, which is involved in various mRNA decay pathways. *RNA.* 13, 1027-1035.
- Vandesompele,J., De,P.K., Pattyn,F., Poppe,B., Van,R.N., De,P.A., and Speleman,F. (2002). Accurate normalization of real-time quantitative RT-PCR data by geometric averaging of multiple internal control genes. *Genome Biol.* 3, RESEARCH0034.
- Vasudevan,S., Tong,Y., and Steitz,J.A. (2007). Switching from repression to activation: microRNAs can up-regulate translation. *Science* 318, 1931-1934.
- Viswanathan,S.R., Daley,G.Q., and Gregory,R.I. (2008). Selective blockade of microRNA processing by Lin28. *Science* 320, 97-100.
- Vlasova,I.A., Tahoe,N.M., Fan,D., Larsson,O., Rattenbacher,B., Sternjohn,J.R., Vasdewani,J., Karypis,G., Reilly,C.S., Bitterman,P.B., and Bohjanen,P.R. (2008). Conserved GU-rich elements mediate mRNA decay by binding to CUG-binding protein 1. *Mol. Cell* 29, 263-270.
- Wagers,A.J. and Conboy,I.M. (2005). Cellular and molecular signatures of muscle regeneration: current concepts and controversies in adult myogenesis. *Cell* 122, 659-667.
- Wang,D., Furuichi,Y., and Shatkin,A.J. (1982). Covalent guanylyl intermediate formed by HeLa cell mRNA capping enzyme. *Mol. Cell Biol.* 2, 993-1001.

- Wang,G.S., Kearney,D.L., De,B.M., Taffet,G., and Cooper,T.A. (2007). Elevation of RNA-binding protein CUGBP1 is an early event in an inducible heart-specific mouse model of myotonic dystrophy. *J. Clin. Invest* *117*, 2802-2811.
- Wang,G.S., Kuyumcu-Martinez,M.N., Sarma,S., Mathur,N., Wehrens,X.H., and Cooper,T.A. (2009a). PKC inhibition ameliorates the cardiac phenotype in a mouse model of myotonic dystrophy type 1. *J. Clin. Invest* *119*, 3797-3806.
- Wang,J.G., Collinge,M., Ramgolam,V., Ayalon,O., Fan,X.C., Pardi,R., and Bender,J.R. (2006). LFA-1-dependent HuR nuclear export and cytokine mRNA stabilization in T cell activation. *J. Immunol.* *176*, 2105-2113.
- Wang,W.X., Wilfred,B.R., Hu,Y., Stromberg,A.J., and Nelson,P.T. (2010). Anti-Argonaute RIP-Chip shows that miRNA transfections alter global patterns of mRNA recruitment to microribonucleoprotein complexes. *RNA.* *16*, 394-404.
- Wang,Y., Liu,C.L., Storey,J.D., Tibshirani,R.J., Herschlag,D., and Brown,P.O. (2002). Precision and functional specificity in mRNA decay. *Proc. Natl. Acad. Sci. U. S. A* *99*, 5860-5865.
- Wang,Y., Opperman,L., Wickens,M., and Hall,T.M. (2009b). Structural basis for specific recognition of multiple mRNA targets by a PUF regulatory protein. *Proc. Natl. Acad. Sci. U. S. A* *106*, 20186-20191.
- Ward,A.J., Rimer,M., Killian,J.M., Dowling,J.J., and Cooper,T.A. (2010). CUGBP1 overexpression in mouse skeletal muscle reproduces features of myotonic dystrophy type 1. *Hum. Mol. Genet.* *19*, 3614-3622.
- Wein,G., Rossler,M., Klug,R., and Herget,T. (2003). The 3'-UTR of the mRNA coding for the major protein kinase C substrate MARCKS contains a novel CU-rich element interacting with the mRNA stabilizing factors HuD and HuR. *Eur. J. Biochem.* *270*, 350-365.
- Williams,A.H., Liu,N., van,R.E., and Olson,E.N. (2009). MicroRNA control of muscle development and disease. *Curr. Opin. Cell Biol.* *21*, 461-469.
- Williams,A.S. and Marzluff,W.F. (1995). The sequence of the stem and flanking sequences at the 3' end of histone mRNA are critical determinants for the binding of the stem-loop binding protein. *Nucleic Acids Res.* *23*, 654-662.
- Wilusz,C.J., Wormington,M., and Peltz,S.W. (2001). The cap-to-tail guide to mRNA turnover. *Nat. Rev. Mol. Cell Biol.* *2*, 237-246.
- Wu,J., Kubota,J., Hirayama,J., Nagai,Y., Nishina,S., Yokoi,T., Asaoka,Y., Seo,J., Shimizu,N., Kajihio,H., Watanabe,T., Azuma,N., Katada,T., and Nishina,H. (2010). p38 Mitogen-activated protein kinase controls a switch between cardiomyocyte and neuronal commitment of murine embryonic stem cells by activating myocyte enhancer factor 2C-dependent bone morphogenetic protein 2 transcription. *Stem Cells Dev.* *19*, 1723-1734.

- Wu,L. and Belasco,J.G. (2008). Let me count the ways: mechanisms of gene regulation by miRNAs and siRNAs. *Mol. Cell* 29, 1-7.
- Wu,M., Nilsson,P., Henriksson,N., Niedzwiecka,A., Lim,M.K., Cheng,Z., Kokkoris,K., Virtanen,A., and Song,H. (2009). Structural basis of m(7)GpppG binding to poly(A)-specific ribonuclease. *Structure*. 17, 276-286.
- Xu,Q. and Wu,Z. (2000). The insulin-like growth factor-phosphatidylinositol 3-kinase-Akt signaling pathway regulates myogenin expression in normal myogenic cells but not in rhabdomyosarcoma-derived RD cells. *J. Biol. Chem.* 275, 36750-36757.
- Yamashita,A., Chang,T.C., Yamashita,Y., Zhu,W., Zhong,Z., Chen,C.Y., and Shyu,A.B. (2005). Concerted action of poly(A) nucleases and decapping enzyme in mammalian mRNA turnover. *Nat. Struct. Mol. Biol.* 12, 1054-1063.
- Yang,E., van,N.E., Zavolan,M., Rajewsky,N., Schroeder,M., Magnasco,M., and Darnell,J.E., Jr. (2003). Decay rates of human mRNAs: correlation with functional characteristics and sequence attributes. *Genome Res.* 13, 1863-1872.
- Yang,L., Duff,M.O., Graveley,B.R., Carmichael,G.G., and Chen,L.L. (2011). Genomewide characterization of non-polyadenylated RNAs. *Genome Biol.* 12, R16.
- Yekta,S., Shih,I.H., and Bartel,D.P. (2004). MicroRNA-directed cleavage of HOXB8 mRNA. *Science* 304, 594-596.
- Yoon,K., Ko,D., Doderer,M., Livi,C.B., and Penalva,L.O. (2008). Over-represented sequences located on 3' UTRs are potentially involved in regulatory functions. *RNA. Biol.* 5, 255-262.
- Yu,Z., Wang,A.M., Robins,D.M., and Lieberman,A.P. (2009). Altered RNA splicing contributes to skeletal muscle pathology in Kennedy disease knock-in mice. *Dis. Model. Mech.* 2, 500-507.
- Zhang,L., Lee,J.E., Wilusz,J., and Wilusz,C.J. (2008). The RNA-binding protein CUGBP1 regulates stability of tumor necrosis factor mRNA in muscle cells: implications for myotonic dystrophy. *J. Biol. Chem.* 283, 22457-22463.
- Zhang,W., Wagner,B.J., Ehrenman,K., Schaefer,A.W., DeMaria,C.T., Crater,D., DeHaven,K., Long,L., and Brewer,G. (1993). Purification, characterization, and cDNA cloning of an AU-rich element RNA-binding protein, AUF1. *Mol. Cell Biol.* 13, 7652-7665.



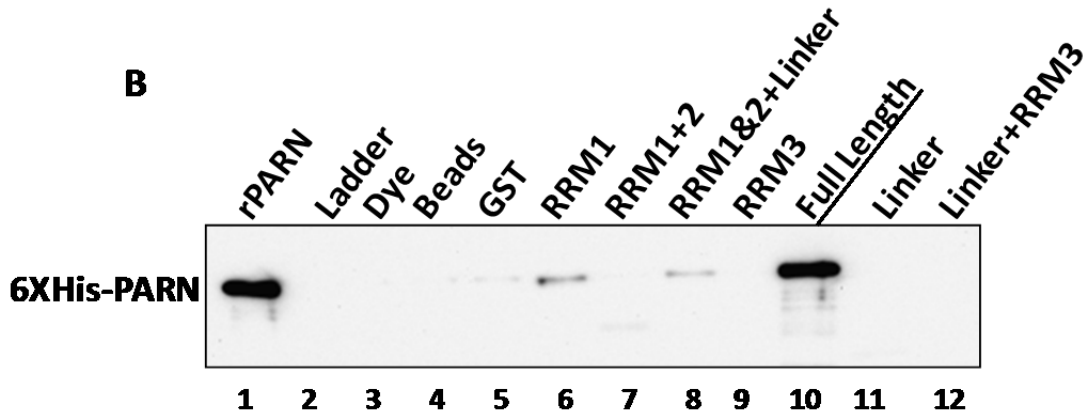
## ***Appendices***

Appendix 1.

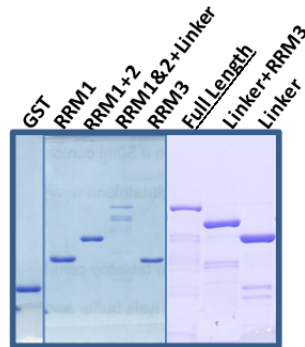
A



B

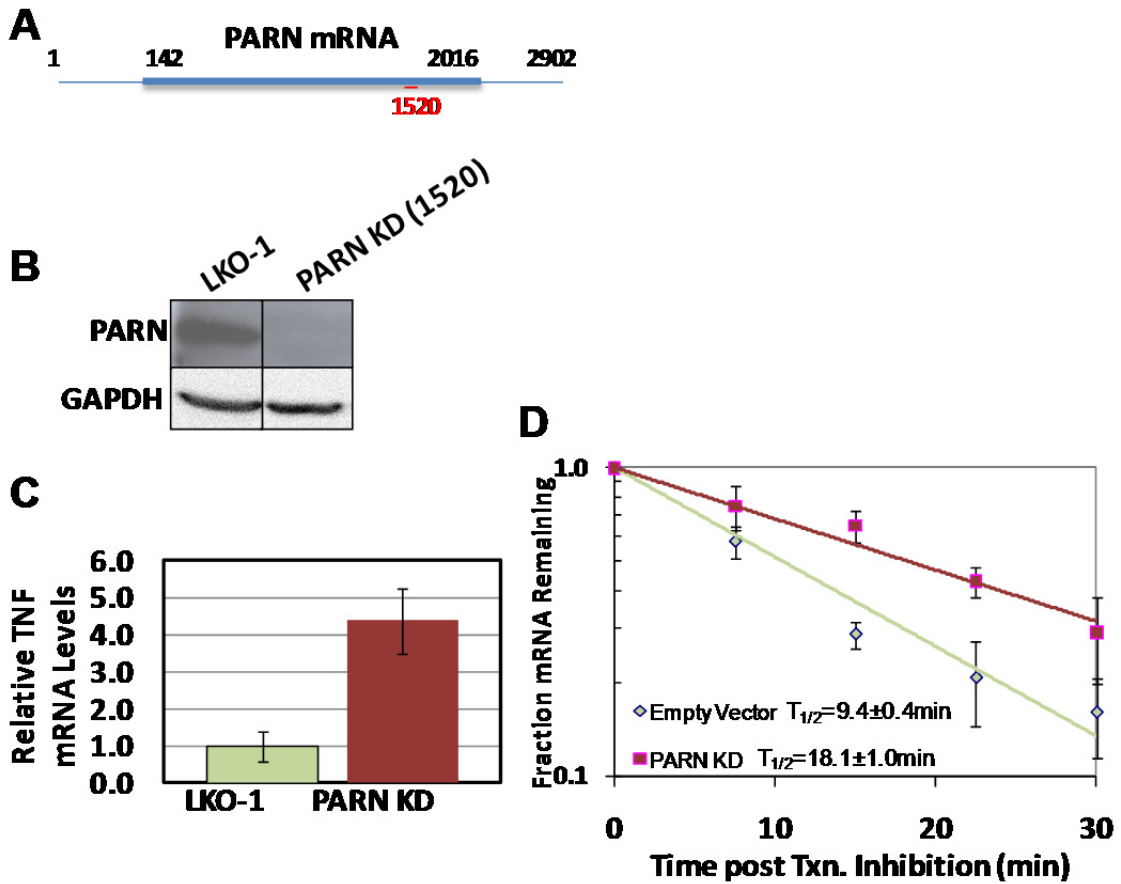


C



**Only full-length CUGBP1 stably interacts with PARN *in vitro*.** (A) Diagram of CUGBP1. RNA recognition motifs (RRM) are shown in blue and linker region is shown as a line. (B) Equal amounts of recombinant PARN were incubated with 5 $\mu$ g of the indicated GST-CUGBP1 protein immobilized on glutathione linked agarose resin in the presence of RNase A. After washing, the proteins were eluted by boiling in 1XSDS loading dye and separated on a 10% SDS polyacrylamide gel. PARN was detected by western blot. (C) Coomassie stained gel showing recombinant proteins used in these experiments.

Appendix 2.

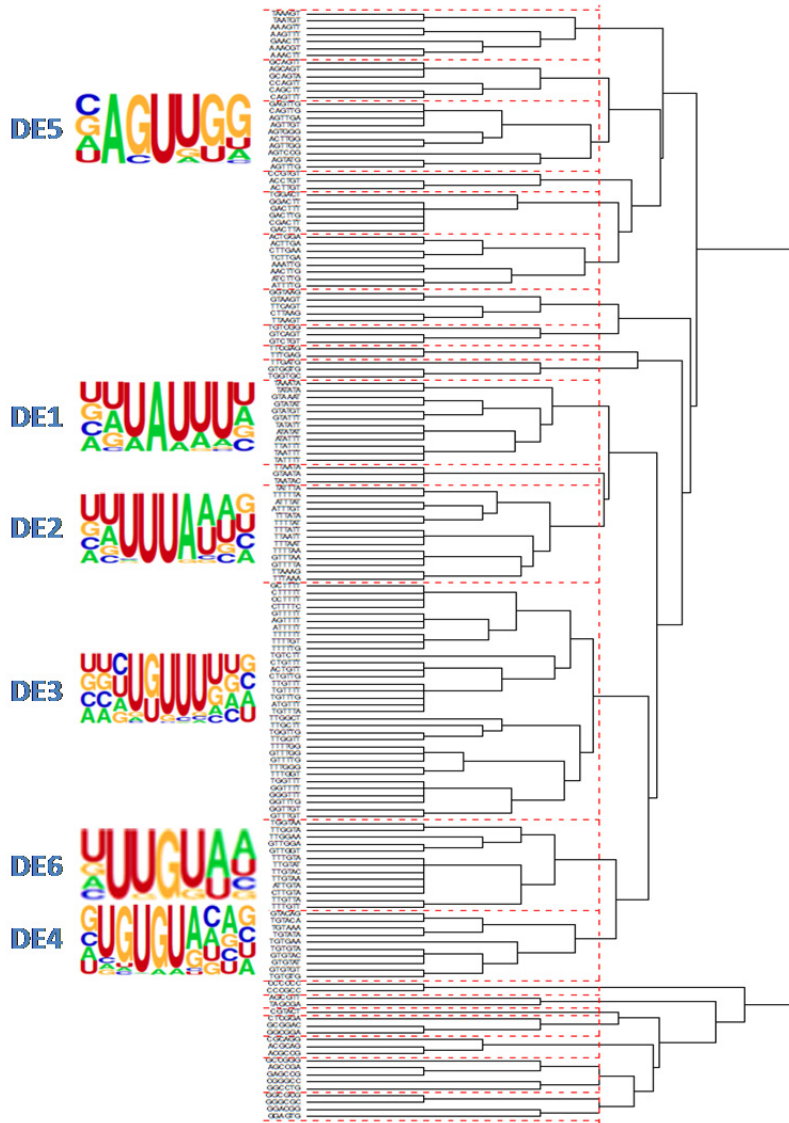


**Knock-down of PARN by shRNA #1520 changes TNF mRNA abundance and half-life.** (A) Schematic of PARN mRNA, ORF as box, lines as UTRs, red line indicates position of targeting shRNA. (B) Western blot for PARN and GAPDH (loading control) of extracts from LKO-1 and PARN knock-down cell lines. (C) TNF mRNA levels assessed by qRT-PCR from LKO-1 and PARN KD cell lines normalized to GAPDH. (E) Rate of decay for TNF mRNA in the LKO-1 (solid line) and PARN KD cell line (dashed line) was assessed following actinomycin-D treatment. mRNA levels were measured at each time point and normalized to GAPDH.

# Appendix 3.

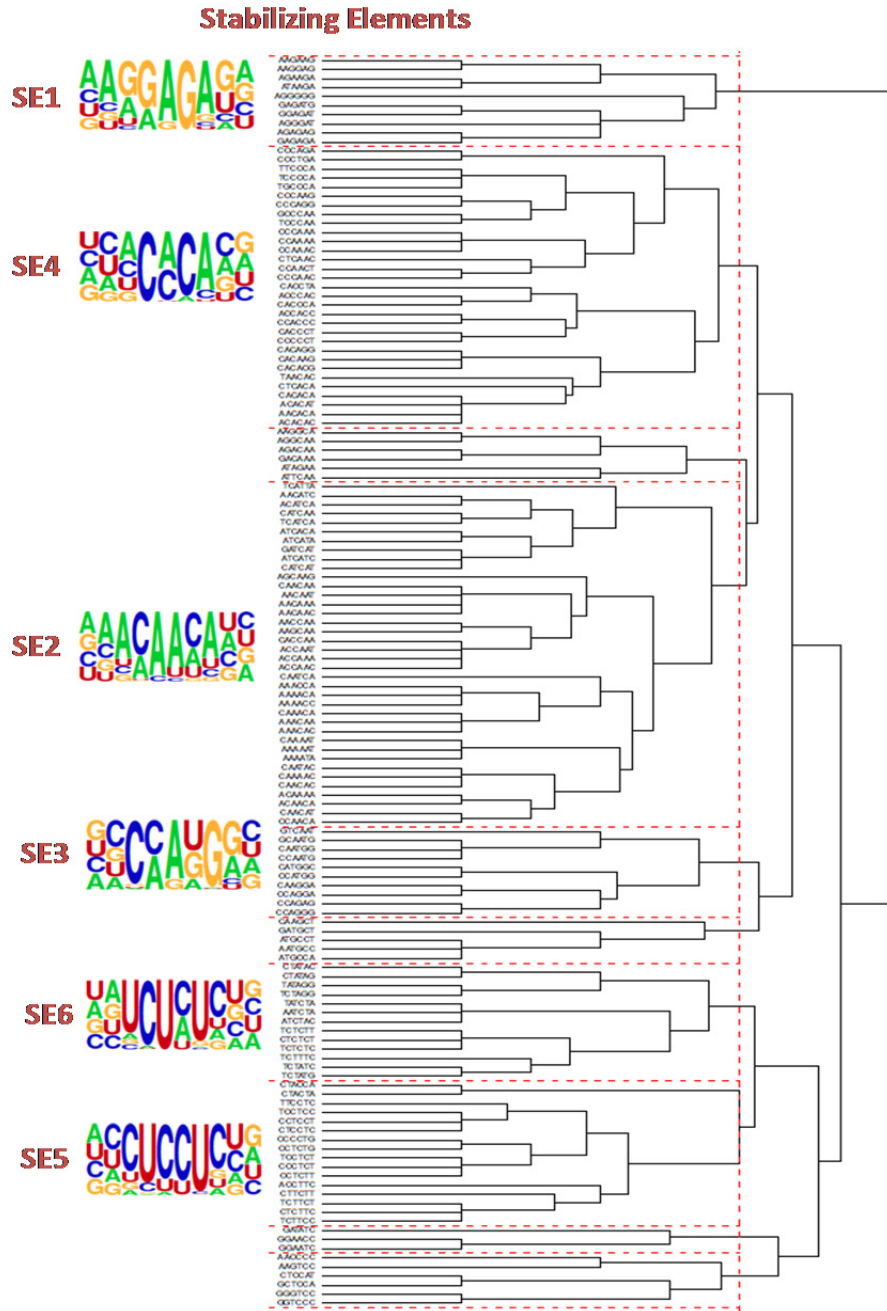
## A

### Destabilizing Elements



Appendix 3. continued

**B**



**Hexamers enriched in the 3'UTRs of the most and least stable mRNAs.** (A) Hexamers enriched in the least stable genes' 3'UTRs and their corresponding sequence logo. (B) Hexamers enriched in the most stable genes' 3'UTRs and their corresponding sequence logo.

#### Appendix 4. Transcripts stabilized upon CUGBP1 knock-down

Gene ID	Gene Name	Control HL (min)	CUGBP1 KD HL (min)	Fold Change	P-value
64113	Moap1	86	458	5.3	3.57E-02
22644	Rnf103	117	613	5.2	4.05E-02
106200	Txndc11	103	418	4.0	1.11E-02
320376	Bcor1	132	531	4.0	4.36E-02
101497	Plekhg2	142	571	4.0	1.83E-02
11911	Atf4	66	258	3.9	7.80E-03
217684	4933426M11Rik	114	448	3.9	1.92E-04
118445	Klf16	102	395	3.9	3.59E-02
268291	Rnf217	72	272	3.8	3.58E-02
72655	2810026P18Rik	60	222	3.7	4.93E-03
13716	Eli	100	373	3.7	1.16E-02
11839	Areg	102	376	3.7	1.40E-02
78266	Zfp687	134	494	3.7	4.92E-05
100038535	ENSMUSG00000075516	117	431	3.7	4.34E-02
29861	Dpf1	179	656	3.7	4.97E-02
109019	Obfc2a	93	335	3.6	3.79E-02
229004	Gmeb2	69	247	3.6	1.33E-02
224118	1700021K19Rik	103	362	3.5	1.66E-02
229543	Ints3	148	522	3.5	4.68E-02
75273	Pelp1	139	489	3.5	3.09E-02
235040	Atg4d	132	463	3.5	4.32E-02
72469	Plcd3	104	361	3.5	1.60E-02
239796	1600021P15Rik	99	340	3.4	5.33E-05
13170	Dbp	91	308	3.4	2.22E-02
170767	Rfxap	109	371	3.4	3.76E-02
110524	Dgkq	220	745	3.4	3.07E-02
74041	4632434I11Rik	77	259	3.4	3.12E-02
72946	Lrrc47	106	356	3.4	2.26E-02
74178	Stk40	96	323	3.3	2.52E-02
52829	D4Bwg0951e	72	239	3.3	3.95E-02
71955	2400003C14Rik	109	358	3.3	4.02E-03
17131	Smad7	61	199	3.3	1.92E-02
69612	2310037I24Rik	95	310	3.3	3.21E-02
67246	2810474O19Rik	59	190	3.2	3.37E-02
97484	Cog8	134	432	3.2	3.87E-02
73122	Tgfbrap1	136	435	3.2	1.79E-02
98402	Sh3bp4	73	232	3.2	3.27E-02
227449	Zcchc2	94	298	3.2	1.92E-02
209212	Osgin2	107	339	3.2	2.85E-02
71254	Naif1	166	517	3.1	3.99E-02
228869	Ncoa5	108	335	3.1	2.22E-03
13557	E2f3	83	258	3.1	1.11E-02
74194	Rnd3	34	106	3.1	1.27E-03
72635	Lins2	126	391	3.1	7.36E-03

#### Appendix 4. continued

11854	Rhod	106	328	3.1	3.27E-03
109136	Mmaa	135	414	3.1	3.46E-02
207932	4921511H13Rik	110	337	3.1	4.46E-02
381306	BC055324	106	322	3.0	5.16E-06
13728	Mark2	100	304	3.0	1.61E-02
242418	Wdr32	84	253	3.0	1.16E-02
69612	2310037I24Rik	102	309	3.0	3.73E-02
69601	Dab2ip	109	328	3.0	2.21E-03
329003	Zfp516	87	260	3.0	3.56E-03
18626	Per1	100	295	3.0	9.19E-04
18844	Plxna1	103	306	3.0	1.68E-02
114604	Prdm15	120	354	3.0	2.26E-02
98999	Znfx1	107	318	3.0	6.30E-03
26939	Polr3e	116	344	3.0	2.40E-02
226182	Taf5	69	204	2.9	1.72E-03
52504	Cenpo	127	373	2.9	9.08E-03
319885	Zcchc7	110	322	2.9	2.22E-02
64453	Zfp280b	75	219	2.9	1.54E-03
230734	Yrdc	96	281	2.9	3.93E-02
68778	1110038D17Rik	95	276	2.9	4.11E-03
74094	Tjap1	85	246	2.9	4.50E-02
99526	Usp53	120	349	2.9	8.81E-03
107305	Vps37c	88	256	2.9	1.30E-02
319583	Lig4	98	286	2.9	3.62E-02
73233	3110048L19Rik	100	291	2.9	2.92E-02
239555	Smcr7l	116	335	2.9	4.18E-02
12296	Cacnb2	113	325	2.9	2.26E-02
13803	Enc1	63	181	2.9	1.15E-03
100978	Nfxl1	94	268	2.9	3.71E-02
67123	Ubap1	75	214	2.8	4.51E-02
56332	Amotl2	44	124	2.8	5.34E-03
54006	Deaf1	118	333	2.8	4.54E-02
71093	Atoh8	108	304	2.8	1.31E-03
232944	Mark4	129	365	2.8	1.74E-02
14312	Brd2	86	243	2.8	1.71E-02
74035	Nol9	85	238	2.8	3.92E-02
192652	Wdr81	143	402	2.8	6.39E-03
80744	BC003993	77	215	2.8	9.07E-03
67619	Nob1	112	313	2.8	3.42E-04
66667	Hspbap1	142	397	2.8	4.32E-02
21665	Tdg	98	275	2.8	2.08E-02
641340	Nrbf2	93	259	2.8	2.28E-02
14573	Gdnf	103	288	2.8	3.03E-02
21665	Tdg	96	267	2.8	3.76E-02
71799	Ptcd1	97	271	2.8	1.69E-02
320790	Chd7	92	255	2.8	3.93E-02
268783	Mtmr12	123	341	2.8	9.32E-03

#### Appendix 4. continued

20779	Src	136	377	2.8	3.03E-02
320790	Chd7	78	218	2.8	2.34E-02
75424	Zfp820	213	589	2.8	2.92E-03
225339	Ammecr1l	109	301	2.7	2.10E-02
227613	Tubb2c1	158	433	2.7	6.17E-04
52552	Parp8	103	283	2.7	1.49E-03
100169	Phactr4	87	238	2.7	1.97E-02
74570	Zkscan1	64	175	2.7	3.41E-02
668940	Myh7b	102	279	2.7	1.39E-02
435684	Shf	128	347	2.7	4.58E-02
15357	Hmgcr	108	294	2.7	2.10E-02
269623	C030048B08Rik	107	289	2.7	4.54E-02
15903	Id3	42	113	2.7	4.18E-02
224648	Uhrf1bp1	110	298	2.7	9.84E-03
14369	Fzd7	72	194	2.7	3.49E-02
63856	Taf8	107	289	2.7	6.57E-03
13875	Erf	119	320	2.7	3.91E-02
14283	Fosl1	59	159	2.7	3.78E-02
14287	Fpgs	116	311	2.7	4.32E-02
72008	Zfyve19	177	472	2.7	3.07E-02
386655	Eid2	189	503	2.7	4.76E-03
75901	Dcp1a	99	263	2.7	2.23E-02
66895	1300014I06Rik	91	241	2.7	4.68E-02
107951	Cdk9	86	227	2.7	5.96E-03
22145	Tuba4a	133	352	2.7	5.88E-03
15117	Has2	48	127	2.6	9.08E-03
77853	Msl2l1	49	129	2.6	3.75E-02
21664	Phlda1	52	138	2.6	1.92E-02
70573	Tbccd1	159	420	2.6	1.22E-03
110816	Pwp2	149	392	2.6	4.78E-02
229599	Gm129	88	233	2.6	3.94E-02
66089	Rmnd5b	127	335	2.6	3.26E-02
23849	Klf6	53	140	2.6	4.62E-02
14200	Fhl2	80	210	2.6	5.06E-03
57170	Dolpp1	117	309	2.6	1.12E-02
66830	Btbd14b	127	334	2.6	1.40E-02
260315	Nav3	126	331	2.6	2.59E-02
69641	Wdr20a	65	169	2.6	3.92E-03
102414	Clk3	93	241	2.6	4.96E-04
12530	Cdc25a	60	156	2.6	4.53E-02
58996	4933428G20Rik	110	286	2.6	2.44E-02
100206	Adprhl2	116	301	2.6	1.49E-02
19206	Ptch1	119	309	2.6	1.67E-03
69577	Fastkd3	104	272	2.6	3.72E-02
67109	Zfp787	132	343	2.6	1.37E-03
217207	Dhx8	89	230	2.6	5.50E-03
20482	Skil	79	205	2.6	2.34E-02



#### Appendix 4. continued

641340	Nrbf2	91	236	2.6	3.70E-02
641340	Nrbf2	91	236	2.6	3.70E-02
234138	BC019943	133	345	2.6	1.94E-02
20623	Snrk	90	234	2.6	1.79E-03
677593	LOC677593	94	244	2.6	1.69E-02
21750	Terf2	109	281	2.6	2.80E-02
30877	Gnl3	77	198	2.6	3.64E-02
57438	7-Mar	64	164	2.6	2.58E-02
74349	4632419K20Rik	117	301	2.6	3.49E-03
233276	Tubgcp5	129	331	2.6	1.21E-03
52231	Ankzf1	156	401	2.6	2.78E-02
16835	Ldlr	88	226	2.6	3.45E-02
381022	Mll2	94	241	2.6	1.87E-02
107765	Ankrd1	72	184	2.6	4.68E-02
213990	Centg3	144	367	2.6	3.55E-02
60532	Wtap	93	236	2.5	6.83E-03
230700	Foxj3	79	202	2.5	3.36E-02
211147	11-Mar	146	371	2.5	3.87E-03
223666	D15Wsu169e	125	317	2.5	5.33E-04
545622	Ptpn3	145	368	2.5	1.05E-02
102423	Mizf	134	339	2.5	1.37E-02
22224	Usp10	86	218	2.5	2.74E-02
72344	Usp36	84	214	2.5	8.68E-04
56503	Ankrd49	81	205	2.5	1.14E-02
223664	Lrrc14	95	238	2.5	2.39E-02
68968	Cdan1	105	264	2.5	2.72E-02
74386	Rmi1	73	184	2.5	2.85E-02
16206	Lrig1	107	268	2.5	6.22E-03
218613	Mier3	60	150	2.5	9.73E-03
107607	Nod1	186	464	2.5	3.46E-03
230661	Tesk2	93	232	2.5	1.24E-02
71458	Bcor	95	237	2.5	2.99E-02
20935	Surf6	110	273	2.5	2.80E-04
29870	Gtse1	106	263	2.5	9.61E-04
57912	Cdc42se1	102	254	2.5	3.10E-02
71804	2610016C23Rik	97	240	2.5	4.84E-02
240880	Scyl3	121	298	2.5	5.82E-03
319719	4732471D19Rik	80	198	2.5	2.84E-02
269060	Dagla	104	257	2.5	4.06E-03
22390	Wee1	46	114	2.5	8.70E-03
381801	Tatdn2	119	292	2.5	4.33E-02
232196	C87436	71	174	2.5	3.25E-02
54131	Irf3	132	325	2.5	7.51E-03
228994	Ythdf1	103	251	2.5	7.76E-03
12193	Zfp3612	58	142	2.4	2.36E-03
98710	Rabif	84	204	2.4	1.92E-02
74549	9130404D08Rik	115	282	2.4	4.18E-02

#### Appendix 4. continued

238871	Pde4d	79	193	2.4	3.00E-02
56632	Sphk2	126	307	2.4	1.89E-02
233904	Setd1a	111	270	2.4	6.18E-04
217039	Ggnbp2	75	181	2.4	1.01E-02
22325	Vav2	131	316	2.4	2.49E-02
228368	Slc35c1	113	271	2.4	3.68E-04
269582	Clspn	125	300	2.4	9.99E-03
21975	Top3a	98	237	2.4	1.34E-02
268933	Wdr24	158	381	2.4	2.91E-02
67164	2610209A20Rik	186	445	2.4	6.92E-03
18130	Ints6	63	150	2.4	2.24E-02
21847	Klf10	58	139	2.4	6.14E-03
78246	Phf23	54	128	2.4	1.70E-02
16319	Incenp	96	230	2.4	4.60E-02
105351	AW209491	105	250	2.4	3.79E-02
226049	Dmrt2	111	264	2.4	1.10E-02
330474	Zc3h4	96	228	2.4	3.94E-02
215748	Cnksr3	70	166	2.4	4.20E-02
11350	Abl1	81	192	2.4	1.72E-02
234678	D230025D16Rik	87	204	2.4	1.52E-02
228140	Tnks1bp1	115	272	2.4	2.26E-02
217127	Myst2	97	228	2.4	3.72E-02
268749	Rnf31	141	331	2.4	1.20E-03
74769	Pik3cb	120	283	2.3	1.93E-02
66690	Tmem186	113	264	2.3	4.13E-02
20677	Sox4	89	209	2.3	1.28E-02
232798	Leng8	162	379	2.3	3.72E-02
210973	Kbtbd2	70	164	2.3	3.78E-02
108673	Ccdc86	93	217	2.3	1.91E-02
22718	Zfp60	121	282	2.3	2.53E-03
229055	Zbtb10	106	247	2.3	1.43E-02
76969	Chst1	97	226	2.3	2.57E-02
244666	Gm505	104	241	2.3	9.03E-04
223642	Zc3h3	162	375	2.3	9.88E-03
104445	Cdc42ep1	52	121	2.3	4.09E-02
226153	Peo1	108	250	2.3	2.86E-03
229584	Pogz	78	181	2.3	9.11E-03
72726	Tbcc	123	283	2.3	1.45E-02
240665	Ccnj	133	306	2.3	4.34E-03
238330	6430527G18Rik	76	176	2.3	5.51E-03
140629	Ubox5	106	243	2.3	1.40E-02
18712	Pim1	87	201	2.3	3.97E-02
235584	Dusp7	72	165	2.3	9.47E-03
67655	Ctdp1	97	223	2.3	1.34E-02
360216	Zranb1	106	244	2.3	8.56E-03
67139	Mis12	82	189	2.3	9.49E-03
65020	Zfp110	114	261	2.3	1.73E-02

#### Appendix 4. continued

320398	Lrig3	56	128	2.3	2.04E-02
101612	Grwd1	93	212	2.3	2.39E-02
81630	Zbtb22	99	226	2.3	3.30E-04
20775	Sqle	95	217	2.3	5.68E-03
240064	6030490I01Rik	127	290	2.3	3.91E-02
276919	Gemin4	74	168	2.3	5.63E-04
101095	Zfp282	86	196	2.3	7.31E-03
320661	D5Erttd579e	80	181	2.3	5.69E-03
109113	Uhrf2	82	185	2.3	4.30E-02
76813	Armc6	123	279	2.3	2.50E-03
24069	Sufu	84	190	2.3	9.02E-03
13163	Daxx	93	210	2.3	3.37E-02
72323	Asb6	86	194	2.3	3.19E-02
101994	Zfp828	80	181	2.3	7.06E-04
319520	Dusp4	39	89	2.2	8.24E-03
112406	Egln2	142	318	2.2	1.55E-02
21815	Tgif1	45	102	2.2	2.18E-02
26889	Cln8	109	244	2.2	2.67E-02
217779	Lysmd1	131	294	2.2	2.28E-02
13548	Dyrk1a	78	174	2.2	3.99E-02
56488	Nxt1	76	170	2.2	3.29E-02
70024	Mcm10	102	227	2.2	1.41E-02
381695	N4bp2l2	101	226	2.2	3.57E-02
16172	Il17ra	81	180	2.2	2.38E-02
20361	Sema7a	65	146	2.2	3.66E-02
68114	Mum1	130	288	2.2	2.18E-02
319594	Hif1an	74	163	2.2	9.58E-03
57434	Xrcc2	117	260	2.2	3.93E-02
231769	Sfrs8	120	267	2.2	2.57E-03
75788	Smurf1	101	224	2.2	2.09E-02
69582	Plekhm2	135	299	2.2	1.80E-02
108961	E2f8	73	160	2.2	4.08E-02
15547	Htf9c	139	305	2.2	2.01E-02
22640	Zfp1	89	195	2.2	6.54E-03
56381	Spen	93	204	2.2	2.72E-03
17691	Snf1lk	62	135	2.2	3.02E-02
625662	LOC625662	66	145	2.2	3.65E-02
12750	Clk4	69	151	2.2	3.24E-02
55942	Sertad1	49	107	2.2	2.33E-02
239719	Mkl2	110	240	2.2	3.84E-02
360216	Zranb1	92	199	2.2	1.03E-02
20525	Slc2a1	127	276	2.2	4.82E-02
209456	Trp53bp2	95	207	2.2	2.13E-02
18044	Nfya	80	173	2.2	2.06E-02
11541	Adora2b	80	174	2.2	2.41E-02
66973	Mrps18b	117	253	2.2	4.12E-03
22156	Tuft1	116	250	2.2	4.54E-03

#### Appendix 4. continued

232879	Zbtb45	96	208	2.2	1.71E-02
231841	AA881470	163	351	2.2	4.60E-02
12042	Bcl10	98	212	2.2	1.29E-02
70052	Prpf4	93	202	2.2	1.07E-02
245877	Mtap7d1	118	255	2.2	4.27E-03
227522	Rpp38	41	89	2.2	2.29E-02
73754	Thap1	127	272	2.1	4.84E-03
215051	Bud13	98	211	2.1	5.17E-03
18181	Nrf1	87	186	2.1	7.66E-03
320790	Chd7	102	217	2.1	2.11E-02
74133	1200011M11Rik	88	187	2.1	9.14E-03
17127	Smad3	86	183	2.1	3.56E-02
74211	14-Sep	63	134	2.1	2.78E-02
227731	Slc25a25	107	228	2.1	8.09E-03
11845	Arf6	106	225	2.1	1.03E-02
212427	A730008H23Rik	74	156	2.1	1.53E-03
56371	Fzr1	81	172	2.1	4.56E-02
17210	Mcl1	55	116	2.1	2.85E-02
235682	Zfp445	87	183	2.1	4.07E-03
57377	Gcs1	114	241	2.1	8.17E-03
74155	Errfi1	38	79	2.1	2.41E-02
30951	Cbx8	109	230	2.1	3.24E-03
231798	Lrch4	116	244	2.1	2.15E-02
17423	Ndst2	96	203	2.1	4.01E-02
26909	Exo1	88	186	2.1	8.18E-03
213499	Fbxo42	76	160	2.1	2.35E-03
67131	Acbd4	183	385	2.1	4.02E-02
243362	Stard13	64	134	2.1	4.36E-03
71393	Kctd6	96	201	2.1	7.18E-03
63953	Dusp10	49	102	2.1	4.03E-02
78581	Utp23	108	227	2.1	2.45E-04
101489	Ric8	168	351	2.1	4.98E-02
59091	Jph2	143	299	2.1	2.91E-02
320790	Chd7	110	230	2.1	1.94E-03
99683	Sec24b	107	224	2.1	3.36E-03
216805	Flcn	82	172	2.1	4.86E-02
99696	Ankrd50	78	163	2.1	2.87E-02
66953	Cdca7	79	164	2.1	2.57E-02
100978	Nfxl1	96	201	2.1	4.21E-02
67308	Mrpl46	139	289	2.1	4.20E-02
20589	Ighmbp2	174	362	2.1	2.07E-02
20893	Bhlhb2	42	87	2.1	2.50E-03
77040	Atg16l1	118	245	2.1	7.14E-03
231915	Usp11	66	137	2.1	2.61E-02
237859	Ccdc55	85	177	2.1	2.64E-02
70686	Dusp16	92	192	2.1	4.86E-02
66591	Mad2l1bp	70	145	2.1	1.99E-03

#### Appendix 4. continued

71865	Fbxo30	73	151	2.1	1.87E-02
13666	Eif2ak3	113	233	2.1	4.19E-02
109075	Exosc4	130	267	2.1	3.14E-02
193796	Jmjd2b	110	226	2.1	1.31E-02
13831	Epc1	80	164	2.0	6.86E-03
93760	Arid1a	87	177	2.0	3.08E-02
223642	Zc3h3	173	353	2.0	2.33E-02
16468	Jarid2	100	203	2.0	1.90E-02
72290	Lsm11	137	279	2.0	1.48E-03
233210	Prr12	100	204	2.0	2.14E-02
109305	Orai1	150	306	2.0	2.77E-02
70044	Tut1	93	190	2.0	2.90E-02
676142	LOC676142	74	150	2.0	3.50E-02
676142	LOC676142	74	150	2.0	3.50E-02
676142	LOC676142	74	150	2.0	3.50E-02
676142	LOC676142	74	150	2.0	3.50E-02
676142	LOC676142	74	150	2.0	3.50E-02
676142	LOC676142	74	150	2.0	3.50E-02
676142	LOC676142	74	150	2.0	3.50E-02
192232	Hps4	118	240	2.0	7.00E-03
103724	Tbc1d10a	134	271	2.0	4.63E-03
14284	Fosl2	75	152	2.0	2.27E-02
320119	Rps6kc1	112	226	2.0	1.68E-02
72454	Ccdc71	104	209	2.0	1.12E-02
66406	Sac3d1	140	281	2.0	4.86E-02
64209	Herpud1	82	163	2.0	2.68E-02
77011	5730590G19Rik	74	147	2.0	1.56E-02
210029	Metrnl	178	355	2.0	1.37E-02
74522	Morc2a	78	155	2.0	2.97E-02
102098	Arhgef18	112	223	2.0	8.12E-03
76793	Snip1	67	134	2.0	3.64E-02
108954	Ppp1r15b	67	134	2.0	6.67E-03
71640	4930422I07Rik	186	368	2.0	4.08E-02
71878	2310007D09Rik	82	162	2.0	3.98E-03
207952	Klhl25	121	240	2.0	3.46E-03
97112	Nmd3	75	148	2.0	4.43E-02
68550	1110002N22Rik	101	200	2.0	6.14E-03
240442	Adnp2	57	113	2.0	6.43E-03
68897	Disp1	94	185	2.0	3.05E-03
211978	Zfyve26	149	295	2.0	7.34E-04
94092	Trim16	87	171	2.0	3.44E-02
12224	Klf5	86	170	2.0	3.18E-02
20460	Stil	69	137	2.0	9.61E-03
29815	Bcar3	63	125	2.0	7.98E-03
72123	2010109K11Rik	132	261	2.0	2.81E-02
67141	Fbxo5	33	65	2.0	1.81E-02
50721	Sirt6	126	248	2.0	1.29E-04

**Appendix 4. continued**

12394	Runx1	108	211	2.0	3.60E-02
20466	Sin3a	93	182	2.0	1.30E-02
13836	Epha2	76	148	1.9	3.06E-02
19671	Rce1	173	336	1.9	1.40E-02
13846	Ephb4	134	260	1.9	5.68E-03
68118	9430023L20Rik	93	180	1.9	8.64E-03
213541	Ythdf2	108	209	1.9	3.26E-02
67760	Slc38a2	71	136	1.9	4.71E-03
11852	Rhob	43	82	1.9	8.25E-03
22689	Zfp27	150	287	1.9	2.79E-03
67311	Nanp	73	139	1.9	4.68E-03
240263	Fem1c	65	123	1.9	2.02E-02
12795	Plk3	125	238	1.9	4.02E-03
80914	Uck2	107	204	1.9	4.74E-03
217333	Trim47	88	167	1.9	4.90E-02
52040	Ppp1r10	41	78	1.9	2.09E-02
15902	Id2	55	105	1.9	1.06E-04
75234	Rnf19b	106	202	1.9	2.37E-02
54399	Bet1l	83	158	1.9	7.67E-03
24001	Tiam2	76	143	1.9	3.95E-03
15937	Ier3	55	105	1.9	3.28E-02
232784	Zfp212	72	135	1.9	2.98E-02
12053	Bcl6	89	166	1.9	2.55E-04
67976	Trabd	166	311	1.9	4.19E-02
106564	Ppcs	157	294	1.9	2.37E-02
30945	Rnf19a	55	102	1.9	6.84E-03
69534	Avpi1	133	247	1.9	3.05E-02
98985	Clp1	58	107	1.9	3.90E-02
72699	Lime1	153	284	1.9	3.18E-02
319266	A130010J15Rik	103	190	1.8	3.68E-02
108829	Jmjd1c	66	121	1.8	9.50E-03
70208	Med23	97	180	1.8	1.68E-02
83486	Rbm5	82	151	1.8	2.27E-02
226154	Lzts2	120	221	1.8	3.06E-02
67842	2610027L16Rik	133	245	1.8	3.27E-02
212632	C79267	112	205	1.8	6.16E-03
20471	Six1	56	102	1.8	1.33E-02
28113	Tinf2	184	336	1.8	1.36E-02
72046	2010005J08Rik	90	164	1.8	2.58E-03
60532	Wtap	96	175	1.8	1.18E-02
235036	Ppan	79	143	1.8	3.30E-02
231872	Jtv1	156	282	1.8	1.44E-02
75871	Zfp821	98	178	1.8	4.50E-02
68295	0610011L14Rik	136	247	1.8	4.73E-03
73338	Itpr1p1	179	319	1.8	1.46E-02
67311	Nanp	91	163	1.8	1.45E-02
100213	Rusc2	100	177	1.8	4.94E-02

#### Appendix 4. continued

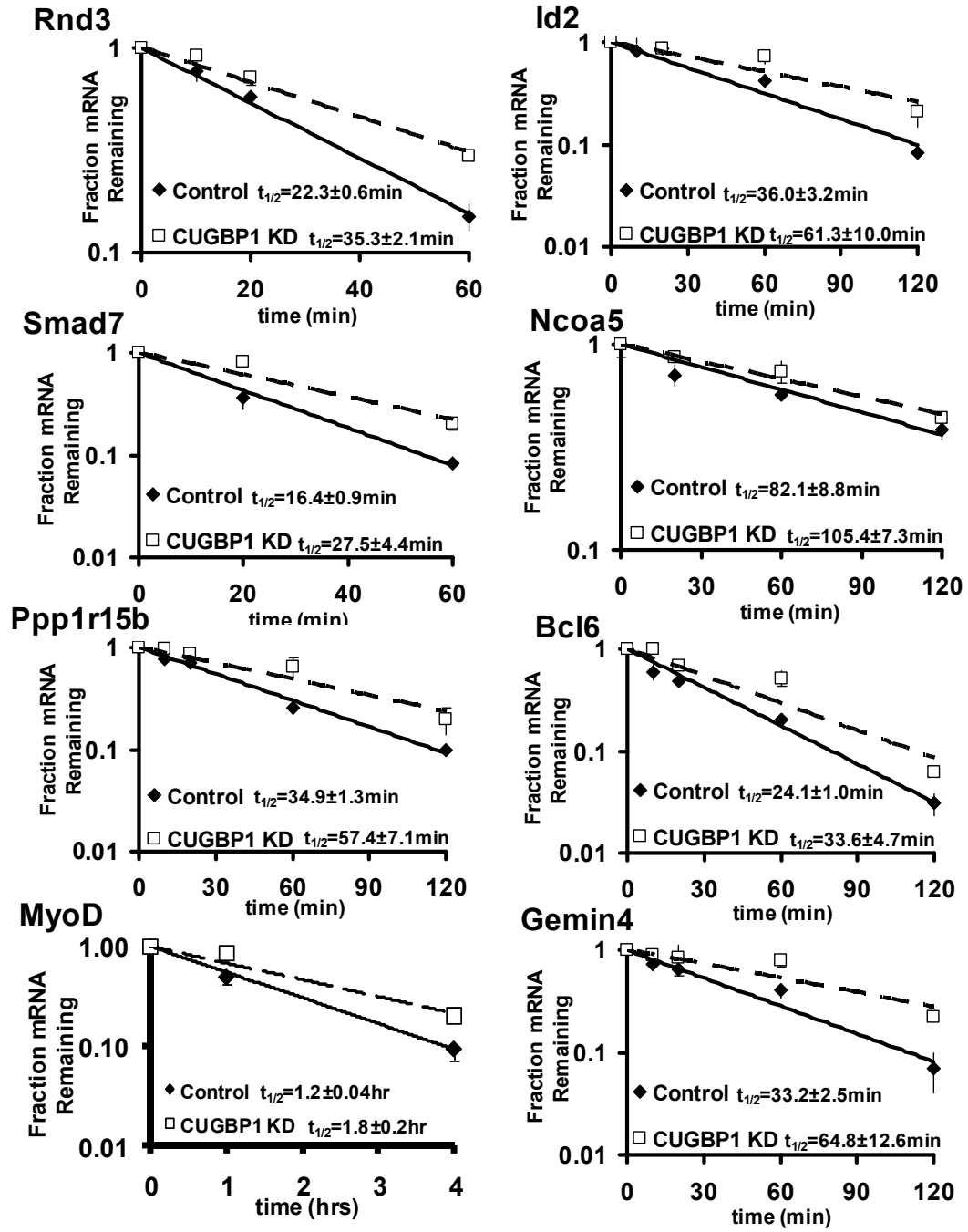
54343	Atf7ip	76	134	1.8	4.57E-02
101471	Phrf1	89	156	1.8	3.17E-02
353190	Edc3	76	134	1.8	1.33E-02
276852	D11Wsu47e	178	312	1.8	1.03E-03
78733	Troap	66	115	1.8	4.98E-02
66617	Mettl11a	129	227	1.8	2.38E-02
214791	Sertad4	78	136	1.7	1.35E-02
217198	Plekhh3	103	179	1.7	1.39E-02
218581	Depdc1b	92	160	1.7	4.09E-02
16475	Jub	43	74	1.7	1.64E-02
12449	Ccnf	45	79	1.7	2.28E-02
22030	Traf2	71	124	1.7	1.28E-02
72549	Reep4	120	208	1.7	1.95E-02
20353	Sema4c	54	93	1.7	1.66E-02
106894	A630042L21Rik	88	153	1.7	3.97E-02
57815	Spata5	83	143	1.7	8.72E-03
66597	Trim13	74	127	1.7	2.74E-03
217331	Unk	101	174	1.7	4.83E-02
53890	Sart3	119	204	1.7	1.44E-02
59016	Thap11	123	211	1.7	2.58E-02
68730	Dus1l	122	209	1.7	3.34E-04
16190	Il4ra	68	116	1.7	4.52E-02
228790	Asxl1	73	124	1.7	7.37E-03
66513	Map3k7ip1	101	171	1.7	2.07E-02
70427	Mier2	103	173	1.7	9.52E-05
17165	Mapkapk5	124	208	1.7	5.87E-03
66680	3230401D17Rik	63	106	1.7	3.63E-02
320790	Chd7	113	187	1.7	1.47E-03
74157	1300018I05Rik	99	164	1.6	5.52E-04
53892	Ppm1d	70	114	1.6	1.82E-02
68350	Mul1	88	144	1.6	2.96E-02
72486	Rnf219	88	143	1.6	6.18E-03
232855	BC023179	135	216	1.6	1.43E-02
108912	Cdca2	79	127	1.6	9.08E-03
209815	Tbc1d25	94	150	1.6	9.98E-03
100047059	LOC100047059	102	164	1.6	8.51E-03
16007	Cyr61	35	56	1.6	1.01E-02
20620	Plk2	34	54	1.6	3.37E-02
72171	Shq1	161	256	1.6	2.40E-02
234582	Ccdc102a	131	204	1.6	4.32E-02
67219	Med18	52	81	1.6	3.37E-02
66680	3230401D17Rik	66	103	1.6	3.87E-02
214855	Arid5a	143	221	1.5	2.35E-02
319192	Hist2h2aa2	53	81	1.5	3.18E-02
16362	Irf1	45	68	1.5	1.98E-02
80838	Hist1h1a	45	68	1.5	1.06E-03
78294	Rps27a	105	159	1.5	4.67E-02

**Appendix 4. continued**

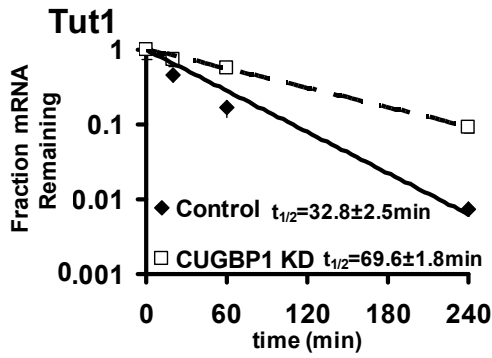
17684	Cited2	65	98	1.5	5.11E-03
67849	Cdca5	79	119	1.5	4.87E-02
18654	Pgf	57	86	1.5	1.67E-02
319192	Hist2h2aa2	65	96	1.5	3.24E-02
22033	Traf5	83	122	1.5	3.72E-02
665433	RP23-480B19.10	51	75	1.5	1.05E-02
66213	Med7	101	146	1.4	2.41E-02
665433	RP23-480B19.10	67	96	1.4	1.95E-02
665433	RP23-480B19.10	67	95	1.4	2.22E-02
665433	RP23-480B19.10	67	95	1.4	2.22E-02
665433	RP23-480B19.10	64	90	1.4	1.61E-02
52521	Zfp622	89	123	1.4	3.61E-02
71952	2410016O06Rik	97	121	1.2	7.15E-03



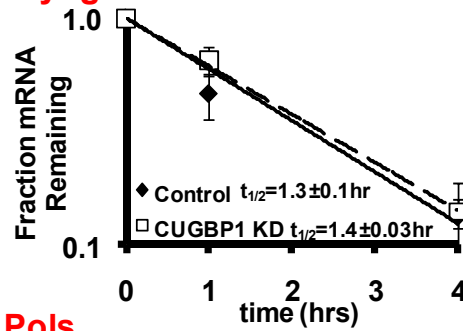
Appendix 5.



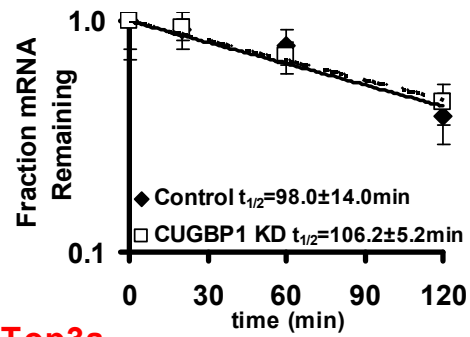
Appendix 5 continued



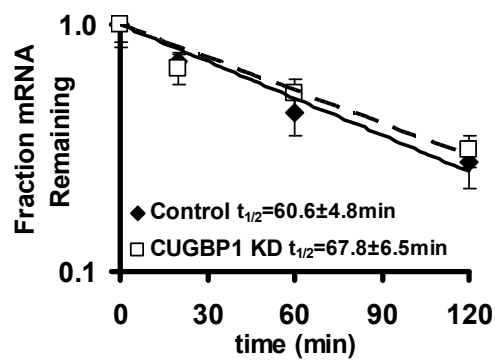
**Myogenin**



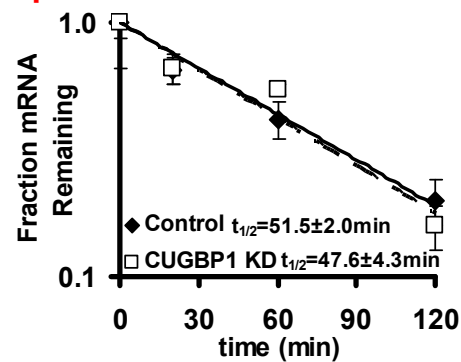
**Runx3**



**Pols**



**Top3a**



**Validation of novel mRNA targets of CUGBP1 in muscle cells.** Half-lives of indicated mRNAs were determined in LKO-1 and CUGBP1 KD cell lines by qRT-PCR. Error bars represent the standard deviation. Transcripts where no difference between LKO-1 and CUGBP1 KD was found are shown in red.

## Appendix 6. Transcripts which immunoprecipitate with CUGBP1

Signal-to-negative ratios for RIP-chip experiment.			
Gene ID	Gene Name	Signal-to-Negative	Rank (%)
21771	Cirh1a	22.96	100.0
98258	Txndc9	20.70	100.0
68724	Arl8a	20.57	100.0
20443	St3gal4	20.33	100.0
109284	C030046I01Rik	18.72	100.0
11984	Atp6v0c	18.18	100.0
54208	Arl6ip1	17.97	100.0
56349	Net1	16.68	100.0
11984	Atp6v0c	16.08	100.0
13358	Slc25a1	16.07	99.9
98258	Txndc9	15.87	99.9
67141	Fbxo5	15.81	99.9
11984	Atp6v0c	15.42	99.9
13663	Ei24	15.12	99.9
12237	Bub3	14.55	99.9
67636	Lym5	14.40	99.9
22154	Tubb5	14.14	99.9
15374	Hn1	13.89	99.9
94280	Sfxn3	13.68	99.9
74194	Rnd3	13.66	99.9
12767	Cxcr4	13.41	99.9
209448	Hoxc10	13.40	99.9
76551	Ccdc6	13.15	99.9
66940	Shisa5	12.77	99.9
14467	Gbas	12.71	99.9
12111	Bgn	12.37	99.9
15081	H3f3b	12.34	99.9
100044509	LOC100044509	12.13	99.8
70088	Z310005N01Rik	12.09	99.8
15081	H3f3b	11.96	99.8
246256	Fcgr4	11.68	99.8
66442	Spc25	11.62	99.8
68969	Eif1b	11.50	99.8
223922	Atf7	11.42	99.8
674164	LOC674164	11.33	99.8
13688	Eif4ebp2	11.31	99.8
213742	Xist	11.26	99.8
15081	H3f3b	11.24	99.8
223922	Atf7	11.20	99.8
15081	H3f3b	11.06	99.8
98711	Rdh10	10.89	99.8
434401	EG434401	10.72	99.8
384009	Glipr2	10.72	99.8
66094	Lsm7	10.68	99.8
56398	1500003O03Rik	10.67	99.8
56457	Cipltm1	10.64	99.7
66094	Lsm7	10.55	99.7
211488	Ado	10.53	99.7
105171	Arrdc3	10.46	99.7
71371	Arid5b	10.30	99.7
15368	Hmox1	10.26	99.7
20610	Sumo3	10.15	99.7
16848	Lfng	10.06	99.7
19108	Prkx	10.05	99.7
74648	S100pbb	10.02	99.7
68929	Mospd3	9.99	99.7
68066	Slc25a39	9.90	99.7
66799	Ube2w	9.89	99.7
22785	Slc30a4	9.87	99.7
51792	Ppp2r1a	9.74	99.7
67942	Atp5g2	9.69	99.7
22004	Tpm2	9.64	99.7
434401	EG434401	9.56	99.6
192662	Arhgdia	9.53	99.6
56693	Crtap	9.52	99.6
77889	Lbh	9.49	99.6
208228	Mobkl2a	9.46	99.6
11555	Adrb2	9.43	99.6
76987	Hdhd2	9.38	99.6
100127111	Snord22	9.32	99.6
114143	Atp6v0b	9.17	99.6
674164	LOC674164	9.17	99.6
67942	Atp5g2	9.11	99.6
26394	Lypla2	9.03	99.6
100048649	LOC100048649	9.03	99.6
97863	C78339	9.01	99.6
14368	Fzd6	9.01	99.6
12540	Cdc42	8.96	99.6
67942	Atp5g2	8.96	99.6
70310	Plscr3	8.79	99.6
20437	Siah1a	8.79	99.5
16647	Kpna2	8.76	99.5
19056	Ppp3cb	8.71	99.5
16647	Kpna2	8.70	99.5
21749	Terf1	8.69	99.5
16478	Jund	8.65	99.5
217558	6030408C04Rik	8.64	99.5
636070	EG636070	8.64	99.5
74868	Tmem65	8.63	99.5
18023	Nfe2l1	8.60	99.5
93686	Rbm9	8.51	99.5

## Appendix 6. continued

16647	Kpna2	8.50	99.5	107566	Arl2bp	6.83	99.2
22240	Dpysl3	8.38	99.5	71833	Wdr68	6.83	99.2
21366	Slc6a6	8.35	99.5	22196	Ube2i	6.82	99.2
223455	6-Mar	8.32	99.5	230125	Mcart1	6.80	99.2
18637	Pfdn2	8.30	99.5	106248	Qtrtd1	6.77	99.2
17927	Myod1	8.30	99.5	239096	Cdh24	6.74	99.2
66234	Sc4mol	8.19	99.4	67515	Ttc33	6.74	99.2
73826	Poldip3	8.18	99.4	20971	Sdc4	6.72	99.2
212111	Inpp5a	8.07	99.4	12443	Ccnd1	6.62	99.2
66508	2400001E08Rik	8.03	99.4	16319	Incenp	6.61	99.2
320267	Fubp3	8.00	99.4	107513	Ssr1	6.56	99.2
17775	Laptm4a	7.98	99.4	11798	Xiap	6.55	99.2
22088	Tsg101	7.95	99.4	83383	Tcfap4	6.53	99.1
54401	Ywhab	7.86	99.4	56351	Ptges3	6.49	99.1
68801	Elovl5	7.85	99.4	101142	Itfg2	6.49	99.1
56473	Fads2	7.85	99.4	665860	EG665860	6.49	99.1
56371	Fzr1	7.83	99.4	71918	Zcchc24	6.48	99.1
68926	Ubp2	7.74	99.4	14674	Gna13	6.47	99.1
226178	D19Wsu162e	7.69	99.4	22088	Tsg101	6.44	99.1
53817	Bat1a	7.65	99.4	66290	Atp6v1g1	6.44	99.1
26416	Mapk14	7.64	99.4	22196	Ube2i	6.43	99.1
67393	Cxzc5	7.62	99.4	20393	Sgk1	6.43	99.1
11777	Ap3s1	7.52	99.4	70546	Zdhhc2	6.38	99.1
56351	Ptges3	7.52	99.4	214459	Fnbp1l	6.38	99.1
11933	Atp1b3	7.49	99.3	50918	Myadm	6.37	99.1
56351	Ptges3	7.48	99.3	68564	Nufip2	6.33	99.1
110454	Ly6a	7.47	99.3	104625	Cnot6	6.31	99.1
19345	Rab5c	7.43	99.3	665860	EG665860	6.29	99.1
208715	Hmgcs1	7.41	99.3	101185	Pot1a	6.28	99.1
17928	Myog	7.41	99.3	12571	Cdk6	6.26	99.1
228005	Ppig	7.38	99.3	50784	Ppap2c	6.26	99.0
54351	Rai12	7.33	99.3	20652	Soat1	6.26	99.0
16476	Jun	7.29	99.3	66632	Atpbd4	6.25	99.0
53945	Slc40a1	7.28	99.3	16323	Inhba	6.24	99.0
19046	Ppp1cb	7.22	99.3	78541	Asb8	6.23	99.0
74747	Ddit4	7.16	99.3	16533	Kcnmb1	6.22	99.0
68799	Rgmb	7.12	99.3	216344	Rab21	6.21	99.0
97820	4833439L19Rik	7.11	99.3	17131	Smad7	6.19	99.0
16835	Ldlr	7.10	99.3	192196	Luc7l2	6.17	99.0
11777	Ap3s1	6.96	99.3	101358	Fbxl14	6.17	99.0
68612	Ube2c	6.96	99.3	382423	ENSMUSG000000	6.16	99.0
107732	Mrpl10	6.95	99.3	14062	F2r	6.14	99.0
66522	Pgpep1	6.94	99.2	19326	Rab11b	6.06	99.0
70296	Tbc1d13	6.93	99.2	81489	Dnajb1	6.05	99.0
56397	Morf4l2	6.93	99.2	23992	Prkra	6.00	99.0
11777	Ap3s1	6.90	99.2	73469	Rnf38	6.00	99.0
71446	Wrb	6.86	99.2	76969	Chst1	5.98	99.0

## Appendix 6. continued

66290	Atp6v1g1	5.95	98.9	224647	D17Wsu92e	5.30	98.7
12934	Dpysl2	5.94	98.9	19231	Ptma	5.26	98.7
29812	Ndr3	5.94	98.9	209497	Tmem164	5.25	98.7
67554	Slc25a30	5.92	98.9	56737	Alg2	5.25	98.7
12527	Cd9	5.92	98.9	66618	2610209M04Rik	5.24	98.7
21750	Terf2	5.90	98.9	18648	Pgam1	5.23	98.7
72999	Insig2	5.90	98.9	18648	Pgam1	5.23	98.7
218793	Ube2e2	5.87	98.9	66390	Slmo2	5.22	98.6
18787	Serpine1	5.84	98.9	640370	EG640370	5.22	98.6
226151	6030443O07Rik	5.82	98.9	100044416	LOC100044416	5.22	98.6
224938	Pja2	5.79	98.9	13972	Gnb1l	5.20	98.6
26905	Eif2s3x	5.76	98.9	83797	Smarcd1	5.18	98.6
100040099	ENSMUSG000000	5.76	98.9	235072	7-Sep	5.18	98.6
16828	Ldha	5.76	98.9	640370	EG640370	5.18	98.6
104318	Csnk1d	5.74	98.9	14904	Gtpbp1	5.18	98.6
21416	Tcf7l2	5.73	98.9	22390	Wee1	5.16	98.6
114128	Laptm4b	5.72	98.9	108705	Pttg1ip	5.16	98.6
170742	Sertad3	5.71	98.9	27801	Zdhhc8	5.14	98.6
218975	Mapk1ip1l	5.70	98.8	52398	11-Sep	5.13	98.6
20682	Sox9	5.68	98.8	240334	Pcyox1l	5.12	98.6
12534	Cdc2a	5.65	98.8	13728	Mark2	5.12	98.6
67125	Tspan31	5.62	98.8	16784	Lamp2	5.11	98.6
192657	Eil2	5.62	98.8	26572	Cops3	5.09	98.6
69065	Chac1	5.61	98.8	12575	Cdkn1a	5.07	98.6
241296	Lrrc8a	5.59	98.8	83486	Rbm5	5.06	98.5
54198	Snx3	5.57	98.8	68581	Tmed10	5.06	98.5
19179	Psmc1	5.56	98.8	63953	Dusp10	5.06	98.5
13990	Smarcad1	5.55	98.8	105440	Kctd9	5.05	98.5
20877	Aurkb	5.54	98.8	14567	Gdi1	5.03	98.5
76178	6330578E17Rik	5.54	98.8	68970	Wdr40a	5.02	98.5
67171	Tmem77	5.54	98.8	381038	Parl	5.01	98.5
59090	Midn	5.53	98.8	268490	Lsm12	4.99	98.5
80904	Dtx3	5.51	98.8	70527	Stambp	4.99	98.5
14026	Em	5.51	98.8	23790	Coro1c	4.97	98.5
12340	Capza1	5.47	98.8	19231	Ptma	4.97	98.5
11909	Atf2	5.45	98.8	18648	Pgam1	4.96	98.5
74137	Nuak2	5.45	98.7	70551	Tmtc4	4.96	98.5
69288	Rhobtb1	5.43	98.7	19231	Ptma	4.96	98.5
11512	Adcy6	5.41	98.7	77644	C330007P06Rik	4.95	98.5
18453	P4hb	5.41	98.7	66140	1110001A07Rik	4.95	98.5
100043982	LOC100043982	5.40	98.7	67468	Mmd	4.94	98.5
12340	Capza1	5.37	98.7	52696	Zwint	4.94	98.5
73137	Prrc1	5.37	98.7	675534	LOC675534	4.94	98.4
63959	Slc29a1	5.36	98.7	64453	Zfp280b	4.93	98.4
66578	2610039C10Rik	5.32	98.7	211347	Pank3	4.92	98.4
66511	2500003M10Rik	5.32	98.7	380959	Alg10b	4.91	98.4
68581	Tmed10	5.31	98.7	109006	Ciapin1	4.90	98.4

## Appendix 6. continued

68911	Pygo2	4.89	98.4	81535	Sgpp1	4.57	98.1
228836	Dlgap4	4.88	98.4	19230	Twf1	4.54	98.1
15395	Hoxa10	4.88	98.4	18708	Pik3r1	4.54	98.1
56376	Pdlim5	4.85	98.4	19156	Psap	4.53	98.1
19330	Rab18	4.84	98.4	16911	Lmo4	4.53	98.1
52635	D12Erd551e	4.83	98.4	17134	Mafg	4.52	98.1
22325	Vav2	4.83	98.4	11842	Arf3	4.51	98.1
72486	Rnf219	4.82	98.4	56233	Hdac7	4.51	98.1
12444	Ccnd2	4.82	98.4	78521	B230219D22Rik	4.51	98.1
15200	Hbegf	4.80	98.4	19179	Psmc1	4.51	98.1
56443	Arpc1a	4.79	98.4	675440	OTTMUSG000000	4.51	98.1
56501	ENSMUSG000000	4.79	98.4	665155	Srp54b	4.50	98.1
75869	Arl5b	4.78	98.3	19206	Ptch1	4.50	98.1
11480	Acvr2a	4.77	98.3	26442	Psma5	4.49	98.1
56878	Rbms1	4.77	98.3	13874	Ereg	4.48	98.1
99151	Cercam	4.76	98.3	140499	Ube2j2	4.47	98.1
98415	Nucks1	4.76	98.3	57339	Jph1	4.47	98.1
20249	Scd1	4.74	98.3	19139	Prps1	4.46	98.1
19230	Twf1	4.71	98.3	67145	Tomm34	4.45	98.0
76303	Osbp	4.71	98.3	11911	Atf4	4.45	98.0
103743	Tmem98	4.71	98.3	22215	Ube3a	4.45	98.0
240028	Lnpep	4.70	98.3	18475	Pafah1b2	4.45	98.0
68713	lftm1	4.70	98.3	20333	Sec22b	4.45	98.0
12531	Cdc25b	4.70	98.3	21973	Top2a	4.44	98.0
18227	Nr4a2	4.70	98.3	218581	Depdc1b	4.44	98.0
12417	Cbx3	4.70	98.3	18174	Slc11a2	4.44	98.0
69085	Zcchc9	4.70	98.3	66206	1110059E24Rik	4.44	98.0
108954	Ppp1r15b	4.69	98.3	20474	Six4	4.43	98.0
66059	Krtcap2	4.68	98.3	66508	2400001E08Rik	4.42	98.0
94275	Maged1	4.67	98.3	229782	Slc35a3	4.42	98.0
24075	Taf10	4.67	98.2	12399	Runx3	4.40	98.0
116940	Tgs1	4.66	98.2	67213	Cmtm6	4.39	98.0
19084	Prkar1a	4.65	98.2	30939	Pttg1	4.39	98.0
19192	Psme3	4.65	98.2	17387	Mmp14	4.38	98.0
14007	Cugbp2	4.65	98.2	71805	Nup93	4.38	98.0
18035	Nfkbia	4.64	98.2	15568	Elav1	4.37	98.0
70319	2600006K01Rik	4.63	98.2	11908	Atf1	4.36	97.9
20315	Cxcl12	4.62	98.2	12848	Cops2	4.36	97.9
107368	Pdzd8	4.62	98.2	236848	BC023829	4.36	97.9
19324	Rab1	4.61	98.2	12417	Cbx3	4.35	97.9
675440	OTTMUSG000000	4.61	98.2	19646	Rbbp4	4.34	97.9
59043	Wsb2	4.61	98.2	12417	Cbx3	4.34	97.9
226251	Ablim1	4.61	98.2	22318	Vamp2	4.34	97.9
675440	OTTMUSG000000	4.60	98.2	101867	1500003O22Rik	4.34	97.9
18605	Enpp1	4.59	98.2	268448	Phf12	4.33	97.9
15939	Ier5	4.57	98.2	56399	Akap8	4.33	97.9
77853	Msl211	4.57	98.2	319622	ltpripl2	4.33	97.9

**Appendix 6. continued**

100201	Tmem64	4.32	97.9	74102	Slc35a5	4.12	97.6
319622	Itprlp2	4.32	97.9	15251	Hif1a	4.12	97.6
214137	Arhgap29	4.32	97.9	223870	Senp1	4.12	97.6
665283	OTTMUSG000000	4.32	97.9	233575	Frag1	4.11	97.6
13046	Cugbp1	4.31	97.9	14451	Gas1	4.11	97.6
215449	Rap1b	4.31	97.9	11652	Akt2	4.10	97.6
22151	Tubb2a	4.29	97.8	74383	Ubap2l	4.10	97.6
14595	B4galt1	4.29	97.8	19252	Dusp1	4.10	97.6
100226	Stx12	4.29	97.8	76789	Z410129H14Rik	4.10	97.6
545085	Wdr70	4.29	97.8	22234	Ugcg	4.09	97.6
218460	Wdr41	4.28	97.8	225995	D030056L22Rik	4.09	97.6
68837	Foxk2	4.28	97.8	76789	Z410129H14Rik	4.09	97.6
194655	Klf11	4.28	97.8	21825	Thbs1	4.09	97.5
68842	Tulp4	4.28	97.8	667723	EG667723	4.09	97.5
638636	638636	4.27	97.8	56356	Gltf	4.09	97.5
107767	Scamp1	4.27	97.8	21859	Timp3	4.09	97.5
21423	Tcfe2a	4.27	97.8	675440	OTTMUSG000000	4.09	97.5
20148	Dhrs3	4.26	97.8	140499	Ube2j2	4.09	97.5
230257	Rod1	4.26	97.8	28042	D5Wsu178e	4.07	97.5
327826	Frs2	4.26	97.8	16011	Igfbp5	4.06	97.5
667723	EG667723	4.25	97.8	12330	Canx	4.04	97.5
675440	OTTMUSG000000	4.24	97.8	76775	Slc10a7	4.04	97.5
12631	Cfl1	4.23	97.8	75841	Rnf139	4.03	97.5
233724	Tmem41b	4.23	97.8	13002	Dnajc5	4.03	97.5
11652	Akt2	4.23	97.7	67501	Ccdc50	4.02	97.5
58523	Elp2	4.21	97.7	12469	Cct8	4.02	97.5
225339	Ammecr1l	4.19	97.7	11966	Atp6v1b2	4.02	97.5
19291	Purb	4.19	97.7	75219	Dusp18	4.02	97.5
23849	Klf6	4.18	97.7	12633	Cflar	4.02	97.5
67219	Med18	4.18	97.7	107971	Frs3	4.01	97.5
71779	8-Mar	4.17	97.7	56442	Serinc1	4.01	97.4
16430	Stt3a	4.17	97.7	269987	Z610024B07Rik	4.01	97.4
19141	Lgmn	4.17	97.7	19042	Ppm1a	3.98	97.4
13557	E2f3	4.16	97.7	22146	Tuba1c	3.97	97.4
17684	Cited2	4.16	97.7	83673	Snhg1	3.97	97.4
12449	Ccnf	4.16	97.7	223989	4921513D23Rik	3.96	97.4
12972	Cryz	4.16	97.7	667723	EG667723	3.96	97.4
17261	Mef2d	4.15	97.7	13046	Cugbp1	3.96	97.4
56494	Gosr2	4.15	97.7	54633	Pqbp1	3.95	97.4
16392	Isl1	4.14	97.7	29864	Rnf11	3.95	97.4
54138	Atxn10	4.14	97.7	19664	Rbpj	3.95	97.4
75734	Mff	4.14	97.6	72183	Snx6	3.94	97.4
67464	Entpd4	4.14	97.6	667723	EG667723	3.94	97.4
66700	Vps24	4.14	97.6	19684	Rdx	3.93	97.4
327900	Ubtcd2	4.13	97.6	98267	Stk17b	3.93	97.4
12520	Cd81	4.13	97.6	19826	Rnps1	3.93	97.4
68441	Rraga	4.13	97.6	14252	Flot2	3.93	97.4

**Appendix 6. continued**

22344	Vezf1	3.92	97.3	56334	Tmed2	3.75	97.1
74287	Kcmf1	3.92	97.3	224903	Safb	3.75	97.1
11787	Apbb2	3.92	97.3	26360	Angptl2	3.74	97.1
72124	Seh1l	3.89	97.3	13135	Dad1	3.74	97.1
381038	Parl	3.88	97.3	19777	C80913	3.73	97.1
65960	Twsg1	3.87	97.3	21372	Tbl1x	3.73	97.1
74012	Rap2b	3.87	97.3	433762	LOC433762	3.73	97.0
67443	Map1lc3b	3.87	97.3	433762	LOC433762	3.73	97.0
228136	Zdhhc5	3.87	97.3	20788	Sreb2	3.73	97.0
71801	Plekhf2	3.86	97.3	78755	4632404H22Rik	3.73	97.0
19826	Rnps1	3.85	97.3	15234	Hgf	3.73	97.0
108645	Mat2b	3.85	97.3	677333	677333	3.72	97.0
13713	Elk3	3.84	97.3	110213	Tegt	3.72	97.0
15481	Hspa8	3.84	97.3	17188	Maz	3.72	97.0
15481	Hspa8	3.84	97.3	72946	Lrrc47	3.72	97.0
22631	Ywhaz	3.84	97.3	12151	Bmi1	3.71	97.0
22146	Tuba1c	3.84	97.3	12306	Anxa2	3.71	97.0
19872	Rny1	3.83	97.3	108911	Rcc2	3.71	97.0
233812	BC030336	3.82	97.2	67898	Pef1	3.71	97.0
80795	Selk	3.82	97.2	67760	Slc38a2	3.71	97.0
100044642	LOC100044642	3.82	97.2	229542	Gatad2b	3.71	97.0
22196	Ube2i	3.82	97.2	109270	Prr5	3.70	97.0
110911	Cds2	3.81	97.2	17449	Mdh1	3.70	97.0
15312	Hmgn1	3.81	97.2	277463	Gpr107	3.70	97.0
100038401	ENSMUSG000000	3.81	97.2	224170	Dzip3	3.69	96.9
13685	Eif4ebp1	3.81	97.2	28193	Reep3	3.69	96.9
68097	Dynl12	3.81	97.2	545216	EG545216	3.69	96.9
13684	Eif4e	3.81	97.2	321022	Cdv3	3.69	96.9
226151	6030443O07Rik	3.80	97.2	68916	Cdkal1	3.68	96.9
108907	Nusap1	3.79	97.2	20878	Aurka	3.68	96.9
71949	Lass5	3.79	97.2	56334	Tmed2	3.68	96.9
65103	Arl6ip6	3.79	97.2	72562	Pcbd2	3.68	96.9
237459	Pctk2	3.78	97.2	67490	1810074P20Rik	3.67	96.9
72972	Gcap14	3.78	97.2	100048094	LOC100048094	3.67	96.9
224105	Pak2	3.78	97.2	14825	Cxcl1	3.66	96.9
229517	Slc25a44	3.77	97.2	12417	Cbx3	3.66	96.9
56878	Rbms1	3.77	97.1	209032	Zc3hav1l	3.66	96.9
56332	Amotl2	3.77	97.1	22388	Wdr1	3.66	96.9
50926	Hnrpd1	3.76	97.1	20729	Spin1	3.65	96.9
16589	Uhmk1	3.76	97.1	210992	Lpcat1	3.64	96.9
13803	Enc1	3.76	97.1	100048094	LOC100048094	3.64	96.9
13798	En1	3.76	97.1	68337	Crip2	3.63	96.8
26442	Psma5	3.76	97.1	236794	Slc9a6	3.63	96.8
19087	Prkar2a	3.76	97.1	18148	Npm1	3.63	96.8
73067	Tmem192	3.75	97.1	215193	AA408296	3.62	96.8
71900	Tmem106b	3.75	97.1	68365	Rab14	3.62	96.8
68108	9430008C03Rik	3.75	97.1	11520	Adfp	3.62	96.8



**Appendix 6. continued**

217653	C79407	3.61	96.8	100048094	LOC100048094	3.48	96.5
110172	Slc35b1	3.61	96.8	100042180	LOC100042180	3.48	96.5
67510	1810036I24Rik	3.60	96.8	22668	Sf1	3.48	96.5
19027	Sypl	3.60	96.8	18578	Pde4b	3.48	96.5
19384	Ran	3.60	96.8	791412	OTTMUSG000000	3.48	96.5
20583	Snai2	3.60	96.8	68473	Mobk1a	3.47	96.5
320213	Senp5	3.60	96.8	68904	Abhd13	3.47	96.5
19353	Rac1	3.59	96.8	56217	Mpp5	3.47	96.5
66661	Srp72	3.59	96.8	72033	Tsc22d2	3.46	96.5
241576	Ldlrad3	3.58	96.8	67704	1810037I17Rik	3.46	96.5
67229	Prpf18	3.57	96.8	213491	D4ErtD22e	3.46	96.5
70620	Ube2v2	3.57	96.8	116891	Der12	3.46	96.5
22319	Vamp3	3.57	96.7	114716	Spred2	3.46	96.5
72018	Fundc1	3.57	96.7	268697	Ccnb1	3.46	96.5
109154	2410014A08Rik	3.57	96.7	76179	Usp31	3.46	96.5
68151	Gpr177	3.57	96.7	207521	Dtx4	3.45	96.5
67698	Fam174a	3.57	96.7	97998	Depdc6	3.45	96.5
22099	Tsn	3.56	96.7	668347	EG668347	3.45	96.5
210998	D15ErtD621e	3.56	96.7	65112	Pmepa1	3.44	96.4
20750	Spp1	3.56	96.7	432537	OTTMUSG000000	3.43	96.4
74026	4121402D02Rik	3.56	96.7	12371	Casp9	3.43	96.4
665155	Srp54b	3.55	96.7	19352	Rabggtb	3.43	96.4
22146	Tuba1c	3.55	96.7	218203	Mylip	3.43	96.4
69082	Zc3h15	3.55	96.7	18515	Pbx2	3.43	96.4
381820	2700089E24Rik	3.54	96.7	329154	Ankrd44	3.42	96.4
20383	Sfrs3	3.54	96.7	13445	Cdk2ap1	3.42	96.4
12336	Capns1	3.54	96.7	56772	Mllt11	3.42	96.4
66492	Zmat2	3.54	96.7	15257	Hipk1	3.42	96.4
22381	Wbp5	3.53	96.7	21415	Tcf3	3.42	96.4
67771	Arpc5	3.53	96.7	22221	Ubp1	3.42	96.4
14958	H1f0	3.52	96.6	56334	Tmed2	3.42	96.4
67958	2610101N10Rik	3.51	96.6	20397	Sgpl1	3.41	96.4
12417	Cbx3	3.51	96.6	109154	2410014A08Rik	3.41	96.4
12417	Cbx3	3.51	96.6	20454	St3gal5	3.41	96.4
75553	Zc3h14	3.51	96.6	13831	Epc1	3.41	96.4
100048094	LOC100048094	3.51	96.6	226026	Smc5	3.41	96.3
22146	Tuba1c	3.51	96.6	268697	Ccnb1	3.41	96.3
71804	2610016C23Rik	3.51	96.6	226154	Lzts2	3.40	96.3
100042180	LOC100042180	3.51	96.6	229279	Hnmpa3	3.40	96.3
234663	Dync1li2	3.51	96.6	16653	Kras	3.40	96.3
208292	9030612M13Rik	3.51	96.6	268697	Ccnb1	3.40	96.3
19821	Rnf2	3.50	96.6	238330	6430527G18Rik	3.40	96.3
229279	Hnmpa3	3.49	96.6	11732	Ank	3.39	96.3
18003	Nedd9	3.49	96.6	68713	Ifitm1	3.39	96.3
68024	Hist1h2bc	3.49	96.6	14234	Foxc2	3.39	96.3
21413	Tcf4	3.49	96.6	103573	Xpo1	3.39	96.3
56294	Ptpn9	3.48	96.6	546080	EG546080	3.39	96.3

**Appendix 6. continued**

72416	Lrp3rc	3.39	96.3	229279	Hnrmpa3	3.30	96.0
433261	EG433261	3.39	96.3	52626	Cdkn2aipnl	3.29	96.0
18858	Pmp22	3.39	96.3	59125	Nek7	3.29	96.0
70420	2610034B18Rik	3.38	96.3	14470	Rabac1	3.29	96.0
100043485	100043485	3.38	96.3	57810	Cdon	3.29	96.0
100043314	Vstm3	3.38	96.3	56496	Tspan6	3.28	96.0
241311	Zbtb34	3.38	96.2	546032	EG546032	3.28	96.0
68051	Nutf2	3.38	96.2	18701	Pigf	3.27	96.0
65247	Asb1	3.38	96.2	11793	Atg5	3.27	96.0
27054	Sec23b	3.38	96.2	22763	Zfr	3.27	96.0
72265	Tram1	3.38	96.2	66143	Eef1e1	3.27	96.0
12417	Cbx3	3.37	96.2	18647	Pfk1	3.26	96.0
70155	Ogfr1	3.37	96.2	20910	Stxbp1	3.26	95.9
217337	Srp68	3.37	96.2	69912	Nup43	3.26	95.9
22152	Tubb3	3.37	96.2	218121	Mboat1	3.26	95.9
71448	Tmem80	3.37	96.2	320063	B230354K17Rik	3.26	95.9
27984	Efhd2	3.37	96.2	66078	Tsen34	3.26	95.9
319448	Fndc3a	3.37	96.2	53331	Stx7	3.25	95.9
66307	Isoc1	3.36	96.2	20539	Slc7a5	3.25	95.9
69568	Vkorc111	3.36	96.2	80912	Pum1	3.25	95.9
72542	Pgam5	3.36	96.2	14824	Gm	3.25	95.9
20383	Sfrs3	3.36	96.2	791412	OTTMUSG000000	3.25	95.9
107358	Tm9sf3	3.36	96.2	434356	EG434356	3.25	95.9
50721	Sirt6	3.36	96.2	17758	Mtap4	3.25	95.9
83602	Gtf2a1	3.36	96.1	15980	lfng2	3.25	95.9
93730	Lztf1	3.36	96.1	14605	Tsc22d3	3.25	95.9
15405	Hoxa9	3.35	96.1	229279	Hnrmpa3	3.25	95.9
18391	Oprs1	3.35	96.1	27494	Amot	3.24	95.9
14700	Gng10	3.35	96.1	66074	Tmem167	3.24	95.9
271981	A630047E20Rik	3.35	96.1	19652	Rbm3	3.24	95.9
321022	Cdv3	3.34	96.1	321022	Cdv3	3.24	95.8
448987	Fbxl7	3.34	96.1	15387	Hnrmpk	3.24	95.8
12317	Calr	3.33	96.1	625801	EG625801	3.24	95.8
72949	Ccnt2	3.33	96.1	68051	Nutf2	3.24	95.8
14688	Gnb1	3.32	96.1	68051	Nutf2	3.24	95.8
56386	B4galt6	3.32	96.1	69554	Klhdc2	3.24	95.8
101476	Plekha1	3.32	96.1	66817	Tmem170	3.24	95.8
214597	Sidt2	3.32	96.1	170791	Rbm39	3.24	95.8
73158	Larp1	3.32	96.1	20362	8-Sep	3.23	95.8
59043	Wsb2	3.32	96.1	226551	AI848100	3.23	95.8
68137	Kdelr1	3.31	96.1	67966	Zcchc10	3.23	95.8
13589	Mapre1	3.31	96.0	67048	2610030H06Rik	3.23	95.8
13390	Dlx1	3.31	96.0	67048	2610030H06Rik	3.23	95.8
13445	Cdk2ap1	3.31	96.0	56612	Pfdn5	3.23	95.8
665250	OTTMUSG000000	3.30	96.0	56314	Zfp113	3.23	95.8
76073	Pcgf5	3.30	96.0	13498	Atn1	3.23	95.8
229279	Hnrmpa3	3.30	96.0	20384	Sfrs5	3.22	95.8

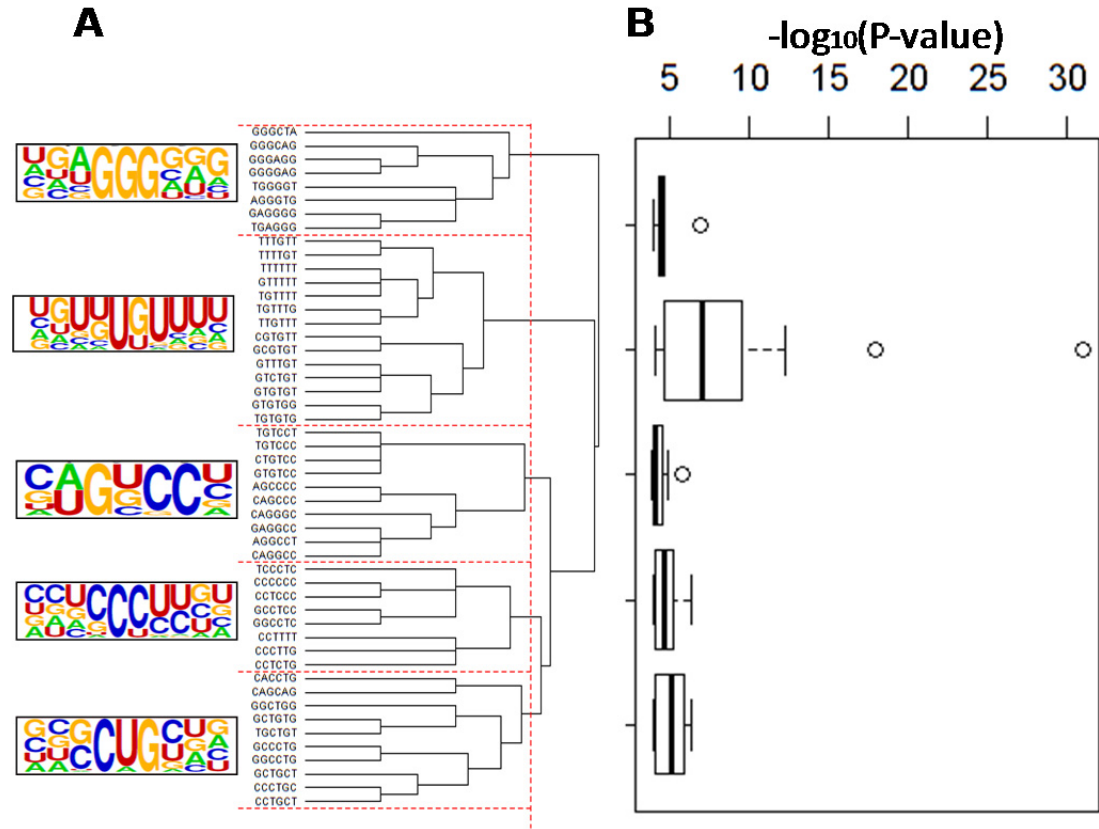
## Appendix 6. continued

69860	Eif1ad	3.22	95.7	229279	Hnmpa3	3.14	95.5
14284	Fosl2	3.22	95.7	209416	Gpkow	3.14	95.5
26939	Polr3e	3.22	95.7	102098	Arhgef18	3.14	95.5
13207	Ddx5	3.22	95.7	20024	Sub1	3.13	95.5
668063	EG668063	3.22	95.7	57437	Golga7	3.13	95.5
270066	Slc35e1	3.22	95.7	56468	Socs5	3.13	95.5
67006	Cisd2	3.22	95.7	66915	Myeov2	3.13	95.4
20623	Snrk	3.22	95.7	54667	Atp8b2	3.12	95.4
232313	Gltd4	3.21	95.7	22193	Ube2e3	3.12	95.4
56418	Ykt6	3.21	95.7	67248	Rpl39	3.12	95.4
622469	OTTMUSG000000	3.21	95.7	70533	Btf3l4	3.12	95.4
20168	Rtn3	3.21	95.7	69563	2310015B20Rik	3.12	95.4
100048094	LOC100048094	3.21	95.7	230779	Serinc2	3.11	95.4
64164	lfrg15	3.20	95.7	97487	Cmtm4	3.11	95.4
12048	Bcl2l1	3.20	95.7	17344	Pias2	3.11	95.4
57436	Gabarapl1	3.20	95.7	277010	Marveld1	3.11	95.4
67248	Rpl39	3.20	95.7	23983	Pcbp1	3.11	95.4
17309	Mgat3	3.20	95.7	246103	Atxn7	3.11	95.4
67963	Npc2	3.20	95.6	20810	Srm	3.11	95.4
66439	2010012O05Rik	3.20	95.6	107765	Ankrd1	3.11	95.4
13852	Stx2	3.19	95.6	13178	Dck	3.10	95.4
67710	Polr2g	3.19	95.6	107975	Pacs1	3.10	95.4
329506	Ctdspl2	3.19	95.6	230761	Zfp362	3.09	95.4
13929	Amz2	3.19	95.6	67876	Coq10b	3.09	95.4
14230	Fkbp10	3.19	95.6	66258	Mrps17	3.09	95.3
68041	Mid1ip1	3.18	95.6	229279	Hnmpa3	3.09	95.3
18005	Nek2	3.18	95.6	15387	Hnmpk	3.09	95.3
17691	Snf1lk	3.18	95.6	72881	Zdhhc4	3.09	95.3
101148	B630005N14Rik	3.18	95.6	59021	Rab2a	3.09	95.3
108946	Zzz3	3.18	95.6	67070	Lsm14a	3.08	95.3
67039	Rbm25	3.17	95.6	17118	Marcks	3.08	95.3
100042107	100042107	3.17	95.6	242291	Impad1	3.07	95.3
72462	Rrp1b	3.17	95.6	74585	Sppl3	3.07	95.3
14955	H19	3.17	95.6	433702	AU014645	3.07	95.3
15382	Hnmpa1	3.16	95.6	66818	9130011J15Rik	3.07	95.3
622845	EG622845	3.16	95.5	78832	2700078E11Rik	3.07	95.3
100042289	100042289	3.16	95.5	100040260	Gm1862	3.06	95.3
268396	Sh3pxd2b	3.16	95.5	78651	Lsm6	3.06	95.3
54196	Pabpn1	3.16	95.5	67857	Ppp6c	3.06	95.3
100434	Slc44a1	3.16	95.5	70144	Lrch3	3.06	95.3
66624	Spcs2	3.15	95.5	20364	Sepw1	3.06	95.3
13196	Ddef1	3.15	95.5	78825	5830417C01Rik	3.06	95.2
19652	Rbm3	3.15	95.5	16562	Kif1c	3.05	95.2
192285	Phf21a	3.15	95.5	26949	Vat1	3.05	95.2
19225	Ptgs2	3.15	95.5	21769	Zfand3	3.05	95.2
14462	Gata3	3.15	95.5	110809	Sfrs1	3.05	95.2
272589	Tbcel	3.15	95.5	19652	Rbm3	3.05	95.2

## Appendix 6. continued

12798	Cnn2	3.05	95.2
15931	lds	3.05	95.2
13865	Nr2f1	3.04	95.2
18148	Npm1	3.04	95.2
13345	Twist2	3.04	95.2
14593	Ggps1	3.04	95.2
215335	Slc36a1	3.04	95.2
22724	Zbtb7b	3.04	95.2
229279	Hnmpa3	3.03	95.2
12868	Cox8a	3.03	95.2
72454	Ccdc71	3.03	95.2
108735	Sft2d2	3.03	95.2
23854	Def8	3.03	95.1
208968	Zfp280c	3.03	95.1
107260	Otub1	3.03	95.1
67733	Irgb3bp	3.03	95.1
219024	Tmem55b	3.03	95.1
20918	Eif1	3.02	95.1
12995	Csnk2a1	3.02	95.1
70510	Rnf167	3.02	95.1
69568	Vkorc1l1	3.01	95.1
56444	Actr10	3.01	95.1
70681	Fam175a	3.00	95.1
22682	Zfand5	3.00	95.1
103583	Fbxw11	3.00	95.1
72640	Mex3a	3.00	95.1
671652	Trav7-1	3.00	95.1
74168	Zdhhc16	3.00	95.1
13205	Ddx3x	3.00	95.1
69082	Zc3h15	3.00	95.0
230721	Pabpc4	2.99	95.0
18226	Nup62	2.99	95.0
16906	Lmnb1	2.99	95.0
11435	Chma1	2.99	95.0
75747	Sesn3	2.99	95.0
12995	Csnk2a1	2.98	95.0
53424	Tsnax	2.98	95.0
53380	Psm10	2.98	95.0
22629	Ywhah	2.98	95.0
69875	Ndufa11	2.98	95.0
74919	4930471M23Rik	2.98	95.0
101187	Parp11	2.97	95.0
18712	Pim1	2.97	95.0
545622	Ptpn3	2.97	95.0
20520	Slc22a5	2.97	95.0
76522	Lsm8	2.97	95.0
240614	Ranbp6	2.97	95.0

Appendix 7.



**Clustering of the top 50 hexamers enriched in CUGBP1 IP dataset reveals binding site.**

(A.)The top 50 hexamers (by P-value ranking) from CUGBP1 bound mRNA 3'UTRs, clustered by relatedness of sequence. (B) Box and whisker plot of p-value ranges for the clustered groups of hexamers, black line represents the mean.

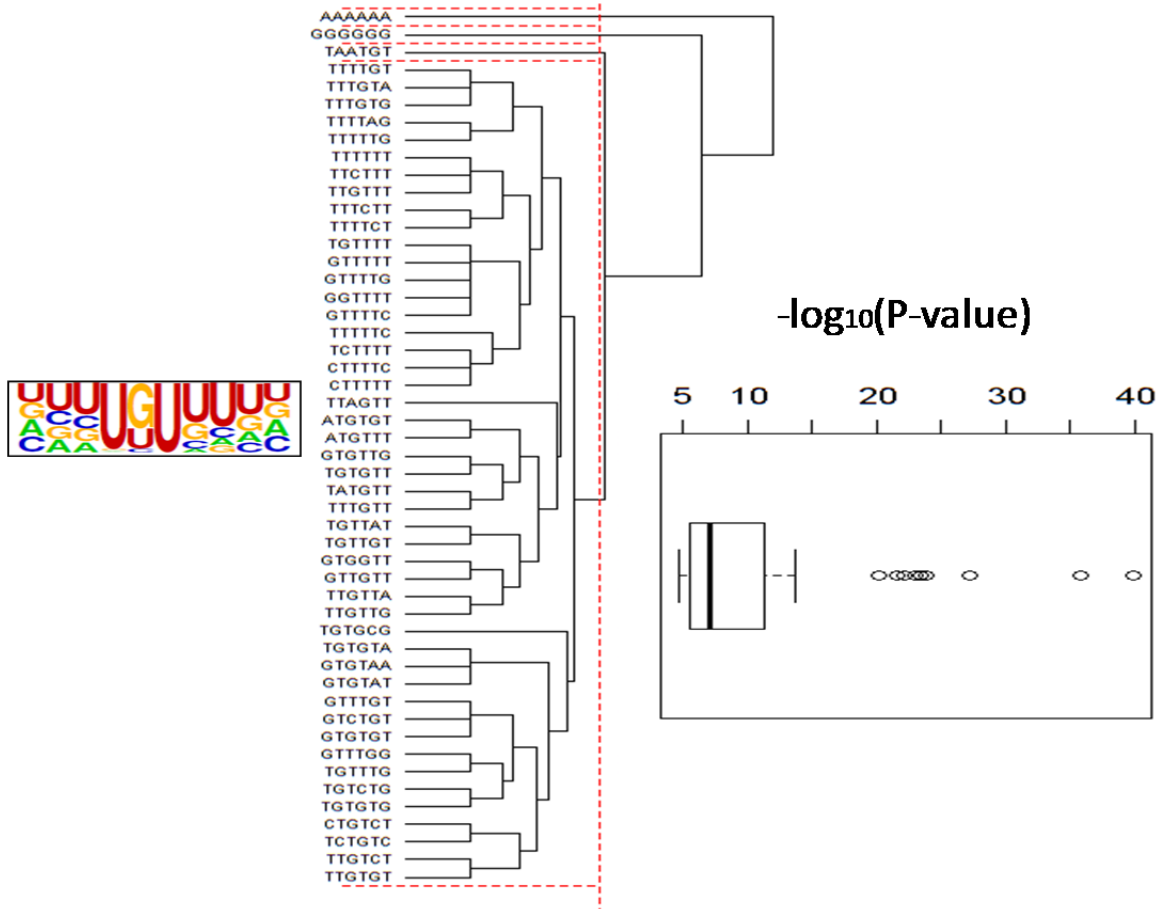
## Appendix 8.

Shared transcripts between stabilized in CUGBP1 KD and top 5% from CUGBP1 RIP-Chip				
Gene ID	Gene Name	RIP Chip Rank(%)	Fold-change in mRNA stability	p-value
68904	Abhd13	98	2.4	1.8E-05
50721	Sirt6	97	2.0	1.3E-04
69860	Eif1ad	97	3.3	5.2E-04
100043982	LOC100043982	99	2.6	8.4E-04
13803	Enc1	98	2.9	1.1E-03
68799	Rgmb	99	2.4	1.2E-03
74194	Rnd3	100	3.1	1.3E-03
64453	Zfp280b	99	2.9	1.5E-03
19206	Ptch1	99	2.6	1.7E-03
20877	Aurkb	99	4.6	1.7E-03
20623	Snrk	97	2.6	1.8E-03
13345	Twist2	97	3.1	3.3E-03
105171	Arrdc3	100	3.2	3.8E-03
67760	Slc38a2	98	1.9	4.7E-03
17684	Cited2	98	1.5	5.1E-03
56332	Amotl2	98	2.8	5.3E-03
238330	6430527G18Rik	97	2.3	5.5E-03
226178	D19Wsu162e	100	3.5	5.8E-03
72486	Rnf219	99	1.6	6.2E-03
26416	Mapk14	100	2.5	6.6E-03
108954	Ppp1r15b	99	2.0	6.7E-03
68911	Pygo2	99	3.3	6.7E-03
114716	Spred2	98	3.0	6.7E-03
13831	Epc1	97	2.0	6.9E-03
11911	Atf4	99	3.9	7.8E-03
102098	Arhgef18	97	2.0	8.1E-03
75841	Rnf139	98	2.1	8.2E-03
22390	Wee1	99	2.5	8.7E-03
241296	Lrrc8a	99	1.8	9.2E-03
16007	Cyr61	95	1.6	1.0E-02
109263	Rlf	96	3.0	1.1E-02
102193	Zdhhc7	96	1.9	1.1E-02
13557	E2f3	95	3.1	1.1E-02
72454	Ccdc71	97	2.0	1.1E-02
11555	Adrb2	100	3.2	1.4E-02
56772	Mllt11	97	3.0	1.5E-02
13728	Mark2	99	3.0	1.6E-02
381085	Tbc1d22b	96	3.0	1.8E-02
76522	Lsm8	96	2.3	1.8E-02
67141	Fbxo5	100	2.0	1.8E-02
16848	Lfng	100	1.9	1.8E-02

**Appendix 8. continued**

16468	Jarid2	96	2.0	1.9E-02
17131	Smad7	99	3.3	1.9E-02
72549	Reep4	96	1.7	1.9E-02
140482	Zfp358	95	2.7	2.0E-02
68041	Mid1ip1	97	3.6	2.0E-02
13990	Smarcad1	99	3.1	2.0E-02
225339	Ammecr1l	98	2.7	2.1E-02
72946	Lrrc47	98	3.4	2.3E-02
14284	Fosl2	97	2.0	2.3E-02
83486	Rbm5	99	1.8	2.3E-02
12449	Ccnf	98	1.7	2.3E-02
75234	Rnf19b	96	1.9	2.4E-02
12531	Cdc25b	99	2.3	2.4E-02
22325	Vav2	99	2.4	2.5E-02
76969	Chst1	99	2.3	2.6E-02
210106	Pols	95	2.3	2.6E-02
268697	Ccnb1	97	4.0	2.8E-02
21750	Terf2	99	2.6	2.8E-02
17691	Snf1lk	97	2.2	3.0E-02
226154	Lzts2	97	1.8	3.1E-02
14739	S1pr2	96	2.6	3.2E-02
219024	Tmem55b	97	1.7	3.3E-02
67219	Med18	98	1.6	3.4E-02
68970	Wdr40a	99	2.8	3.4E-02
16835	Ldlr	99	2.6	3.5E-02
27058	Srp9	96	2.7	3.5E-02
20937	Suv39h1	96	2.7	3.6E-02
232798	Leng8	95	2.3	3.7E-02
77853	Msl2l1	99	2.6	3.7E-02
18712	Pim1	96	2.3	4.0E-02
63953	Dusp10	99	2.1	4.0E-02
218581	Depdc1b	99	1.7	4.1E-02
19822	Rnf4	95	3.0	4.1E-02
66140	1110001A07Rik	99	3.1	4.1E-02
210982	BC032203	95	2.7	4.3E-02
12064	Bdnf	96	3.2	4.5E-02
56371	Fzr1	100	2.1	4.6E-02
16319	Incenp	99	2.4	4.6E-02
66665	5730528L13Rik	96	2.9	4.6E-02
23849	Klf6	98	2.6	4.6E-02
107765	Ankrd1	97	2.6	4.7E-02
170742	Sertad3	99	2.3	4.7E-02
73847	5430432M24Rik	96	2.7	4.7E-02
230761	Zfp362	97	2.9	4.8E-02
71804	2610016C23Rik	98	2.5	4.8E-02
29861	Dpf1	96	3.7	5.0E-02

## Appendix 9.

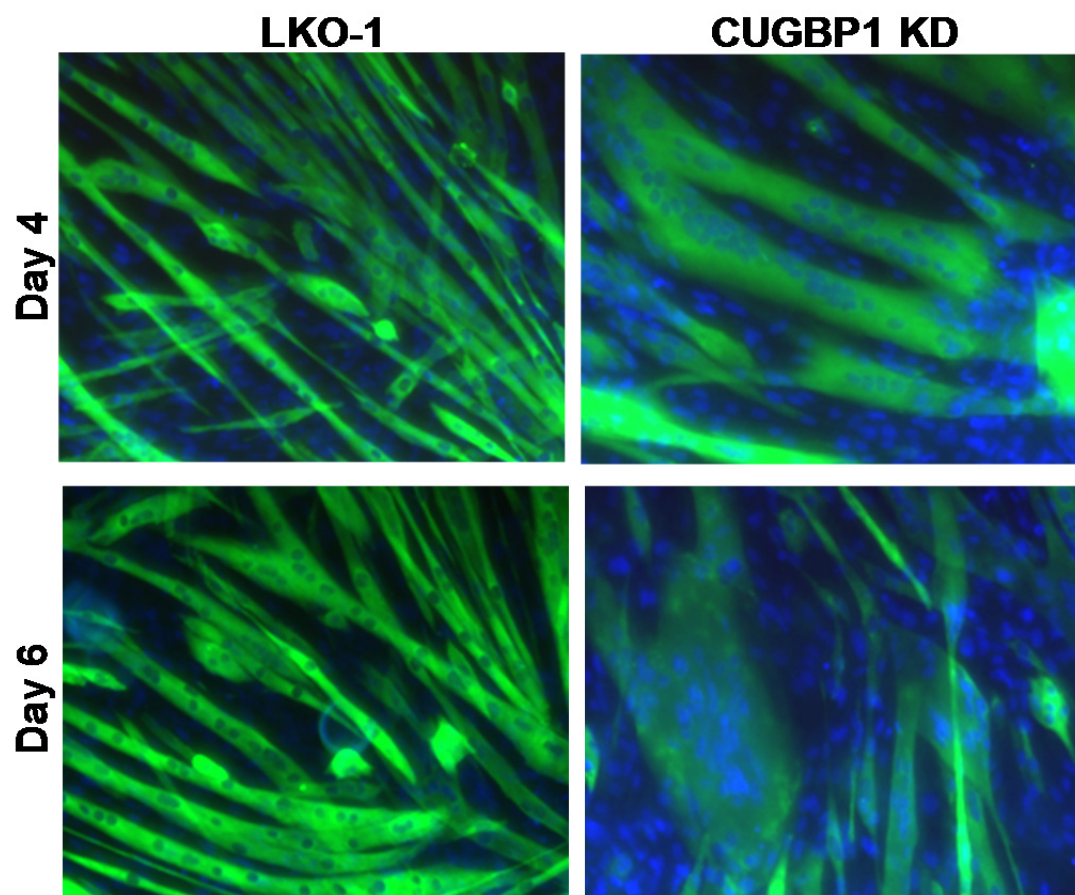


**Top 50 hexamers from transcripts stabilized in the CUGBP1 knock-down dataset and in the top 5% of the CUGBP1 IP dataset.** (A.) The top 50 hexamers (by P-value ranking) from CUGBP1 bound mRNA 3'UTRs, and the stabilized in the CUGBP1 KD half-life array clustered by relatedness of sequence, and the corresponding sequence logo. (B) Box and whisker plot of p-value ranges for the clustered group of hexamers, black line represents the mean.

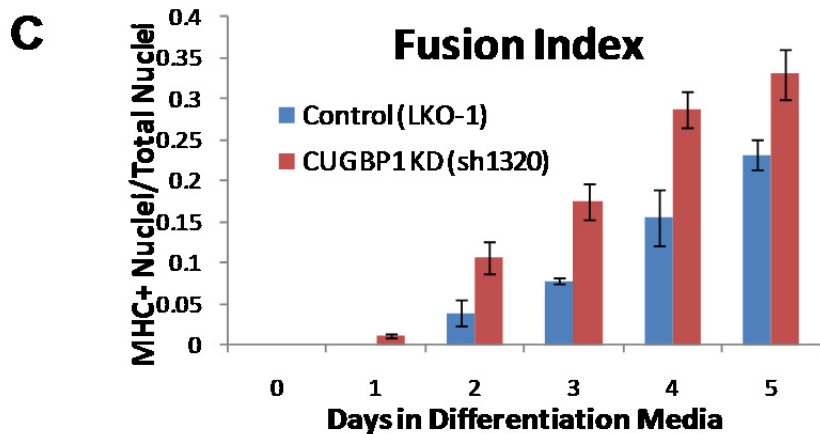
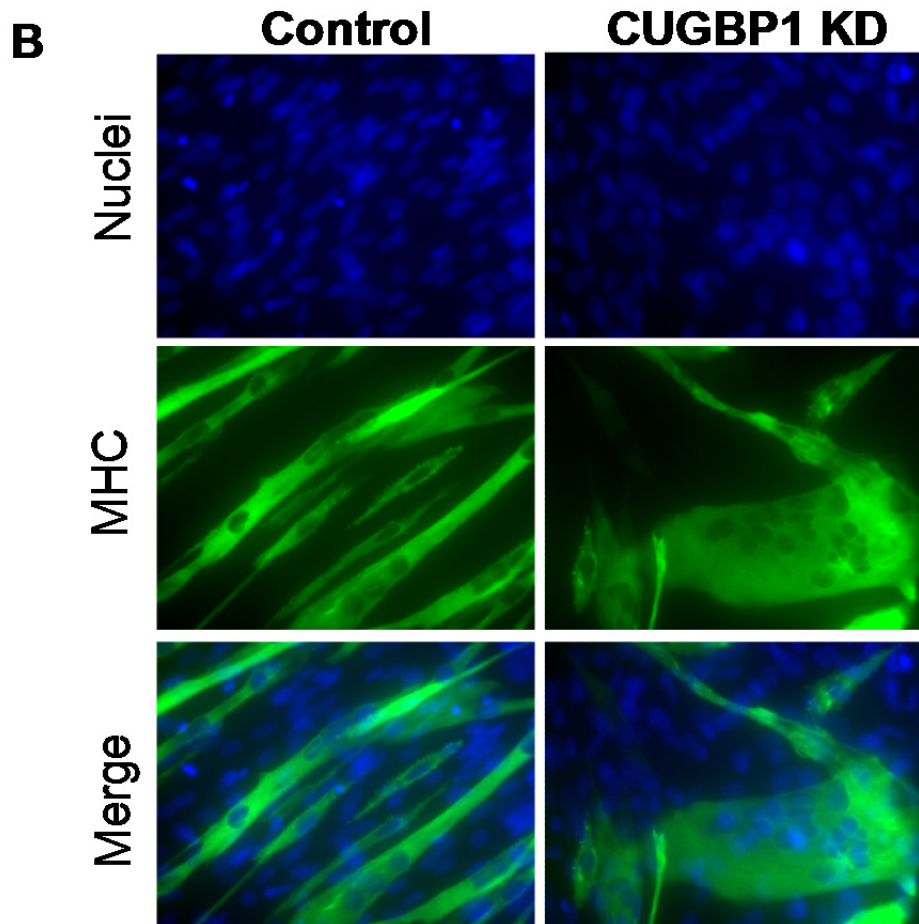


Appendix 10.

**A**



Appendix 10 cont.

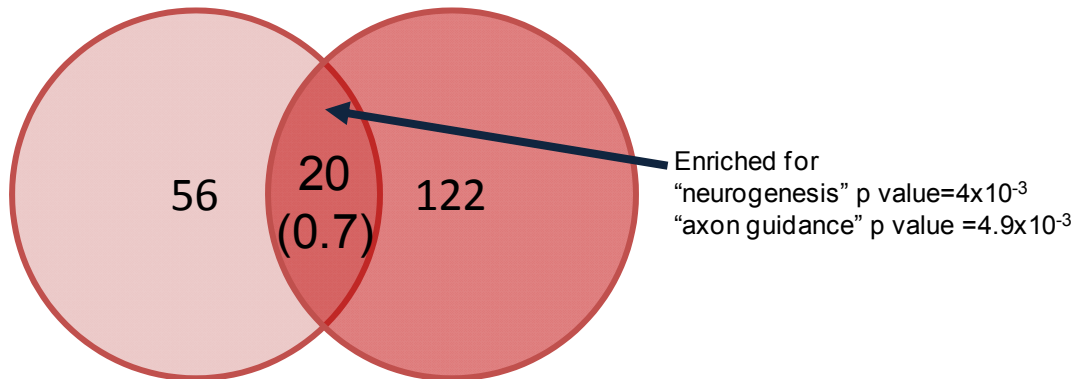


**CUGBP1 knock-down cell line and alternative shRNA (#1320) result in myosac formation and enhanced differentiation.** (A) Immunofluorescence microscopy of 6 day differentiated myotubes from LKO-1 and CUGBP1 KD cell lines from Chapter 3. (B) Immunofluorescence microscopy of 5 day differentiated myotubes from control and CUGBP1 KD cell pools sh1320 (nuclei were stained with DAPI and are colored blue, MHC was detected with monoclonal antibody MF20 (colored green)). (C) Fusion index of myoblast differentiation in control and CUGBP1 KD cell pools sh1320 (average of 3 independent experiments) where error bars represent the standard error.

Appendix 11.

Up in PARN KD

Up in CUGBP1 KD



**A significant number of mRNAs are increased in abundance in both PARN and CUGBP1 knock-down cells.** Of the 144 mRNAs whose abundance was increased in the CUGBP1 KD cells, 20 were also elevated >2-fold in the PARN KD cells. This was significantly more than expected at random (number indicated in parentheses). GO terms enriched in the shared mRNAs are shown.